

*Exploratory Multivariate Data Analysis
with Applications in Food Technology*

PhD Dissertation by
Claus A. Andersson, M.Sc., Chem. Eng.

Supervisor
Professor, Fil. Dr. Lars Munck
Chemometrics Group, Food Technology
The Department of Dairy and Food Science
The Royal Veterinary and Agricultural University
Rolighedsvej 30, DK-1958 Frederiksberg, Denmark

Title: Exploratory Multivariate Data Analysis with Applications in Food Technology

Author: Claus A. Andersson

Keywords: exploratory data analysis, multivariate data analysis, chemometrics, multiway, multimode, PCA, PARAFAC, CANDECOMP, Tucker, multivariate statistics

202 pages

ISBN 87-987937-0-5

July 1st, 2000

Printed by DSR Grafik, Frederiksberg, Denmark

Cover The words on the front and back cover pages have been ordered by letting MATLAB[®] choose randomly and uniformly from a list of selected keywords.

Preface

This PhD dissertation is based on a series of research projects conducted at The Royal Veterinary and Agricultural University (KVL), in the Chemometrics Research Group of Professor Lars Munck and colleagues during the period 1996-99. Parts of the theoretical research were accomplished during a part-time position as guest researcher at Humboldt University of Berlin (HUB), Dept. of Analytical Chemistry, Germany, in the group of Prof. G. Henrion during 1996-98.

I am greatly indebted to the many skilled and visionary people with whom I have had the great privilege to collaborate. The very competent chemometrics and spectroscopic groups at Food Technology are gratefully thanked for offering numerous interesting challenges. First and foremost, my colleagues in the group of Food Technology and in particular Lars Munck who through numerous discussions on the importance of context in relation to the exploratory spirit elevated my scope to look beyond the limits of the many isolated projects to find the “principal components” of successful solutions to problems based on data from systems of high complexity. With regards to algorithms and models, much appreciated professional and personal inspiration has come from Rasmus Bro and Lars Nørgaard. Søren B. Engelsen introduced me to the challenges of molecular modelling during a joint research project. Appreciation goes to Gilda Kischinovsky for proofreading of the text.

Dr. Rene Henrion, Weierstrass Institute for Applied Analysis and Stochastics, Berlin, and Prof. Gunther Henrion, Institute of Analytical Chemistry, Humboldt University, Berlin, are thanked for a very educational stay in Berlin and for the close collaboration.

Danisco Sugar Development Center, Nakskov, is thanked for providing industrial samples and data that have allowed for exploratory application of multivariate data analysis and, thus, many of the results reported in this dissertation.

Salaries, computers and travels have been funded by The Nordic Industrial Fund and the European Commission projects AFFLUENCE (CT 94-1416) and NWAYQUAL (GRD1-1999-10337). The funds are much appreciated for the required financial support during the period.

The thesis is based on work published in the following peer-reviewed papers which are included as off-prints at the back of the thesis and are referred to throughout the text by labels P1-P10:

- P1 **Direct orthogonalization**, C. A. Andersson, *Chemometrics and Intelligent Laboratory Systems*, 47, 51-63 (1999)
- P2 **A new criterion for simple-structure transformations of core arrays in N -way principal components analysis**, R. Henrion and C. A. Andersson, *Chemometrics and Intelligent Laboratory Systems*, 47, 189-204 (1999)
- P3 **A general algorithm for obtaining simple structure of core arrays in N -way PCA with application to fluorometric data**, C. A. Andersson and R. Henrion, *Computational Statistics and Data Analysis*, 31, 255-278 (1999)
- P4 **Improving the speed of multiway algorithms. Part I: Tucker3**, C. A. Andersson and R. Bro, *Chemometrics and Intelligent Laboratory Systems*, 42, 93-103 (1998)
- P5 **Improving the speed of multiway algorithms. Part II: Compression**, R. Bro and C. A. Andersson, *Chemometrics and Intelligent Laboratory Systems*, 42, 105-113 (1998)
- P6 **Further improvements of the speed of the three-way Tucker3 algorithm**, P. Paatero and C. A. Andersson, *Chemometrics and Intelligent Laboratory Systems*, 47, 17-20 (1999)
- P7 **Chemometrics in food science - a demonstration of the feasibility of a highly exploratory, inductive evaluation strategy of fundamental scientific significance**, L. Munck, L. Nørgaard, S. B. Engelsen, R. Bro and C. A. Andersson, *Chemometrics and Intelligent Laboratory Systems*, 44, 31-60 (1998)
- P8 **Multi-way chemometrics for mathematical separation of fluorescent colorants and colour precursors from spectrofluorimetry of beet sugar and beet sugar thick juice as validated by HPLC analysis**, D. Baunsgaard, C. A. Andersson, A. Arndal and L. Munck, *Food Chemistry*, 70, 113-121 (2000)
- P9 **Analysis of N -dimensional data arrays from fluorescence spectroscopy of an intermediate sugar product**, C. A. Andersson, L. Munck, G. Henrion and R. Henrion, *Fresenius Journal of Analytical Chemistry*, 359, 138-142 (1997)
- P10 **PARAFAC2 - Part II. Modeling chromatographic data with retention time shifts**, R. Bro, C. A. Andersson and H. A. L. Kiers, *Journal of Chemometrics*, 13, 295-309 (1999)

Summary

The subject of this PhD dissertation concerns the use of multivariate models in the service of exploratory data analysis in food technology. In this context the exploratory approach implies a computer-based evaluation of data from multivariate observations in a dialogue with *a priori* knowledge through an interactive hypothesis generating process. A review of principal component analysis as part of exploratory and multivariate data analysis is conducted in the introductory part of the thesis. The exploratory multivariate tools are compared to the classical hypothesis driven approach, and the differences are discussed. It is clarified that the success of exploratory multivariate data analysis is due to the context-driven analysis of high quality data, constantly anchored in the realm of the problem rather than in an abstract mathematical formulation.

The core of the dissertation consists of 10 peer-reviewed papers, proposing new mathematical models and algorithms designed specifically to assist the analyst in situations where an exploratory data analysis is to be preferred. The mathematical models and exploratory approaches are presented as a background to the research projects and to clarify on the applicability of the tools. The following models are covered: Principal component analysis (PCA), principal component regression (PCR), partial least squares regression (PLSR), parallel factors (PARAFAC) and canonical decomposition (CANDECOMP), Tucker3 modelling, and multi-way factor analysis.

A novel preprocessing tool for bi- and multilinear models is presented as *Direct Orthogonalization* (DO) [P1] which separates systematic phenomena that are *independent* of the response variables from the systematic phenomena that are *dependent*. The reported work shows that the model provides extended possibilities for exploratory analysis and outlier detection in diverse calibration problems. Two papers address the issues of rotational indefiniteness in some classes of multi-way models by providing a new measure of model simplicity [P2] and a general mathematical algorithm [P3] that by orthogonal transformations can optimize any differentiable function. Simplification of complex multi-way models that suffer from rotational indeterminacy is required to allow for use as exploratory tools.

To reduce the computational requirements for conducting data experiments, three research papers [P4, P5, P6] deal specifically with developing efficient implementations of algorithms for estimating parameters of multi-way models. The following three publications [P7, P8, P9] exemplify how exploratory multivariate data analysis could be performed in the sugar industry. The papers serve to visualize the advantages of using multi-way exploratory data analysis on real multivariate fluorescence measurements on sugar and sugar production streams.

Finally, a novel model termed PARAFAC2 [P10] for three-way data analysis is applied to real data from chromatography with similar spectral axes but dissimilar time axes. The results prove that significant advantages are gained when PARAFAC2 is compared to the ordinary PARAFAC-CANDECOMP resolution, since the model error is reduced by not assuming trilinearity and the factors are thus valid as estimates of the pure contributors.

The thesis concludes by focussing on the potential of exploratory data analysis in science. Data sets used in scientific publications should be made public on the Internet, allowing for an open dialogue on how data should be treated and interpreted in order to further stimulate the advancement of science.

Sammenfatning

Emnet for denne ph.d. afhandling er, hvordan multivariate modeller kan anvendes til eksplorativ dataanalyse i levnedsmiddelteknologi. I denne sammenhæng omfatter den eksplorative metode en computerbaseret evaluering af multivariate respons gennem en interaktiv og hypotese genererende process. I den indledende del af afhandlingen er der foretaget en litteraturundersøgelse af principal komponent analyse som en del af eksplorativ og multivariat dataanalyse. De eksplorative multivariate værktøjer sammenlignes med den klassiske hypotesebaserede tilgang, og forskellene diskuteres. Det understreges, at succes, hvormed multivariat og eksplorativ dataanalyse er blevet anvendt, skyldes den kontekstdrevne dataanalyse, som konstant er forankret i opgavens virkelighed i stedet for en abstrakt matematisk formulering.

Afhandlingens emneområde udgøres af 10 censorede publikationer, der indeholder forslag til nye matematiske modeller og algoritmer, som er specifikt designet for at hjælpe analytikeren i situationer, hvor eksplorativ dataanalyse kan anvendes. De matematiske modeller og eksplorative metoder præsenteres i kort form som baggrund for forskningsprojekterne og for at anskueliggøre værktøjernes anvendelsesmuligheder. Følgende modeller diskuteres: Principal komponent analyse, principal komponent regression, delvis mindste kvadraters regression, parallelle profiler og kanonisk dekomposition, Tucker3 modellering og multivejs faktoranalyse.

En ny metode til forbehandling af bi- og trilineære modeller præsenteres som Direkte Orthogonalisering (DO) [P1], som separerer systematiske fænomener, der er *uafhængige* af responsvariablene fra systematiske variationer, der er *afhængige*. De rapporterede resultater viser, at modellen giver udvidede muligheder for eksplorativ dataanalyse og identifikation af problematiske prøver i diverse kalibreringsopgaver. To artikler omhandler rotationsmæssig ubestemthed i enkelte klasser af multivejs modeller ved at tilbyde et mål for modellens simpelhed [P2] og en generel matematisk algoritme [P3], som ved orthogonale transformationer kan optimere alle differentiable funktioner. Simplificeringen af komplekse multivejs modeller er påkrævet for anvendelse i eksplorative sammenhænge.

Med henblik på at reducere de beregningsmæssige krav for at kunne udføre dataeksperimenter, omhandler tre forskningspublikationer [P4, P5, P6] specifikt, hvorledes mere effektive implementeringer af algoritmer til estimering af parametre i multivejs modeller kan foretages. De tre efterfølgende publikationer [P7, P8, P9] viser ved eksempler, hvorledes eksplorativ multivariat dataanalyse kan anvendes i sukkerindustrien. Publikationerne viser fordelene ved at anvende multivejs eksplorativ dataanalyse på virkelige multivariate fluorescensmålinger af sukker og strømme fra sukkerproduktion.

Endelig anvendes en ny model kaldet PARAFAC2 [P10] til analyse af virkelige trevejs data fra kromatografi med ens spektrale akser, men med forskellige tidsakser. Resultaterne viser, at betydelige fordele opnås når PARAFAC2 sammenlignes med den almindelige PARAFAC-CANDECOMP resolvering, eftersom modelfejlen reduceres ved ikke at antage trilinearitet.

Afhandlingen fokuserer afslutningsvis på potentialet af eksplorativ dataanalyse i videnskaben. Datamateriale som bruges i videnskabelige publikationer bør gøres frit tilgængeligt på Internettet for at muliggøre en åben dialog om hvorledes data skal behandles og fortolkes for at stimulere videnskabens videre udvikling.

Contents

Section I. Exploratory multivariate data analysis

1. Introduction	1
2. Exploratory multivariate data analysis	5
2.1 Exploratory data analysis	5
2.2 Multivariate data analysis	6
2.3 Exploratory multivariate data analysis revisited	8
3. Exploratory multivariate models	13
3.1 Principal component analysis (PCA)	13
3.2 Principal component regression (PCR)	14
3.3 Partial least squares regression (PLSR)	15
3.4 Direct orthogonalization (DO)	16
3.5 PARAFAC-CANDECOMP (PC)	17
3.6 TUCKER	18
3.7 A note on multi-way factor rotations	19
3.8 Validation	21
4. Applications of the exploratory multivariate tools	23
5. Conclusion	35
6. Reference list	39
7. Author's full publication list	51

Section II. Algorithms, models and applications

P1. Direct orthogonalization	53
P2. A new criterion for simple-structure transformations of core arrays in N -way principal components analysis	67
P3. A general algorithm for obtaining simple structure of core arrays in N -way PCA with application to fluorometric data	85
P4. Improving the speed of multiway algorithms. Part I: Tucker3	111
P5. Improving the speed of multiway algorithms. Part II: Compression	123
P6. Further improvements of the speed of the three-way Tucker3 algorithm	133
P7. Chemometrics in food science - a demonstration of the feasibility of a highly exploratory, inductive evaluation strategy of fundamental scientific significance	139
P8. Multi-way chemometrics for mathematical separation of fluorescent colorants and colour precursors from spectrofluorimetry of beet sugar and beet sugar thick juice as validated by HPLC analysis	171
P9. Analysis of N -dimensional data arrays from fluorescence spectroscopy of an intermediate sugar product	181
P10. PARAFAC2 - Part II. Modeling chromatographic data with retention time shifts	187

1. Introduction

What has modern multivariate data analysis, as performed in chemometrics, to offer that is not already offered by established scientific data analytic disciplines, such as statistics? What does multivariate data analysis bring to the market that makes it deserve special attention, e.g. by this thesis? In attempting to answer these questions, first of all an elucidation of the term *exploratory multivariate data analysis* is required. Next, a distinction between the mathematical models and their applications in chemometrics and statistics has to be made.

The development in sensors during the last decades provides academia and industry with more information than ever before. The new spectral sensors are characterized by high data quality, good sensitivity, fast responses and wide measuring ranges for rapid fingerprinting of vast amounts of samples. Furthermore, the complexity of a single measurement is increasing from spectra to higher-order structures, e.g. spectral data from 2D electrophoresis, hyphenated chromatography and fluorescence spectroscopy. Today, most chemists discard much of this information by making problem reduction or non-intelligent data reduction, selecting only the wavelength and fraction for analysis for which there is an *a priori* established hypothesis and model. This leads to a dramatic loss of information, and especially loss of important new information that would not initially be anticipated. Instead, the increased amount of complex data demands effective tools for data mining and reversed engineering first to explore connections, correlations and groupings and afterwards to help the analyst to generate hypotheses.

The realm of modern science and industry needs rapid solutions to complex biologically based problems as found in the strongly competitive food industry, thus demanding versatile, robust and unbiased methods for successful handling of complex measuring conditions. The focus has shifted from general and long-term fundamental research to solving specific here-and-now problems with clearly formulated success criteria. It is thus necessary to translate the parameters from more or less abstract mathematical models to real world language expressions of the functional factors for making decisions and for inducing new, more adequate and precise hypotheses. Consequently, tools are required to facilitate optimal exploitation of the vast amount of the often intercorrelated information provided by the new instruments. It is here that exploratory multivariate data analysis plays a key role by combining multivariate mathematical tools and exploratory approaches for analysing data sets with correlated variables.

I. Exploratory multivariate data analysis

In looking through the literature, it becomes clear that a new exploratory technology has emerged in parallel with new mathematical developments. The versatility of the multivariate tools and the few assumptions required by multivariate analysis (other than those inherent in the models) makes this technology a cardinal and indispensable tool for exploratory purposes required to efficiently solve R&D problems today.

In particular, it is the intention to discuss here two core features of multivariate data analysis: First, the scientific process leading from multivariate observations to information, and secondly, the mathematical development with a description of how some of the most versatile multivariate models can be used in chemometrics. The dissertation is divided into two sections. Section I is outlined as follows: The development of modern multivariate data analysis up to today is depicted in the context of principal component analysis, and the exploratory multivariate scientific process going from observation to knowledge is presented and compared to the classical scientific approach. Furthermore, some fundamental and general exploratory mathematical models are briefly presented. Section I ends with a presentation of the applications and a conclusion on the use of exploratory multivariate data analysis is made. Section II consists of off-prints of the peer-reviewed published papers that constitute the thesis.

The concepts and tools for multivariate data analysis are collectively referred to as *chemometrics* in the context of chemistry. Chemometrics, being a juxtaposition of *chemo* (*latin*, chemistry) and *metrics* (*greek*, measure) is the common denominator of all possible tools applied to make rational analysis of chemical measurements. Several publications cover the history of chemometrics [Kowalski (1984), Anderson (1984), Beebe & Kowalski (1987), Meuzelaar & Isenhour (1987), Geladi & Esbensen (1990), Esbensen & Geladi (1990), Wold (1996)]. Using the term chemometrics serves an important purpose: It makes clear that the whole of the problem is to be observed, analysed and interpreted in a direct or indirect chemical context. The issue of proper context will later be shown to be consistent with the success of biometrics, econometrics, psychometrics, and in our case, chemometrics.

For the engaged practitioner, chemometrics offers significant new possibilities in the approach towards multivariate problems that perfectly complements the classical scientific methodology, thus providing a *technology* in the sense that it is a holistic pragmatic solution combining strategies and tools in the very centre of the application. It is important to stress the difference between a technology and a discipline. *Disciplines* evolve by budding off, thus establishing new borders by making subclasses of existing scientific disciplines. A *technology* is comprised of a set of tools with interdisciplinary applicability and is defined by its operational aims rather than by its formal scientific heritage. Exploratory data

I. Exploratory multivariate data analysis

analysis, chemometrics and multivariate analysis are technologies rather than disciplines, since they are tools that work in the context of different disciplines and are adapted to the circumstances at hand, such as chemistry, biology or psychology.

The two chemometrics journals, *Journal of Chemometrics* (Wiley) and *Chemometrics and Intelligent Laboratory Systems* (Elsevier) demonstrate an active international society pursuing chemometrics as a technology that is constantly developing theory and applications for the multivariate domains, including signal processing and image analysis. Now and then there is a tendency also in chemometrics to form borders and to be self-sufficient as a discipline, leaving out the flexibility of a technological approach. To serve science in the best way such tendencies should be combatted [Wold (1994)]. As is apparent from the two mentioned journals, chemometrics covers all types of models and data analysis approaches applied to chemical and physical data. Soft multivariate data analysis makes up the major part of chemometrics, but it is not solely about multivariate modelling, since many hard models have found their way into chemometrics. Chemometrics is thus open for inspiration from areas outside the natural sciences, i.e. getting inspiration from areas as different as engineering, psychology and economics. This openness is particularly evident for the establishment of multi-way mathematical tools which will be discussed in more detail at the end of this section.

I. Exploratory multivariate data analysis

2. Exploratory multivariate data analysis

Exploratory multivariate data analysis is the unification of *exploratory data analysis* and *multivariate data analysis*. Henceforth, we will initiate the discussion by describing what these two terms represent in order to have useful definitions in place. The effect of combining the two historically different approaches is multiplicative rather than additive in the sense that new possibilities and paths are offered to solve complex scientific and industrial problems.

2.1 Exploratory data analysis

The term *exploratory data analysis* [Hoaglin et al. (1983), Weihs (1993), Minton & Rose (1997)] was first used in the psychological and behavioural sciences. In spite of extensive literature searches, no formal definition of exploratory data analysis could be found, but perhaps the closest and most direct is given by Hoaglin et al. (1983): “In brief, exploratory data analysis emphasizes flexible searching for clues and evidence, whereas confirmatory data analysis stresses evaluating the available evidence”. In the context of factor analysis [Thurstone (1931), Anderson & Rubin (1956), Horst (1965)], which is central to all models based on principal components, Harshman (1970), p. 5, proposes the following distinction between *descriptive* and *explanatory* analysis: “While descriptive factor analysis seeks merely to find a convenient, condensed representation of data relationships, explanatory factor analysis seeks to discover good estimates of the structure of ‘true underlying’ influences that are responsible for the observed data relationships.”. Exploratory analysis is concerned with both: The exploratory approach is focussed on making the data analysis in a stepwise manner, evaluating at each step the appropriateness of the model and the data, and if necessary, modifying the model and/or the data basis. At each step, new insight is gained in terms of correlations between objects or variables, outlying samples or the effects of preprocessing, or numerous other important conditions necessary to reach valid conclusions. The exploratory approach lets the results from the iterative exploratory procedure help the analyst to define and find the combinations of analysis conditions that provide the optimal understanding of data. The comprehensive book on exploratory data analysis by Tukey (1977), p. 3, has the following dictum “Exploratory data analysis can never be the whole story, but nothing else can serve as the foundation stone - as the first step.”, and in the same reference, the necessity for confirmatory analysis is also stressed. Tukey compares the task of doing exploratory analysis with that of a detective looking for clues and hints to be able to find the truth.

I. Exploratory multivariate data analysis

Due to the ever accelerating improvement of the computer, it is now possible to conduct new exploratory analysis in pure electronic form by using digital representations of the system under investigation in combination with an interactive graphical interface between the observations and the model parameters. Having the data in the computer allows for examinations of subsets of objects and variables, and for applying different preprocessing methods among a host of possible mathematical treatments. Thus, once having data represented in the computer allows for extensive *data experimentation* in the same sense as when a chemist conducts experiments in the laboratory. The high-performing and efficient mathematical environments for doing such experiments can run on every modern computer, thus opening the way for scientists to take responsibility for exploration of the structure of their own data by not considering measured data as something static, but rather regarding them as symbols of dynamic systems that can be recombined and transformed into meaningful information by the use of exploratory multivariate chemometrics.

It is noteworthy that in several places in the statistics literature [Anderson (1984)] the term *descriptive* data analysis is used as a synonym for *exploratory* data analysis. These unfortunate choices of definitions are incompatible and do not fully conform to the reality of exploratory analysis.

2.2 Multivariate data analysis

One multivariate tool has, in particular, formed the conceptual basis from which the central part of multivariate tools of concurrent multivariate data analysis and chemometrics has been derived. This is principal component analysis (PCA). PCA represents the core idea of condensing large amounts of data to a few representative parameters (*principal components* or *latent factors*) which capture the levels of, and differences between, objects and variables in the data under investigation. Patterns and clusters in the parameters are easily represented in the form of scatter plots in the Euclidian plane with an exploratory choice of different principal components as axes. By nature, PCA implies that the world is under indirect observation as variations in data are caused by *principal* components in the sense that these are hidden and underlying instead of manifest and directly observable. After estimation, these parameters can subsequently be treated in numerous ways to facilitate optimal representations of the original data and in this regard visualization provides an indispensable and very effective path for analysts to identify similarities and dissimilarities of objects and variables in large data sets. The latent factors may under favourable conditions be interpreted as functional factors recognizable in real world terms. According to Jolliffe (1986), the approaches towards PCA taken by Pearson (1901), Hotelling (1933a) and Hotelling (1933b) are the earliest. But Fisher & MacKenzie (1923) also explicitly mention

I. Exploratory multivariate data analysis

PCA and even include a simple algorithm for estimating principal components, similar to the so-called non-linear iterative least squares (NIPALS) algorithm. Albeit, decades earlier in a rather compressed communication, Adcock (1878) formulated a least squares problem that resembles the decompositional approach taken in PCA. According to Wold (2000), an even earlier, yet non-verified, reference dates back to Cauchy (1829). Several reviews on PCA have been published in different application areas [Kruskal (1978), Jackson (1980), Jolliffe (1986), Wold et al. (1987), Mardia et al. (1992), Horst (1992), Wold (1996)].

A fundamental feature of PCA is the minimization of sums of squared errors between observations and the model predictions, i.e. the well-known least squares approach. Least squares approaches, which constitute a significant part of multivariate data analysis, can be traced back to 1795-1799. Several references ascribe the first publication of the least squares principle to Legendre (1805), but Gauss (1809) (written 1809) claimed to have used least squares since 1795. More references on error functions in multivariate modelling can be found elsewhere, e.g. [Goldstine (1977), Björck (1990)]. Markoff (1912) notes that Gauss [Gauss (1821), Gauss (1823)] proved that least squares provides the least biased estimator as optimal feature when the distribution is unknown.

Principal components can be estimated as *eigenvectors* because they represent the phenomena that will grow out of data, if data is amplified with itself iteratively. See references [Bauer (1957), Rutishauser (1969), Longley (1984)] for algorithmic descriptions on finding eigenvectors, which in the simplest forms works by growing eigenvectors out of data by projecting data onto itself.

Multivariate statistics is established as a discipline under applied statistics [Afifi & Elashoff (1966), Bryant & Atchley (1975), Gordon (1981), Anderson (1984), Krzanowski (1988)], but multivariate statistical data analysis has since long been regarded as an independent statistical discipline [Gordon (1981), Anderson (1984)]. However, due to the complexity of dealing with multivariate distributions this mathematical-statistical treatment has moved to the background of statistics. Since the introduction of the computer, multivariate modelling has been conducted separately from theoretical statistics as applied data analysis in various application areas, e.g. psychometrics, biometrics and chemometrics. There appears to be a paradox between the refined, and thus rarely used, statistical methods which require the handcraft of a professional statistician to provide valid conclusions on the one hand, and the easily applicable and interpretable multivariate models like PCA on the other. In spite of the fundamental significance of the computer, multivariate models have not received enough attention from the statistical community due to lack of methods to characterize distributions for multivariate responses with correlated parameters. In this

I. Exploratory multivariate data analysis

respect, it is noteworthy that the idea of PCA was first conceived by scientists with high mathematical capabilities working in the social sciences and psychology, outside the field of pure statistics.

2.3 Exploratory multivariate data analysis revisited

Statistics dates back several hundreds of years to a time when theories of gambling and insurance policy were developed, and when the numerical and computational tools were extremely limited compared to today. Thus, the mathematical abstraction of any kind of problem had to be represented by a very simple mathematical relation requiring estimation of only a few parameters. Before the computer, i.e. up to around 1950, statisticians were forced to transcribe their problems into forms that were solvable, thus implicitly restricting the viable domain to consist of uni- and oligovariate models. Since 1950 higher numbers of parameters have been easy to estimate, and thus the more demanding multivariate models now provide resourceful alternatives to the classical approaches, e.g. hypothesis testing and analysis of variance.

On three particular points the exploratory multivariate approaches, here in terms of the essentially exploratory principal component analysis, offer significant and new possibilities which are of fundamental importance to the way research is conducted. The first aspect is the way naturally occurring correlations between observations are exploited to improve the understanding of complex systems by identifying the latent factors of the observations. This is done with a minimum of *a priori* assumptions and with models that are optimal when applied to unknown distributions [Markoff (1912)]. Secondly, direct application of PCA in screening setups helps the analyst to narrow in on the important factors and conditions of the system under observation. Finally, the methods are well suited for application as close to the context of the problem as possible by introducing mathematical metaphors which correspond to real life factors, thereby diminishing the requirement for creating abstract mathematical or chemical representations of the real problem. In the following, these three aspects and their premises will be advanced in terms of modern food technological problems and chemometrics.

Since around 1950 science has had access to estimating soft, adaptive and yet still interpretable models of observations. These novel *soft* data analysis tools are based on formal mathematics not assuming any *hard* explicit model, as required by classical deductive modelling. It is important to note that soft models, e.g. PCA, neural nets and genetic algorithms, are intrinsically preconceived due to the mathematical models on which they are based, i.e. linear relations, exponential functions and logical operators, and that their

I. Exploratory multivariate data analysis

adaptability is due to a high number of parameters involved in the many intrinsic repetitions of the basis functions. A normative approach, as listed in Table 1, assumes that data conform to an *a priori* defined mathematical relationship or distribution, thus requiring the analyst to have a hypothesis on the structure of the data before doing the analysis. In contrast, the novel exploratory multivariate tools are *hypothesis generating*, and require less *a priori* knowledge at the outset of a new research project. Table 2 gives a schematic overview of the exploratory multivariate strategy towards solving research problems. The table is inspired by the sequence of exploratory events as explained in the concept of the *selection cycle* by Munck [Munck (1991), Munck (2000)], and in thesis paper P7. In the textbook by Massart et al. (1997), p. 1-2, a brief discussion of the Arch of Knowledge by Oldroyd (1986) is given in terms of inductive versus deductive analysis in the context of chemometrics. The main conclusion by Oldroyd is that the optimal conditions for scientific research are defined by clever and relevant experiments with a rational subsequent analysis of the results, i.e., an intensive dialogue between knowledge and experiment.

Both the normative and the exploratory approaches require *a priori* knowledge, but the stages in the processes at which it is used differ significantly. As is apparent from Table 1, the classical scientific approach implies a high risk of forming a hypothesis that is biased by what is already known. Thus, the objective is formulated at the first step of the analysis in a rigid and abstract way, by which the real problem is reduced and simplified. Before and after the introduction of inductive inference [Fischer (1935)] and formal significance testing [Fischer (1922)], statisticians Neyman & Pearson (1928) argued in favour of *an informed personal judgement*. Informed judgement expresses an intention to respect that the systems under observation are never identical and it depicts a consciousness of ensuing proper context. Despite this very early realization by Neyman and Pearson, statistics has continuously aimed at developing tools that works for all data analysis situations, as claimed for significance testing by Fischer (1925). It should be remembered that chemometrics integrates mathematics and chemistry throughout the analysis due to the data analyst's understanding of the research context, while chemometrics without understanding of chemistry is reduced to statistics.

An inherent limitation of the classical hypothesis-testing principle in Table 1 is the problem of making ground-breaking discoveries, since the analyst can only test hypotheses that can be imagined mentally, as it is only possible to formulate new ideas in terms of what is already known. At best, new possibilities may be realized by considering interferences to the ruling hypotheses in experiments. By letting the data talk through a more sophisticated dialogue as suggested in exploratory multivariate data analysis in Table 2, new ideas can be

I. Exploratory multivariate data analysis

formed in the mind of the investigator by a kind of supervised intuition made possible by the synergy with the computer through the graphical display.

Table 1: Simplified presentation of the classical scientific one-shot approach to data analysis for a given data set.

1	Hypothesis based on problem reduction of prior knowledge Mathematical tailoring of the hypothesis into a mechanistic model. Assumptions are made on intersample/intergroup relations observed from experiments designed to test the hypothesis. The problem of recognizing the effects is reformulated in a mathematical abstraction of the original problem.
2	Parameter estimation A mathematical/statistical model that aims at capturing the essence of the scientific problem is deduced from the mechanistic assumptions. The model parameters are estimated.
3	Hypothesis testing The analysis ends by a statistical test of confidence of the parameters or the observables in the framework of assumptions required by the initial mechanistic model or the statistical models applied during analysis.
4	Hypothesis reformulation If the hypothesis is rejected, a new fundamental mechanistic model needs to be formulated, or the data material is discarded. The outcome is a simple yes/no to the proposed hypothesis, depending on the significance test of the null hypothesis.

In multivariate analysis performed as experimental mathematics outlined in Table 2, no initial hypothesis is necessitated prior to the analysis other than that implicit in the experimental screening analyses and the mathematical tools. Thus, it is initially data that is reduced and simplified rather than the problem. Looking at the data in terms of fewer parameters as provided by the modelling tools will allow for an enhanced graphic and thus more effective interfacing between the observed variations in the data set and the mind of the researcher which again will initiate ideas for new connections and groupings. Thus, the analyst will be inspired to form new hypotheses from the insight provided by the new representations of the data. The *a priori* knowledge is used for validation after the PCA model has been estimated and is used as an inspiration for generating new relevant hypotheses and to ensure that the conclusions are valid in the context of the analysis. Thus, the known features of the system under investigation are used in an interactive fashion that ensures validity by constantly comparing with the known variations and groupings in data as well as with external knowledge.

I. Exploratory multivariate data analysis

Table 2: Typical application of iterative and interactive multivariate models to explore problems, thereby performing data reduction in a stepwise manner for a given data set.

1	Estimation of a multivariate model in an inventory analysis Exploits correlations of observables with a broad aim of establishing the character of the underlying principal components. Often the first choice of model is principal component analysis (PCA) for screening purposes. The aim is unbiased reduction of the primary data with a minimum loss of information.	
2	Graphic representation Exploits human cognition for interpretation of plots of classes, outliers, correlations and patterns in a close dialogue with the context.	Numerical representation Figures of merits filter and simplify the estimated parameters. Provides tools for automated analysis.
3	Evaluation Conclusions are induced from graphs and plots of patterns of objects and variables by comparing to prior knowledge. The results are validated by contextual measures and comparisons.	
4	Hypothesis generation by data management and/or model reformulation New models are built on subclasses, outliers are removed, other preprocessing is chosen or a different type of multivariate model may be applied. Depending on the evaluation, a new measurement technology may be introduced, thus producing entirely new data sets for the problem that can be used in combination with what is already known.	
5	The gained knowledge is applied. A new iteration is made beginning with Step 1.	

For different reasons, during the last century the general demand for new knowledge has changed from dealing with general, existential and fundamental issues towards solving concurrent specific problems. Political and commercial administrations have a preference for evaluating and monitoring the effects of scientific, economic and social initiatives in detail in order to design new solutions. The objective is formulation of effective and precise indicators for efficiency and success. In consequence, a large fraction of public and commercial scientific research is aimed directly at mending current problems, e.g. improving nutritional value of foods, identifying the mechanisms of viruses or finding a cure for cancer. These complex, often biological, areas are difficult to address with a design strategy, like that used for building cars, as there are no known simple mathematical and theoretical relationships between the unknown factors and the effects. The objectives for addressing these problems today are not so much curiosity about nature, nor the gain of fundamental knowledge, but rather in the short perspective to solve the problems that are currently in the eye of an increasingly critical society. To comply with this demand for obtaining a fast fix of the underlying, yet unknown, nature, inventories of problem areas using fast, sensitive,

I. Exploratory multivariate data analysis

and reproducible holistic screening methods are required that, in short time and at affordable costs, can provide decision makers at all levels with high quality data which can be evaluated by multivariate methods to produce sufficient insight and knowledge to allow for managing and controlling the various kinds of problems.

The quality of data is an important aspect in improving the outcome of multivariate investigations as pointed out by Wold (1994). As advocated in Step 1 of Table 2, a first screening step is introduced which will indicate whether there are systematic relations between the objects in the sense that objects that are similar should be assigned the same properties and objects that are dissimilar should be assigned different properties by the chosen model. Accordingly, the analyst should be able to identify known intersample patterns or groupings by comparing to his/her *a priori* knowledge of the samples from the system under observation and furthermore to identify the physical/chemical character of the underlying principal components selected by the multivariate model. Thus, this screening step is an intrinsic part of a successful application, since the screening step serves to test for meaningful systematic variation before more elaborate examinations are conducted later in the sequence.

3. Exploratory multivariate models

In the preceding text historical references have been given for the PCA model and its exploratory application in sciences. In the sequel the focus widens from PCA to chemometric models that are relevant for the research conducted in relation to this thesis. Giving a complete description of multivariate data analysis, or even just chemometrics, is an impossible task, since chemometrics is a technology in constant pragmatic development. As such, the re-introduction of the models in the following does not aspire for completeness or adequateness beyond the use in this work. However, exhaustive textbooks on chemometrics are available [Kowalski (1984), Martens & Næs (1989), Nøtvedt et al. (1996), Massart et al. (1997)].

A significant part of the methods listed in the following require a conscious and premeditated attitude towards the preprocessing of variables, e.g. mean-centering [Seasholtz & Kowalski (1992), Pell et al. (1992), Faber (1998)], scaling [Torgerson (1958), Simeon & Pavkovic (1992), Gulliksson (1994)], linearization [Box & Cox (1964), Geladi et al. (1985), Klicka & Kubacek (1997)], warping [Kassidas et al. (1998a)] or scatter-correction [Isaksson & Næs (1988), Næs et al. (1990), Isaksson & Kowalski (1993), Helland et al. (1995)]. A new preprocessing method has been devised [P1] for removing systematic, but irrelevant, phenomena.

3.1 Principal component analysis (PCA)

Let the data matrix \mathbf{X} (I, J) denote a table of I samples, each evaluated at J variables. The R ($R \leq \min(I, J)$) component PCA model [Aitchison (1983), Wold et al. (1987), Wu et al. (1997), Vaira et al. (1999)] is defined in (1) where the parameters in matrices \mathbf{A} (I, R) and \mathbf{B} (J, R) are referred to as scores and loadings, and residuals are contained in \mathbf{E} (I, J). In PCA, component matrix \mathbf{A} is columnwise orthogonal and \mathbf{B} is columnwise orthonormal, whereas in multivariate curve resolution the component matrices are either left unconstrained or are assigned other types of constraints.

$$\mathbf{X} = \mathbf{AB}^T + \mathbf{E}$$

$$(1) \quad x_{ij} = \sum_{r=1}^R a_{ir} b_{jr} + e_{ij}$$

The number of components, R , expresses the complexity of the observed variations in data and may to some extent be regarded as the number of independent phenomena that cause the observed variations. The principal components are ordered according to their

I. Exploratory multivariate data analysis

significance, i.e. the amount by which the residual sum of squares of \mathbf{X} is successively reduced as more components are modelled. Thus, the first principal components are the ones that capture the boldest patterns; however, more and more refined information may be captured by later principal components. Given any dimensionality R , the PCA model fits \mathbf{X} as a minimization of the squared errors, i.e. in a least squares sense. Several approaches towards determining the correct dimensionality have been proposed [Horn (1965), Cattell (1966), Malinowski (1977), Malinowski (1991), Faber & Kowalski (1997)]. These references also propose methods for validating the model dimensionality as well as the models themselves, but more suggestions may be found elsewhere [Scarponi et al. (1990), Næs & Ellekjær (1993), Krzanowski & Kline (1995), Biscay et al. (1997)].

As stated above, PCA has a wide application area. It is perhaps the most versatile exploratory tool and it can be used from the first screening to the last classification. A full-fledged application of PCA and other exploratory multivariate models to facilitate understanding of the highly complex variations within a sugar process is given in thesis paper P7.

PCA forms the basis of many classification methods [Gordon (1981)], in particular soft independent modelling of class analogies (SIMCA) [Wold (1976), Albano et al. (1978), Frank & Lanteri (1989), Mertens et al. (1994), Dunn & Wold (1995)]. In many practical chemical measuring setups the resulting data have missing observations for reasons that may, or may not, be controlled. For PCA, methods for handling missing data have been proposed in various disciplines which further stresses the real-data application of PCA [Afifi & Elashoff (1966), Gleason & Staelin (1975), Frane (1976), Little & Rubin (1987), Grung & Manne (1998)].

3.2 Principal component regression (PCR)

If K response values are known for the I samples defined in the previous chapter, an additional matrix \mathbf{Y} (I,K) is defined, such that the i th row of \mathbf{X} corresponds to the same row in \mathbf{Y} . The two matrices are respectively referred to as the independent and the dependent observations, although in the context of causal relationships it may actually be the reverse. In PCA, these dependent observations are not used at all in the modelling part of the data analysis. Turning to regression, the well-known statistical multiple linear regression (MLR) model attempts to find regression coefficients $\boldsymbol{\beta}$ (J,K) that establish a connection between \mathbf{X} and \mathbf{Y} , as defined by (2).

$$(2) \quad \mathbf{X}\boldsymbol{\beta} = \mathbf{Y}$$

I. Exploratory multivariate data analysis

As noted very early by Gauss, there is no solution to this model when there are more variables than objects, i.e. ($J > I$). Furthermore, there is no solution if the \mathbf{X} matrix is singular, rendering a unique estimation of $\boldsymbol{\beta}$ impossible. In most spectroscopic applications, the variables are correlated such that \mathbf{X} does not have full rank, but merely consists of a few pure spectral phenomena. Finding a sufficient full-rank subspace of \mathbf{X} , as is done with PCA, will provide regressors that are independent due to orthogonality. Using the scores from a PCA as a basis of MLR results in the principal components regression (PCR) [Jolliffe (1982), Mason & Gunst (1985), Glenn et al. (1989), Vaira et al. (1999)] which has well-conditioned numerical properties allowing for a good estimation of the $\boldsymbol{\beta}$ parameters since the columns of \mathbf{X} ($J < I$) are independent, and the rank is full.

The purpose of regression can be multi-faceted. An exploratory application of PCR is that of relating functional factors with *a priori* knowledge to allow for an interpretation of functional or class relationships. Using the PCR for calibration is perhaps the most common application seeking to estimate the parameters of a model that will predict new samples with the lowest possible future random error and bias. To achieve this goal it is important to use the correct dimensionality of the PCA model which can be found by various validation schemes, as will be touched upon later.

3.3 Partial least squares regression (PLSR)

Since the factors from the PCA are found by successively reducing the residual sums of squares of \mathbf{X} with no consideration to \mathbf{Y} , there is no predictive optimality connected to the factors that will subsequently be used for regression onto \mathbf{Y} . A method called partial least squares regression (PLSR) [Jöreskog & Wold (1982), Wold et al. (1984)] has evolved that aims to improve the efficiency of the scores as correlated estimators of \mathbf{Y} . The PLSR model is an algorithmic prescription aiming to improve the predictive efficiency of the regression model by finding score vectors for \mathbf{X} that are more likely to correlate to the columns of \mathbf{Y} . No direct closed form mathematical description can be made for PLSR [de Jong & Phatak (1997)], but the algorithm is given below. In Algorithm 1, the involved variables are \mathbf{y} ($I,1$), \mathbf{w} ($J,1$), \mathbf{t} ($I,1$), \mathbf{p} ($J,1$) and \mathbf{q} ($1,1$)

I. Exploratory multivariate data analysis

Algorithm 1: The PLSR algorithm for modelling a univariate response \mathbf{y} .

1. For each component 1, 2, ..., R
2. $\mathbf{w} = \mathbf{X}^T \mathbf{y} / \|\mathbf{X}^T \mathbf{y}\|$
3. $\mathbf{t} = \mathbf{X} \mathbf{w}$
4. $\mathbf{p} = \mathbf{X}^T \mathbf{t} / \mathbf{t}^T \mathbf{t}$
5. $\mathbf{q} = \mathbf{y}^T \mathbf{t} / \mathbf{t}^T \mathbf{t}$
6. $\mathbf{X} = \mathbf{X} - \mathbf{t} \mathbf{p}^T$
7. $\mathbf{y} = \mathbf{y} - \mathbf{t} \mathbf{q}$
8. Save the current intermediate factors and goto 1

For the sake of commenting on the PLSR algorithm and preparing for the subsequent discussion of Direct Orthogonalization some remarks are necessary. From Algorithm 1, it is seen that in some cases the weight vector \mathbf{w} , which is derived from \mathbf{X} and \mathbf{Y} , *may* be under control of a strong eigenstructure in \mathbf{X} , so that the obtained score \mathbf{t} (step 3) is only expressing variability in \mathbf{X} and not in \mathbf{Y} , thereby reducing the predictive performance of that particular component. The listed PLSR algorithm depicts a method that aims at providing scores that are relevant for the explanation of both \mathbf{X} and \mathbf{Y} by means of optimizing the covariance between the scores of the two structures. The PLSR algorithm is in all aspects dependent on data and the treatment and a characterization of this method is rather limited due to this fact, but from a pragmatic point of view, as undertaken by chemometrics, the PLSR generally performs well. For the instances where the derived scores, \mathbf{t} , are guided solely by \mathbf{X} , new preprocessing methods have been proposed that will be discussed briefly.

3.4 Direct orthogonalization (DO)

In order to eliminate the problem of having many PCR or PLS components that are explaining significant, but irrelevant, phenomena in \mathbf{X} , a novel method called direct orthogonalization (DO) [P1] has been proposed. Rather than applying the PCR or PLS on the data directly, a preprocessing step is suggested that ensures that principal components that have no impact on the predictive performance with respect to \mathbf{Y} are removed. Conceptually, the DO procedure can be regarded as splitting the \mathbf{X} array into two additive parts: A first part that is systematic in terms of \mathbf{X} , but irrelevant in terms of \mathbf{Y} , and a second part that is used for the core calibration problem, as depicted by (3).

$$(3) \quad \mathbf{X} = \mathbf{X}^i + \mathbf{X}^c$$

On page 53 in the publication P1, an algorithm is devised for the estimation of the irrelevant part, \mathbf{X}^i , and the relevant part that is used for calibration, \mathbf{X}^c . The principle is as follows: A PCA model is established to model the \mathbf{X}^i part upon orthogonalizing \mathbf{X}

I. Exploratory multivariate data analysis

columnwise with each column of \mathbf{Y} . This provides an improved basis for calibration since the large but irrelevant eigenstructures of \mathbf{X} are removed. By separating the observations into individual models, it is possible to interpret the systematic background variations that are independent of \mathbf{Y} , e.g. baseline drift, light-scatter in instruments, and so on.

A similar approach for dealing with significant background phenomena called orthogonal scatter correction (OSC) has been proposed by Wold et al. (1998). Whereas OSC orthogonalizes the principal components from the initial bilinear model, the DO does not assume bilinearity until after the initial orthogonalization. Both models require that the dependent responses are of high quality for the filtration to be successful, since reference values with high levels of noise may introduce error in the subsequent calibration.

3.5 PARAFAC-CANDECOMP (PC)

Parallel factors (PARAFAC) by Harshman (1970) and canonical decomposition (CANDECOMP) by Carroll & Chang (1970) designate a multilinear model that was initially proposed in psychometrics, generally referred to as the PARAFAC-CANDECOMP (PC) model. See Kiers (2000) for a proposal of a general multi-way notation. Recent papers on applications in chemometrics hint that the data provided by spectrophotometers as often encountered in chemical applications exploit the full potential of the PARAFAC-CANDECOMP model as a curve resolution model, e.g. [P7, P8, P9, Bro (1999)]. Tutorials on the use of PARAFAC can be found in Geladi (1989), Bro (1998a), Bro (1998b).

Given a three-way data array $\underline{\mathbf{X}}(I,J,K)$, the R -dimensional PARAFAC-CANDECOMP model defined by (4) is a multilinear PCA analog in the sense that PARAFAC-CANDECOMP parameters are latent factors describing the variations in the observed three-way array, as defined by (4).

$$(4) \quad x_{ijk} = \sum_{r=1}^R a_{ir} b_{jr} c_{kr} + e_{ijk}$$

The PARAFAC-CANDECOMP model provides unique factor estimates and, except for shift of signs and indeterminate scaling, the factors $\mathbf{A}(I,R)$, $\mathbf{B}(J,R)$ and $\mathbf{C}(K,R)$ cannot be changed or rotated without changing the error of the model. The uniqueness of the PARAFAC-CANDECOMP factors makes the model outstanding in curve resolution applications, since the bilinear models suffer from the same rotational indeterminacy as the PCA model. In the multilinear case, the PARAFAC-CANDECOMP model explicitly estimates the underlying curves with no need for subsequent rotation, provided that the number of PARAFAC-CANDECOMP components does not exceed the rank. The maximum

I. Exploratory multivariate data analysis

number of PARAFAC-CANDECOMP components for any given array coincides with the multilinear rank per definition, e.g. Kruskal (1989). To underline the difference between bilinear and multilinear modelling, the maximum rank of a (2, 2, 2) array is three and the maximum rank of a (3,3,3) array is 5 [Kruskal (1977), Kruskal (1989)].

The use of multi-way models implies more structure (multilinearity) in the data which requires the analyst to validate this assumption, e.g. by comparison towards the bilinear model. However, if the multilinear model-error is insignificant such that the multi-way model can be deployed, the number of parameters involved in the model can be dramatically reduced compared to estimating simple bilinear models of the matricized data.

3.6 TUCKER

In 1963, Ledyard Tucker proposed a sophisticated multilinear model [Tucker (1963), Tucker (1966)] which is referred to as the Tucker3 model. The reader is directed to dedicated publications [Kroonenberg (1983), Henrion (1994)] for detailed presentations of the class of Tucker models. The Tucker3 model is defined in (5).

$$(5) \quad x_{ijk} = \sum_{p=1}^P \sum_{q=1}^Q \sum_{r=1}^R a_{ip} b_{jq} c_{kr} g_{pqr} + e_{ijk}$$

The Tucker model allows for individual numbers of parameters in each of the three modes, thus, the complexity of the model is described by a three-tuple (P, Q, R) rather than a simple scalar dimensionality. The factors in the columns of matrices, \mathbf{A} (I, P), \mathbf{B} (J, Q) and \mathbf{C} (K, R) are interacting through the elements of the three-way core array $\underline{\mathbf{G}}$ (P, Q, R) to allow for interaction between factors. In case the factors are independent, i.e. columnwise orthogonal matrices \mathbf{A} , \mathbf{B} and \mathbf{C} , the squared elements of the core array express the relative importance of each individual factor combination out of the PQR possible. Thus, in order to find the most significant combinations of latent phenomena eligible for interpretation, the analyst has to locate the largest absolute entries of the core array.

In contrast to the PARAFAC-CANDECOMP model, the Tucker models have an inherent rotational freedom that can be exploited to simplify the representation. Reformulating the summation expression in (5) to matrix form yields (6), where the three-way array $\underline{\mathbf{X}}$ has been matricized into a two-way matrix form by right-appending the K frontal slices of the (I, J, K) cube to form matrix $\mathbf{X}^{(1)}$ (I, JK). Likewise, the core array $\underline{\mathbf{G}}$ (P, Q, R) is matricized into $\mathbf{G}^{(1)}$ (P, QR).

$$(6) \quad \mathbf{X}^{(1)} = \mathbf{A} \mathbf{G}^{(1)} (\mathbf{C}^T \otimes \mathbf{B}^T) + \mathbf{E}^{(1)}$$

I. Exploratory multivariate data analysis

The expressions in (7) are obtained by multiplication by non-singular rotation matrices \mathbf{L} (P,P), \mathbf{M} (Q,Q) and \mathbf{N} (R,R). Letting \mathbf{I} designate the identity matrix of correct order, \mathbf{L}^+ designate the pseudo-inverse of \mathbf{L} and \otimes designate the right Kronecker product, the rotational invariance of the model estimates can be described by (7).

$$\begin{aligned}
 & \mathbf{A}\mathbf{G}^{(1)}(\mathbf{C}^T \otimes \mathbf{B}^T) \\
 &= \mathbf{A}\mathbf{I}\mathbf{G}^{(1)}\left(\left(\mathbf{C}\mathbf{I}\right)^T \otimes \left(\mathbf{B}\mathbf{I}\right)^T\right) \\
 &= \mathbf{A}\mathbf{L}\mathbf{L}^+\mathbf{G}^{(1)}\left(\left(\mathbf{C}\mathbf{N}\mathbf{N}^+\right)^T \otimes \left(\mathbf{B}\mathbf{M}\mathbf{M}^+\right)^T\right) \\
 (7) \quad &= \mathbf{A}\mathbf{L}\mathbf{L}^+\mathbf{G}^{(1)}\left(\left(\mathbf{C}\mathbf{N}\right)^T \otimes \left(\mathbf{B}\mathbf{M}\right)^T\right)\left(\mathbf{N}^{+T} \otimes \mathbf{M}^{+T}\right) \\
 &= \mathbf{A}\mathbf{L}\left(\mathbf{L}^+\mathbf{G}^{(1)}\left(\mathbf{N}^{+T} \otimes \mathbf{M}^{+T}\right)\right)\left(\left(\mathbf{C}\mathbf{N}\right)^T \otimes \left(\mathbf{B}\mathbf{M}\right)^T\right) \\
 &= \tilde{\mathbf{A}}\tilde{\mathbf{G}}^{(1)}\left(\tilde{\mathbf{C}}^T \otimes \tilde{\mathbf{B}}^T\right)
 \end{aligned}$$

From (7) we derive that instead of the specific component matrices \mathbf{A} , \mathbf{B} and \mathbf{C} , an infinite manifold of component matrices connected by the non-singular rotation matrices \mathbf{L} , \mathbf{M} and \mathbf{N} exists with exactly the same model predictions. Thus, by controlling the rotation matrices the analyst is able to obtain the same fit to data, but can optimize criteria formulated in terms of the core array or component matrices to provide the simplest model for interpretation. In particular, a simple core array is desirable with few but very large elements and as many near-zero entries as possible, as this provides a simple model for subsequent interpretation. For this purpose a novel simplicity measure has been proposed and applied [P2, P9] and an algorithm for optimizing this measure, as well as other continuous and differentiable measures, by orthogonal rotation matrices has been proposed [P3].

3.7 A note on multi-way factor rotations

In the dissertation papers [P2, P3] concerning rotation of Tucker models, only orthogonal rotation matrices have been considered. However, orthogonality is an unwanted constraint, and by using non-singular oblique transformation matrices the simplicity measures may be improved further. As a supplement to the papers on the subject, a practical illustration of the effect of using oblique transformations is given. Several authors have proposed algorithms for rotation by non-orthogonal rotation matrices [Kiers (1994), Kiers (1997)].

We consider 5 fluorescence landscapes of three amino acids (tyrosine, phenyl-alanine and tryptophane) in a buffered aqueous solution at pH 7.0. Samples 1-3 are the pure amino acids and samples 4-5 are mixtures thereof. As the chemical multi-way rank is three, a number of

I. Exploratory multivariate data analysis

three profiles are resolved by means of the PARAFAC-CANDECOMP model, yielding a sum of squared residuals at $1.445143 \cdot 10^6$ out of a total sum of squares at $2.303227 \cdot 10^9$, explaining 99.93% of the variation. As explained above, the PARAFAC-CANDECOMP model implies super-diagonality in the corresponding Tucker3 core array.

On the same data, the more complex (3,3,3) Tucker3 model, with orthogonal component matrices provides a sum of squared residuals at $1.378327 \cdot 10^6$ explaining 99.94% of the variation. The super diagonal holds 64.47% of the sum of squares in the initial Tucker3 core array. Since the PARAFAC-CANDECOMP parameters providing the optimal diagonality are known, we can now examine to what extent the super-diagonality of the core can be optimized by means of orthogonal rotation matrices as opposed to oblique rotation matrices. Using the algorithm published as [P3] the following *orthonormal* rotation matrices provide a super-diagonality at 73.87%:

$$\mathbf{L}^o = \begin{bmatrix} -0.19 & -0.98 & -0.06 \\ -0.66 & 0.18 & -0.73 \\ -0.72 & 0.10 & 0.69 \end{bmatrix}, \mathbf{M}^o = \begin{bmatrix} 0.22 & -0.97 & 0.06 \\ 0.84 & 0.22 & 0.50 \\ 0.50 & 0.06 & -0.86 \end{bmatrix}, \mathbf{N}^o = \begin{bmatrix} -0.22 & -0.97 & 0.07 \\ 0.97 & -0.22 & 0.09 \\ -0.07 & 0.09 & 0.99 \end{bmatrix}$$

In order to estimate the optimal oblique rotation matrices we apply a simple Procrustes rotation according to the following: We seek the oblique unconstrained rotation matrix, \mathbf{L}^u , that in a least squares sense maps the corresponding Tucker3 component matrix, \mathbf{S} , into the PARAFAC-CANDECOMP component matrix \mathbf{T} by the formula $\mathbf{T} = \mathbf{S}\mathbf{L}^u$, which is found as $\mathbf{L}^u = \mathbf{S}^+ \mathbf{T}$. The following unconstrained oblique matrices are found, providing a super diagonality of 99.86% :

$$\mathbf{L}^u = 10^5 \begin{bmatrix} 0.30 & 0.15 & 0.11 \\ -0.15 & 0.13 & 0.12 \\ 0.03 & -0.14 & 0.14 \end{bmatrix}, \mathbf{M}^u = \begin{bmatrix} 0.84 & 0.70 & 0.49 \\ 0.54 & -0.58 & -0.75 \\ -0.07 & 0.41 & -0.44 \end{bmatrix}, \mathbf{N}^u = \begin{bmatrix} 0.99 & 0.96 & 0.71 \\ 0.12 & 0.23 & -0.70 \\ -0.10 & 0.18 & 0.00 \end{bmatrix}$$

To conclude the discussion of the use of orthogonal vs. oblique rotation matrices, we find that this real data example clearly illustrates that significant gains in simplicity can be expected by using the lesser constrained oblique methods. In the actual situation, a gain of approx. 30% of diagonality was reached by using oblique rotation matrices. In exploratory situations there is a risk that the analyst will be unable to verify the presence of PC-structure by a simplifying rotation of the Tucker3 model and this form of validation should be avoided unless oblique methods are used. Future work on how to derive optimal oblique rotation matrices is required to improve the exploratory and validatory applicability of the Tucker3 model and optimization of simplicity measures.

3.8 Validation

Validation is a fundamental property of exploratory data analysis, allowing the analyst to maintain focus on the real problem and to ensure that correct hypotheses are induced. A general and elaborate discussion on validation of exploratory models is given by Harshman (1984).

For the sake of a meaningful discussion on the issue of validity of results, it is required that the sampling (see e.g. Gy (1998)) has been carried out carefully so that the data set mirrors the realm of the problem, i.e. that the samples comprising the data collected for exploration with reasonable certainty can be said to be representative of the manifold of the types of samples upon which the model is supposed to work. Assuming that this important requirement is met, two sources of potential problems need discussion. To avoid incorrect inductions from the collected data, it is of utmost importance to have thorough validation in place to i) detect incorrect model estimates (e.g., numerical problems, outliers, incorrect dimensionality, invalid model type, and so on), and ii) prevent invalid inductions from the estimated model parameters, leading to erroneous conclusions.

Incorrect factor estimates may be due to numerical errors, invalid handling of data, inappropriate model complexity or model error in the sense that data do not comply to the assumptions, e.g. linearity, additivity, etc. Model errors can be detected by looking for abnormalities in the estimated factors and systematic variations in the residuals, whereas other types of errors can be detected by validation schemes like cross-validation, test-set validation or more complicated forms thereof. As mentioned earlier, cross-validation and test-set validation schemes are firmly integrated into chemometrics, e.g. [Efron & Gong (1983), Osten (1988), Gemperline & Salt (1989), Feinberg & Bugner (1989), Martens & Dardenne (1998), Rivals & Personnaz (1999), Esbensen & Huang (2000)]. The issue of proposing one validation method over another is outside the scope of this thesis, but there appears to be no single general optimal solution to this question. Depending on the context, e.g. calibration or classification, the objectives of the validation schemes are the same, namely to provide the analyst with information such as indications of outliers, model dimensionality, future prediction error, and bias. Thus, it is suggested to apply several methods to ensure that a consensus between the different methods can be obtained. In case this is not possible, the analyst will know that an exceptional behaviour has occurred and that special caution should be exercised.

The idea of cross-validation may be explained in the following way: The data set is randomly, or ordered, divided into a number segments of one or more samples so that no

I. Exploratory multivariate data analysis

overlap occurs between any segments. By excluding a segment and treating it as a new (unknown) set of samples, the future error of a model with a particular model dimensionality can be estimated. In turn, *included* calibration segments are used to estimate the model parameters, and the *excluded* test segments are kept out to assess the error measures. Thus, models of several dimensionalities are fitted to the included data segments and the excluded segments are predicted and the future error is estimated. All samples are left out once in each model calculation. The overall model dimensionality that provides the optimal model as evaluated on the left-out calibration data is the one that with highest probability performs optimally on future samples as simulated by the successively excluded segments. Several validation schemes have been proposed with different attention to various modelling aspects [Scarponi et al. (1990), Næs & Ellekjær (1993), Krzanowski & Kline (1995), Biscay et al. (1997)]. A recent approach by Martens & Martens (1999) is based on jackknife resampling techniques and provides uncertainty estimates on the principal components and the regression coefficients. It is likely that more such exhaustive resampling techniques will emerge, heavily facilitated by the increase in computational capacity.

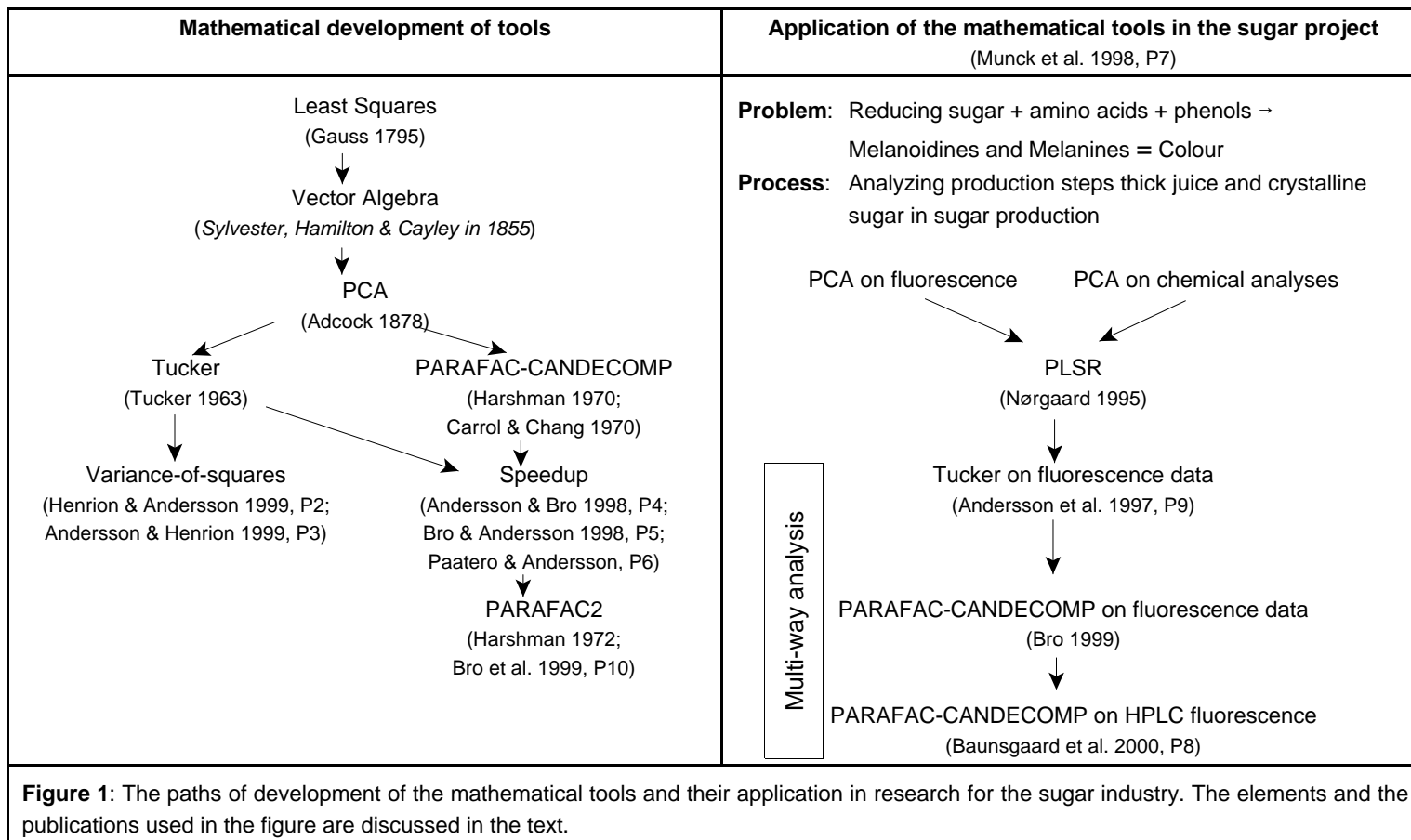
To ensure a *valid interpretation* of the observations and the model, the focus turns to the context of the problem and external knowledge may be critically required. Preferably, the analyst has proper knowledge about the system under observation but it is advisable to interview experts in the field and interrogate external sources of information, as demonstrated in the paper P7 of this thesis. In exploratory procedures of data evaluation in, for instance, industry it may be difficult by virtue of their exploratory nature to provide supplemental information. However, in many cases there are laboratory reports and process information that describe deviations from normal conditions which can be used to explain and to justify outlying or extreme samples. This type of external validation obtained by communicating with laboratory and process engineers is important in keeping the exploratory analysis in line with the problem in order to avoid an undesired shift of focus or immersion into unnecessary or irrelevant details.

4. Applications of the exploratory multivariate tools

The development of multivariate chemometrics tools within the framework of this thesis has been driven by the need for rational analysis of the complex data provided by the chemical applications to obtain optimal and unbiased information. In the following it will be described how the new models and algorithms compare to the existing tools, and differences and improvements on established methods are discussed. For elaborations and details the reader is referred to the publications P1-P6 on mathematical tools, and papers P7-P10 on applications in the last section of this thesis. Here, the intention is to provide an overview of the successive steps towards controlling and understanding the problem of formation of colour in sugar production which is the main application area. The following text is supported by Figure 1 that serves as the storyboard in which the development of algorithms can be compared to the developments in the applications.

Turning to the applications of the exploratory technologies in a broader context, publication P7 has been dedicated to illustrating a complex holistic approach and an in-depth discussion of exploratory multivariate data analysis in a specific context. For many years the formation of colour during the production of sugar has been an important issue to the sugar producers, and the increasing demands regarding the purity of sugar require tools for monitoring and controlling the formation of colour during the process. Sugar, chemically termed *sucrose*, is one of the purest food products with a typical purity above 99.99%, but still, colour and purity are key parameters in an increasingly competitive and sensitive market. By accident, in the Danish sugar factories around 1940 it was experienced that an early indicative analytical assessment of the purity of crystalline sugar could be performed by the use of a UV-lamp and a filter: The more blue light emitted by the sugar crystals, the lower the purity. On this basis a collaboration with Danisco Sugar Development was initiated in 1993 with the aim of detecting and subsequently reducing the formation of colour in sugar by means of sensitive fluorescence measurements evaluated by exploratory multivariate data analysis.

In the complex chemical reaction leading to formation of coloured substances, primarily the Maillard reactions play a key role. According to the non-enzymatic Maillard reaction schemes, interaction between small amounts of reducing sugars and amino acids in the process streams forms the macromolecular melanoidines, whereas other reaction paths with phenols lead to melanines, both having a polymer/macromolecular structure. These two component classes are coloured.



I. Exploratory multivariate data analysis

As depicted in Figure 2, the sugar process is very complex due to a large number of composite unit operations. The sugar beets entering the process are washed, sliced and boiled to extract the sugar into the water. After several filtrations and addition of lime to raise pH and lower the amount of reducing sugars, the *thin juice* is boiled under vacuum to form *thick juice*. During this process the temperature rises to levels at which caramelization (and thus undesired colouring) may begin to take place. After addition of a reductive polymerization inhibitor (SO_2) and reboiling, the stream is mixed with one or more re-fluxed streams to form the *standard liquor*. Standard liquor is spiked with icing sugar to initiate the crystallization. After crystallization has begun, the juice is centrifuged to isolate the sugar crystals from the syrup. The sugar crystals from this process is typically more than 99.99% pure.

With a minimum of *a priori* assumptions a screening analysis was conducted by Nørgaard (1995), see also P7. The very first 34 crystalline sugar samples were provided by Danisco Sugar Development and an immediate PCA of the matricized fluorescence landscapes of the samples diluted in phosphate-buffered water revealed that three clusters were present. By interviewing the sugar specialists we were informed that we had received samples from three factories in accordance with the three clusters, as depicted on Figure 1B (page 34, P7). This validation of fluorescence as a relevant source of information motivated the requisition of more data. Thus, for the same samples Danisco Sugar provided 10 chemical reference measurements for each sample. A separate PCA of these chemical reference values again indicated the presence of three clusters constituted by the same samples as the model for the spectral measurements, as is shown in Figure 1D (page 35, P7). By using the graphical tools of multivariate data analysis as in Figure 1E (page 36, P7), we found that the samples differed in all chemical measurements except flocculation (FLOC).

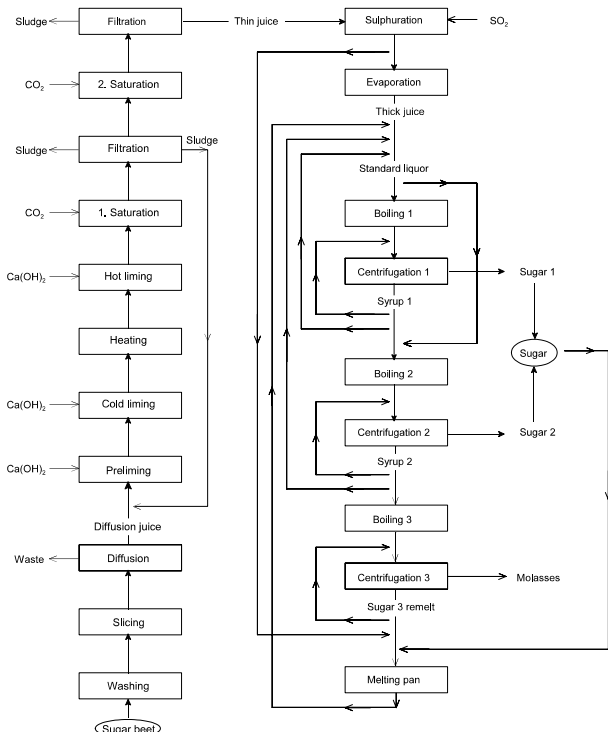


Figure 2: Schematic illustration of the sugar process in a modern sugar factory. See the text for details.

I. Exploratory multivariate data analysis

The observation that the same clusters were observed in the model for fluorescence measurements and the models for the 10 chemical measurements indicated that the chemical reference values could be predicted by the use of fluorescence. A PLSR model gave a correlation coefficient of 0.91 between the fluorescence measurements and the reference value for ash. The ash content was systematically highest for samples with the highest fluorescence intensities, but as ash is not fluorescent, the model is based on predicting the amount of ash *indirectly*. This illustrates how the multivariate models allow for predicting features that are not directly measurable by the spectroscopic technique in question. This indirect modelling is possibly due to fluorescence signals from fluorophores which, through unknown complex chemical mechanisms, depend on the levels of ash. In contrast, the prediction of colour and amino-N is based on a direct chemical relation with the fluorescent amino acids and phenols and provided regression coefficients above 0.94. It should be noted that the fluorescent amino acids and phenols only represent a selection of the total concentration of the different amino acids and phenols involved in the colour formation. The ability of the model to predict total amino-N, is thus possible due to the natural correlation between the various amino acids and other chemical compounds under the control of the biological equilibria in the cells of the beets. As the applied models are not black-box solutions, the parameters can be interpreted exploratively, in e.g. biplots, to allow for a spectroscopist's interpretation of the spectra that covaries with the reference values at hand, thereby helping to induce hypotheses on the structure of the involved chemical species, and thus, the underlying mechanisms.

Several different data sets from different years and factories have been explored by the multivariate models and the results consistently confirm the first experiences regarding fluorescence as a relevant spectroscopic measurement technique with respect to the prediction of the chemical measurements. The sequence of successive inductions from PCA and PLSR models of sample sets from 1993 and up to 1998 led to a deeper understanding of the conditions that cause the formation of colour.

To further scrutinize the information present in fluorescence measurements of thick juice, a collection of 47 fluorescence landscapes taken from 5 factories over a period of 10 weeks were explored by means of a Tucker3 model of a 4-way data array [P9]. The 4-way array consisted of 47 samples, two levels of dilution, 311 emission wavelengths and 20 excitation wavelengths, i.e. a 4-way array with dimensions (47, 2, 311, 20). The Tucker model explained 96.16% of the variation and after rotation to optimal variance-of-squares by the methods described in papers P2 and P3, score vectors number two and three revealed that fluorescence measurements contain high-quality information about the temporal state of the sample in the sugar campaign *and* the factory relationship, as illustrated in Figure 5 (page

I. Exploratory multivariate data analysis

142, P9). However, two-way PCA of fluorescence measurements from different factories showed that sugar samples could be classified only according to factory. To visualize the temporal development throughout the sugar campaign local PCA models had to be made individually for each factory, as depicted in Figure 2AB (page 38, P7). However, with the 4-way PCA model, each of the 47 samples were clustered both according to factory and to sampling week, as seen in Figure 3C (page 41, P7). This surprising finding illustrates the importance of respecting the structure of data in order to obtain the optimal yield of information in the sense that the 4-way data required a 4-way model to allow for an exploration on a detailed level. Thus, the fluorescence landscape is a fingerprint that describes the history and state of each sample. In this sense, each sample is its own bar code with a unique identifier that can be read with a spectrofluorometre and interpreted by using an optimal multi-way model.

At this stage it was evident that the increased amounts of multi-way data from fluorescence measurements required exploration by multi-way methods to reach the finer details of the data. The low efficiency of the existing algorithms for multi-way modelling gave rise to investigations towards faster and more efficient algorithms for estimation of PARAFAC-CANDECOMP and Tucker3 models. Multi-way models like PARAFAC-CANDECOMP and Tucker3 are much more time-consuming with regards to computing time than their two-way counterparts, i.e. PCA and PLSR. Although the two-way and multi-way algorithms are different and thus difficult to compare, a properly validated PCA model may take perhaps 5 minutes, whereas the same task on the same amount of observations in a true three-way constellation may take 5-100 times longer due to the lack of direct methods for estimating the parameters of the PARAFAC-CANDECOMP and Tucker3 models.

Thus, to reduce the analysis time for the iterative multi-way models, an efficient algorithm for estimating Tucker3 parameters was sought [P4]. By combining different schemes for approximating eigenvectors in new ways, significant improvements were found. The algorithms were kept in the alternating least squares (ALS) form, without assuming special structures like having one mode with many variables, as exploited in other works [Kiers et al. (1992)]. The algorithm based on non-linear iterative partial least squares (NIPALS) required the least computations in order to reach convergence. However, issues like numerical stability and robustness were not touched upon in the publication. Since 1996 the algorithms have been implemented in the *N*-way Toolbox for MATLAB [Bro & Andersson (1999)]. A later publication [P6] led to an improved scheme that further reduced the time by rearranging the order of the least squares regression problems. The fast Tucker3 algorithm is exploited further in the following method proposed for fast and efficient estimation of PARAFAC-CANDECOMP models [P5].

I. Exploratory multivariate data analysis

In most cases the PARAFAC-CANDECOMP model is estimated by using unconstrained factors, and the ALS algorithm for estimating the PARAFAC-CANDECOMP factors is prone to poor convergence properties due to correlated factors and near-singular component matrices. However, a method is proposed [P5] for efficient calculation of unconstrained PARAFAC-CANDECOMP factors by fitting the PARAFAC-CANDECOMP model to a subspace of the original data represented by a core array from the Tucker3 model. Thus, it is proposed to estimate a Tucker3 model which natively has better convergence properties due to the use of orthogonality constrained component matrices. Compared to the size of the original data, the significantly reduced core array is then used to estimate PARAFAC-CANDECOMP factors that are later expanded by the subspaces represented by the component matrices of the Tucker3 model. A similar approach termed canonical decomposition with linear constraints [Carroll et al. (1980)] has been proposed; however, it is limited to orthogonality and has not been proposed for compression. In the CANDECOMP paper by Carroll & Chang (1970) it is suggested to use two-way PCA to find the compression bases, whereas in P5, the core array of the Tucker3 model ensures that multi-linearity is preserved. Significant reductions in computational requirements are observed when applied to real data. In paper P5 considerations are also made with respect to the stringency of the convergence criteria and missing values, and the methods are applied to real data. The improved methods published as papers P4, P6 and P5 are prerequisite for being able to make validation possible for the computationally intensive multi-way models and to allow for industrial applications where time is a decisive factor. Whereas we formerly could use 5-7 days to reach an acceptable convergence criterion of the least squares PARAFAC-CANDECOMP algorithm, it became possible to conduct the same computations in roughly 1-2 hours on the same data.

As the more efficient Tucker3 algorithm published in P4 has been used extensively in complex exploratory problems, the interpretational ambiguity of the multi-way PCA due to the rotational indeterminacy required further elaboration. From a pragmatic multivariate point of view, the rotational abilities of the model can be exploited to yield the simplest possible model which in return requires less interpretation. Thus, a measure of model simplicity was postulated [P2] along with an algorithm for optimizing this and other simplicity measures [P3]. The interdependent publications P2 and P3 present respectively a figure of merit for the simplicity of a given core array and a general algorithm that can be used to optimize any differentiable measure as a function of orthonormal rotation matrices.

The simplicity measure for assessing the structure of core arrays is named *variance-of-squares*, and has later been found to be a special case of Orthomax [Kiers (1997)] in the case of orthogonal rotations. The value of the variance-of-squares merit is high in the desirable

I. Exploratory multivariate data analysis

situation where there are few, but very significant, core entries and many near-zero elements. This structure of the core array will allow the analyst to focus on a few significant combinations of factors in the analysis and interpretation.

A novel algorithm has been proposed as a means of optimizing any differentiable measure, e.g., variance-of-squares [P2]. This algorithm is based on the necessary and sufficient criterion that a certain interim product of the rotation matrices must have diagonal structure at stationary points of the objective function. In the published paper P3, the derivatives for three simplicity measures are developed: variance-of-squares, diagonality and slice-wise diagonality.

The assumption of bilinearity of excitation-emission matrices from fluorometric landscape measurements has been proposed for resolution of the underlying excitation and emission profiles of the fluorophores by several authors [Warner et al. (1977), Lee et al. (1991)]. Leurgans & Ross (1992) showed that, in theory, the mathematical relationship between the concentrations of fluorophores and fluorescence intensities, using the ordinary assumptions with respect to linearity and additivity, complies with the PARAFAC-CANDECOMP model. Thus, a first justification for the use of the PARAFAC-CANDECOMP for resolving the profiles of the pure underlying fluorophores was established. By using the PARAFAC-CANDECOMP model, Bro (1999) resolved excitation and emission spectra identical with the PARAFAC-CANDECOMP loadings of 4 fluorophores from fluorescence landscapes of 268 process sugar samples dissolved in water. These 4 components were later used as *indicator substances* and exhibited strong a correlation to important quality and process parameters. The emission spectra are shown in Figure 5BCD (page 44-45 in P7). Due to the mathematical uniqueness of the PARAFAC-CANDECOMP model these pseudocomponents can be interpreted directly in terms of spectroscopy which makes the PARAFAC-CANDECOMP model an efficient tool for exploratory data analysis. Thus, with such profiles in almost-natural-language we could immediately use our long term experience with spectra to understand the factors from the PARAFAC-CANDECOMP model, and we directly identified the emission spectra of two of the components to be the amino acids tyrosine and tryptophane. The other two components resolved from the sugar samples exhibited emission in the visible spectral area above 400 nm, and could thus be classified as possible direct contributors to colour in the final product. The fact that the latter two unknown components have very wide emission peaks makes it probable that the components are macromolecular or polymers, belonging to the classes of melanoidines and melanines was subsequently confirmed. The results from this direct spectroscopic exploration were checked by chemical identification through size-exclusion high performance liquid chromatography (HPLC) [P8].

I. Exploratory multivariate data analysis

To ensure that the exploratory models are formulated in a meaningful context, constraints can be used in the dialogue between the observations and the model. As stressed in Appendix A of P7 and elsewhere in the literature [Bro 1998a, de Juan et al. (1997), Bro & Sidiropoulos (1998)], constraints like non-negativity and unimodality can be used in the least-squares optimization schemes to guarantee that the functional factors can be interpreted and provide knowledge from which new hypotheses can be made. For example, when resolving the underlying profiles of the pure fluorophores from the complex fluorescence landscapes, it is physically impossible to have negative excitation and emission profiles, since this is in conflict with the quantum chemical models of electron systems of the fluorophores. Since the use of constraints can be overly focussed on obtaining results that are in accordance with the *a priori* assumptions, it is important to use an extensive validation scheme that ensures that the obtained factors have a general validity. In most cases, it suffices to compare the factors and the residuals obtained from unconstrained and constrained models of the system under investigation. If deviations occur, they should be explained to provide more information on the appropriateness of the exploratory model in use. As an example, such deviations can be observed in PC models of fluorescence landscapes where non-linear behaviour caused by quenching and light scattering violates the assumption of linearity and additivity of the PC model. Thus, frequently, the unconstrained profiles may suffer from minor wavelength regions that are negative at the wavelengths where the stronger absorbing fluorophores overlap and quench the signals of the other fluorophores.

In order to explore the functional relevance of the 4 resolved pseudocomponents, they were regressed upon reference measurements of colour and ash [Bro (1999), P7] obtaining reasonable predictions. The most important components with respect to colour proved to be the two macromolecular components, whereby we were inspired to introduce the concept of *potential colour* as a measure of the amount of colourless substances (e.g., tyrosine and tryptophane) present that could produce coloured substances through reaction with reducing sugars. Further examinations in the direction of potential colour were deferred for later investigations. Factory records as well as interviews with the process engineers revealed that sugar beets are stored longer during weekends which may produce heat due to microbiological activity which is reflected in higher fluorescence intensities, hence scores, for all 4 resolved components. This is seen as correlated cyclic changes in intensities in Figure 5E (page 46, P7). It is important to note that around sample number 200 an increasing trend of Component 4 is depicted which coincides with the event of frozen sugar beets. Further elaboration on this issue with the production engineers revealed that the variation of the 4 indicator substances diminished through the campaign due to decreasing outdoor

I. Exploratory multivariate data analysis

beet storage temperatures. The concept of using the PC loadings representing *indicator substances* or *functional factors* to explain important process parameters and chemical properties has a high potential as a tool for monitoring and controlling complex processes.

At the time of the collection of sample 200 (November 15th) the beets had been exposed to temperatures far below 0 °C, causing Component 4 to increase in concentration. Thus, a preliminary hypothesis was generated that in future campaigns it should be checked if Component 4 could be used as an indicator for frozen beets. The increasing formation of colour during the remaining time of the sampling was reflected by Component 4 which may thus serve as an indicator substance of both colour and frozen beets. Even more, it was shown in a process analysis [Bro (1999), P7] that it was possible to use the 4 indicator substances to predict, retrospectively, important process parameters (pH and CaO) along with chemical parameters (colour and ash) throughout the process. This experience should be used in implementing the more difficult process control aspect.

To validate and provide additional information about the indicator substances just described, extensive examinations by column chromatography were performed, as published in P8 and P10. Here, the mathematical separation of the fluorophores was compared with high performance liquid chromatography (HPLC) on a size-exclusion column, separating the high molecular coloured polymers from the potential colour, e.g. tyrosine and tryptophane. It is noteworthy that research has been conducted in the field of sugar production since 1869 [Scheibler (1869)], and that the functional importance of fluorescent constituents of the sugar streams has not yet been characterized in any way by means of fluorescence. With the mathematical resolution of the pure spectral profiles checked with HPLC, it is proven that fluorescent *indicator substances* for the chemical parameters provide a feasible solution to the complex problem of understanding the processes leading to formation of colour in the sugar streams.

In order to address the identification and validation issues raised by the preceding resolution of the 4 components from sugar, more chemically based investigations were conducted. Because of the minute traces of these components in the crystalline sugar it is difficult to perform the chromatographic validation of the fluorometric results on such a pure product. In the hope of identifying even more components in the sugar streams, the intermediary unrefined product, *thick juice*, was subjected to high performance liquid chromatography, as described in P8. For the detailed chemical identification one thick juice sample was analysed by HPLC. To reduce the risk of model errors caused by quenching, the thick juice sample was separated into 41 fractions according to a combined effect of molecular size and affinity to the HPLC column material. The fractions, thus containing only

I. Exploratory multivariate data analysis

one or a few chemical components, were measured by spectrofluorometry, yielding a landscape for each single fraction, as illustrated in Figure 5 of P8. With the exploratory use of the PARAFAC-CANDECOMP model, 7 fluorophores could be resolved from the complex fluorescence landscapes of the fractions obtained by HPLC. Among them were tyrosine and tryptophane, which were identified by spiking samples with solutions of the pure amino acids, as shown in Figure 3 of P8. The application of HPLC to avoid quenching and thereby to significantly reduce the model error is novel, and the awareness of the modelling tools at the chemist's level has facilitated the results. The identifications were not only based on the similarity of the resolved profiles for excitation and emission, but also on chromatographic retention time. Due to the elution order, the 7 fluorophores could be assigned approximate molecular sizes and 4 large coloured macromolecules or polymers were found which all displayed absorption in the visible range. Three of the macromolecular constituents exhibit absorptivity in a wide range of the ultraviolet spectrum, depicting various complex molecular structures. This is in accordance with the understanding of the Maillard reaction mechanisms that suggest the formation of polymers by polymerization of the amino acids present. Thus by fluorescence analysis we have been able to select 4 chemical components, or indicator substances, which were found to be representative in modelling a wide range of different aspects of the sugar process.

Besides confirming the presence of tryptophane and tyrosine in thick juice and sugar, two other observations are made from the chromatograms: The profiles of tryptophane are preserved in the fluorescent molecular melanoidine fractions, while the fluorescence signature of tyrosine is absent (Figure 6, P8). This is in accordance with the molecular structure of the two amino acids, since tryptophane is a large, irregular and rigid molecule compared to tyrosine which is less complex thus making it more likely to lose its fluorescence signature when incorporated into polymer structures.

Thus, we have come the full circle. At this stage important chemical knowledge and chemically based hypotheses have been induced by the successive steps of increasingly more extensive multivariate analyses initiated in 1995 [Nørgaard (1995)] as a screening with PCA. The use of increasingly complex models has provided equally more detailed information on the different organisational levels [Munck (2000)] with respect to the multivariate context of the sugar production. These contextual levels may be defined as i) The biology of the sugar beet including the effects of production and storage, ii) The parameters of the sugar production process, and, iii) The characteristics of the raw materials, process streams and sugar as evaluated by (a) spectroscopy and by (b) physical/chemical properties. The utilization of continuous inventory analyses and validations in the stepwise exploratory approach is described in Table 2.

I. Exploratory multivariate data analysis

In chromatography, a fundamental problem has to be addressed when several chromatograms are included in the same multivariate model. The problem occurs if the time axes are different, corresponding to differing elution times for the same chemical components. If this is the situation, the assumption of trilinearity is violated, since there is no common time-factor that can be exploited to find principal components, and attempts to do so will introduce model errors and bias. This problem is general in nature, since existing component models assume that the variables have the same meaning for all samples, which is not the case if an axis is shifted from sample to sample. A unique model that implicitly handles this problem by the use of general cross-product matrices was proposed as PARAFAC2 by Harshman (1972), and recently an algorithm was proposed for fitting it [Kiers et al. (1999)]. In P10 the algorithm is applied for analysis of liquid chromatography data for resolution of spectral profiles with significant success compared to the ordinary PARAFAC-CANDECOMP model parameters. The approach differs from preprocessing techniques like warping [Kassidas et al. (1998b)] in the implicit handling of the time axes by elegantly replacing the problematic axis for each sample by the covariance matrix of time profiles calculated across one of the other modes. In this particular application the covariances are calculated across the spectral mode in order to treat each sample separately. A necessary but rather unrestrictive constraint ensures that the PARAFAC2 factors maintain uniqueness as in the PARAFAC-CANDECOMP model. In the application paper P10, the profiles resolved by PARAFAC2 and ordinary PARAFAC-CANDECOMP were compared in terms of similarity and explained variation. The PARAFAC2 components were significantly closer to the known spectra of the pure chemical components. Applying the PARAFAC-CANDECOMP model to data with non-aligned modes involves a risk of obtaining erroneous and misleading factors in the results. Thus, it is advocated to apply both models and compare residuals and estimated profiles in order to gain a fundamental understanding of the data at hand and to obtain the optimal model.

The common problem of having significant and systematic background signals that quench the part of the analytical signal that correlates to the reference measurements has been described earlier under direct orthogonalization. High background signals due to scattered light or temperature differences are well-known causes of model deviations in spectroscopy. Several methods address these problems by applying pre-transformations of the signals by means of theoretically based models, e.g. multiplicative scatter correction [Martens et al. (1983), Geladi et al. (1985)] or Kubelka-Munck theory [Law et al. (1996)]. However, in many cases the background signals do not conform to the underlying mathematical expression of the assumed physical/chemical relationships and a more adaptive alternative is appreciated. One soft model that aims at describing the significant,

I. Exploratory multivariate data analysis

but uncorrelated, signals is Direct Orthogonalization (DO) [P1]. The method suggests including a preregression step on the part of data that is independent of the reference measurements. For the DO method to be effective it is a prerequisite that the reference measurements have sufficiently low errors in order for the preregression step not to remove information that would otherwise stabilize the regression model. Some suggestions on how to use DO for multi-way calibrations are made at the end of publication P1. Wold et al. (1998) propose a somewhat similar approach termed orthogonal signal correction (OSC), by which a bilinear model of the data is orthogonalized with the reference measurements, and not the data themselves. Both approaches offer some exciting possibilities for exploratory as well as industrial and scientific uses. By inspecting the principal components of what is independent of the reference measurements, the analyst and the process engineer have significantly improved means for identifying outlying observations. In essence, it is possible to define the normal patterns in both the independent and the analytical parts of the data, so that models can be established for the background signal as well as the analytical signal.

5. Conclusion

Working exploratively with complex composite problems requires continuous involvement by specialists from the various implicated application fields, as has just been illustrated by the applications of multivariate models in the sugar production. As an example (page 48, P7) of the efficiency and success of the exploratory multivariate approach we could compare with the strategy of Madsen et al. (1978), using classical chromatography and statistics in analysing the compounds in sugar responsible for the formation of colour. In traditional chemical analysis, one starts by defining the hundreds of chemical substances involved in a process, as was done for the sugar industry by Madsen et al. in order to understand colour formation. If the target hypothesis is to find easily identifiable *indicator substances* by which to model quality and process characteristics, it is suggested that the exploratory method of introducing a multivariate screening method would be more economical than a deductive strategy based only on *a priori* chemical knowledge, chromatography and classical statistics as studied in the research laboratory. In contrast to the deductive approach, the *a priori* knowledge in the exploratory method is used after the primary data evaluation and then stepwise throughout a hypothesis generating process to ensure that the obtained preliminary conclusions are on track with the problem at hand and that the results are validated at each step. If the *a priori* knowledge is used *only* to formulate the model without the prior support by an exploratory screening analysis, the resulting interpretations and conclusions may be unnecessarily biased to fulfill the assumptions of the analyst. It should be noted that *a priori* knowledge is of crucial importance also to the exploratory strategy for validation and in order to navigate in the selection process.

For chemometrics to be successful, access to a full chain of interdisciplinary resources including, e.g. analytical chemical analysis, spectroscopy, mathematics, computer programming and IT is required by the researcher. Every link in this chain has to have basic understanding of multivariate data analysis in order to contribute optimally to the solution to the problem, since issues like repeatability, variation, validation and data quality are of fundamental importance to the exploratory multivariate data analysis. For researchers educated to have fundamental working knowledge of the multivariate tools it will be possible to take responsibility not only for the collection of data, but also for the analysis of their own data. Otherwise, the researcher will just hand over data for statistical analysis by methods which have not been developed for that particular problem and its context and the interactive part of exploratory analysis is lost.

The birth of exploratory multivariate data analysis occurred by breaking multivariate models away from multivariate statistics to be placed in the core of the specific application

I. Exploratory multivariate data analysis

fields as exemplified by Figure 1. There is a danger that multivariate analysis within chemistry, i.e. chemometrics, will be drawn back into unapplied and theoretical statistics by becoming overly sophisticated, general and not enough specific to be directly applicable for researchers from non-mathematical and non-statistical disciplines. It is vital to uphold a balance between pragmatics and theory in the multivariate society. Bearing in mind that chemometrics owes its success to its applicability in chemistry and that these multivariate technologies are often applied more by researchers with experimental and modelling skills rather than by statisticians with skills in the application, it must be avoided that research in multivariate data analysis goes solely in the direction of static generalized theory.

The modern spectral sensors offer data of high quality with regards to relevance and signal-to-noise ratio, and the exploratory multivariate technologies offer a host of possibilities to natural sciences, technology and human sciences. The speed and robustness of the spectral sensors and the novel mathematical tools as provided by chemometrics already now allow for implementation in high-sensitivity laboratory systems and high-speed process systems. The most important benefit from multivariate analysis is the much overlooked possibility of making qualified estimations on the quality of a sample by applying methods for outlier-identification utilizing the multivariate advantage as a fingerprint. By comparing with the samples used during the calibration, it is possible to assess the discrepancy between what is known by the model to be normal and any new sample. Due to the advantages of using spectroscopy over traditional wet chemistry, we will see spectrophotometers in more places in the coming years. It is already possible to mount spectral sensors on urinals and toilets to give indications of latent diabetes, blood alcohol level and even some forms of cancer.

The Internet has made distribution of data and information possible throughout the world. The next paradigm shift may allow users to formulate their own information analyses of data directly from the original data bases to suit individual purposes rather than having only a preformulated and prefabricated result offered with no possibilities for examining other scenarios than those dictated by the data provider. Much like the way it is possible to search for literature in the library data bases via the web, it will in the future hopefully be possible to browse and screen larger amounts of data like the archives of the National Bureau of Statistics to explore own hypotheses by making tailor-made models. This data mining task could in many instances be that of exploring patterns in large tables comprised of data from relevant observations. Here the multivariate technologies will provide the ideal tools. Using soft, adaptive and graphical tools, users will be able to verify the calculations and interpretations of those responsible for the data, and furthermore, users will have the possibility to formulate and explore their own individual problems and interpret these, e.g.

I. Exploratory multivariate data analysis

relations between production parameters in the agricultural and food industry with instances of food poisoning or comparisons of the economical figures of merit between different countries. Mediation by the intuitive and graphical tools for multivariate data analysis will make it possible for every Internet surfer to investigate his or her own idea, if the proper sources of data are available.

Publication of original data sets and the conditions used during data collection together with research papers should be compulsory in science to provide the most transparent background for the drawn conclusions. This should also be mandatory for the more official data gathered at national level, e.g. by the European Commission, and would thereby contribute significantly to an improvement in the economical and political democracy. Turning that kind and amount of information into useful knowledge would require the involvement of exploratory multivariate data analysis for easy and efficient data mining interpreted in dialogue with different experienced members of society.

I. Exploratory multivariate data analysis

6. Reference list

1. Adcock, R. J. (1878), A problem in least squares, *The Analyst*, **5**, 53-54
2. Afifi, A. A. and Elashoff, R. M. (1966), Missing observations in multivariate statistics I. Review of the literature, *Journal of American Statistical Association*, **81**, 595-604
3. Aitchison, J. (1983), Principal component analysis of compositional data, *Biometrika*, **70**, 57-65
4. Albano, C., Dunn, W. J., Edlund, E., Johansson, E., Nordén, B., Sjøstrøm, M., and Wold, S. (1978), Four levels of pattern recognition, *Analytica Chimica Acta*, **103**, 429-443
5. Anderson, T. W. (1984), An introduction to multivariate statistical analysis, 2nd ed., John Wiley & Sons, New York
6. Anderson, T. W. and Rubin, H. (1956), Statistical inference in factor analysis, 5 ed., pp. 111-150, University of California Press, Los Angeles, USA
7. Bauer, F. L. (1957), Das Verfahren der Treppeniterationen und verwandte Verfahren zur Lösung algebraischer Eigenwertprobleme, *Zeitschrift für angewandte Mathematik und Physik*, **8**, 214-235
8. Beebe, K. R. and Kowalski, B. R. (1987), An introduction to multivariate calibration and analysis, *Analytical Chemistry*, **59**, 1007A-1017A
9. Biscay, R., DiazFrances, E., and Rodriguez, L. M. (1997), Cross-validation of covariance structures using the Frobenius matrix distance as a discrepancy function, *Journal of Statistical Computation and Simulation*, **58** (3), 195-215
10. Björck, Å. (1990), *Least squares methods* in Handbook of numerical analysis Vol. I. Finite difference methods (part 1), Ed.: Ciarlet, P. G. and Lions, J. L., pp. 467-635
11. Box, G. and Cox, D. (1964), An Analysis of Transformations, *Journal Of The Royal Statistical Society Series B Statistical Methodology*, **26**, 211-243
12. Bro, R. (1998a), Multi-way Analysis in the Food Industry. Models, Algorithms, and Applications, University of Amsterdam, The Netherlands, Ph.D. thesis

I. Exploratory multivariate data analysis

13. Bro, R. (1998b), PARAFAC: Tutorial and applications, *Chemometrics and Intelligent Laboratory Systems*, **38**, 149-171
14. Bro, R. (1999), Exploratory study of sugar production using fluorescence spectroscopy and multi-way analysis, *Chemometrics and Intelligent Laboratory Systems*, **46**, 133-147
15. Bro, R. and Andersson, C. A. (1999), The N-way toolbox for MATLAB. Version 1.04, Dept. Food Technology, Dairy and Food Science, Royal Veterinary and Agricultural University, <http://www.models.kvl.dk/source>
16. Bro, R. and Sidiropoulos, N. D. (1998), Least squares algorithms under unimodality and non-negativity constraints, *Journal of Chemometrics*, **12**, 223-247
17. Bryant, E. H. and Atchley, W. R. (1975), *Multivariate Statistical Methods: Within-group Covariation*, Halsted Press, Stroudsburg
18. Carrol, J. D. and Chang, J. (1970), Analysis of individual differences in multidimensional scaling via an n-way generalization of "Eckardt-Young" decomposition, *Psychometrika*, **35**, 283-319
19. Carroll, J. D., Pruzansky, S., and Kruskal, J. B. (1980), CANDELINC: A general approach to multidimensional analysis of many-way arrays with linear constraints on parameters, *Psychometrika*, **45**, 3-24
20. Cattell, R. B. (1966), The scree test for the number of factors, *Multivariate Behavioral Research*, **1**, 245-276
21. Cauchy, A. L. (1829), *OEvres IX*, **2**, 172-175
22. de Jong, S. and Phatak, A. (1997), *Partial least squares regression* in Recent Advances in Total Least Squares Techniques and Errors-in Variables Modeling, Ed.: van Huffel, S. , SIAM, Philadelphia, pp. 25-36
23. de Juan, A., van der Heyden, Y., Tauler, R., and Massart, D.-L. (1997), Assessment of new constraints applied to the alternating least squares method, *Analytica Chimica Acta*, **346** (3), 307-318
24. Dunn, W. J. and Wold, S. (1995), *SIMCA Pattern recognition and classification* in Chemometric methods in molecular design, Ed.: Waterbeemd, H. v., Weinheim, New York, pp. 179-193

I. Exploratory multivariate data analysis

25. Efron, B. and Gong, G. (1983), A leisurely look at the Bootstrap, the Jackknife, and the cross-validation, *American Statistician*, **37**, 36-48
26. Esbensen, K. H. and Geladi, P. (1990), The start and early history of chemometrics: selected interviews. Part II, *Journal of Chemometrics*, **4**, 389-399
27. Esbensen, K. H. and Huang, J. (2000), Principles of proper validation, *Journal of Chemometrics* (In prep.)
28. Faber, N. M. (1998), Mean centering and computation of scalar net analyte signal in multivariate calibration, *Journal of Chemometrics*, **12** (6), 405-409
29. Faber, N. M. and Kowalski, B. R. (1997), Critical evaluation of two F-tests for selecting the number of factors in abstract factor analysis, *Analytica Chimica Acta*, **337**, 57-71
30. Feinberg, M. and Bugner, E. (1989), Chemometrics and food chemistry: data validation, *Analytica Chimica Acta*, **223** (1), 223-235
31. Fischer, R. A. (1922), On the mathematical foundation of theoretical statistics, *Philosophical Transactions of the Royal Society of London*, **222** (A), 309-368
32. Fischer, R. A. (1925), *Statistical methods for research workers*, Oliver & Boyd, Edinburgh, Ireland
33. Fischer, R. A. (1935), *The design of experiments*, Oliver & Boyd, Edinburgh, Ireland
34. Fisher, R. and MacKenzie, W. A. (1923), Studies in Crop Variation. II. The manurial response of different potato varieties, *Journal of Agricultural Science*, **13**, 311-320
35. Frane, J. W. (1976), Some simple procedures for handling missing data in multivariate analysis, *Psychometrika*, **41**, 409-415
36. Frank, I. E. and Lanteri, S. (1989), Classification models: discriminant analysis, SIMCA, CART, *Chemometrics and Intelligent Laboratory Systems*, **5**, 247-256
37. Gauss, C. F. (1821), *Theoria combinationis observationum erroribus minimis obnoxiae, pars prior*, Vol. IV, Königlichen Gesellschaft der Wissenschaften zu Göttingen, Göttingen, Germany, pp. 1-26

I. Exploratory multivariate data analysis

38. Gauss, C. F. (1823), *Theoria combinationis observationum erroribus minimis obnoxiae, pars prior*, Vol. IV, Königlichen Gesellschaft der Wissenschaften zu Göttingen, Göttingen, Germany, pp. 27-53
39. Gauss, C. F. (1963), *Theory of the motion of the heavenly bodies moving around the Sun in conic sections*, Dover, New York, USA (Translated by C. H. Davis. First published in 1809.)
40. Geladi, P. (1989), Analysis of multi-way (multi-mode) data, *Chemometrics and Intelligent Laboratory Systems*, **7**, 11-30
41. Geladi, P. and Esbensen, K. H. (1990), The start and early history of chemometrics: selected interviews. Part I, *Journal of Chemometrics*, **4**, 337-354
42. Geladi, P., MacDougall, D., and Martens, H. (1985), Linearization and scatter-correction for near-infrared reflectance spectra of meat, *Applied Spectroscopy*, **39**, 491-500
43. Gemperline, P. J. and Salt, A. (1989), Principal components regression for routine multicomponent UV determinations: a validation protocol, *Journal of Chemometrics*, **3**, 343-357
44. Gleason, T. C. and Staelin, R. (1975), A proposal for handling missing data, *Psychometrika*, **40**, 229-252
45. Glenn, W. G., Dunn, W. J., and Scott, D. R. (1989), Principal components analysis and partial least squares regression, *Tetrahedron Computer Methodology*, **2**, 349-376
46. Goldstine, H. H. (1977), *A history of numerical analysis from the 16th through the 19th century*, Springer-Verlag, New York, USA
47. Gordon, A. D. (1981), *Classification. Methods for the exploratory analysis of multivariate data*, Chapman and Hall, New York, USA, ISBN 0-412-22850-5
48. Grung, B. and Manne, R. (1998), Missing values in principal component analysis, *Chemometrics and Intelligent Laboratory Systems*, **42**, 125-139
49. Gulliksson, M. (1994), Iterative refinement for constrained and weighted linear least squares, *BIT*, **34**, 239-253
50. Gy, P. (1998), *Sampling for analytical purposes*, John Wiley & Sons Ltd., Baffins Lane, Chichester, West Sussex, England, ISBN 0471979562 (In French in 1996)

I. Exploratory multivariate data analysis

51. Harshman, R. (1970), Foundations of the PARAFAC procedure: Models and conditions for an 'explanatory' multi-modal factor analysis, *UCLA working papers in phonetics*, **16**, 1-84
52. Harshman, R. A. (1972), PARAFAC2: Mathematical and technical notes, *UCLA working papers in phonetics*, **22**, 30-47
53. Harshman, R. A. (1984), *How can I know it's real? A catalog of diagnostics for use with three-mode factor analysis and multidimensional scaling* in Research Methods for Multimode Data Analysis, Ed.: Law, H. G., Snyder, C. W., Jr., Hattie, J., and McDonald, R. P., Praeger, New York, pp. 566-591
54. Helland, I. S., Næs, T., and Isaksson, T. (1995), Related versions of the multiplicative scatter correction method for preprocessing spectroscopic data, *Chemometrics and Intelligent Laboratory Systems*, **29**, 233-241
55. Henrion, R. (1994), N-way principal component analysis theory, algorithms and applications, *Chemometrics and Intelligent Laboratory Systems*, **25**, 1-23
56. Hoaglin, D. C., Mosteller, F., and Tukey, J. W. (1983), Understanding robust and exploratory data analysis, John Wiley & Sons, Inc., New York, USA, ISBN 0-471-09777-2
57. Horn, J. L. (1965), A rationale and test for the number of factors in factor analysis, *Psychometrika*, **30** (2), 179-185
58. Horst, P. (1965), Factor Analysis of Data Matrices, Rhinehart and Winston, New York
59. Horst, P. (1992), Sixty years with latent variables and still more to come, *Chemometrics and Intelligent Laboratory Systems*, **14**, 5-21
60. Hotelling, H. (1933b), Analysis of a complex of statistical variables into principal components, *Journal of Educational Psychology*, **24**, 498-520
61. Hotelling, H. (1933a), Analysis of a complex of statistical variables into principal components, *Journal of Educational Psychology*, **24**, 417-441
62. Isaksson, T. and Kowalski, B. R. (1993), Piece-wise multiplicative scatter correction applied to near-infrared diffuse transmittance data from meat products, *Applied Spectroscopy*, **47**, 702-709

I. Exploratory multivariate data analysis

63. Isaksson, T. and Næs, T. (1988), The effect of multiplicative scatter correction (MSC) and linearity improvement in NIR spectroscopy, *Applied Spectroscopy*, **42**, 1273-1284
64. Jackson, J. E. (1980), Principal components and factor analysis: part I - principal components, *Journal of Quality Technology*, **12**, 201-213
65. Joliffe, I. T. (1982), A note on the use of principal components in regression, *Applied Statistics*, 300-303
66. Joliffe, J. (1986), Principal Component analysis, Springer Verlag , Berlin
67. Jöreskog, K. G. and Wold, H. (1982), Systems under indirect observation, North-Holland, Amsterdam
68. Kassidas, A., MacGregor, J. F., and Taylor, P. A. (1998a), Synchronization of batch trajectories using dynamic time warping, *AIChE Journal*, **44** (4), 864-875
69. Kassidas, A., MacGregor, J. F., and Taylor, P. A. (1998b), Synchronization of batch trajectories using dynamic time warping, *AIChE Journal*, **44** (4), 864-875
70. Kiers, H. A. L. (1994), SIMPLIMAX: oblique rotation to an optimal target with simple structure, *Psychometrika*, **59** (567), 579
71. Kiers, H. A. L. (1997), Three-mode orthomax rotation, *Psychometrika*, **62**, 579-598
72. Kiers, H. A. L. (2000), Towards a Standardized Notation and Terminology in Multiway Analysis, *Journal of Chemometrics*, **14** (3), 105-122
73. Kiers, H. A. L., Kroonenberg, P. M., and ten Berge, J. M. F. (1992), An efficient algorithm for TUCKALS3 on data with large numbers of observation units, *Psychometrika*, **57**, 415-422
74. Kiers, H. A. L., ten Berge, J. M. F., and Bro, R. (1999), PARAFAC2 - Part I. A direct fitting algorithm for the PARAFAC2 model, *Journal of Chemometrics*, **13**, 275-294
75. Klicka, R. and Kubacek, L. (1997), Statistical properties of linearization of the Arrhenius equation via the logarithmic transformation, *Chemometrics and Intelligent Laboratory Systems*, **39**, 69-75
76. Kowalski, B. R. (1984), Chemometrics: Mathematics and statistics in chemistry, D. Reidel, Dordrecht, The Netherlands

I. Exploratory multivariate data analysis

77. Kroonenberg, P. M. (1983), Three-mode Principal Component Analysis. Theory and Applications, DSWO Press, Leiden
78. Kruskal, J. B. (1977), Three-way arrays: rank and uniqueness of trilinear decompositions with applications to arithmetic complexity and statistics, *Linear Algebra and its Applications*, **18**, 95-138
79. Kruskal, J. B. (1978), *Factor analysis and principal components* in International Encyclopedia of Statistics, 1st ed., The Free Press, New York, pp. 307-337
80. Kruskal, J. B. (1989), *Rank, decomposition, and uniqueness for 3-way and N-way arrays* in Multiway Data Analysis, Ed.: Coppi, R. and Bolasco, S., Elsevier, Amsterdam, pp. 8-18
81. Krzanowski, W. J. (1988), Principles of multivariate analysis. A users perspective, Oxford Science Publications, Oxford , ISBN 0198522118
82. Krzanowski, W. J. and Kline, P. (1995), Cross-validation for choosing the number of important components in principal component analysis, *Multivariate Behavioral Research*, **30** (2), 149-165
83. Law, D. P., Blakeney, A. B., and Tkachuk, R. (1996), The Kubelka-Munk equation: some practical considerations, *Journal of Near Infrared Spectroscopy*, **4**, 189-193
84. Lee, C., Kim, K., and Ross, R. T. (1991), Trilinear analysis for the resolution of overlapping fluorescence spectra, *Korean Biochem.J.*, **24**, 374-379
85. Legendre, A. M. (1805), Nouvelles méthodes pour la détermination des orbites de comètes, Courcier, Paris, France
86. Leurgans, S. E. and Ross, R. T. (1992), Multilinear models: Applications in spectroscopy, *Statistical Science*, **7**, 289-319
87. Little, R. J. A. and Rubin, D. B. (1987), Statistical analysis with missing data, John Wiley & Sons, New York, ISBN 0-471-80254-9
88. Longley, J. W. (1984), Least squares computations using orthogonalization methods, Marcel Dekker, New York
89. Madsen, R. F., Kofod Nielsen, W., Winstrøm-Olsen, B., and Nielsen, T. E. (1978), Formation of colour compounds in production of sugar from sugar beet, *Sugar Technological Reviews*, **6**, 49-115

I. Exploratory multivariate data analysis

90. Malinowski, E. R. (1977), Theory of error in factor analysis, *Analytical Chemistry*, **49**, 606-617
91. Malinowski, E. R. (1991), Factor Analysis in Chemistry, John Wiley and Sons, New York
92. Mardia, K. V., Kent, J. T., and Bibby, J. M. (1992), Multivariate Analysis, Academic Press, Inc., San Diego, CA, USA
93. Markoff, A. A. (1912), Wahrscheinlichkeitsrechnung, 2 ed., H. Liebmann, Leipzig, Germany
94. Martens, H., Jensen, S. A., and Geladi, P. (1983), Multivariate linearity transformations for near-infrared reflectance spectrometry, Nordic Symposium on Applied Statistics, pp. 205-233, Stokkand Forlag Publishers, Stavanger
95. Martens, H. A. and Dardenne, P. (1998), Validation and verification of regression in small data sets, *Chemometrics and Intelligent Laboratory Systems*, **44** (1-2), 99-121
96. Martens, H. and Martens, M. (1999), Modified Jack-knife estimation of parameter uncertainty in bilinear modelling by partial least squares regression (PLSR), *Food Quality and Preferences*
97. Martens, H. and Næs, T. (1989), Multivariate calibration, Wiley, England
98. Mason, R. L. and Gunst, R. F. (1985), Selecting principal components in regression, *Statistics & Probability Letters*, **3**, 299-301
99. Massart, D. L., Vandeginste, B. G. M., Buydens, L. M. C., de Jong, S., Lewi, P. J., and Smeyers-Verbeke, J. (1997), Handbook of Chemometrics and Qualimetrics, Vol. 20, Elsevier Science, Amsterdam, The Netherlands, ISBN 0-4444-82854-0
100. Mertens, B., Thompson, M., and Fearn, T. (1994), Principal component outlier detection and SIMCA: A synthesis, *Analyst*, **119**, 2777-2784
101. Meuzelaar, H. L. C. and Isenhour, T. L. (1987), Computer-enhanced analytical spectroscopy, Plenum Press, New York
102. Minton, A. P. and Rose, R. L. (1997), The effects of environmental concern on environmentally friendly consumer behavior: an exploratory study, *Journal Of Business Research*, **40** (1), 37-48

I. Exploratory multivariate data analysis

103. Munck, L. (1991), *Man as a selector -- A Darwinian boomerang striking through natural selection* in Environmental Concerns, Ed.: Hansen, J. A., Elsevier Scientific, pp. 211-227
104. Munck, L. (2000), *Detecting diversity - a new holistic exploratory approach* (Chapter 12) in Diversity in Barley, Ed.: von Bothmer, R., Elsevier Scientific (in press)
105. Neyman, J. and Pearson, E. S. (1928), On the use and interpretation of certain test criteria for purposes of statistical inference, *Biometrika*, **20**, 175-240
106. Nortvedt, R., Brakstad, F., Kvalheim, O. M., and Lundstedt, T. (1996), Anvendelse av kjemometri innen forskning og industri, John Grieg AS, Bergen, Norway, ISBN 82-91294-01-1 (In Swedish/Norwegian/Danish)
107. Næs, T. and Ellekjær, M. R. (1993), Cross-validation and leverage-correction revisited, *NIR news*, **4**, 8-9
108. Næs, T., Isaksson, T., and Kowalski, B. R. (1990), Locally weighted regression and scatter correction for near-infrared reflectance data, *Analytical Chemistry*, **62**, 664-673
109. Nørgaard, L. (1995), Classification and prediction of quality and process parameters of beet sugar and thick juice by fluorescence spectroscopy and chemometrics, *Zuckerindustrie*, **120** (11), 970-981
110. Oldroyd, D. (1986), *The Arch of Knowledge. An Introductory Study of the History of the Philosophy and Methodology of Science*, Methuen, New York
111. Osten, D. W. (1988), Selection of optimal regression models via cross-validation, *Journal of Chemometrics*, **2**, 39-48
112. Pearson, K. (1901), On lines and planes of closest fit to points in space, *Philosophical Magazine*, **2** (6), 559-572
113. Pell, R. J., Seasholtz, M. B., and Kowalski, B. R. (1992), The relationship of closure, mean centering and matrix rank interpretation, *Journal of Chemometrics*, **6**, 57-62
114. Rivals, I. and Personnaz, L. (1999), On cross validation for model selection, *Neural Computation*, **11**, 863-870

I. Exploratory multivariate data analysis

115. Rutishauser, H. F. L. (1969), Computational aspects of Bauers simultaneous iteration method, *Numerical Mathematics*, **13**, 4-13
116. Scarponi, G., Moret, I., Capodaglio, G., and Romanazzi, M. (1990), Cross-validation, influential observations and selection of variables in chemometric studies of wines by principal component analysis, *Journal of Chemometrics*, **4**, 217-240
117. Scheibler, C. (1869), Über das Betaïn, eine in dem Saft der Zuckerrüben (*Beta Vulgaris*) vorkommende Pflanzenbase., *Zeitschrift des Vereines für die Rübenzucker-Industrie im Zollverein*, **19**, 549-558
118. Seasholtz, M. B. and Kowalski, B. R. (1992), The effect of mean centering on prediction in multivariate calibration, *Journal of Chemometrics*, **6**, 103-111
119. Simeon, V. and Pavkovic, D. (1992), Weighted analysis of principal components: two approximations to statistical weights, *Journal of Chemometrics*, **6**, 257-266
120. Thurstone, L. L. (1931), Multiple factor analysis, *Psychological Review*, **38**, 406-427
121. Torgerson, W. S. (1958), *Theory and methods of scaling*, Wiley and Sons, New York
122. Tucker, L. R. (1963), *Problems in measuring change*, Ed.: Harris, C. W., University of Wisconsin Press, Madison
123. Tucker, L. R. (1966), Some mathematical notes on three-mode factor analysis, *Psychometrika*, **31**, 279-311
124. Tukey, J. W. (1977), *Exploratory data analysis*, Addison-Wesley Publishing Company, USA, ISBN 0-201-07616-0
125. Vaira, S., Mantovani, V. E., Robles, J. C., Sanchis, J. C., and Goicoechea, H. C. (1999), Use of chemometrics: Principal Component Analysis (PCA) and principal component regression (PCR) for the authentication of orange juice, *Analytical Letters*, **32** (15), 3131-3141
126. Warner, I. M., Christian, G. D., Davidson, E. R., and Callis, J. B. (1977), Analysis of multicomponent fluorescence data, *Analytical Chemistry*, **49**, 564-573
127. Weihs, C. (1993), Multivariate exploratory data analysis and graphics: a tutorial, *Journal of Chemometrics*, **7**, 305-340

I. Exploratory multivariate data analysis

128. Wold, S. (1976), Pattern recognition by means of disjoint principal components models, *Pattern Recognition*, **8**, 127-139
129. Wold, S. (1994), Chemometrics; what do we mean with it, and what do we want from it?, *Chemometrics: Philosophy, History and Directions*, Ed.: Aloke Phatak, http://www.emsl.pnl.gov:2080/docs/incinc/chem_phd/SWdoc.html
130. Wold, S. (1996), *Kemometri - historik och filosofi* (Chapter 1.1) in *Anvendelse af kjemometri innen forskning og industri*, Ed.: Nortvedt, R., Brakstad, F., Kvalheim, O. M., and Lundstedt, T., John Grieg AS, Bergen, Norway, pp. 33-51, ISBN 82-91294-01-1 (In Swedish)
131. Wold, S. (2000), Personal communication via ICS-L (International Chemometrics Society E-mail Listserver) on March 1st, 2000
132. Wold, S., Antti, H., Lindgren, F., and Öhman, J. (1998), Orthogonal signal correction of near-infrared spectra, *Chemometrics and Intelligent Laboratory Systems*, **44** (1-2), 175-185
133. Wold, S., Esbensen, K. H., and Geladi, P. (1987), Principal component analysis, *Chemometrics and Intelligent Laboratory Systems*, **2**, 37-52
134. Wold, S., Ruhe, A., Wold, H., and Dunn, W. J. (1984), The collinearity problem in linear regression. The partial least squares (PLS) approach to generalized inverses, *SIAM Journal of Scientific and Statistical Computing*, **5**, 735-743
135. Wu, W., Massart, D.-L., and de Jong, S. (1997), The kernel PCA algorithm for wide data. Part I: Theory and Algorithms, *Chemometrics and Intelligent Laboratory Systems*, **36**, 165-172

I. Exploratory multivariate data analysis

7. Author's full publication list

The following chronological list contains peer-reviewed research papers published by the author 1996-2000.

- 1 Dorrit Baunsgaard, Claus A. Andersson, Allan Arndal and Lars Munck (2000), *Multi-way chemometrics for mathematical separation of fluorescent colorants and colour precursors from spectrofluorimetry of beet sugar and beet sugar thick juice as validated by HPLC analysis*, Food Chemistry, **70**, 113-121
- 2 Claus A. Andersson and Søren B. Engelsen (1999), *The mean hydration of carbohydrates as studied by normalized 2-D radial pair distributions*, Journal of Molecular Graphics and Modeling **17**, 101-105 & 131-133
- 3 Claus A. Andersson and René Henrion (1999), *A new general algorithmic approach for obtaining simple-structure N-way core arrays with an application to a 3-way data array from fluorometry*, Computational Statistics & Data Analysis **31**, 255-278
- 4 Pierluigi Barbieri, Claus A. Andersson, D. L. Massart, S. Predonzani, G. Adami and E. Reisenhofer (1999), *Modeling bio-geochemical interactions in the surface waters of the Gulf of Trieste by three-way principal component analysis (PCA)*, Analytica Chimica Acta **398**, 227-235
- 5 Pentti Paatero and Claus A. Andersson (1999), *Further improvements of the speed of the TUCKER3 three-way algorithm*, Chemometrics and Intelligent Laboratory Systems **47**, 17-20
- 6 Rasmus Bro, Claus A. Andersson and Henk A. L. Kiers (1999), *PARAFAC2 - Part II. Modeling chromatographic data with retention time shifts*, Journal of Chemometrics **13**, 295-309
- 7 Claus A. Andersson (1999), *Direct orthogonalization*, Chemometrics and Intelligent Laboratory Systems **47**, 51-63
- 8 René Henrion and Claus A. Andersson (1999), *A new criterion for simple-structure transformations of core arrays in N-way principal components analysis*, Chemometrics and Intelligent Laboratory Systems **47**, 189-204
- 9 Lars Munck, Lars Nørgaard, Søren B. Engelsen, Rasmus Bro and Claus A. Andersson (1998), *Chemometrics in food science - a demonstration of the feasibility of a highly exploratory, inductive evaluation strategy of fundamental scientific significance*, Chemometrics and Intelligent Laboratory Systems **44**, 31-60

I. Exploratory multivariate data analysis

- 10 Claus A. Andersson and Rasmus Bro (1998), *Improving the speed of multi-way algorithms. Part I: Tucker3*, Chemometrics and Intelligent Laboratory Systems **42**, 93-103
- 11 Rasmus Bro and Claus A. Andersson (1998), *Improving the speed of multi-way algorithms. Part II: Compression*, Chemometrics and Intelligent Laboratory Systems **42**, 105-113
- 12 Claus A. Andersson, Lars Munck, René Henrion and Gunther Henrion, (1997), *Analysis of N-dimensional data arrays from fluorescence spectroscopy on an intermediary sugar product*, Fresenius Journal of Analytical Chemistry **359**, 138-142

P1
Direct orthogonalization

Claus A. Andersson



Direct orthogonalization

Claus A. Andersson *

Food Technology, Royal Veterinary and Agricultural University, Rolighedsvvej 30, DK-1958 Frederiksberg, Denmark

Received 3 July 1998; revised 9 September 1998; accepted 9 September 1998

Abstract

A multivariate method called *direct orthogonalization* is proposed for removing factors that describe irrelevant phenomena from data in calibration situations. The method is suggested for improving regression of data sets with systematic, but irrelevant, variations. The method is applied to FT-IR spectral data measured on dry pectin powder samples with the purpose of predicting the degree of esterification. Direct orthogonalization is compared with piecewise multiplicative scatter correction (PMSC) schemes and second order derivatives on the predictive performance of principal component regression (PCR) and partial least squares regression (PLSR) models. When applying direct orthogonalization to the FT-IR spectral data under investigation, the number of significant PLSR and PCR components was lowered significantly while facilitating a qualitative discussion of the scatter phenomena, and at the same time providing a means to identify outliers prior to prediction. In terms of root mean square error of prediction (RMSEP), the proposed method resulted in error measures at the same level as the applied PMSC schemes. Application of second order derivatives to the same data resulted in significantly poorer models. © 1999 Elsevier Science B.V. All rights reserved.

Keywords: Noise filtration; Baseline correction; Background correction; Scatter correction; Orthogonalization; Pretreatment of data; Outlier detection; Low-pass filtration

Contents

1. Introduction	52
2. Theory.	52
2.1. Nomenclature and notation	52
2.2. Direct orthogonalization	53
2.3. Multiplicative scatter correction.	54
2.4. Second order derivatives	55
3. Application to diffuse FT-IR on pectin powder samples.	56
3.1. Experimental.	56
3.2. Results and discussion.	56

* E-mail: ca@kvl.dk

4. Further applications and improvements	61
5. Conclusions	62
Acknowledgements	62
References	62

1. Introduction

In some analytical situations, the measured data are severely affected by shifts and trends in baseline. Typical areas are spectroscopic applications (e.g., IR, NIR and Raman) and process applications where the data have low-frequency fluctuations that, in a systematic way, influence the level of signals. Modelling becomes difficult because the relevant variation is quenched by irrelevant, but systematic, variation. In IR spectroscopy, it is a well-known problem that light scattering causes a high background level that may vary greatly between and within samples. The level of light scatter is rarely useful in modelling because it is related to physical rather than chemical phenomena in the samples. The problem of variations in the background signal is often mended by multiplicative scatter correction (MSC), see Refs. [1–3], or second order derivatives (SOD), see Refs. [4]. However, MSC and SOD may eliminate analytical information that is required to establish efficient models. When reference values exist, they can be used to guide the filtration/pre-treatment, so that only a minimum of relevant information is removed.

From the viewpoint of modelling, it is desirable to use as few regression components as possible, since this reflects that the phenomena described by the model are the major sources of variation. This allows for easy interpretation and for identifying and explaining outlying observations. This is the motivation for suggesting direct orthogonalization as a means of reducing the number of regression components and facilitating early detection of outliers. With direct orthogonalization, a separate model is established prior to regression that extracts the systematic, but irrelevant, factors. The principle of direct orthogonalization is (i) to establish an orthogonal model with scores

independent of the variable(s) being modelled, and (ii) a conventional regression model on the data *not* extracted by the orthogonal model.

To evaluate direct orthogonalization, we will compare the predictive abilities of partial least squares regression (PLSR) and principal components regression (PCR) models where the data have been pretreated according to direct orthogonalization (DO), second order derivatives (SOD), multiplicative scatter correction (MSC) and piecewise MSC (PMSC). High-pass filtering methods like Fourier transformation and Savitsky–Golay smoothing are not in the scope of the current work which is focused on the domain of methods that are based on eigenanalysis or least squares regression. For more complete reviews on methods for standardization and pretreatment, the reader is referred to Refs. [5,6].

2. Theory

The method of DO is presented and an algorithm is devised. Subsequently, the applied approaches to MSC and PMSC are described.

2.1. Nomenclature and notation

In the following, scalars will be represented by italic typefaces, e.g., *a*, whereas column vectors are written as bold lower case, e.g., **y**, and matrices are written with bold uppercase letters, e.g., **X**. Transposition of matrix **X** will be expressed as **X**^T. Let \bar{x} denote the columnwise mean of **X** and let \tilde{X} be the columnwise mean-centred **X**. In line with the common terminology, **X** denotes a matrix of independent

measurements and \mathbf{y} denotes dependent observations between which we intend to establish a relation.

A common measure of model efficiency, namely the root mean square error of prediction (RMSEP), will be used as a basis for comparing the different methods. For a number of I samples, this is defined as $\text{RMSEP} = \sqrt{\frac{1}{I} \sum_{i=1}^I (y_i^{\text{true}} - y_i^{\text{pred}})^2}$. Errors determined from cross validation segments are referred to as RMSECV.

2.2. Direct orthogonalization

The DO ensures that information in \mathbf{X} which correlates perfectly to \mathbf{y} is not removed during pretreatment, since this will reduce the predictive abilities of the model. The number of parameters (components) of PCR and PLSR models increases when there are sources of irrelevant variation. If the data under investigation has irrelevant and significant structures, the first number of PLSR components will account for these variations, rather than focusing on modelling \mathbf{y} . By removing irrelevant variation from \mathbf{X} , the dimensionality of the final regression model is lowered and, in some cases, it may be determined with less ambiguity. Direct orthogonalization is a simple pretreatment of data in such a way that the structures of \mathbf{X} that are insignificant to modelling of \mathbf{y} may be removed prior to regression. The proposed DO method may be regarded either as a two-step procedure consisting of a pretreatment step and a regression step, or as a closed form method for regression.

A closed form algorithm for making a regression based on DO is proposed. The algorithm is based on eigendecomposition as done by, for example, nonlinear iterative partial least squares (NIPALS) or singular value decomposition (SVD). During preliminary studies bi-linear resolution was explored—constraining the resolved scores to be orthogonal to the given \mathbf{y} , while minimizing an ordinary least squares error term. However, due to the low time consumption, stable convergence and the good numerical stability, an eigenproblem-based algorithm is preferred to a constrained resolution technique. The high potential of constrained multi-linear resolution with regard to pretreatment of data is discussed later.

In Algorithm (1), it is described how DO may be applied by orthogonalizing the calibration data $\tilde{\mathbf{X}}_c$

$(i_c \times j)$ with the corresponding reference values, $\tilde{\mathbf{y}}_c$ ($i_c \times 1$). In step 1, the data matrices are centred. In step 2, the vector \mathbf{w} ($j \times 1$) represents the columnwise covariation between $\tilde{\mathbf{X}}_c$ and $\tilde{\mathbf{y}}_c$ used for deriving matrix $\tilde{\mathbf{X}}_c$ ($i_c \times j$) such that it is columnwise orthogonal to $\tilde{\mathbf{y}}_c$. In step 3, the columnwise orthogonal matrix $\hat{\mathbf{T}}_c$ ($i_c \times a$) and the columnwise orthonormal matrix $\hat{\mathbf{P}}_c$ ($j \times a$) are found by NIPALS or SVD as an a dimensional subspace of $\tilde{\mathbf{X}}_c$ that describes the systematic part of $\tilde{\mathbf{X}}_c$ being independent of $\tilde{\mathbf{y}}_c$. The loadings in $\hat{\mathbf{P}}_c$ describe the uncorrelated components of the native data $\tilde{\mathbf{X}}_c$. Thus, in step 4, these components are quantified as scores $\tilde{\mathbf{T}}_c$ by regression onto $\tilde{\mathbf{X}}_c$, and are subtracted from $\tilde{\mathbf{X}}_c$ to yield a matrix $\tilde{\mathbf{X}}_c^{\text{DO}}$ ($i_c \times j$) with a rank being a lower than the rank for $\tilde{\mathbf{X}}_c$. In the final step, the corrected data $\tilde{\mathbf{X}}_c^{\text{DO}}$ are used for regression, that typically being PLSR or PCR.

1. \mathbf{X}_c and \mathbf{y}_c are centred to give $\tilde{\mathbf{X}}_c$ and $\tilde{\mathbf{y}}_c$
2. $\tilde{\mathbf{X}}_c$ is orthogonalized w.r. to $\tilde{\mathbf{y}}_c$

$$\mathbf{w} = \tilde{\mathbf{X}}_c^T \tilde{\mathbf{y}}_c (\tilde{\mathbf{y}}_c^T \tilde{\mathbf{y}}_c)^{-1}$$

$$\tilde{\mathbf{X}}_c = \tilde{\mathbf{X}}_c - \tilde{\mathbf{y}}_c \mathbf{w}^T$$
3. PCA of $\tilde{\mathbf{X}}_c$ using a components (1)

$$\hat{\mathbf{T}}_c \hat{\mathbf{P}}_c^T \approx \tilde{\mathbf{X}}_c \text{ s.t. } \hat{\mathbf{T}}_c^T \hat{\mathbf{T}}_c \text{ diagonal and } \hat{\mathbf{P}}_c^T \hat{\mathbf{P}}_c = \mathbf{I}$$
4. The amount of independent phenomena is extracted
$$\tilde{\mathbf{T}}_c = \tilde{\mathbf{X}}_c \hat{\mathbf{P}}_c$$

$$\tilde{\mathbf{X}}_c^{\text{DO}} = \tilde{\mathbf{X}}_c - \tilde{\mathbf{T}}_c \hat{\mathbf{P}}_c^T$$
5. Regression of $\tilde{\mathbf{y}}_c$ onto $\tilde{\mathbf{X}}_c^{\text{DO}}$ using b regression components

The term *direct orthogonalization* stems from the single direct application of the orthogonalization with \mathbf{y} . In the case where the regressors are not univariate but multivariate, i.e., \mathbf{Y} , step 2 must be repeated for every column in $\tilde{\mathbf{Y}}_c$. Thereby, all significant information that is linearly dependent on \mathbf{Y}_c is removed prior to finding the orthogonal components in step 3.

When predicting new samples, the regression parameters, the means of \mathbf{X}_c and \mathbf{y}_c and the components in $\hat{\mathbf{P}}_c$ ($j \times a$) are used. The samples to be predicted, denoted by \mathbf{X}_p ($i_p \times j$), are treated according

to Algorithm (2). Matrix $\hat{\mathbf{T}}_p$ ($i_p \times a$) holds the scores of the samples to be predicted and the corrected data are represented by $\tilde{\mathbf{X}}_p^{\text{DO}}$.

1. \mathbf{X}_p is centred as in Alg. (1), step 1, giving $\tilde{\mathbf{X}}_p$
2. The amount of independent phenomena (2)

is extracted

$$\tilde{\mathbf{T}}_p = \tilde{\mathbf{X}}_p \hat{\mathbf{P}}_c$$

$$\tilde{\mathbf{X}}_p^{\text{DO}} = \tilde{\mathbf{X}}_p - \tilde{\mathbf{T}}_p \hat{\mathbf{P}}_c^T$$

3. Predict using $\tilde{\mathbf{X}}_p^{\text{DO}}$

In steps 3 and 5 of Algorithm (1), it is recognized that the two parameters, a and b , must be chosen. It is suggested to do this by simultaneous validation, that is, for a range of combinations of a and b apply Algorithm (1) using a calibration data set and subsequently apply Algorithm (2) using some test object(s). The combination of a and b that yields the lowest RMSEP will represent the optimum combination. As an alternative to the time-consuming simultaneous validation of a and b , one could apply an individually automated approach, e.g., according to the proposal by Malinovski [7] for finding a and a validation scheme for finding b . However, without simultaneous optimization of both parameters, one is not guaranteed to obtain the optimal parameters.

The scores $\tilde{\mathbf{T}}_p$ belonging to the samples being predicted can be used as a diagnostic tool in detecting abnormal spectra, i.e., spectra with particularly low or high levels of uncorrelated components. This feature may have applications in process control and systems for automated data analysis. The principal components of DO are adaptive in the sense that the scatter is found from the data itself and no a priori knowledge is required.

With DO, it is important to evaluate the quality of the reference values, i.e., \mathbf{y} , since the effect of orthogonalizing \mathbf{X} with bad estimates on \mathbf{y} may derail subsequent modelling. The consequence of orthogonalizing with inaccurate \mathbf{y} values is that the inner PCA, i.e., Algorithm (1) step 3, will remove relevant systematic variation from \mathbf{X} , thereby leaving only weakly correlated information for the final regression step.

Another procedure for filtering data, Orthogonal Signal Correction (OSC), has recently been proposed

[8,9]. The first step of the OSC algorithm is to obtain a bi-linear model of the initial data by an iterative approach such that the scores in the model are orthogonal to \mathbf{y} . Next, a so-called inverse PLSR model is established between the initial data and the orthogonal score. The scores and loadings of this PLS model are then subtracted from the initial data, whereby uncorrelated information is removed and the filtered data is applicable for further modelling. The filtration stages of DO and OSC methods differ algorithmically since for DO it is data itself that is orthogonalized with \mathbf{y} prior to bi-linear modelling whereas OSC makes use of a constrained bi-linear model and the inverse PLSR model to remove uncorrelated information.

2.3. Multiplicative scatter correction

An approach to scatter correction that is often used for pretreatment of NIR and IR spectra is multiplicative scatter correction (MSC), see Refs. [1,2]. The MSC approach is to some extent inspired by theoretical considerations, i.e., Kubelka–Munk theory [10], dealing with optical phenomena that cause light scattering. The principle behind MSC is as follows: From the calibration samples an *ideal* spectrum is derived as the mean spectrum, $\bar{\mathbf{x}}$. Subsequently, for the i th sample ($i = 1, 2, \dots, I$) a set of parameters a_i and b_i is estimated by least squares regression of the sample spectrum \mathbf{x}_i onto $\bar{\mathbf{x}}$:

$$\mathbf{x}_i = a_i + b_i \bar{\mathbf{x}} + \mathbf{e}_i \quad (1)$$

Using these parameters, the MSC spectrum is found by backtransformation of the measured spectrum \mathbf{x}_i according to Eq. (2).

$$\mathbf{x}_i^{\text{MSC}} = \frac{\mathbf{x}_i - a_i}{b_i} \quad (2)$$

It should be noted that MSC does not aim at eliminating the scatter but rather aims at reducing the inter-sample variations of the scatter by applying an additive and multiplicative transformation of the individual spectrum into the common idealized average spectrum. This may be derived from Eq. (1) where an intercept and a slope, denoted by a and b , are found that lines up the idealized spectrum with the measured spectrum under minimization of a least squares error term. Since all samples will be lined up

against the same idealized spectrum, the differences in background levels are minimized upon correction. However, wavelength regions that are suitable for finding a and b must be selected. Since there are wavelengths where the variation is not solely due to scatter effects (e.g., wavelengths correlated to the reference values), it is generally advisable not to include the whole spectra for parameter estimation. Thus, intervention is required to select wavelength regions that carry scatter information solely to obtain an efficient and robust MSC.

The MSC approach may be applied to data for which there are no reference measurements. Furthermore, since only two parameters are estimated for each sample, MSC uses relatively few degrees of freedom. Since MSC does not take into account that unique information may be removed by the correction, MSC cannot guarantee that subsequent modelling will benefit from the transformation. Also, cases exist in which the simple two-parameter MSC does not align the spectra adequately, since the linearity assumption in Eq. (1) does not hold. There may even be cases where artificial variation is introduced into the corrected data due to poorly estimated MSC parameters. For example, if there are significant differences in particle size distributions, one is likely to observe different phenomena in the scattered light. Such different backgrounds may be problematic for the MSC based approaches, since only *one* idealized spectrum applies for standardization. An important and necessary assumption underlying MSC is that the relation between the idealized spectrum and the individual spectra is independent of wavelength, i.e., one set of a_i and b_i parameters suffices for the i th sample in its full wavelength range. If this assumption does not hold, local MSC may be performed on sub-ranges of the spectra where it is more likely that a linear relation between the idealized spectrum and the individual spectra applies. Dividing the spectra into, say K , different wavelength regions, K pairs of coefficients are obtained for each spectrum. Here, two approaches to MSC have been implemented: Simple PMSC (SPMSC) and the more advanced PMSC.

The SPMSC method divides the full spectral range into non-overlapping subranges of equal width. Thus, the one-segment SPMSC corresponds to the ordinary MSC. In the reported studies, we will refer to MSC as a special case of SPMSC.

The PMSC method, as proposed in Ref. [3], uses a fixed-width moving window designating the variables used for finding a and b . For the present applications, only symmetric windows have been used.

It should be noted that for SPMSC the number of segments and for PMSC the width of the moving windows can severely affect the subsequent predictive abilities of the model. Thus, the parameters must be included in the validation step to ensure the optimal model. When increasing the number of segments in SPMSC or when narrowing the window width in PMSC, the corrected spectra may become too similar, ruling out significant differences between the spectra and thereby making subsequent modelling difficult. In order to make the SPMSC plausible, one should consider building in a priori spectroscopic knowledge, leaving significant wavelengths out when estimating a and b coefficients. In the current application of SPMSC, a simple non-supervised approach has been taken, in which all variables of the segments are used for finding the coefficients.

2.4. Second order derivatives

A commonly used approach to spectral correction is second order derivation. Second order derivation removes not only simple additive offsets, but also first order effects like drift in baseline. In Ref. [11], a list of approximations for second order derivatives are given for increasing number of neighbouring points. The simplest approximation, i.e., using only two neighbouring points, of the second order derivative in the i th point of a spectrum with equidistant variables is obtained as described in Eq. (3):

$$\ddot{x}_i \approx x_{i-1} - 2x_i + x_{i+1} \quad (3)$$

If required, the approximation given in Eq. (3) may be improved by application of extrapolation schemes.

Neither multiple neighboring points nor gaps have been used in this investigation. Including more neighboring points than the two in Eq. (3) will smooth the derivatives to some extent. In addition, when using several neighboring points, it is common that a gap is introduced around the i th element. The observations belonging to the gap are simply excluded from the approximation of the derivative, and a modified form of Eq. (3) is used. By including several neighboring points and gaps, the derived transform is

no longer a second order derivative per se, as the transformation approaches Savitsky–Golay convolution [12]. Nevertheless, these two modifications have in some instances been justified as useful approaches, improving the predictive abilities of models, see for example Refs. [5,13].

3. Application to diffuse FT-IR on pectin powder samples

Using PCR and PLSR, the focus of this investigation is on the effects of DO as compared to existing approaches to spectral correction for inter-sample variations. For this study, we will model the degree of esterification (%DE) of dried pectin powders. The reader is referred to Ref. [14] for a specific discussion and interpretation of the spectral information.

3.1. Experimental

With the purpose of predicting the degree of esterification (%DE), 97 pectin powder samples were

measured as dried powder on a Perkin-Elmer System 2000. The 97 samples were randomly divided into three segments with 33 or 34 objects. In turn, one segment was left out and predicted from a model calibrated on objects in the two complementary segments. In one cycle, each object was predicted once. Ten such cycles were performed as to re-sample the three segments randomly in each cycle. The RM-SEC values are mean values of the 10 cycles. For computations, a 200 MHz Pentium Pro running Windows NT and MATLAB 5.1 was used. The values of %DE ranges from 21.40% to 54.10% with a mean value 31.87%. Neither accuracy nor precision of the reference measurements have been examined. However, the absolute error is estimated to be less than 1.5% in the measured range, see Ref. [14].

3.2. Results and discussion

In Fig. 1, the raw FT-IR spectra are depicted. As stated in Ref. [14], the absorbances at 1752, 1686, 1650 and 950 cm^{-1} are expected to correlate to some extent with the degree of esterification. However, as

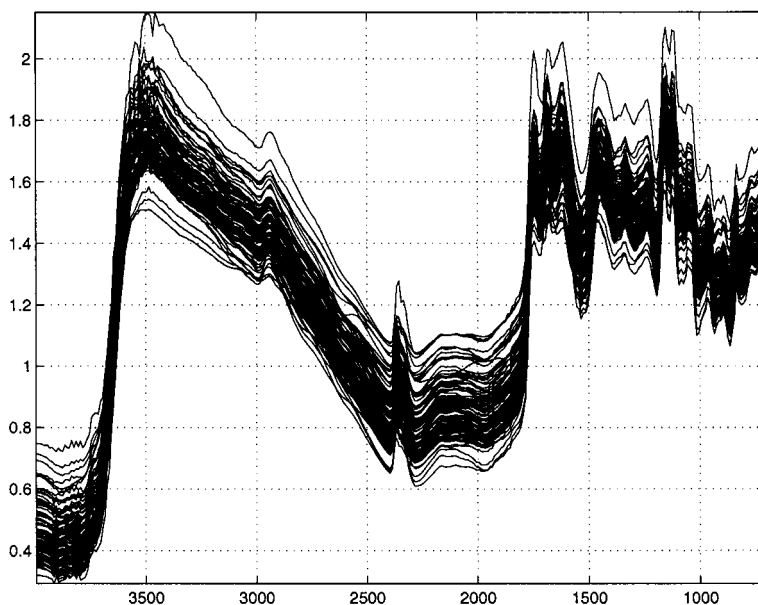


Fig. 1. The raw and untreated FT-IR spectra from the pectin powder samples. The wavelength axis is in cm^{-1} .

II. Algorithms, models and applications

seen in Fig. 1, interpretation of the raw data is difficult due to the large differences in scatter. After extracting three DO components according to Algorithm (1), the spectra are somewhat more equivalent as seen from Fig. 2. In Fig. 2, the variation is not significantly higher for the 4 expected wavelengths which indicates that the information is more dispersed than what the hard molecular theory allows us to assume. In other words, data requires a multivariate approach to attain optimal results. This finding is supported by the DO components in Fig. 3, since there are no wavelength ranges with zero elements. Such zero ranges describe wavelengths where the information is perfectly correlated to the reference value and thus have been completely removed prior to the inner PCA. The DO components are shown in Fig. 3 as normalized vectors. The un-nuanced and constant level of the first DO component (dashed line) indicates that this factor models the offset of the scatter. The second DO component (dash-dot line)

resembles the general curvatures of the measured spectra. Hence, we conclude that this component explains the common scatter signal. The two first factors explain respectively approx. 45% and 23% of the variance of the orthogonalized matrix, whereas the third DO component (solid line) explains 9%. Only minor patterns in the third component can be recognized as stemming from the raw spectra. However, it is important to remember that the interpretability is obscured by the orthogonality of the PCA solutions. In this light, the components cover to some extent a behaviour that can be found to be present in the raw spectra. It is noteworthy that the peak at 1752 cm^{-1} constitutes a major part of the third component.

Turning to second order derivatives, the spectra move from the spectroscopist's domain to an abstract mathematical form where interpretation is rendered difficult, as depicted in Fig. 4. Here, the SOD spectra indicate that approx. 1752 cm^{-1} is a region in which major variations occur. Although SOD may be used

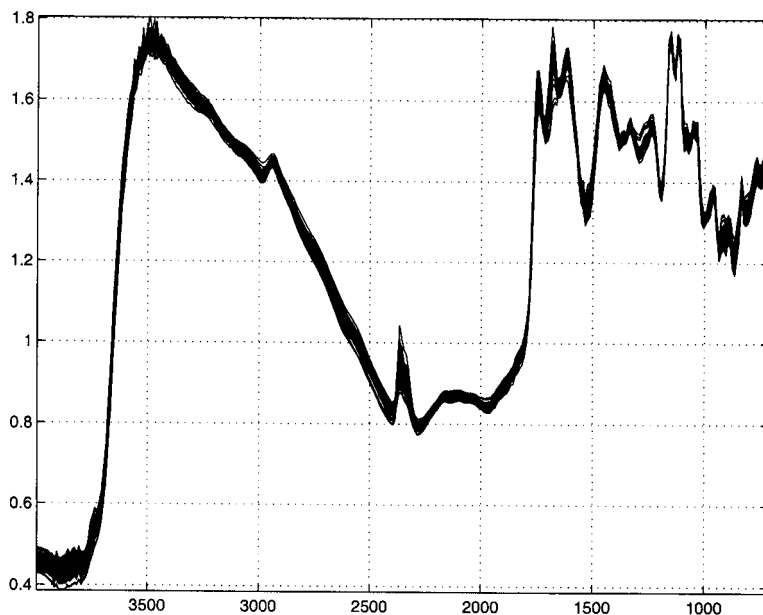


Fig. 2. FT-IR spectra with three orthogonal components removed. The components are depicted in Fig. 3. The wavelength axis is in cm^{-1} . Compare with Fig. 1.

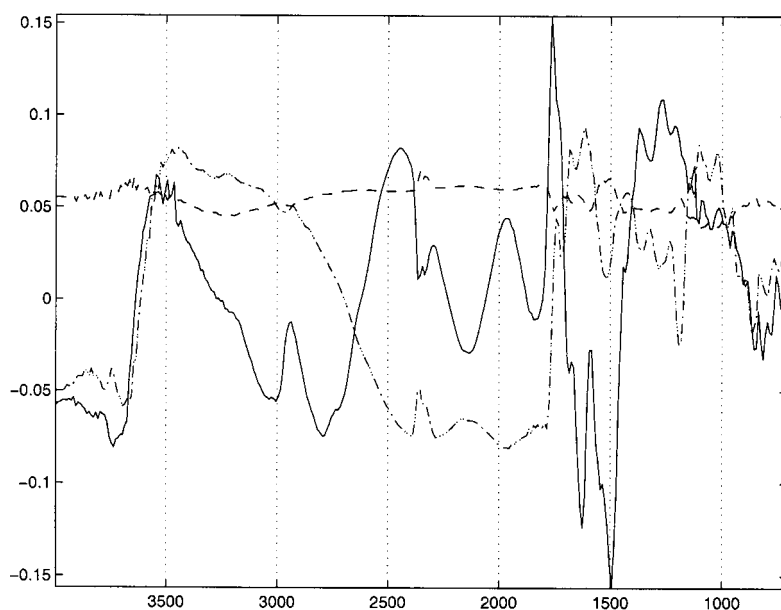


Fig. 3. Scatter components found and removed by direct orthogonalization in Fig. 2. The components explain 45% (dashed line), 23% (dash-dot line) and 9% (solid line) of the variance of the FT-IR spectra. The wavelength axis is in cm^{-1} . Compare with Fig. 1.

to locate wavelengths with high variations, pretreatment of the spectra with SOD does not improve the correlation between the spectra and the reference values, as will be shown later.

The methods based on multiplicative scatter correction, SPMSC and PMSC, give spectra that can be interpreted and evaluated in relation to the degree of esterification. The effect of pretreating with PMSC using a symmetric window width of 190 cm^{-1} is shown in Fig. 5. The similarity with SPMSC with eight intervals is very high; thus, only the effect of PMSC is illustrated. When applying the MSC approaches, as well as DO, the spectroscopist is allowed to evaluate the relative responses and couplings when interpreting the corrected spectra. Note, that the variation around 1752 cm^{-1} is high, this meaning that variability has been preserved throughout correction. There is, however, no guarantee that the variability qualifies for a better correlation to the reference values. As will be seen, DO, SPMSC and PMSC not only improve the qualitative information

present in the spectra, but the quantitative part of the analysis benefits from these methods of pretreatment as well.

Now turning to modelling, the point of interest becomes the modelling error in terms of the applied cross validation, i.e., RMSECV. In Table 1, the RMSECV values for modelling the degree of esterification are listed for using PLSR. The four different approaches are listed in groups of rows, and each column represents the RMSECV from segmented cross validation of PLSR models using from 1 to 10 components. The optimal dimensionality of each model is indicated by boldfacing the respective RMSECV value. The chosen dimensionality has been determined (subjectively) in such a way that the simplicity of the model is ensured while providing satisfactory fit to data. Including too many components in the regression step increases the risk of overfitting data whereby future samples will be poorly predicted. The first row, denoted as Raw, illustrates the development in RMSECV when applying an increasing

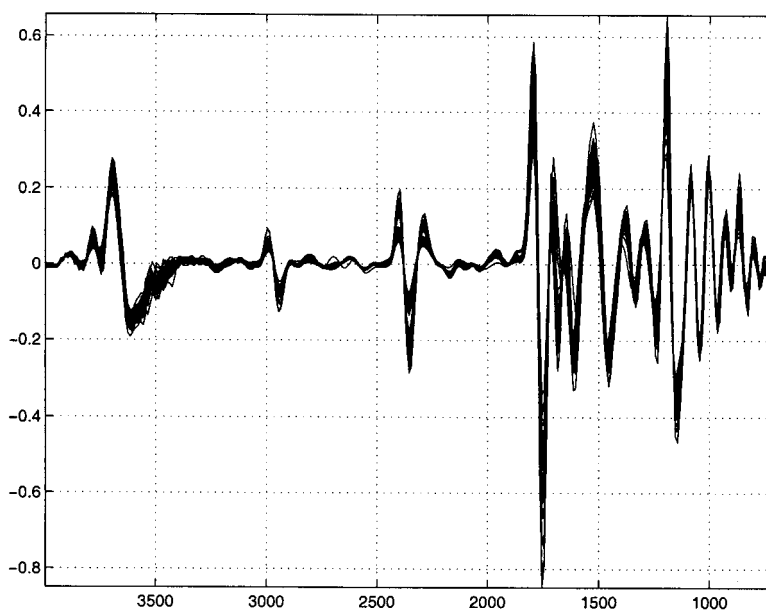


Fig. 4. Second order derivatives of the FT-IR spectra. The wavelength axis is in cm^{-1} . Compare with Fig. 1.

number of PLSR components to the raw data. A number of eight PLSR components offers the optimal model dimensionality at a RMSECV of 1.84. The estimated error of the reference method is 1.5%. Thus, the obtained validation error is close to the optimal value.

When extracting one DO component, the same error in terms of RMSECV, i.e., 1.84, is achieved with one less PLSR component. This behaviour is repeated when extracting successive numbers of DO components. When removing six DO components, the RMSECV increases slightly to 1.90. This indicates that, even upon orthogonalization, there is variation left in the data that is not perfectly correlated with y , but sufficiently correlated to be significant and have a stabilizing effect on the factors of the regression model. The proposed effect of DO, with respect to removing information that is orthogonal to y , is clearly recognized in the pattern of the optimal dimensionality of the subsequent PLSR models. The argumentation is verified by the explained variance of %DE, as depicted in Table 2. Table 2 lists the cumu-

lated explained variance of all 97 FT-IR spectra from calibration when extracting from 1 to 8 DO components and using 1 to 10 PLSR components. While the raw (untreated) spectra use eight PLSR components to explain a total of 97.9% of the variance, the extraction of one DO component reduces this number to 7. Removing one more DO component lowers the number to six PLSR components. This behaviour continues up the extraction of 4 DO components. When removing the effect of five DO components, vital information is removed from the spectra and the optimal number of PLSR components stop to decrease. This observation is explained by the lack of accuracy of the measurements in y , i.e., %DE. If the reference values are not accurate, the effect of orthogonalization is diminished, since the orthogonalization is dependent on the existence of a relationship between y and X . Thus, from Table 2 we induce that the sum of the two model dimensionalities a and b is constant. Accordingly, Table 1 indicates the existence of a closed relation between the number of PLSR and DO components to sum up to 8 for the data

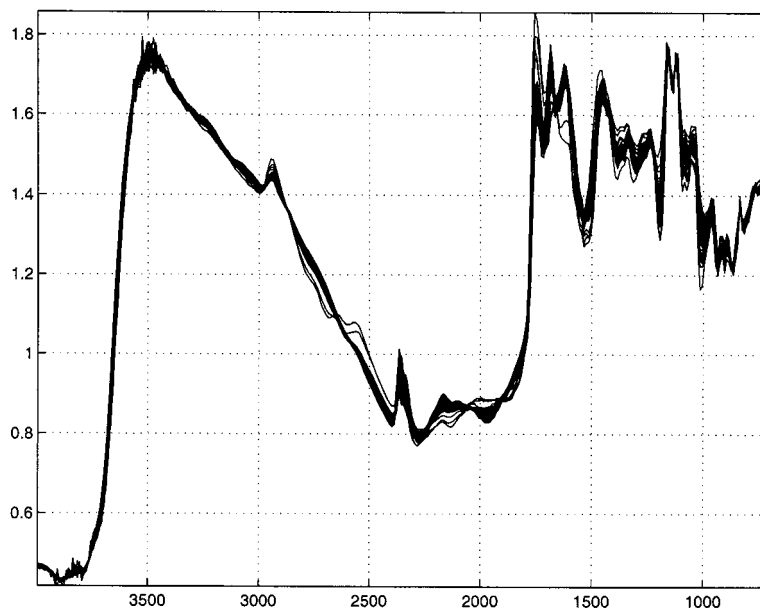


Fig. 5. Piecewise multiplicative scatter correction (PMSC) of the FT-IR spectra using symmetric windows 190 cm^{-1} wide. The visual effect of SPMSC with eight intervals is similar to this case. The wavelength axis is in cm^{-1} . See Fig. 1 for the raw spectra.

at hand. In general, we expect the dimensions of the DO model and the PLSR model to add up to a constant—close to the optimal dimensionality of a PLSR model on the raw data.

The application of SOD yields the highest values of RMSECV as listed in Table 1. With an RMSECV of 2.01, the optimal PLSR model uses only four

components but this error is approx. 10% higher than the lowest overall RMSECV at 1.83.

Models based on both MSC methods provide RMSECV values comparable to PLSR models on the raw data—the PMSC even slightly lower, see Table 1. For the PMSC approach, window widths between 15 cm^{-1} and 500 cm^{-1} have been tested, and the

Table 1
RMSECV values for FT-IR spectra using from 1 to 10 PLSR components

	1	2	3	4	5	6	7	8	9	10
Raw	6.29	5.78	4.01	2.65	2.29	2.06	1.96	1.84	1.99	2.11
DO, 1 comp	5.89	4.01	2.65	2.29	2.06	1.96	1.84	1.99	2.11	2.11
DO, 2 comp	4.12	2.66	2.30	2.06	1.96	1.84	1.99	2.11	2.11	2.09
DO, 3 comp	2.90	2.39	2.10	1.97	1.83	1.98	2.10	2.11	2.08	2.09
DO, 4 comp	2.81	2.24	2.02	1.84	1.96	2.09	2.11	2.08	2.09	2.09
DO, 5 comp	2.67	2.11	1.85	1.92	2.08	2.11	2.08	2.09	2.09	2.09
DO, 6 comp	2.52	1.90	1.89	2.06	2.12	2.08	2.09	2.09	2.09	2.12
SOD	3.77	2.51	2.16	2.01	2.09	2.10	2.08	2.08	2.08	2.11
PMSC, 190 cm^{-1} width	4.91	2.44	2.03	1.89	1.83	1.84	1.90	1.92	1.88	1.83
SPMSC, eight intervals	3.79	2.10	1.94	1.89	1.86	1.94	2.16	2.15	2.33	2.21

II. Algorithms, models and applications

Table 2

Cumulated explained variance (%) for %DE for all 97 calibration FT-IR spectra when extracting 1 to 8 DO components of uncorrelated information from **X** prior to PLSR with 1 to 10 components

	1	2	3	4	5	6	7	8	9	10
Raw	13.2	29.8	74.3	91.7	96.2	97.1	97.9	98.2	99.0	99.3
1	29.6	74.4	91.7	96.2	97.1	97.9	98.3	99.0	99.3	99.5
2	71.5	91.6	96.1	97.0	97.9	98.3	99.0	99.3	99.5	99.7
3	90.5	95.0	96.8	97.8	98.3	98.9	99.3	99.5	99.7	99.9
4	90.5	96.2	97.5	98.2	98.9	99.3	99.5	99.7	99.9	99.9
5	90.6	96.4	98.0	98.7	99.3	99.5	99.7	99.9	99.9	100.0
6	92.2	97.3	98.3	99.2	99.4	99.7	99.9	99.9	100.0	100.0
7	94.0	97.7	99.1	99.3	99.6	99.8	99.9	100.0	100.0	100.0
8	96.8	98.4	99.2	99.6	99.8	99.9	100.0	100.0	100.0	100.0

Compare Table 1.

optimal window width found from full cross-validation was 190 cm⁻¹. For SPMSC, all intervals from 1 (corresponding to ordinary MSC) up to 10 have been tested, and the optimal number of intervals was found to be 8. The PMSC approach, although very time-consuming, provides good estimates providing an error of 1.83 when using five PLSR components. The SPMSC approach yields an insignificantly less optimal RMSECV value at 1.86 for the same number of PLSR components.

In Table 3, the RMSECV values from PCR are listed. Comparing the values to Table 1, we find that PCR can perform almost as well as PLSR on the data under investigation, albeit generally requiring two more regression components. When comparing DO against raw spectra, the closure between the number of regression components and DO components is verified. The sum of the dimensionalities of the DO and the PLSR models appears to be 11. For example,

it is possible to choose between a model with one DO component and 10 PLSR components, or say, five DO components and six PLSR components. The RMSECV values for SOD for both PCR and PLSR models are the highest, and for the data at hand SOD is the least feasible approach. For SPMSC and PMSC, seven PCR components are required and yields an RMSECV of 1.91—this is in the same range as models based on PLSR. The optimal parameters for SPMSC as well as PMSC prove to be independent of the choice of regression model since the number of intervals is found to be 8 and the window width to be 190 cm⁻¹ as in the case of PLSR.

4. Further applications and improvements

There are several approaches and possible applications for using DO as a tool for pretreatment of

Table 3

RMSECV values for FT-IR spectra using PCR with 1 to 11 components

	1	2	3	4	5	6	7	8	9	10	11
Raw	6.40	6.30	5.92	5.72	4.44	3.20	2.96	2.75	2.24	2.01	1.92
DO, 1 comp	6.20	5.87	5.67	4.39	3.18	2.94	2.74	2.23	2.00	1.92	1.92
DO, 2 comp	5.88	5.64	4.34	3.14	2.92	2.73	2.23	2.00	1.91	1.92	1.94
DO, 3 comp	5.33	4.13	3.07	2.85	2.69	2.20	1.98	1.90	1.91	1.93	1.94
DO, 4 comp	4.14	3.07	2.85	2.69	2.20	1.99	1.90	1.91	1.94	1.94	1.96
DO, 5 comp	3.04	2.83	2.67	2.20	1.98	1.90	1.91	1.94	1.95	1.96	1.98
DO, 6 comp	2.76	2.66	2.19	1.98	1.91	1.92	1.94	1.95	1.97	1.99	2.01
SOD	5.66	3.36	2.96	2.20	2.10	2.08	2.08	2.09	2.11	2.13	2.15
PMSC, 190 cm ⁻¹ width	6.45	6.49	4.58	2.70	2.23	2.09	1.91	1.95	2.01	2.08	2.11
SPMSC, eight intervals	6.26	6.14	4.78	3.86	3.16	2.15	1.94	1.93	2.11	2.10	2.13

data. In addition to the reported algorithm, a bi-linear alternating least squares (ALS) resolution algorithm was also implemented and applied to data. The implemented resolution scheme constrains the scores to be orthogonal to y while minimizing a least squares error term. The effects were exactly the same as the results derived from the proposed eigenproblem-based algorithm. The possibility of implementing DO in the form of bi- and multi-linear resolution schemes brings new issues into perspective, e.g., in the form of constrained PARAFAC models. If certain chemical/physical behaviours make some modes of the data conform to e.g., unimodality, non-negativity and/or monotonicity, such constraints may be applied during decomposition in addition to the orthogonality constraint. For multi-way data arrays, the common multi-way alternating least squares (ALS) resolution schemes can be modified to yield scores that are independent of y , thus, allowing to filter the arrays for systematic, but irrelevant information. The ALS schemes give scatter components that need not be orthogonal to each other, and may thus be easier to interpret. Drawbacks are (i) the much higher time consumption of the resolution schemes, and (ii) the problem of rotation remains for the bi-linear case.

Process data is another field in which DO is believed to be feasible. Process data often have fluctuations of different frequencies and since these fluctuations will not depend on the reference parameter(s) being modelled, drift in baseline will be extractable as DO components. It has been proposed to use DO for correlation studies between different kinds of spectra where effects of scatter can be eliminated prior to investigations.

5. Conclusions

In the present paper, a method is proposed for supervised multivariate filtration and the method has been applied to spectral data from FT-IR measurements. For the spectral data under investigation, the method of direct orthogonalization provides a viable approach to pretreatment of spectra with high levels of scatter. Compared to common approaches as second order derivatives, simple interval piecewise scatter correction and windowed piecewise scatter correction, the validation error in terms of RMSECV are

comparable. In contrast to the existing methods, the proposed supervised method provides a means of identifying possible outliers in the filtration step and the phenomena constituting the background are decomposed for possible interpretation. In addition, direct orthogonalization is fast due to the one-step orthogonalization requiring only one low-dimensional principal component analysis. Finally, a range of possible applications of DO have been outlined.

Acknowledgements

Thanks to Börkur Arnvidarson, ARCTIC, for talks about applications and theory. Søren B. Engelsen is thanked for sharing his expertise in IR spectroscopy and for providing data for the applications. Lars Nørgaard has supported and encouraged the work. The support and inspiration of Prof. Lars Munck is greatly appreciated. Tormod Næs and Tomas Isaksson, MATFORSK, Norway, and Harald Martens, BTI, DTU, Denmark are thanked for their practical and philosophical remarks. Financing support is due to EU funding Affluence and FØTEK 2.

References

- [1] H. Martens, S. Jensen, P. Geladi, Proceedings, Nordic Symposium on Applied Statistics, Stavanger, Stokkand Forlag Publishers, Skagenkaiaen 12, Stavanger, Norway, ISBN 82-90496-02-8, 1983, pp. 205–234.
- [2] P. Geladi, D. McDougall, H. Martens, Linearization and scatter corrections for near infrared reflectance spectra of meat, *Appl. Spectrosc.* 39 (1985) 491–500.
- [3] T. Isaksson, B. Kowalski, Piece-wise multiplicative scatter correction applied to near-infrared diffuse transmittance data from meat products, *Appl. Spectrosc.* 47 (1993) 702–709.
- [4] L. Horváth, K.H. Norris, M. Horváth-Mosonyi, J. Rigó, E. Hegedüs-Völgyesi, Study into determining dietary fiber of wheat bran by NIR-technique, *Acta Alimentaria* 13 (1984) 355–382.
- [5] O.E. de Noord, Multivariate calibration standardization, *Chem. Intell. Lab. Syst.* 25 (1994) 85–97.
- [6] P.R. Mobley, B.R. Kowalski, J.J. Workman, R. Bro, Review of chemometrics applied to spectroscopy: 1985–1995, *Appl. Spectrosc. Rev.* 31 (1996) 347, Part II.
- [7] E.R. Malinovski, *Factor Analysis in Chemistry*, 2nd edn., Wiley, New York, 1980, pp. 199–206.
- [8] J. Sjöblom, O. Svensson, M. Josefson, H. Kulberg, S. Wold, Evaluation of orthogonal signal correction applied to calibra-

II. Algorithms, models and applications

- tion transfer of near infrared spectra, Poster presented at SSC5, Lahti, Finland, 1997.
- [9] S. Wold, H. Antti, F. Lindgren, J. Öhman, Orthogonal signal correction of near-infrared spectra, *Chem. Intell. Lab. Syst.*, 1998, to appear.
- [10] P. Kubelka, F. Munck, *Z. Tech. Phys.* 12 (1931) 593.
- [11] L. Råde, B. Westergren, *Beta Mathematics Handbook*, 2nd edn., Studentlitteratur, Lund, 1990, p. 347.
- [12] A. Savitsky, M.J.E. Golay, Smoothing and differentiation of data by simplified least squares procedures, *Anal. Chem.* 36 (1964) 1627–1639.
- [13] T.V. Karstang, O.M. Kvalheim, Multivariate prediction and background correction using local modelling and derivative spectroscopy, *Anal. Chem.* 63 (1991) 767–772.
- [14] S.B. Engelsen, L. Nørgaard, Comparative vibrational spectroscopy for determination of quality parameters in aminated pectins as evaluated by chemometrics, *Carbohydr. Polym.* 30 (1996) 9–24.

P2

**A new criterion for simple-
structure transformations of
core arrays in N -way principal
components analysis**

Rene Henrion and Claus A. Andersson



A new criterion for simple-structure transformations of core arrays in N -way principal components analysis

René Henrion ^{a,*}, Claus A. Andersson ^b

^a Weierstrass Institute for Applied Analysis and Stochastics, Mohrenstr. 39, D-10117 Berlin, Germany

^b Royal Veterinary and Agricultural University, Department of Food Science, Chemometrics Group, DK-1871 Copenhagen, Denmark

Abstract

Among the possible (orthogonal) transformations of core arrays in N -way principal components analysis (PCA), the conventional approach of body diagonalization turns out not to provide the simplest structure (in the sense of minimizing the number of significant entries). As an alternative, the maximization of the variance-of-squared core entries is proposed. Both criteria are equivalent in a two-way constellation but may differ markedly for $N \geq 3$. Actually, using the variance criterion may provide more insight into the rank structure of the given data, and it is also easily applied to general rectangular core arrays. In order to clarify the relation between body diagonality and variance-of-squares, we prove the following main result of the paper: If some cubic N -way core array can be transformed to exact body diagonality, then the same transformation yields maximum variance-of-squared entries. This result implies the equivalence in the two-way case mentioned above. A solution algorithm is formulated and illustrated with a small numerical example. The application to data examples from environmental chemistry and chromatographic analysis is briefly discussed. © 1999 Elsevier Science B.V. All rights reserved.

Keywords: N -way-principal components analysis; Tucker3 model; Core array; Simple-structure transformation; Body diagonality; Variance-of-squares

1. Introduction

N -way data analysis has become an efficient tool for solving chemometric problems which are based on complex (N -dimensional or N -way) data arrays as they arise, for instance, from hyphenated instrumentation. For early papers in this direction, we refer to Refs. [1,2]. Since then, a lot of contributions mainly to three-way data analysis have appeared. Chemometrically-oriented introductions to three-way analysis may be found in Refs. [3,4]. Meanwhile, at least the case $N = 4$ must be considered practically relevant (e.g., emission/excitation data from fluorescence measurements of different samples under changing conditions like pH [5]). Maybe the most important methods involved are Parallel Factor Analysis (PARAFAC) [6], Canonical Decomposition (CANDECOMP) [7] and the Tucker3 model of (three-way) Principal Components Analysis (PCA) [8], but also some variants of three-way Partial Least Squares (PLS) [9–11].

* Corresponding author. Fax: +49-30-2044975; E-mail: henrion@wias-berlin.de

The present paper addresses a specific problem of N -way PCA (for an introduction see Ref. [12]). More precisely, a new approach of transforming core arrays to simple structure is proposed and compared to the conventional diagonalization procedure.

2. Transformation of core arrays to simple structure

The general model of N -way PCA is (compare Ref. [13])

$$\text{vec } \mathbf{X} \approx (\mathbf{A}_1 \otimes \cdots \otimes \mathbf{A}_N) \text{vec } \mathbf{C} \quad (1)$$

Here, \mathbf{X} denotes an N -way data array of order (n_1, \dots, n_N) , the \mathbf{A}_i are component matrices of orders (n_i, s_i) , where, usually, the s_i 's are small numbers for the purpose of data reduction, and \mathbf{C} is the so called N -way core array of order (s_1, \dots, s_N) . Furthermore, vec and \otimes denote the vectorization operator and the Kronecker product, respectively. It is emphasized, that in the following vec will be understood as an operator unfolding the given array in a way that the first index runs fast and the last index slowly. For matrices, this corresponds to the usual stacking of columns (note that there is some inconsistency in the definition in Ref. [13], pages 30 and 363). Accordingly, we understand the Kronecker product in the sense

$$\mathbf{A} \otimes \mathbf{B} = \begin{pmatrix} b_{11}\mathbf{A} & \cdots & b_{1m}\mathbf{A} \\ \vdots & \ddots & \vdots \\ b_{n1}\mathbf{A} & \cdots & b_{nm}\mathbf{A} \end{pmatrix}.$$

The aim of N -way PCA is, given \mathbf{X} , to find the component matrices (sometimes additionally required to be column-wise orthonormal) and the core array such that the above approximation is optimal in the sense of least squares deviations. The component matrices \mathbf{A}_i allow to plot the basic factors in each of the N modes influencing the total variation in the array \mathbf{X} . The core array \mathbf{C} , on the other hand, indicates how factor combinations from different modes interact. For instance, in a three-way constellation ($N = 3$) with orthonormal component matrices, the squared core element c_{121}^2 measures the amount of data variance covered by combining the first factor of the first mode with the second factor of the second mode and the first factor of the third mode. Such consideration of interactions is not necessary in conventional two-mode PCA since the core matrix can always be diagonalized there. Hence, the information in data tables is exhausted efficiently by independent extraction of successive factors for objects and variables. The explanatory effect of interactions (say by combining the first factor of objects with the second factor of variables) can always be made zero. Things become different for data arrays of dimensions larger than two. Of course, one might still suppress interactions by restricting the model of decomposition, which is the case in the PARAFAC approach. However, such decomposition is no longer the most efficient one. Indeed, using the Tucker3 model with possible interactions between different factors of different modes, the same amount of data variation as in a PARAFAC decomposition might be explained by a smaller number of factors. On the other hand, interactions are more difficult to interpret. In particular, a generalization of the well-known bi-plots from two-way PCA to 'tri-plots' or ' N -plots' is not straightforward. Therefore, a common strategy is to simplify the interaction structure among factors after a Tucker3 analysis as far as possible. This is the aim of simple-structure transformations of core arrays. In the ideal case, one could remove all the interactions and would arrive at the same result as with a direct PARAFAC approach. Unfortunately, this is not possible in general, so one has to be satisfied with structures simplified according to suitable criteria which will be discussed in the sequel. For an illustration of the PCA decomposition according to the Tucker3 model (1) and for an interpretation of the core elements, we refer to the data example in Section 5.

While the optimal component matrices in (1) may be determined by an alternating least squares algorithm (see Ref. [14]), the corresponding optimal core array results from them according to (compare Ref. [13])

$$\text{vec } \mathbf{C} = (\mathbf{A}_1^T \otimes \cdots \otimes \mathbf{A}_N^T) \text{vec } \mathbf{X}$$

II. Algorithms, models and applications

On the other hand, neither the component matrices \mathbf{A}_i , nor the core array \mathbf{C} are uniquely determined in the decomposition (1). Indeed, using nonsingular matrices \mathbf{P}_i of orders (s_i, s_i) , this same decomposition transforms to (by $\mathbf{P}_i \mathbf{P}_i^{-1} = \mathbf{I}_{s_i}$):

$$\begin{aligned} \text{vec } \mathbf{X} &\approx (\mathbf{A}_1 \otimes \cdots \otimes \mathbf{A}_N) \text{vec } \mathbf{C} \\ &= (\mathbf{A}_1 \otimes \cdots \otimes \mathbf{A}_N) (\mathbf{I}_{s_1} \otimes \cdots \otimes \mathbf{I}_{s_N}) \text{vec } \mathbf{C} \\ &= (\mathbf{A}_1 \otimes \cdots \otimes \mathbf{A}_N) (\mathbf{P}_1 \otimes \cdots \otimes \mathbf{P}_N) (\mathbf{P}_1^{-1} \otimes \cdots \otimes \mathbf{P}_N^{-1}) \text{vec } \mathbf{C} \\ &= (\mathbf{A}'_1 \otimes \cdots \otimes \mathbf{A}'_N) \text{vec } \mathbf{C}', \end{aligned}$$

where $\mathbf{A}'_i = \mathbf{A}_i \mathbf{P}_i$ are the transformed versions of the original component matrices \mathbf{A}_i , and \mathbf{C}' is the new core array which relates to the old one through

$$\text{vec } \mathbf{C}' = (\mathbf{P}_1^{-1} \otimes \cdots \otimes \mathbf{P}_N^{-1}) \text{vec } \mathbf{C} \quad (2)$$

Along with the transformed core \mathbf{C}' , the \mathbf{A}'_i provide the same approximation of \mathbf{X} as the original \mathbf{A}_i and \mathbf{C} . Actually, corresponding to the manifold of possible nonsingular matrices \mathbf{P}_i , there is an infinite number of equally good approximations of the given data array. For simplicity and comparison to existing methods, we restrict the further presentation mainly to orthogonal transformations. Then, the inverses \mathbf{P}_i^{-1} in (2) simply become the transposed matrices \mathbf{P}_i^T . Furthermore, in this case, the transformed component matrices \mathbf{A}'_i remain orthonormal if so were the original ones \mathbf{A}_i and, hence, the entries of the transformed core \mathbf{C}' may be interpreted as variance contributions of factor combinations from different (transformed) components \mathbf{A}'_i as it held true for the original core \mathbf{C} and the original components \mathbf{A}_i (see above).

A reasonable choice of a particular solution in (1) would require the core array to have as few significant entries as possible in order to arrive at a model with a minimum number of describing factors. Doing so, the interpretational effort of the results obtained may be considerably reduced. For the purpose of illustration, consider the following three-mode core arrays of order (2,2,2), in unfolded form (i.e., the third index refers to the slice left or right to the separation line while the first two indices are read in the slices as for usual matrices):

$$\left(\begin{array}{cc|cc} \frac{1}{\sqrt{2}} & \frac{1}{\sqrt{2}} & \frac{1}{\sqrt{2}} & \frac{1}{\sqrt{2}} \\ \frac{1}{\sqrt{2}} & -\frac{1}{\sqrt{2}} & \frac{1}{\sqrt{2}} & -\frac{1}{\sqrt{2}} \end{array} \right); \left(\begin{array}{cc|cc} 1 & 0 & 1 & 0 \\ 0 & 1 & 0 & 1 \end{array} \right); \left(\begin{array}{cc|cc} \sqrt{2} & 0 & 0 & 0 \\ 0 & \sqrt{2} & 0 & 0 \end{array} \right) \quad (3)$$

All these cores can be transformed into each other by using appropriate orthogonal matrices in (2). It is clear that the structure simplifies from the left to the right: in the situation of the very left core one would have to interpret eight equally important factor combinations of the N -way PCA model. This number reduces to four in the second and to two in the third core. Sometimes, additional knowledge about the model allows to fix specific core elements as zero and to consider restricted core arrays from the very beginning of analysis. This approach is discussed in Ref. [15] and it has been applied to a selected calibration problem of analytical chemistry in Ref. [16]. In general, however, the insight into the problem structure is rather limited, so premature restrictions of the core might not be advisable. Instead, one can admit a completely loaded core as the output of any N -way PCA algorithm and afterwards use the degree of freedom in the decomposition (1) discussed above, in order to find transformation matrices \mathbf{P}_i , such that the new core resulting from Eq. (2) has a simple structure. In the following, we restrict considerations to cubic core arrays of order (s, \dots, s) . This restriction is not necessary for the approach to be described here, but it allows comparison with existing methods. In the sense of the discussion above, one may imagine several criteria for measuring 'simple structure'. In Ref. [17], the simple structure was formulated as a slice-wise diagonality of the (three-way) core array. The theoretical argument behind this is, that

in case of a possible exact slice-wise diagonalization, the Tucker3 model reduces to a PARAFAC model as soon as one renounces the orthogonality of the components. For instance, both, the second and third core in (3) are slice-wise diagonal.

On the other hand, with orthogonality constraints imposed on the components—and this may have certain advantages—Tucker3 reduces to PARAFAC (also with orthogonal components) only in case that the core has so-called body diagonal shape. By this, it is meant that the entries of \mathbf{C} satisfy $C_{i_1 \dots i_N} = 0$ if not $i_1 = \dots = i_N$. None of the cores in (3) are body diagonal, since, in all cases there are nonzero entries outside the left upper and right lower corners of the unfolded arrays. Indeed, in this data example, there does not exist any orthogonal transformation of the given cores to exact body diagonality. Body diagonality is a desirable property of the core in that it avoids interaction between unequal components from different modes. From a more practical standpoint, body diagonality allows superposition and joint interpretation of component plots. As in the example, exact body diagonalization of core arrays fails in most cases. At least, one can try to fit body diagonality as close as possible, which amounts to maximize the sum of squared body diagonal entries $\text{diag} = \sum_{i=1}^s C_{i \dots i}^2$. The total sum of squared core entries being invariant under the transformation (2) with orthogonal \mathbf{P}_i , this means to minimize the squared off-diagonal entries, hence, a body diagonal shape of the core is approached.

In (3), one computes the values $\text{diag}_1 = 1$, $\text{diag}_2 = 2$, $\text{diag}_3 = 2$ for the succeeding cores. Actually, the value 2 represents the maximum of diag among all possible transformations (2) with orthogonal cores \mathbf{P}_i , so the second and third core are not only slice-wise diagonal, but they have maximum body diagonal shape at the same time. If exact body diagonality was possible here, then one should obtain $\text{diag} = 4$, a value which is equal to the total sum of squares in the cores. An algorithm for (maximum) body diagonalization of three-way core arrays was suggested in Ref. [18]. In Ref. [19], theoretical bounds for the success of body diagonalization of three-way core arrays were derived. For the special case of cores of order (2,2,2)—which is important in exploratory diagram analysis of components—a degree of 80–90% of body diagonality (= diag divided by the total sum of squared entries) may be expected on the average. This makes diagonalization a useful approach for obtaining simple structure of cores.

Simple structure of the core can be understood, however, in a sense different from diagonality. It seems natural to look for transformations providing the smallest number of significant core entries, or equivalently, the largest number of negligible (if not zero) entries. This is a direct formulation of minimizing the effort of interpretation of components. It is intuitively clear, that this aim is not automatically realized by body diagonalization since the latter restricts not only the number of significant elements but simultaneously the shape of the core. Renouncing the diagonality shape, one has hope to find cores with fewer significant entries although not necessarily located on the diagonal. Although, due to its simplicity, the example (3) is not capable of completely highlighting this aspect, it suffices to demonstrate that maximum body diagonality is not directly related with simple structure. As already stated above, both the second and third core in (3) have the same degree of body diagonality while the structure of the third core is much simpler with only two significant entries as compared to the second core. Much more evident examples will be provided in the following sections.

3. Variance-of-squares

3.1. Definition of the criterion

As a quantitative criterion directly oriented towards maximizing the number of negligible entries in the core, we propose to use the variance of the squared entries of the core. More precisely, we define

$$\text{var} = \sum_{i_1=1}^s \dots \sum_{i_N=1}^s (C_{i_1 \dots i_N}^2 - \bar{C})^2 \quad (4)$$

where

$$\bar{C} = \sum_{i_1=1}^s \cdots \sum_{i_N=1}^s C_{i_1 \dots i_N}^2 / s^N = [\text{vec } \mathbf{C}]^T [\text{vec } \mathbf{C}] / s^N \quad (5)$$

is the mean of squared entries.

Eq. (4), as a numerical entity, is identical with the quartimax criterion defined for simple structure transformations of loading matrices in factor analysis [20], but it must not be confused with these. Optimizing the two-way quartimax measure, which relates to loading matrices rather than core matrices, does not necessarily produce simple core arrays which is the aim of the current discussion. Therefore, we keep the name ‘variance-of-squares’ criterion in order to avoid any confusion with concepts from factor analysis.

The justification of the variance-of-squares criterion relies on the following simple observation: If a set of vectors $(\mathbf{x}_1, \dots, \mathbf{x}_n)$ is restricted to have non-negative components x_i which sum up to a constant value, then the variance of the components attains its maximum at those vectors having exactly one component different from zero. In order to translate this result to the context of core arrays, consider now the set of vectors $(\mathbf{x}_1, \dots, \mathbf{x}_n)$ which are vectorizations of squared entries of core arrays related by transformations of type (2). Obviously, the components x_i are non-negative, and they sum up to a constant value, since the sum of squares in a core array does not change under the considered transformation (2) with orthogonal \mathbf{P}_i (compare also the first statement in the proof of the Theorem in Section 3.3). Therefore, maximum variance of the x_i , which is the maximum variance of the squared core entries, aims at reducing the number of nonzero core elements to one. In Eq. (3), the third core has maximum variance-of-squares among all possible transformations. The concrete values $\text{var}_1 = 0$, $\text{var}_2 = 2$, $\text{var}_3 = 6$ for the three cores reflect quite well the increasing simplicity of their structure.

Note that, although the justification given above relates to orthogonal transformation matrices \mathbf{P}_i in (2), the variance-of-squares criterion itself may be applied to general nonsingular transformation matrices \mathbf{P}_i . In the special case of orthogonal transformations which we focus on in this paper, the objective of maximizing the variance-of-squares measure becomes similar to a special case of the three-mode Orthomax criterion proposed by Kiers [21]. The three-mode Orthomax measure is optimized successively for each of the three modes by maximizing the ORMAX matrix operator

$$\text{ORMAX}(\Lambda, \gamma) = \sum_{l=1}^r \left(\sum_{i=1}^m \lambda_{il}^4 - \frac{\gamma}{m} \left(\sum_{i=1}^m \lambda_{il}^2 \right)^2 \right) \quad (6)$$

with λ_{il} denoting the element in the i th row and the l th column of the matrix Λ . A scalar γ weighs the squared mean of the squared column entries of Λ . In the three-mode Orthomax approach, ORMAX is applied alternately to the three unfoldings of the core to yield an overall optimization. Setting $\gamma = 0$ for all three modes, the criterion simplifies to the three-mode Quartimax measure. This situation entails that the squared mean values of the squared entries are neglected, causing the sum of the fourth powers of the core elements to be maximized. Similarly, for orthogonal transformation matrices the variance-of-squares measure (4) will have an invariant mean value of the squares, implicitly resulting in maximization of the fourth powers of the core elements (compare (7)). Whereas, the three-mode Quartimax procedure operates on the unfoldings of the core, the variance-of-squares procedure addresses the problem by optimizing the core directly. Also, both approaches differ when general nonsingular (not just orthogonal) transformations are allowed, since the mean of squares is no longer invariant and, hence, the maximization of the variance-of-squares is no longer equivalent to the maximization of fourth powers then. In terms of understanding the effects of core transformations, we prefer the variance-of-squares measure since variance has an intuitive meaning for analysts while the Quartimax measure is somewhat abstract. Recently, an approach for simultaneous optimization of the orthogonality of the core and the component matrices has been proposed, see Ref. [22].

3.2. On the relations between body diagonality and variance-of-squares

Let us now check the relations between the body diagonality and variance-of-squares criteria. The second and the third core in (3) show that maximum body diagonality does not automatically provide maximum variance-of-squares. The example was for three-way cores, but what about the simpler two-way case ($N = 2$), where body diagonality reduces to conventional diagonalization of square matrices? The answer is given by the Corollary to the Theorem in Section 3.3: In the two-way case, the maximization of ‘body diagonality’ implies the maximization of the variance-of-squares of a quadratic core matrix. In other terms: For $N = 2$, there is no gain by introducing the variance criterion, and the core simplification is completely achieved by singular value decomposition, which is an admissible transformation in the sense of (2). This equivalence in the two-way case might explain why the consideration of the quite natural variance-of-squares criterion has been ignored so far in favour of different diagonality criteria.

A misleading feature of the example in (3) is that the core with maximum variance-of-squares (third core) is contained in—although not identical with—the set of cores having maximum body diagonality. This is not true in general. In order to obtain a more general impression, consider Fig. 1 where variance vs. diagonality plots for three different cores each subject to 5000 random orthogonal transformations are given. Here, the plots (a), (b), and (c) refer to transformations of the cores

$$C = \left(\begin{array}{cc|cc} 1 & \alpha & 1 & \beta \\ \alpha & 1 & \beta & 1 \end{array} \right),$$

where $\alpha = \beta = 0$ in (a), $\alpha = \beta = -0.1$ in (b), and $\alpha = -0.1$, $\beta = 0.1$ in (c). Obviously, Fig. 1(a) relates to transformations of the cores in (3) since, for $\alpha = \beta = 0$, C is equal to the second core there. As a consequence, the three cores of (3) are contained in the plot of Fig. 1(a) as points with the coordinates (diag, var) = (1,0), (2,2), and (2,6), respectively. Note that the vertical line, joining the last two of these points, represents an infinite number of transformed cores with maximum body diagonality but with varying values for the variance-of-squares. Such a phenomenon is not stable since an arbitrarily small perturbation of the core entries (e.g., the parameters α , β) will destroy this vertical line, and a constellation as in Fig. 1(b) and (c) is likely to occur. Here, the qualitative relationship between the diagonality and variance criteria is quite different: In Fig. 1(b), maximum body diagonality implies maximum variance-of-squares (which was not true in Fig. 1(a)), while in Fig. 1(c), the maxima of diag and var are completely unrelated: indeed, the maximum of diag leads only to a value of var, which is less than half the maximum of var. In contrast to Fig. 1(a), both situations are stable with respect to small perturbations of the core entries (due to the fact that var and diag are continuous functions of the core), hence, both of them are typically observed.

Now, the question arises, under which conditions does the one or the other situation occur. As the main result in this direction the following statement, which even relates to general (cubic) N -way cores, is proved in the Theorem of Section 3.3: If the given core array may be transformed according to (2) to exact (!) body diagonality, then the resulting diagonal core array has maximum variance-of-squares at the same time. This result is mainly of theoretical interest in that it connects the relation between both criteria with the structure of the core array. By contraposition, one concludes that neither the cores in Fig. 1(a) nor those in Fig. 1(c) can be transformed to exact body diagonality (since there are transformations providing maximum diagonality but not maximum variance-of-squares). From the practical point of view, one has to take into account of course that a transformation of cubic N -way cores to exact body diagonality is possible for $N \geq 3$ in exceptional cases only.

By the way, Fig. 1 also shows, that even minimum diagonality can lead to maximum variance-of-squares. At least for two-way matrices of order (2,2), this is not surprising since the diagonal elements may be placed as

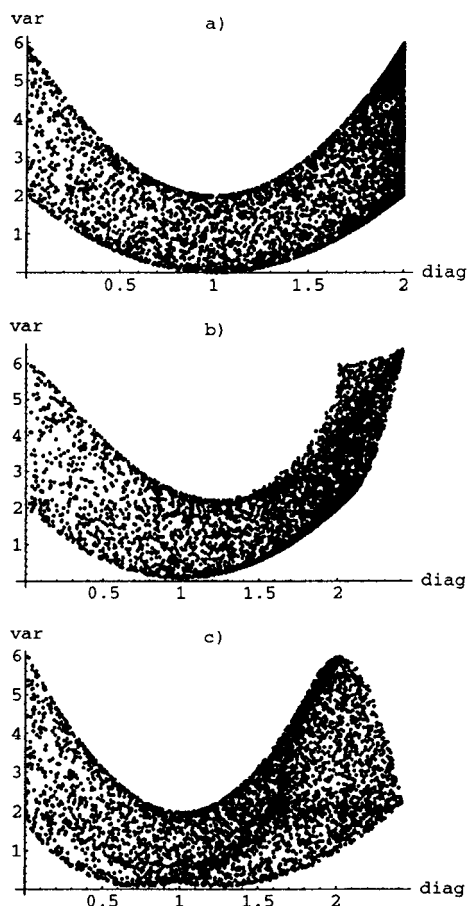


Fig. 1. Plot of variance-of-squared entries vs. body diagonality for 5000 random orthogonal transformations of three different core arrays.

well on the anti-diagonal without changing the variance. For higher order, this is no longer true as can be seen from the simple two-way example:

$$\begin{pmatrix} 0 & 1 & 1 \\ 1 & 0 & 1 \\ 1 & 1 & 0 \end{pmatrix}$$

This matrix has evidently minimum diagonality with variance-of-squares equal to 2, whereas maximum diagonality is attained (after a similarity transformation) when the eigenvalues 2, -1, -1 are placed on the diagonal. This gives a variance-of-squares equal to 14, which must be the maximum according to the Corollary proved in Section 3.3. Consequently, in this example, minimum diagonality yields a variance-of-squares value which is far from the maximum.

3.3. Theoretical results

Now, we prove the statements referred to above. To this aim, let \mathbf{C} denote a cubic N -way core array of order (s, \dots, s) . Given any N -tuple of orthogonal matrices $\mathbf{P}_1, \dots, \mathbf{P}_N$ of common order (s, s) , the following functions are introduced:

$$T(\mathbf{P}_1, \dots, \mathbf{P}_N) = \text{vec}^{-1} [(\mathbf{P}_1^T \otimes \dots \otimes \mathbf{P}_N^T) \text{vec } \mathbf{C}]$$

$$\text{var}(\mathbf{P}_1, \dots, \mathbf{P}_N) = \sum_{i_1=1}^s \dots \sum_{i_N=1}^s (T_{i_1 \dots i_N}^2(\mathbf{P}_1, \dots, \mathbf{P}_N) - \bar{T}(\mathbf{P}_1, \dots, \mathbf{P}_N))^2$$

Here, vec^{-1} refers to the operator which assigns to each vector with s^N components the uniquely defined N -way array of order (s, \dots, s) the vectorization of which gives this vector. Obviously, $T(\mathbf{P}_1, \dots, \mathbf{P}_N)$ is exactly the transformed core array \mathbf{C}' from (2). In the second definition, $\bar{T}(\mathbf{P}_1, \dots, \mathbf{P}_N)$ denotes the mean of squares of the transformed core array (compare (5)), so $\text{var}(\mathbf{P}_1, \dots, \mathbf{P}_N)$ is the variance of squared entries in the transformed core array.

Theorem 3.1. *If there exist orthogonal matrices \mathbf{P}_i^* ($i = 1, \dots, N$) of common order (s, s) such that $T(\mathbf{P}_1^*, \dots, \mathbf{P}_N^*)$ is body diagonal, then $\text{var}(\mathbf{P}_1^*, \dots, \mathbf{P}_N^*)$ maximizes the expression $\text{var}(\mathbf{P}_1, \dots, \mathbf{P}_N)$ among all N -tuples of orthogonal matrices $\mathbf{P}_1, \dots, \mathbf{P}_N$ of common order (s, s) .*

Proof. We start with the obvious observation that the mean of squares of a core array is invariant under the transformation T . In fact, due to the orthogonality of the \mathbf{P}_i , one has

$$\begin{aligned} \bar{T}(\mathbf{P}_1, \dots, \mathbf{P}_N) &= [\text{vec } T(\mathbf{P}_1, \dots, \mathbf{P}_N)]^T [\text{vec } T(\mathbf{P}_1, \dots, \mathbf{P}_N)] / s^N \\ &= [(\mathbf{P}_1^T \otimes \dots \otimes \mathbf{P}_N^T) \text{vec } \mathbf{C}]^T [(\mathbf{P}_1^T \otimes \dots \otimes \mathbf{P}_N^T) \text{vec } \mathbf{C}] / s^N \\ &= [\text{vec } \mathbf{C}]^T ((\mathbf{P}_1 \mathbf{P}_1^T) \otimes \dots \otimes (\mathbf{P}_N \mathbf{P}_N^T)) [\text{vec } \mathbf{C}] / s^N \\ &= [\text{vec } \mathbf{C}]^T [\text{vec } \mathbf{C}] / s^N \\ &= \bar{C}, \end{aligned}$$

where \bar{C} refers to the mean of squares of \mathbf{C} (see (5)). Therefore, the variance criterion, as a function of the chosen transformation, written as

$$\begin{aligned} \text{var}(\mathbf{P}_1, \dots, \mathbf{P}_N) &= \sum_{i_1=1}^s \dots \sum_{i_N=1}^s (T_{i_1 \dots i_N}^2(\mathbf{P}_1, \dots, \mathbf{P}_N) - \bar{C})^2 \\ &= \sum_{i_1=1}^s \dots \sum_{i_N=1}^s T_{i_1 \dots i_N}^4(\mathbf{P}_1, \dots, \mathbf{P}_N) + s^N \bar{C}^2 \\ &\quad - 2\bar{C} \sum_{i_1=1}^s \dots \sum_{i_N=1}^s T_{i_1 \dots i_N}^2(\mathbf{P}_1, \dots, \mathbf{P}_N) \\ &= \sum_{i_1=1}^s \dots \sum_{i_N=1}^s T_{i_1 \dots i_N}^4(\mathbf{P}_1, \dots, \mathbf{P}_N) - s^N \bar{C}^2 \end{aligned} \tag{7}$$

II. Algorithms, models and applications

In the following, we shall make use of the known or easy to verify relations

$$(\mathbf{Q} \otimes \mathbf{R}) \text{vec } \mathbf{S} = \text{vec}(\mathbf{QSR}^T) \tag{8}$$

$$\sum_{ij} \mathbf{Q}_{ij}^4 \leq \text{tr}[\mathbf{Q}^T \mathbf{Q}]^2 \tag{9}$$

between Kronecker product, matrix product, vectorization and trace of matrices \mathbf{Q} , \mathbf{R} , \mathbf{S} with suitable orders. Now, for a cubic N -way array \mathbf{M} of order (s, \dots, s) , define its unfolding $u(\mathbf{M})$ to be the uniquely determined matrix of order (s, s^{N-1}) such that $\text{vec } \mathbf{M} = \text{vec } u(\mathbf{M})$. Then, using (8), one gets

$$\begin{aligned} \text{vec } u(T(\mathbf{P}_1, \dots, \mathbf{P}_N)) &= \text{vec } T(\mathbf{P}_1, \dots, \mathbf{P}_N) = (\mathbf{P}_1^T \otimes \dots \otimes \mathbf{P}_N^T) \text{vec } u(\mathbf{C}) \\ &= \text{vec}[\mathbf{P}_1^T u(\mathbf{C})(\mathbf{P}_2 \otimes \dots \otimes \mathbf{P}_N)] \end{aligned}$$

Consequently, $u(T(\mathbf{P}_1, \dots, \mathbf{P}_N)) = \mathbf{P}_1^T u(\mathbf{C})(\mathbf{P}_2 \otimes \dots \otimes \mathbf{P}_N)$ which implies

$$\begin{aligned} \text{tr}[u(T(\mathbf{P}_1, \dots, \mathbf{P}_N))^T u(T(\mathbf{P}_1, \dots, \mathbf{P}_N))]^2 &= \text{tr}[(\mathbf{P}_2^T \otimes \dots \otimes \mathbf{P}_N^T) u(\mathbf{C})^T u(\mathbf{C})(\mathbf{P}_2 \otimes \dots \otimes \mathbf{P}_N)]^2 \\ &= \text{tr}(\mathbf{P}_2^T \otimes \dots \otimes \mathbf{P}_N^T) [u(\mathbf{C})^T u(\mathbf{C})]^2 (\mathbf{P}_2 \otimes \dots \otimes \mathbf{P}_N) \\ &= \text{tr}[u(\mathbf{C})^T u(\mathbf{C})]^2 \end{aligned} \tag{10}$$

On the other hand, for the particular choice of transformation matrices providing body diagonality (see statement of the theorem), one has

$$\text{tr}[u(T(\mathbf{P}_1^*, \dots, \mathbf{P}_N^*))^T u(T(\mathbf{P}_1^*, \dots, \mathbf{P}_N^*))]^2 = \sum_{i_1=1}^s \dots \sum_{i_N=1}^s T_{i_1 \dots i_N}^4(\mathbf{P}_1^*, \dots, \mathbf{P}_N^*) \tag{11}$$

This follows from the fact that body diagonality of $T(\mathbf{P}_1^*, \dots, \mathbf{P}_N^*)$ implies its unfolded copy $u(T(\mathbf{P}_1^*, \dots, \mathbf{P}_N^*))$ to have in each column and each row at most one entry different from zero. Combining (7), (9), (10) (which in particular holds for the transformation matrices \mathbf{P}_i^*) and (11), one arrives at

$$\begin{aligned} \text{var}(\mathbf{P}_1, \dots, \mathbf{P}_N) &\leq \text{tr}[u(T(\mathbf{P}_1, \dots, \mathbf{P}_N))^T u(T(\mathbf{P}_1, \dots, \mathbf{P}_N))]^2 - s^N \bar{C}^2 \\ &= \text{tr}[u(\mathbf{C})^T u(\mathbf{C})]^2 - s^N \bar{C}^2 \\ &= \text{tr}[u(T(\mathbf{P}_1^*, \dots, \mathbf{P}_N^*))^T u(T(\mathbf{P}_1^*, \dots, \mathbf{P}_N^*))]^2 - s^N \bar{C}^2 \\ &= \sum_{i_1=1}^s \dots \sum_{i_N=1}^s T_{i_1 \dots i_N}^4(\mathbf{P}_1^*, \dots, \mathbf{P}_N^*) - s^N \bar{C}^2 \\ &= \text{var}(\mathbf{P}_1^*, \dots, \mathbf{P}_N^*) \end{aligned}$$

Since the \mathbf{P}_i 's were chosen arbitrarily among all orthogonal matrices of common order (s, s) , this last inequality proves that $\text{var}(\mathbf{P}_1, \dots, \mathbf{P}_N)$ is maximized by the transformation matrices \mathbf{P}_i^* . \square

Corollary 3.2. *In the two-way case ($N = 2$), maximization of diagonality implies maximization of the variance-of-squares of a quadratic core matrix.*

Proof. Since any (square) matrix \mathbf{C} may be transformed to diagonal shape via a singular value decomposition $\mathbf{P}^T \mathbf{C} \mathbf{Q}$ with orthogonal \mathbf{P} and \mathbf{Q} , and since this is an admissible transformation in the sense of (2) (recall that $\text{vec}(\mathbf{P}^T \mathbf{C} \mathbf{Q}) = (\mathbf{P}^T \otimes \mathbf{Q}^T) \text{vec } \mathbf{C}$), the same transformation yields maximum variance-of-squares according to the Theorem. \square

4. A transformation algorithm

In this section, we formulate an algorithm in order to find the optimal orthogonal matrices \mathbf{P}_i in (2) transforming the given core array \mathbf{C} , which is the output of any N -way PCA algorithm, into one with a maximum variance-of-squares value. We omit the theoretical derivation of the algorithm and refer to Ref. [23].

1. Set $\mathbf{C}^{\text{new}} := \mathbf{C}$ (= original core array) and $\mathbf{P}_i^{\text{new}} := \mathbf{I}_{s_i}$ ($i = 1, \dots, N$)
2. Set $j := 0$
3. Set $j := j + 1$, $\mathbf{C}^{\text{old}} := \mathbf{C}^{\text{new}}$, $\mathbf{P}_j^{\text{old}} := \mathbf{P}_j^{\text{new}}$ and compute an orthogonal matrix \mathbf{P} such that $\mathbf{P}^T \mathbf{A}$ becomes a symmetric matrix, where the general entry of \mathbf{A} is ($1 \leq k \leq s_j$; $1 \leq l \leq s_j$)

$$A_{kl} = \sum_{i_1=1}^{s_1} \cdots \sum_{i_{j-1}=1}^{s_{j-1}} \sum_{i_{j+1}=1}^{s_{j+1}} \sum_{i_N=1}^{s_N} \left(C_{i_1 \dots i_{j-1} l i_{j+1} \dots i_N}^2 - \bar{C} \right) C_{i_1 \dots i_{j-1} l i_{j+1} \dots i_N}^{\text{old}} C_{i_1 \dots i_{j-1} k i_{j+1} \dots i_N}^{\text{old}}$$

Define \mathbf{C}^{new} by $\text{vec } \mathbf{C}^{\text{new}} := (\mathbf{I}_{s_1} \otimes \dots \otimes \mathbf{I}_{s_{j-1}} \otimes \mathbf{P} \otimes \mathbf{I}_{s_{j+1}} \otimes \mathbf{I}_{s_N}) \text{vec } \mathbf{C}^{\text{old}}$ and $\mathbf{P}_j^{\text{new}} := \mathbf{P}_j^{\text{old}} \mathbf{P}$. If $j < N$, then goto 3.

4. If $\text{var}(\mathbf{C}^{\text{new}})$ differs significantly from $\text{var}(\mathbf{C}^{\text{old}})$, then goto 2.
5. Stop.

The final \mathbf{C}^{new} is the optimally transformed core array and the final \mathbf{P}_j are the corresponding transformation matrices for the transition from \mathbf{C} to \mathbf{C}^{new} via (2). The decisive step in this algorithm is the symmetrification of $\mathbf{P}^T \mathbf{A}$ in 3. This can be realized by a singular value decomposition of \mathbf{A} by means of orthogonal matrices \mathbf{U} , \mathbf{V} of order s_j , which yields $\mathbf{U} \mathbf{A} \mathbf{V} = \mathbf{D}$ with diagonal \mathbf{D} . Then, setting $\mathbf{P} = \mathbf{U}^T \mathbf{V}^T$, one gets

$$\mathbf{P}^T \mathbf{A} = \mathbf{V} \mathbf{U} \mathbf{A} = \mathbf{V} \mathbf{U} \mathbf{U}^T \mathbf{D} \mathbf{V}^T = \mathbf{V} \mathbf{D} \mathbf{V}^T,$$

which is the desired symmetric matrix. A numerical example shall serve as an illustration of the algorithm. Consider the maximization of the variance-of-squares criterion var for the three-dimensional core array of order (2,2,2) given by

$$\mathbf{C} = \begin{pmatrix} C_{111} & C_{121} & C_{112} & C_{122} \\ C_{211} & C_{221} & C_{212} & C_{222} \end{pmatrix} = \begin{pmatrix} 0 & 1 & 1 & 2 \\ 1 & 1 & 0 & 1 \end{pmatrix}$$

The mean of squared entries is $\bar{C} = 1.125$ and the variance-of-squares criterion for the initial core is $\text{var}(\mathbf{C}) = 10.875$. In the first step of the algorithm, one has to compute the matrix \mathbf{A} with general element

$$A_{kl} = \sum_{i_2=1}^2 \sum_{i_3=1}^2 \left(C_{i_2 i_3}^2 - \bar{C} \right) C_{i_2 i_3} C_{k i_2 i_3} \quad (k = 1, 2; l = 1, 2)$$

For instance, $A_{11} = 0 - 0.125 - 0.125 + 11.5 = 11.25$. For the whole matrix, one has

$$\mathbf{A} = \begin{pmatrix} 11.25 & -0.375 \\ 5.625 & -0.375 \end{pmatrix}$$

From singular value decomposition of this matrix, one finds that $\mathbf{P}^T \mathbf{A}$ becomes symmetric for

$$\mathbf{P} = \begin{pmatrix} 0.911 & 0.412 \\ 0.412 & -0.911 \end{pmatrix}$$

Applying the transformation $(\mathbf{P} \otimes \mathbf{I}_2 \otimes \mathbf{I}_2) \text{vec } \mathbf{C}$ to the original core array yields the new core array

$$\mathbf{C}^{\text{new}} = \begin{pmatrix} 0.412 & 1.323 & 0.911 & 2.234 \\ -0.911 & -0.500 & 0.412 & -0.088 \end{pmatrix}$$

II. Algorithms, models and applications

with a significantly increased variance-of-squares value of $\text{var}(\mathbf{C}^{\text{new}}) = 19.36$. In the next iteration, the matrix \mathbf{A} has to be considered with $j = 2$. Accordingly, its general element is

$$A_{kl} = \sum_{i_1=1}^2 \sum_{i_3=1}^2 (C_{i_1 i_3}^2 - \bar{C}) C_{i_1 i_3} C_{i_1 k i_3} \quad (k, l = 1, 2)$$

where \mathbf{C} refers to the previously obtained \mathbf{C}^{new} . Proceeding as before, one finds a transformation matrix \mathbf{P} symmetrifying $\mathbf{P}^T \mathbf{A}$ and a new core via $\text{vec } \mathbf{C}^{\text{new}} = (\mathbf{I}_2, \mathbf{P}, \mathbf{I}_2) \text{vec } \mathbf{C}$. The new variance-of-squares value then becomes $\text{var}(\mathbf{C}^{\text{new}}) = 27.64$. Finally, after three main iterations (i.e., $3 \times 3 = 9$ single iterations), the var-value reaches a relative precision of 0.001 at $\text{var} = 48.6$. The resulting core is

$$\mathbf{C} = \begin{pmatrix} -0.12 & 0.29 & -0.15 & 2.76 \\ -0.83 & 0.63 & 0.08 & -0.41 \end{pmatrix}$$

Although the sum of squares is the same as in the original core, there is practically only one significant entry left now (after squaring in mind all contributions).

5. Applications

Two applications shall illustrate the ideas discussed so far. The first application is a data example considered in more detail in Ref. [12]. It relates to a water quality study carried out in the course of 1 year in the Niger delta area. More precisely, 13 physicochemical parameters were measured 22 times at 10 sampling stations, thus, yielding a three-way data array of order (10, 13, 22). The data were scaled in a way to give all physicochemical parameters zero mean and unit variance (over all sampling stations and sampling times). The first column of diagrams in Fig. 2 provides the loading plots resulting from a Tucker3 decomposition of the array with two components considered for each mode. Thus, the diagrams correspond to the component matrices \mathbf{A}_j in (1). The first diagram reveals a strong grouping among sampling stations ('a' and 'b') in accordance with their known degree of pollution. The second diagram refers to the physicochemical parameters among which a salinity-related group (conductivity 'co', chloride concentration 'Cl' and hardness 'hr') shows high loadings on the first factor and the chemical oxygen demand 'cO₂' has a high loading on the second factor. In the third diagram, successive sampling times (1,2 = February, ..., 21,22 = December) have a strong temporal trend along the first factor. For better visualization the loadings of this first factor are plotted vs. time in the diagram at the very bottom. The resulting curve indicates a clear temporal factor in the data. In order to detect how these factors of different modes relate to each other, one has to study the core array, which in unfolded form, is given by

$$\mathbf{C} = \begin{pmatrix} 1.36 & 0.48 & 0.35 & -0.35 \\ -0.37 & -0.11 & 1.02 & -0.57 \end{pmatrix}$$

Accordingly, two major entries seem to be present, namely $c_{111} = 1.36$ and $c_{212} = 1.02$. The first one relates to the joint effect of all first factors in the three modes. Re-inspecting the diagrams one recognizes this factor as a seasonal change of salinity which is almost uniform for all stations (similar loadings of stations on the first factor). Indeed, the time curve reflects quite well the rainfall period (September to November) with low salinity. The second contribution relates to the combination of the second factors of sampling stations and times with the first factor of physicochemical parameters. Hence, again salinity is involved, but now with a geographical rather than seasonal meaning: the vertical arrangement of sampling stations corresponds quite well to their geographical positions with increasing distance to the shore resulting in decreasing salinity, while there is no systematic variation of the loadings of sampling times on the second factor.

Among the remaining entries of the core array there are five with comparable contributions, and it seems hard to decide whether all or which of these have additional importance in the explanation of data structure. To

II. Algorithms, models and applications

200

R. Henrion, C.A. Andersson / *Chemometrics and Intelligent Laboratory Systems* 47 (1999) 189–204

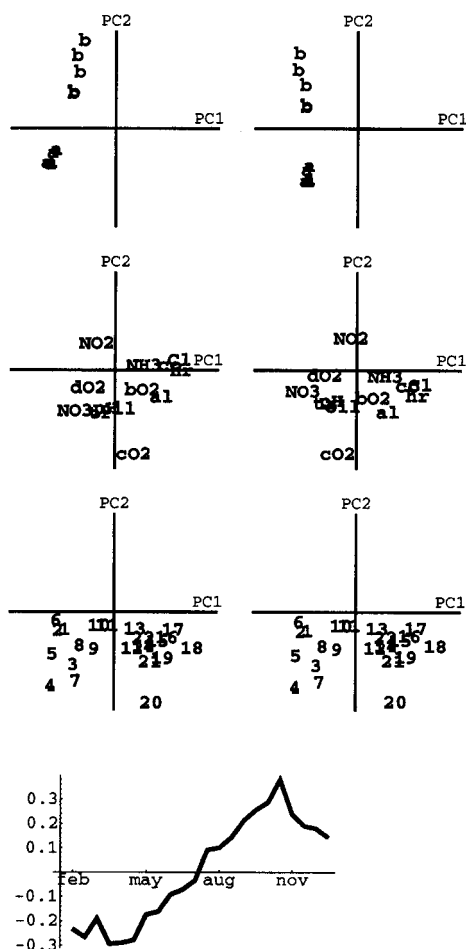


Fig. 2. Original (first column) and rotated (second column) loading plots for sampling stations, physicochemical parameters and sampling times in the water chemistry example. The loadings with respect to the first factor of sampling times are plotted as a curve over time (the same curve refers to both original and rotated loading plots for sampling times).

answer this question, a simple-structure transformation was realized according to the variance-of-squares criterion. The optimally transformed core array turns out to be

$$C = \begin{pmatrix} 1.48 & 0.11 & 0.05 & -0.04 \\ 0.00 & 0.16 & 0.72 & 1.02 \end{pmatrix}$$

In contrast to the original core array, a distinction between significant and nonsignificant contributions is much more evident now. This fact is also supported by the increase of the variance-of-squares criterion from 2.83 to 4.41. Obviously, three relevant factor combinations have to be taken into account. The corresponding rotated

loading diagrams leading to this core array are plotted in the second column of Fig. 2. It is remarkable that only a slight change takes place in the component matrices, nevertheless providing a much clearer core structure. In particular, all sampling stations get even more equal weights on the first factor. Minor changes take place for the parameters, too, whereas the loadings of sampling times remain practically unchanged (in particular the seasonal curve is the same as before). Apart from the two factor combinations c_{111} , c_{212} already discussed before (but now with changed importance), a third combination $c_{222} = 1.02$ —namely the one of all second factors—is found to be significant. According to the vertical axes in the diagrams, this relates to a distinction of sampling stations into groups ‘a’ and ‘b’ mainly due to differing values of chemical oxygen demand uniformly over time. Some effect of pollution is likely to be hidden in this factor combination. However, we do not go into further details of possible interpretations since the main objective of the example is to illustrate the Tucker3 model and the effect of core simplifications.

In order to emphasize the benefits of core rotation, we shall give another example dealing with the differences between cores with optimum variance-of-squares and optimum diagonality. To keep the discussion focused and aimed at core rotation, no explicit chemical interpretation of the factors will be given. The data to be analyzed are derived from fluorescence intensity measurements of 13 *thick juice* samples. Thick juice is an intermediary product in the production of sugar and ongoing projects aim at obtaining means to control and decrease the unwanted formation of colour during the process, see Refs. [5,24].

The 13 thick juice samples have been separated into 28 fractions (each of 700 μl) on a 200 mm Sephadex G25M column that separates components according to molecular size in the approximate range of 1000 to 5000 MW. A sample volume of 300 μl was introduced into the isocratic and aqueous 0.01 w/w% NaCl carrier running with a flow of 0.8 ml/min. For each fraction, six preselected combinations of excitation and emission wavelengths have been measured using spectrofluorometry. The filter combinations were found in earlier investigations [25]. The six combinations of excitation and emission wavelengths cover the range 270 nm to 390 nm of the excitation range and 280 to 420 nm of the emission wavelength range. The collected three-way data array has dimensions (13,28,6) where the respective modes refer to sample number, fraction number and combination of excitation–emission wavelengths.

For exploration of the data, we have chosen to analyze the data by N -way PCA, whereby the significant variation of the data is condensed into a few factors allowing for easy interpretation. In order to illustrate the benefits of core rotation, we will compare two cores derived from rotation of the initial core according to the maximum variance-of-squares measure and the maximum diagonality measure. From the cores discussed in the sequel, it will appear that the PARAFAC model is inadequate of handling the data in question due to severe non-diagonality of the core.

Prior to analysis, the data were mean-centred across the third mode since the filter combinations of the apparatus result in quite different levels of signals. This pretreatment ensures that the arbitrary differences between the response levels are removed from the modelling step in accordance with the aim of the investigation.

A three-way model with three factors in each mode was chosen as a compromise between having a small number of factors and a close fit to the data. The SVD-based algorithm used to calculate the PCA model is described in Ref. [26]. The model explains 71.7% of the variation of data (i.e., sum of squares) and the initial core was found to be

$$C = \begin{pmatrix} \mathbf{3383} & \mathbf{2805} & 493 & \mathbf{2600} & \mathbf{-2300} & -215 & -220 & -477 & 110 \\ \mathbf{-2037} & \mathbf{2116} & 124 & 1096 & 888 & -1484 & 16 & 530 & 213 \\ -284 & 526 & -1208 & 246 & 4 & 1353 & -251 & 554 & -454 \end{pmatrix}$$

where the elements have been rounded to the nearest integer to provide a clear view of the significant elements. The variance-of-squares of C is 2.26×10^{14} and the degree of diagonality is 25.2%. Apparently, there are up to six significant elements in the unrotated core. The sum of squares of the three largest squared elements explains 52.8% of the total sum of squares in C .

II. Algorithms, models and applications

Upon maximization of the variance-of-squares, the core takes the form of

$$\tilde{\mathbf{C}} = \left(\begin{array}{ccc|ccc|ccc} \mathbf{4516} & -87 & 4 & 122 & -\mathbf{3377} & -152 & -114 & 94 & 167 \\ -194 & \mathbf{2837} & -229 & 1388 & -441 & -1495 & 112 & 744 & 318 \\ -33 & 320 & -912 & 263 & -78 & 1546 & -19 & 607 & -744 \end{array} \right)$$

where the variance-of-squares measure increases to 5.37×10^{14} and the degree of diagonality is 42.8%. Now, the three largest squared elements are responsible for 80.7% of the total sum of squares. As seen directly from $\tilde{\mathbf{C}}$, the interpretation has become easier since much variation accounted for by several less significant factor combinations has been condensed into a lower number of more significant ones.

When optimizing the diagonality of \mathbf{C} instead, the core transforms into

$$\hat{\mathbf{C}} = \left(\begin{array}{ccc|ccc|ccc} \mathbf{4424} & -484 & 12 & -407 & -1156 & \mathbf{2857} & 444 & -285 & 562 \\ -705 & -667 & 1747 & -794 & \mathbf{2700} & -67 & -322 & -396 & 87 \\ -139 & 225 & -1796 & 1285 & -35 & 978 & -48 & 165 & -1093 \end{array} \right)$$

with a degree of diagonality at 56.8%. The variance-of-squares measure becomes 4.40×10^{14} . For comparison with the core shown above, the three largest elements account for 70.9% of the total variation in the model, this is approximately 10%—points less than the core that is optimal in the variance-of-squares sense. This means that the analyst, by using the variance-of-squares optimized core $\tilde{\mathbf{C}}$ rather than the diagonalized core $\hat{\mathbf{C}}$, will include what corresponds to 10%-points more variation of data in his interpretation. It is noteworthy that the structure in the data does not conform with the PARAFAC model, since diagonality of the core $\hat{\mathbf{C}}$ cannot be obtained.

In Fig. 3, the 15 largest squared elements from the cores \mathbf{C} , $\tilde{\mathbf{C}}$ and $\hat{\mathbf{C}}$ are plotted. The line denoted by (a) represents the largest squared elements from \mathbf{C} . The differences between successive squared core elements are small, leading to a rather flat line that indicates the low variance of the core elements. Without core rotation, the analyst has to interpret, perhaps, five factor combinations in order to give a detailed picture of data. Line (b) describing $\tilde{\mathbf{C}}$ depicts a much higher variation in the core elements. We see that the three largest elements are all much higher than the fourth. This allows the analyst to focus on three factor combinations. Note, that the *three* largest elements from the rotated core explain the same amount of variation (80.7%) as the *five* largest elements from the initial core (80.9%). Line (c) describes the elements in the core with optimal diagonality, i.e., $\hat{\mathbf{C}}$. The indication of the presence of three significant factor combinations is more clear than with the unrotated core, but

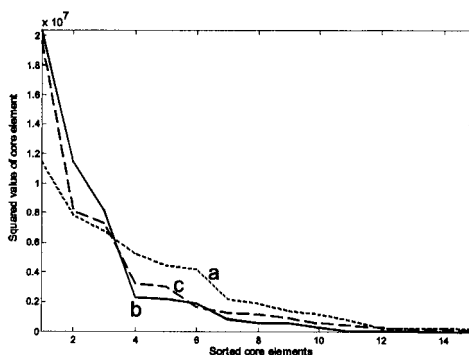


Fig. 3. The 15 largest squared core elements of the three cores are sorted and plotted. Line (a) represents the 15 largest squared core elements of the untreated core. Line (b) are the 15 largest squared elements of the core with optimal variance-of-squares measure, and (c) shows the 15 largest squared elements of the core with optimal diagonality.

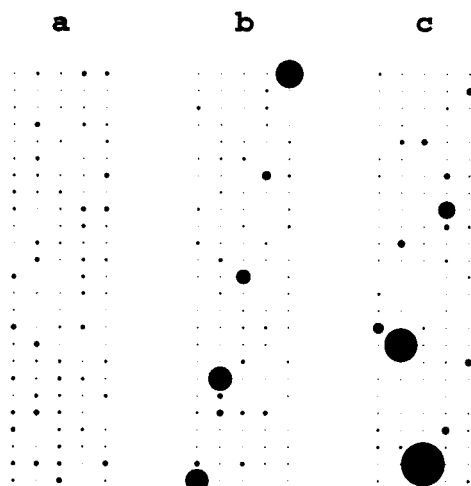


Fig. 4. Symbolic plots of core arrays of order (5,5,5) unfolded to matrices of order (25,5). The left array refers to the original core, the medium one to the transformed core with maximum body diagonality and the right one to the transformed core with maximum variance-of-squares. The squared entries of the cores are translated to diameters of filled circles.

not as clear as with the core with optimal variance-of-squares. The core \hat{C} suffers from the fact that the core could not be diagonalized, since this structure is not present in data. Furthermore, we see that the levels of the remaining squared core elements remain high for C and \hat{C} . This is sub-optimal, because the size of the elements reflects what is not included in the interpretation of the model. The low level of all elements but the significant ones for the line (b) is a direct consequence of maximizing the variance-of-squares measure in \tilde{C} .

Finally, we want to indicate the potentials of maximizing the variance-of-squares criterion in a higher-dimensional setting. To this aim, a random three-way core array of order (5,5,5) was created with entries uniformly distributed between -1 and 1 . This original core was transformed both to maximum body diagonality and maximum variance-of-squares. The results for the unfolded cores (= matrices of order (25,5)) are shown in Fig. 4. For better visualization, the squared values of the entries are translated into diameters of filled circles. Due to the random nature of the original core, there are many positions of medium relevance in the first array (a). In contrast, the two transformed cores show a clear distinction between significant and nonsignificant elements. Not surprisingly, in the core with maximum body diagonality (b), the five major entries are distributed along the diagonal of the unfolded core. Such diagonal structure is lost in the array with maximum variance-of-squares (c), but this loss is in favour of a yet smaller number of significant elements. Comparing (c) with (b) on a rough scale, two rather than three entries are found to be significant. On a finer level, three rather than five entries are clearly distinguished from the rest.

6. Conclusion

The proposed variance-of-squares criterion has a great potential for simplifying the structure of core arrays in N -way PCA and, hence, for facilitating the interpretation of solutions obtained. Its main advantage over the well-established method of body diagonalization is directly to aim at a reduction of the number of significant entries. Moreover, its application is not restricted to cubic cores. The maximization of the criterion can be car-

II. Algorithms, models and applications

ried out by an iterative solution algorithm providing reliable results in a short period of time, thus, higher dimensional arrays (e.g., $N = 7$) may be easily treated as well. Some theoretical results giving insight into the relations between the variance-of-squares and body diagonality criteria have been derived. A convergence proof for the algorithm is given in Ref. [23].

Acknowledgements

The authors wish to thank Prof. L. Munck (Royal Veterinary and Agricultural University Copenhagen) and Prof. G. Henrion (Humboldt University Berlin) for facilitating the present cooperation. The second author wishes to thank the EU Affluence AIR project and the National Danish fund FØTEK2.

References

- [1] C.J. Appellof, E.R. Davidson, *Anal. Chem.* 53 (1981) 2053–2056.
- [2] C. de Ligny, M. Spanjer, J. van Houwelingen, H. Weesie, *J. Chromatogr.* 301 (1984) 311–324.
- [3] P. Geladi, *Chemom. Intell. Lab. Syst.* 7 (1989) 11–30.
- [4] A.K. Smilde, *Chemom. Intell. Lab. Syst.* 15 (1992) 143–157.
- [5] C.A. Andersson, Master Thesis, Royal Veterinary and Agricultural University, Copenhagen, Denmark, 1995.
- [6] R.A. Harshman, *UCLA Working Papers in Phonetics* 16 (1970) 1–84.
- [7] J.D. Carrol, C.C. Chang, *Psychometrika* 35 (1970) 283–319.
- [8] L.R. Tucker, in: C.W. Harris (Ed.), *Problems of Measuring Change*, Univ. of Wisconsin Press, Madison, 1963, p. 122.
- [9] L. Stähle, *J. Pharm. Biomed. Anal.* 9 (1991) 671–678.
- [10] Y.L. Xie, J.J. Baezabaeza, G. Ramisramos, *Chemom. Intell. Lab. Syst.* 27 (1995) 211–220.
- [11] R. Bro, *J. Chemometrics* 10 (1996) 47–61.
- [12] R. Henrion, *Chemom. Intell. Lab. Syst.* 25 (1994) 1–23.
- [13] J.R. Magnus, H. Neudecker, *Matrix Differential Calculus with Applications in Statistics and Econometrics*, Wiley, Chichester, 1988.
- [14] P.M. Kroonenberg, J. de Leeuw, *Psychometrika* 45 (1980) 69–97.
- [15] H.A.L. Kiers, *Statistica Applicata* 4 (1992) 659–667.
- [16] A.K. Smilde, R. Tauler, J.M. Henshaw, L.W. Burgess, B.R. Kowalski, *Anal. Chem.* 66 (1994) 3345–3351.
- [17] P.M. Kroonenberg, *Three-Mode Principal Component Analysis: Theory and Applications*, DSWO Press, Leiden, 1983.
- [18] H.A.L. Kiers, *Statistica Applicata* 4 (1992) 7–15.
- [19] R. Henrion, *J. Chemometrics* 7 (1993) 477–494.
- [20] J.D. Jobson, *Applied Multivariate Data Analysis*, Springer, New York, 1992.
- [21] H.A.L. Kiers, *Psychometrika* 62 (1997) 579–598.
- [22] H.A.L. Kiers, *J. Classification* 15 (1998) 245–268.
- [23] C.A. Andersson, R. Henrion, submitted to *Comp. Stat. Data Anal.*
- [24] L. Nørgaard, *Zuckerindustrie* 120 (1995) 970–981.
- [25] C.A. Andersson, L. Munck, R. Henrion, G. Henrion, *Fresenius J. Anal. Chem.* 359 (1997) 138–142.
- [26] C.A. Andersson, R. Bro, *Chemom. Intell. Lab. Syst.* 42 (1998) 93–105.

II. Algorithms, models and applications

P3

**A general algorithm for
obtaining simple structure of
core arrays in N -way PCA with
application to fluorometric data**

Claus A. Andersson and Rene Henrion



ELSEVIER

Computational Statistics & Data Analysis 31 (1999) 255–278

COMPUTATIONAL
STATISTICS
& DATA ANALYSIS

www.elsevier.com/locate/csda

A general algorithm for obtaining simple structure of core arrays in N -way PCA with application to fluorometric data

Claus A. Andersson^{a,*}, Rene Henrion^b

^a*Royal Veterinary and Agricultural University, Department of Food Technology, Chemometrics Group, Rolighedsvej 30, DK-1958 Frederiksberg, Denmark*

^b*Weierstraß Institute for Applied Analysis and Stochastics, Mohrenstr. 39, D-10117 Berlin, Germany*

Received 1 February 1998; received in revised form 1 January 1999; accepted 18 March 1999

Abstract

Simplifying the structure of core arrays from N -way PCA or Tucker3 models is desirable to allow for easy interpretation of the factor estimates. In the present paper, first a general algorithm for maximizing a differentiable goal function depending on a set of orthogonal matrices is formulated and then specified to the problem of estimating orthonormal transformation matrices for rotating core arrays to simpler structure. The generality of the chosen approach allows to cope with all possible transformation criteria by just changing one command in the implementation. In particular, the classical body- and slice-wise diagonalization of core arrays as well as the recently proposed maximization of the variance of squared entries are covered. The stability of the algorithm is addressed by a simulation study using 120 three-way core arrays of dimension (4,4,4). Each core array instantiates a class of 50 equivalent cores by random orthonormal transformations. Theoretically, each core within a given class has the same optimum with respect to the chosen criterion, and the ability of the algorithm to provide that result has been investigated. The algorithm proves to work with a high degree of stability and consistency in optimizing the three discussed goal functions. In addition, theoretical convergence results of the algorithm are provided. In particular, monotonic convergence of functional values and convergence of iterates towards a stationary solution are proven. To illustrate the effect of maximizing the variance-of-squares and the functionality of the algorithm, the proposed method is applied to a three-way data array from fluorometric analysis of fractions obtained from low-pressure chromatographic separation of a preliminary sugar product, *thick juice*. A significant gain in simplicity is achieved, and in particular optimizing variance-of-squares provides a simple core structure for the data

* Corresponding author. Fax: +45-352-83502.

E-mail addresses: claus@andersson.dk (C.A. Andersson), henrion@wias-berlin.de (R. Henrion)

under investigation. The proposed algorithms for maximizing variance-of-squares, body diagonality and slice-wise diagonality have been implemented in MATLAB and are available by contact to the authors. © 1999 Elsevier Science B.V. All rights reserved.

Keywords: N -way principal component analysis; N -mode factor analysis; Multi-linear modelling; Tucker3 model; Core array; Body diagonality; Variance-of-squares; Factor rotation; Orthogonal transformation; Exploratory modelling; PCA

1. Introduction

Having its roots in the field of psychometrics, the Tucker3 model of N -way principal component analysis (PCA), see Tucker (1966) and Kapteyn et al. (1986), is applied more and more often within chemometrics in the context of multivariate calibration or explanatory data analysis, see e.g. De Ligny et al. (1984), Zeng and Hopke (1990), Smilde (1992), Henrion et al. (1997) and Andersson et al. (1997). In both cases, a huge amount of data, arranged in higher-dimensional arrays, is produced by modern analytical devices. N -way PCA serves as one possible tool for subsequent data reduction. The corresponding model reads as (see Magnus and Neudecker, 1988 for details):

$$\text{vec } \mathbf{X} \approx (\mathbf{A}_1 \otimes \cdots \otimes \mathbf{A}_N) \text{vec } \mathbf{C}. \quad (1)$$

Here, \mathbf{X} represents the N -way data array of order (n_1, \dots, n_N) and \mathbf{A}_i of order (n_i, s_i) is the orthonormal component matrix belonging to the i th way. The array \mathbf{C} of order (s_1, \dots, s_N) designates the core array, while vec and \otimes refer to vectorization and Kronecker product, respectively.

A specific aspect of the N -way PCA model is its non-uniqueness in the sense that the factors, together with the core array, can be rotated without loss of fit: Transforming each of the component matrices \mathbf{A}_i in (1) to $\mathbf{A}_i \mathbf{P}_i$ by means of orthonormal matrices \mathbf{P}_i of order (s_i, s_i) , the same approximation to the data array in (1) is obtained when transforming the original core array \mathbf{C} to

$$\text{vec } \tilde{\mathbf{C}} = (\mathbf{P}_1^T \otimes \cdots \otimes \mathbf{P}_N^T) \text{vec } \mathbf{C}. \quad (2)$$

The resulting core, designated by $\tilde{\mathbf{C}}$, is of equal order as \mathbf{C} . For later argumentation, it is important to note that the sum of squared elements of core arrays is invariant under the above transformation.

The core array provides a way to interpret the solutions since its squared entries represent the relative importance of the factor combinations from different (orthonormal) component matrices in terms of explained variability. Therefore, it is desirable to have a few significant entries in the core array allowing for easy identification of the significant factor combinations. Such factor combinations will reflect the latent behaviour or pattern in the data. But, often the core array does not facilitate direct interpretation because the squared entries are of equal magnitude giving no direct pointer to major trends and systematics in data. Then, the rotational degree of freedom described by (2) may be used to accommodate for this situation. A common

feature of different approaches in this direction is the aim of giving the core a simple structure by optimizing a well-defined goal function that quantifies the simplicity of the core.

Much of the work devoted to increasing the interpretability of the N -way PCA model has been concerned with estimating orthogonal rotation matrices that could transform the solution to give a more unambiguous interpretation, see Kiers (1992). The present work will focus on the common algorithmic aspect of applying orthonormal core transformations (2) for optimizing any differentiable criterion of core simplicity (for the latest work on *oblique* rotations the reader is referred to Kiers, 1999). Special attention will be paid to the variance-of-squares criterion as a recently proposed goal function, see Henrion and Andersson (1999), as well as to some more classical diagonalization criteria. The potential of the presented approach lies in its generality, so for a new criterion of core simplicity, no specific algorithm has to be re-designed. The stability of the algorithm is illustrated by application to a large amount of synthesized, well-characterized, cores. Furthermore, theoretical convergence properties are studied. The discussion concludes with an application to data collected at-line in industrial production of sugar.

2. Criteria for simple-structure transformations

The squared core entries reflect the significance of the factor combinations in the model. In order to allow for easy and correct interpretation, it is desirable to obtain as simple a core structure as possible. If the core can be brought to a simple structure where only a few but very large elements are present, the analyst may focus on these respective factor combinations. The worst case is the situation where all elements in the core are equal, thereby indicating that no significant single factor combination could be found. The concept of rotating core arrays from three-way PCA originates from Tucker (1966) and the field of multidimensional scaling, e.g. De Leeuw and Pruzansky (1978) and Carroll and Wish (1974). For the moment we will leave out of discussion *how* the measures are maximized and focus on the goal functions.

Classical criteria of core simplicity refer to diagonal shapes. Understanding diagonalness of a square N -way core array of order (s, \dots, s) in a strict sense means that all non-zero elements should be located on the so-called body diagonal of the array, i.e. $C_{i_1, \dots, i_N} = 0$ unless $i_1 = \dots = i_N$. In general, of course, core arrays cannot be transformed via (2) to exact body diagonality. All one can do is to maximize the sum of the squared entries on the body diagonal:

$$\max \sum_{i=1}^s C_{i, \dots, i}^2 \tag{3}$$

Since the total sum is invariant under the transformation (2), this will simultaneously minimize the off-diagonal sum of squares, hence body diagonal shape is approached as close as possible. An algorithm for maximizing the body diagonal of three-way cores has been proposed by Kiers (1992). The whole approach applies to square N -way cores of order (s, \dots, s) only. An N -way PCA model with all

off-diagonal core elements being zero corresponds to the N -way PARAllel FACTors (PARAFAC) model (Harshman, 1970) and the CANonical DECOMPosition (CAN-DECOMP) model (Carroll and Chang, 1970), with the factors being constrained to orthogonality. The term *degree of diagonality* refers to the ratio between the sum of squares of the diagonal elements and the total sum of squares of the core array. According to the statements above, this degree has values between zero and one (exact body diagonality), and it may serve to compare the diagonality structure of cores with different total sum of squares.

A weaker concept of diagonality refers to slices of the core array along one fixed, say the N th, mode. In order to give sense to the concept of slice diagonality, the $(N - 1)$ -dimensional slices of the core have to be square arrays, i.e. the core has to have the order (s, \dots, s, s_N) . For $N = 3$, the slices are square matrices then, but the entire array need not be square. For slice-wise diagonal cores, the N -way PCA model reduces to a PARAFAC model again, but now with factors that are not necessarily independent. An algorithm for slice-wise diagonalization of 3-way arrays has been proposed by Kroonenberg (1983). The goal function to be maximized now becomes

$$\max \sum_{j=1}^{s_N} \sum_{i=1}^s C_{i, \dots, i, j}^2. \tag{4}$$

In analogy with diagonality, the *degree of slice-wise diagonality* refers to the ratio between the sum of squared slice-wise diagonal elements and the total sum of squared core elements.

Both of the diagonalization approaches focus on optimizing pre-defined elements in the core array, hence, it is implicitly assumed that the data are well described by these respective factor combinations. Possibly significant off-diagonal entries are not maximized. The variance-of-squares measure, recently introduced in Henrion and Andersson (1999), allows to detect significant factor combinations without using any *a priori* assumption on the structure like diagonality. This more flexible approach to core simplification usually leads to a smaller number of significant core entries than with diagonalization procedures. Of course, an interpretation in terms of PARAFAC, as given above, fails then, since the significant elements can be located anywhere in the core. The criterion to be maximized measures the variance of the squared core entries:

$$\max \sum_{i_1=1}^{s_1} \dots \sum_{i_N=1}^{s_N} (C_{i_1, \dots, i_N}^2 - \bar{C})^2, \tag{5}$$

$$\bar{C} = \prod_{i=1}^N s_i^{-1} \sum_{i_1=1}^{s_1} \dots \sum_{i_N=1}^{s_N} C_{i_1, \dots, i_N}^2. \tag{6}$$

In contrast to any measures of diagonality the variance-of-squares is defined for cores that are non-square. To summarize, Fig. 1 depicts what elements are used during optimization of the three goal functions. Fig. 1a illustrates two elements on a body diagonal of an array of order (2,2,2). Accordingly, Fig. 1b shows the diagonal elements taken slice-wise in the third way. In Fig. 1c the variance-of-squares expression is indicated by letting all entries in the core array contribute to the goal function.

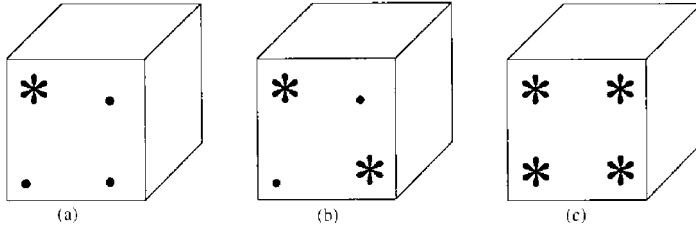


Fig. 1. The differences between the three discussed goal functions for a core array of order (2,2,2) are depicted (a) Maximizing sum of squares of the body diagonal elements, (b) maximizing sum of squares of the slice-wise diagonal elements and (c) maximizing the variance-of-squares using all elements in the core.

In accordance with the diagonality criteria, it would be desirable to define a degree for the variance-of-squares criterion in order to compare different cores. For the diagonality criteria, the maximum possible value which could be obtained within a class of cores of common order and having equal sum of squares is the total sum of squares. Since this value and, hence, the mean value in (6), are invariant under the transformation (2), it is easy to show that the theoretical maximum of the variance-of-squares criterion is attained in the situation where all core elements but one are zero. Then, the non-zero element has to account for the total sum of squares of the core, which is the constant $p\bar{C}$, where $p = \prod_{i=1}^N s_i$ refers to the total number of elements (cf. (6)). Therefore, the variance of squares for such a core equals $(p\bar{C} - \bar{C})^2$ (deviation from mean of the non-zero element) plus $(p - 1)(0 - \bar{C})^2$ (deviation from mean of the $p - 1$ zero elements) which gives $p(p - 1)\bar{C}^2$. In general, a given core cannot be transformed into one with a single non-zero element only, hence this situation is the theoretical limit which the actual transformation may be related to. Due to the invariance of the mean value \bar{C} , this limit can be calculated from any given core. Now, the *degree of variance-of-squares* is defined as the ratio between the actual variance-of-squares and the theoretical maximum $p(p - 1)\bar{C}^2$.

3. An algorithm for optimal orthogonal core transformations

In this section, we develop a general algorithm for finding an optimal orthonormal N -way core transformation according to a specific criterion. In particular, the above-described variance-of-squares maximization, and also the classical body and slicewise diagonalization are included. Since all these transformations can be simultaneously realized by a procedure with common basic structure, we establish a general-purpose algorithm first, which applies to the optimization of any (differentiable) criterion of orthonormal matrices and not just to the three special cases mentioned above in the context of core transformations.

II. Algorithms, models and applications

3.1. Proposal for a general-purpose algorithm

Denote by $\mathcal{O}(n)$ the manifold of orthogonal matrices of order (n, n) and consider the optimization problem

$$(P) \quad \max\{v(P_1, \dots, P_N) \mid P_i \in \mathcal{O}(n_i); i = 1, \dots, N\},$$

where $v: \mathcal{M}(n_1) \times \dots \times \mathcal{M}(n_N) \rightarrow \mathbb{R}$ is a differentiable function and $\mathcal{M}(n)$ refers to the space of matrices of order (n, n) . The orthogonality constraints above may be written as $P_i^T P_i = I_{n_i}$ ($i = 1, \dots, N$). Denoting by A_i ($i = 1, \dots, N$) any multiplier matrix, we define the Lagrangian function

$$f: \mathcal{M}(n_1) \times \dots \times \mathcal{M}(n_N) \times \mathcal{M}(n_1) \times \dots \times \mathcal{M}(n_N) \rightarrow \mathbb{R}$$

via

$$f(P_1, \dots, P_N, A_1, \dots, A_N) = v(P_1, \dots, P_N) - \sum_{i=1}^N \text{tr} [A_i (P_i^T P_i - I_{n_i})].$$

Now, since the orthogonality constraints define a regular surface in $\mathcal{M}(n_1) \times \dots \times \mathcal{M}(n_N)$, it follows that, if $(\bar{P}_1, \dots, \bar{P}_N)$ is a solution of the Problem (P), then there exist *symmetric* multiplier matrices A_i ($i = 1, \dots, N$) (see Magnus and Neudecker, 1988), such that $(\bar{P}_1, \dots, \bar{P}_N, A_1, \dots, A_N)$ is a stationary point of f (i.e. the derivative of f vanishes at that point).

Writing down the stationary conditions gives

$$\frac{\partial v}{\partial P_i}(\bar{P}_1, \dots, \bar{P}_N) - 2\bar{P}_i A_i = 0 \quad (i = 1, \dots, N), \tag{7}$$

$$\bar{P}_i^T \bar{P}_i - I_{n_i} = 0 \quad (i = 1, \dots, N). \tag{8}$$

Here, we made use of the convention that $\partial v / \partial P_i$ is a matrix of same order as P_i with general entry $(\partial v / \partial P_i)_{kl} = \partial v / \partial p_{kl}$, where the last expression refers to the usual partial derivative of v with respect to the general entry p_{kl} of P_i . This special arrangement of partial derivatives is useful in the context of matrix calculus. Later, we shall also work with the conventional definition of the partial gradient $\nabla_{P_i} v$ considered as a linear function assigning to each $Q \in \mathcal{O}(n_i)$ the scalar

$$\langle \nabla_{P_i} v, Q \rangle = \sum_{k,l} \frac{\partial v}{\partial p_{kl}} q_{kl}.$$

From here, the following relation between the two notions is obvious:

$$\langle \nabla_{P_i} v, Q \rangle = \text{tr} \left[\frac{\partial v}{\partial P_i} Q^T \right]. \tag{9}$$

Of course, (8) means nothing else than the required orthogonality of $\bar{P}_1, \dots, \bar{P}_N$, so the interesting part is contained in (7). Multiplying the i th condition of this set from the left by \bar{P}_i^T , provides (by orthogonality)

$$\bar{P}_i^T \frac{\partial v}{\partial P_i}(\bar{P}_1, \dots, \bar{P}_N) = 2A_i \quad (i = 1, \dots, N).$$

II. Algorithms, models and applications

From these equations it follows that for any stationary solution $(\bar{P}_1, \dots, \bar{P}_N)$ of the problem (P) the matrices on the left-hand side have to be symmetric. Conversely, if we find orthogonal \bar{P}_i , such that the mentioned matrices are symmetric, then we have obtained a stationary solution of problem (P) . This follows after left-multiplication of the above relation by \bar{P}_i leading back to (7) and (8) due to orthogonality of the \bar{P}_i . Summarizing, $(\bar{P}_1, \dots, \bar{P}_N)$ is a stationary solution of problem (P) if and only if the matrices

$$\bar{P}_i^T \frac{\partial v}{\partial \bar{P}_i}(\bar{P}_1, \dots, \bar{P}_N) \quad (10)$$

are symmetric for $i=1, \dots, N$. Therefore, it is desirable to have an algorithm iterating on orthogonal P_i , thereby ‘symmetrifying’ the above matrices. This is realized by the following algorithm:

Algorithm 1.

1. Set $P_i^0 := I_{n_i}$ ($i=1, \dots, N$) and $k:=0$
2. Set $k:=k+1$ and $i:=0$
3. Set $i:=i+1$ and compute an orthogonal matrix $P_i^k := U^T V^T$, such that

$$U \left[\frac{\partial v}{\partial P_i}(P_1^k, \dots, P_{i-1}^k, P_i^{k-1}, \dots, P_N^{k-1}) \right] V = \text{diag}[d_1, \dots, d_{n_i}],$$

where $U, V \in \mathcal{O}(n_i)$, $d_1 \geq \dots \geq d_{n_i} \geq 0$ (i.e. U and V provide a singular value decomposition of the derivative matrix). If $i < N$, then goto 3.

4. If $v(P_1^k, \dots, P_N^k)$ significantly differs from $v(P_1^{k-1}, \dots, P_N^{k-1})$, then goto 2.
5. Stop

The motivation behind step 3 is that it provides a symmetrification in the sense of (10). Indeed, one has

$$P_i^{kT} \left[\frac{\partial v}{\partial P_i}(P_1^k, \dots, P_{i-1}^k, P_i^{k-1}, \dots, P_N^{k-1}) \right] = V \text{diag}[d_1, \dots, d_{n_i}] V^T = S$$

where S is a symmetric matrix.

Note that the proposed method does not depend on the concrete structure of the function v to be maximized in problem (P) , therefore it applies as a general-purpose algorithm for maximizing (or minimizing after passing to $-v$) a differentiable function of N orthogonal matrices of possibly differing orders.

3.2. Application to core transformations

Now, we are going to specialize the developed general algorithm to the case of core transformations. All one has to do, according to the preceding section, is to calculate the partial derivatives $\partial v / \partial P_i$ of the corresponding criteria v with respect to the transformation matrices P_i . This turns out to be rather difficult, however, when evaluating at general current iterates whereas it is quite easy to compute at identity matrices. In the following, we shall develop an appropriate modification

II. Algorithms, models and applications

of the algorithm described above taking into account the specific structure of core transformations.

It is important to note that, in the context of core transformation, the criteria depend on the transformation matrices in a composite way: the criterion is a function of the core array which in turn depends on the transformation matrices. Given a core array C and orthonormal matrices P_1, \dots, P_N , we denote the core array transformed according to (2) by

$$T(P_1, \dots, P_N; C) = (\mathbf{P}_1^T \otimes \dots \otimes \mathbf{P}_N^T) \text{vec } C. \tag{11}$$

Now, the criterion as a function of transformation matrices writes as a composition

$$v(P_1, \dots, P_N) = \tilde{v}(T(P_1, \dots, P_N; C^0)),$$

where C^0 is the original core array and \tilde{v} denotes the criterion as a function of the core array. For the three transformations to be considered here, one has

$$\text{variance of squares} \quad \tilde{v}_1(C) = \sum_{i_1=1}^{s_1} \dots \sum_{i_N=1}^{s_N} (C_{i_1, \dots, i_N}^2 - \bar{C})^2, \tag{12}$$

$$\text{body diagonality} \quad \tilde{v}_2(C) = \sum_{i=1}^s C_{i, \dots, i}^2, \tag{13}$$

$$\text{slice diagonality} \quad \tilde{v}_3(C) = \sum_{j=1}^{s_N} \sum_{i=1}^s C_{i, \dots, i, j}^2. \tag{14}$$

Let us consider the very first step ($k = 1, i = 1$) of the algorithm above: The initial transformation matrices are identity matrices and in step 3 one has to compute the partial derivative

$$\frac{\partial v}{\partial P_1}(I_{s_1}, \dots, I_{s_N}) = \frac{\partial \tilde{v}}{\partial C}(C^0) \frac{\partial T}{\partial P_1}(I_{s_1}, \dots, I_{s_N}; C^0) \tag{15}$$

according to the chain rule. The right-hand side matrices are easily calculated as will be seen later on. First note, however, that in the following iteration ($k = 1, i = 2$) of the algorithm, the partial derivative is no longer taken at a complete set of identity matrices but at $(P_1^1, I_{s_2}, \dots, I_{s_N})$, where P_1^1 is the current iterate obtained in step 3 of the previous iteration. So, in the course of iterations, the convenient possibility of evaluating the partial derivatives at identity matrices gets lost. Yet, by a simple modification, this difficulty may be overcome. Let us illustrate this for the second iteration: Define a function

$$v^*(P_1, \dots, P_N) := v(P_1^1 P_1, P_2, \dots, P_N).$$

Obviously, the maximization of v^* is equivalent to the maximization of v , since any solution of the one criterion is immediately transformed into a solution of the other.

Therefore, instead of continuing the maximization of v as proposed in the original algorithm (with $k = 1, i = 2$), one may restart the whole algorithm at the beginning, but now maximizing v^* and iterating on P_2 instead. Starting again with identity

II. Algorithms, models and applications

matrices means to keep the current value of the old criterion, since $v^*(I_{s_1}, \dots, I_{s_N}) = v(P_1^1, I_{s_2}, \dots, I_{s_N})$. From the definitions, one gets

$$v^*(P_1, \dots, P_N) = \tilde{v}(T(P_1^1 P_1, \dots, P_N; C^0)) = \tilde{v}(T(P_1, \dots, P_N; C^1)),$$

where $C_1 = T(P_1^1, I_{s_2}, \dots, I_{s_N}; C^0)$ is the updated core array after applying the transformation matrices $P_1^1, I_{s_2}, \dots, I_{s_N}$ to the original core C^0 . In order to apply step 3 of the algorithm, one has to calculate now the partial derivative $\partial v^*/\partial P_2$ at the identity matrices, so – again by the chain rule – it results

$$\frac{\partial v^*}{\partial P_2}(I_{s_1}, \dots, I_{s_N}) = \frac{\partial \tilde{v}}{\partial C}(C^1) \frac{\partial T}{\partial P_2}(I_{s_1}, \dots, I_{s_N}; C^1).$$

Now it is clear how to proceed: calculate the second transformation matrix P_1^2 as to symmetrize the matrix $P_1^{2T}(\partial v^*/\partial P_2)(I_{s_1}, \dots, I_{s_N})$ (compare step 3 of the algorithm), update the core array by $C^2 = T(I_{s_1}, P_1^2, I_{s_3}, \dots, I_{s_N}; C^1)$, and, in the next iteration evaluate the partial derivative according to

$$\frac{\partial \tilde{v}}{\partial C}(C^2) \frac{\partial T}{\partial P_3}(I_{s_1}, \dots, I_{s_N}; C^2)$$

(without explicit reference to a newly defined v^{**}). In this way, one gets a sequence of core arrays maximizing the considered criterion.

Summarizing, the following algorithm for optimal core transformation with respect to one of the three criteria \tilde{v} introduced above is proposed:

Algorithm 2.

1. Set $C^{\text{new}} := C^0$ (=original core array), $P_j^{\text{new}} := I_{s_j}$ ($j = 1, \dots, N$) and $k := 0$
2. Set $k := k + 1$ and $j := 0$
3. Set $j := j + 1$, $C^{\text{old}} := C^{\text{new}}$, $P_j^{\text{old}} := P_j^{\text{new}}$ and compute an orthonormal matrix $P := U^T V^T$ such that

$$U \left[\frac{\partial \tilde{v}}{\partial C}(C^{\text{old}}) \frac{\partial T}{\partial P_j}(I_{s_1}, \dots, I_{s_N}; C^{\text{old}}) \right] V = \text{diag}[d_1, \dots, d_{n_i}],$$

where $U, V \in \mathcal{O}(n_i)$, $d_1 \geq \dots \geq d_{n_i} \geq 0$.

Set $C^{\text{new}} := T(I_{s_1}, \dots, I_{s_{j-1}}, P, I_{s_{j+1}}, \dots, I_{s_N}; C^{\text{old}})$ and $P_j^{\text{new}} := P_j^{\text{old}} P$. If $j < N$, then goto 3.

4. If $\tilde{v}(C^{\text{new}})$ significantly differs from $\tilde{v}(C^{\text{old}})$, then goto 2.
5. Stop

The transformation matrices, leading from the original core array C^0 to the final core array C^{new} are given by P_j^{new} , i.e. $C^{\text{new}} = T(P_1^{\text{new}}, \dots, P_N^{\text{new}}; C^0)$. Step 3 is performed by singular-value decomposition as in Algorithm 1, so it remains to compute the matrix in brackets. The general element of the second factor in (15), which is common to all procedures, is obtained as

$$\left[\frac{\partial T_{i_1, \dots, i_N}}{\partial P_j}(I_{s_1}, \dots, I_{s_N}; C^{\text{old}}) \right]_{k,l} = \begin{cases} C_{i_1, \dots, i_{j-1}, k, i_{j+1}, \dots, i_N}^{\text{old}} & l = i_j, \\ 0 & l \neq i_j. \end{cases}$$

The general element of the first factor calculates for the three criteria according to

$$\begin{aligned} \left[\frac{\partial \tilde{v}_1}{\partial C} (C^{\text{old}}) \right]_{i_1, \dots, i_N} &= 4(C_{i_1, \dots, i_N}^{2, \text{old}} - \bar{C}) C_{i_1, \dots, i_N}^{\text{old}}, \\ \left[\frac{\partial \tilde{v}_2}{\partial C} (C^{\text{old}}) \right]_{i_1, \dots, i_N} &= \begin{cases} 2C_{i_1, \dots, i_1}^{\text{old}} & i_1 = \dots = i_N, \\ 0 & \text{else} \end{cases} \\ \left[\frac{\partial \tilde{v}_3}{\partial C} (C^{\text{old}}) \right]_{i_1, \dots, i_N} &= \begin{cases} 2C_{i_1, \dots, i_1, i_N}^{\text{old}} & i_1 = \dots = i_{N-1}, \\ 0 & \text{else.} \end{cases} \end{aligned}$$

Now, the expressions in brackets in step 3 become (by multiplication of the corresponding factors) for the three different methods

$$\begin{aligned} []_{k,l}^1 &= 4 \sum_{i_1=1}^{s_1} \dots \sum_{i_{j-1}=1}^{s_{j-1}} \sum_{i_{j+1}=1}^{s_{j+1}} \sum_{i_N=1}^{s_N} (C_{i_1, \dots, i_{j-1}, l, i_{j+1}, \dots, i_N}^{2, \text{old}} - \bar{C}) C_{i_1, \dots, i_{j-1}, l, i_{j+1}, \dots, i_N}^{\text{old}} C_{i_1, \dots, i_{j-1}, k, i_{j+1}, \dots, i_N}^{\text{old}}, \\ []_{k,l}^2 &= 2C_{l, \dots, l}^{\text{old}} \cdot C_{l, \dots, l, k, l, \dots, l}^{\text{old}} \quad (k \text{ at position } j), \\ []_{k,l}^3 &= \begin{cases} 2 \sum_{i_N=1}^{s_N} C_{l, \dots, l, i_N}^{\text{old}} \cdot C_{l, \dots, l, k, l, \dots, l, i_N}^{\text{old}} & (k \text{ at position } j) \quad \text{if } j < N, \\ 2 \sum_{i=1}^s C_{i, \dots, i, l}^{\text{old}} \cdot C_{i, \dots, i, k}^{\text{old}} & \text{if } j = N. \end{cases} \end{aligned}$$

It is interesting to note that the matrix $[]_{k,l}^3$ is automatically symmetric for $j = N$. Henceforth, the slice-wise diagonality remains unaffected by rotation for $j = N$, and with regard to algorithmic efficiency this last inner iteration should be omitted from the optimization scheme.

4. Validation of the algorithm

A large quantity of well-characterized core arrays have been simulated for the purpose of assessing the robustness of the proposed algorithm with respect to finding global, rather than local, optima. The core arrays have been synthesized especially for investigating the ability of the algorithm to find the global optima of the three discussed goal functions; variance-of-squares, diagonality and slice-wise diagonality. The amount and features of cores required for such an analysis can only be provided by synthesis.

4.1. Experimental

A number of 120 core arrays of dimensions (4,4,4) with random elements in the range -100 to $+100$ were synthesized. Each of the 120 synthesized cores were used to establish a class containing 50 core arrays by random orthonormal transformations of the same synthesized core array as described by (2). This ensures that all 50 core arrays within one class can be obtained from each other by an orthonormal transformation, and they are equal in this sense. By comparing the values of the 50 optimized measures within each class, an estimate can be made towards the ability

II. Algorithms, models and applications

of the algorithm to locate the global optimum. Rotated cores within each class have the same optimal value with regard to the three investigated measures. However, preliminary calculations on 80 simulated cores showed that for 11 core arrays the optimal value of the goal function was not found in approx. 10% of the cases. Thus, to enhance the probability of locating the global optimum, the algorithm was restarted 5 times with each core using random initial orthonormal rotation matrices. Additional restarts were performed until the two largest values of the goal function differed less than 1%. This scheme was used throughout the calculations and appears to be a feasible approach to the problem of non-global optima.

Computations were performed on a DELL 200 MHz Pentium Pro running MATLAB 5.1.0.421 under Windows NT 4.0. The MATLAB built-in function `rand()` was used for the purpose of generating random numbers.

4.2. Results

The results from applying the proposed algorithm to the synthesized cores are depicted in Fig. 2a–c. For each class two groups of core arrays are available; the

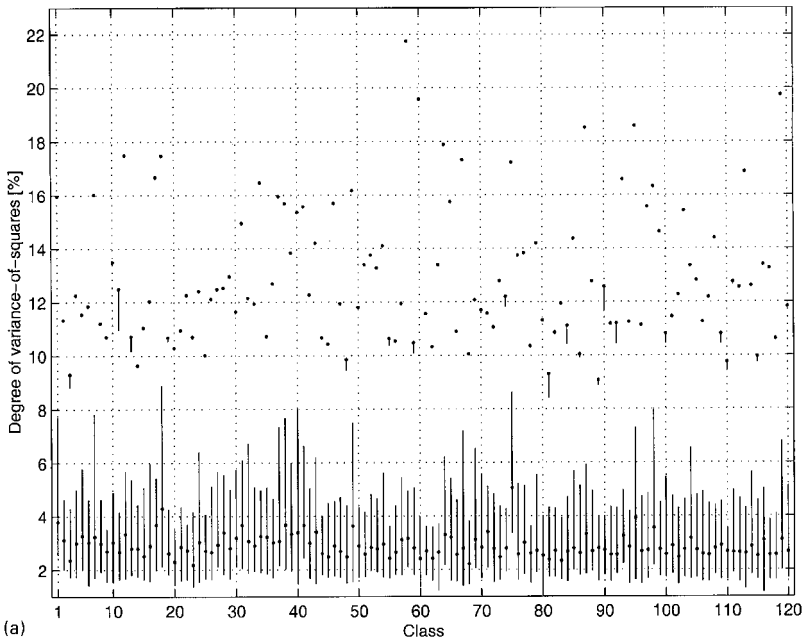


Fig. 2. Summary of the 120 classes each containing 50 cores derived from the same synthesized core array by random orthonormal transformations. The figure depicts the distribution of un-optimized and optimized goal function values for (a) variance-of-squares, (b) body diagonality and (c) slice-wise diagonality. The vertical line indicates the range from the minimum value to the highest value of the goal function. The dots indicate the medians of the two sets. See Section 4.2 for a detailed discussion.

II. Algorithms, models and applications

266

C.A. Andersson, R. Henrion / *Computational Statistics & Data Analysis* 31 (1999) 255–278

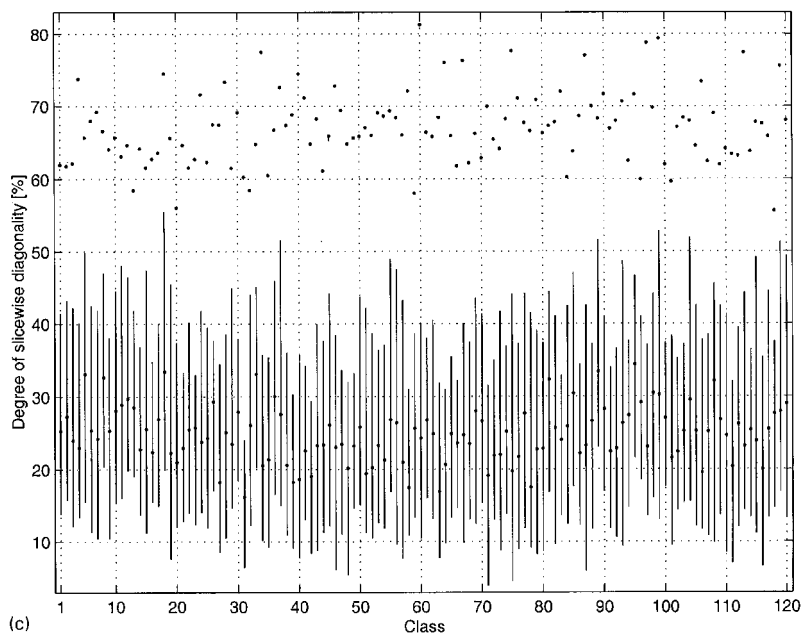
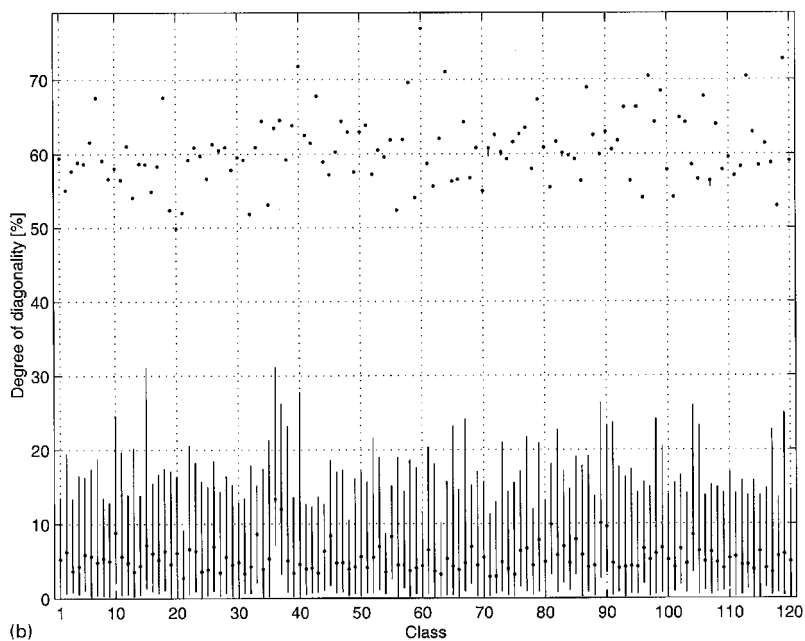


Fig. 2. Continued.

50 un-optimized core arrays and their optimized equivalents. The differences in the goal function values of the two groups are illustrated in Fig. 2a–c. For each distribution a vertical line connects the lowest observed value with the highest observed value and serves to illustrate the range of observations. The dot on each vertical line depicts the median of the observations. The goal function values for the un-optimized core arrays are, as expected, lower than the values of the same optimized core arrays. This is seen as a clear-cut separation between the two groups; the goal function values of the un-optimized core arrays are clearly lower and more spread than the goal function values of the core upon maximization. The function values upon optimization are in most cases so similar that there is no difference between the lowest and the highest of the returned goal function values. The gain of optimization is illustrated by the large differences between the respective measures before and after applying the algorithm. In addition, there is no overlap of the highest values of un-optimized cores with the lowest values of optimized cores, thus, all cores have gained in goal function value. Fig. 2a illustrates the degree of variance-of-squares before and after optimization. There generally is a tri-fold gain for this measure, providing a significant gain in simplicity for all classes. Within some classes, the optimal variance-of-squares core arrays obtained by the algorithm differ significantly in function values. E.g., for class no. 11 at least one of the returned cores have a suboptimal function value at approx. 11%, whereas the median clearly shows that the large part of the estimated optima are equal in value at approx. 12.5%. An important observation is that for all classes the median is similar to the highest value, this indicating, that by applying the algorithm several times a good estimate on the global optimum is found as the highest value. Fig. 2b represents the parameters for the optimization of the body diagonality. For the body diagonality version of the algorithm, the ranges within classes of the calculated optima are quite small. This observation confirms what was apparent during iterations; the optimal degrees of body diagonality within classes were more similar than for the values for variance-of-squares. The median of the distributions typically increase 8 times by optimization. Fig. 2c depicts the parameters for the optimization of slice-wise diagonality. The calculated optima are very close within classes, hence the algorithm for slice-wise diagonalization is slightly more stable in providing the global optima. This behaviour may be explained as follows: since there is no transformation matrix for the last mode, there is one less derivative matrix to return a non-global optimum and the algorithm is less prone to obtain a suboptimal rotation.

5. A three-way PCA of fluorometric measurements of thick juice

To exemplify the principle of maximizing the variance-of-squares and the use of the algorithm described in Section 3, we will apply the method to a core array derived from fluorometric measurements. To keep the focus on the proposed method we will restrict ourselves to discuss solely the core array and leave out detailed chemical interpretation.

In northern Europe white crystalline sugar is produced from sugar beets, i.e. *Beta Vulgaris*. The process is extremely complex and many of the unit processes involve recycled streams, see Larsson (1989). At different stages in the production, colour is formed due to combined effects of pH, temperature and the natural presence of colour precursors, polyphenolic oxidases, phenolic amino acids, carbonylic components and amino-N. The colour is a quality parameter which, in part, has influence on the classification of the final crystalline sugar product. From an economical standpoint it is therefore of great importance to be able to automatically control the operating conditions to give the whitest possible sugar and the most uniform product. Among the many possible intermediary products *thick juice* was chosen as a potential indicator of the degree of colouration in the final sugar. Thick juice is comparable in colour and viscosity to syrup. Spectrofluorometry has been selected for screening due to its sensitivity towards phenolic compounds and, to some extent, amino acids. See Nørgaard (1995) for a discussion of the suitability of spectrofluorometry as a screening method in the sugar process.

5.1. Experimental

From the 1994 production period, 15 thick juice samples were chosen. Each sample was separated into 28 fractions in a low-pressure liquid chromatography (LPLC) system. For each fraction, the fluorescence intensity for six combinations of excitation and emission wavelengths have been measured, thereby yielding a three-way array of order (15, 28, 6) corresponding to (samples, fraction, filter combination). Since the sensitivity and noise levels are equal for the measured filter combinations, it was chosen not to scale the data prior to modelling. However, due to the significant differences in levels of the intensities measured over the filter combinations data were centred over the latter mode.

5.2. Results

To determine the correct dimensionality of the model, a number of three-way PCA models were calculated and the fit to the data was evaluated for each model. The dimensions ranged from one to four factors in all modes, thus, a total of 37 valid models were calculated. It applies that not all combinations of 1–4 factors are valid since the product of the two smallest dimensions of the core must be equal to, or greater than, the largest dimension. E.g., valid dimensions are (1, 2, 2) and (2, 4, 2), whereas (1, 1, 2) and (1, 1, 4) are not. The dimensionality of the model is found under consideration of parsimony, and the chosen model must describe data well with as little complexity as possible since this minimizes the risk of overfit. In order to identify the model that is optimal in this sense, the 37 models were arranged in 13 groups according to the number of parameters in the core. For each group of cores with equal number of elements, the model explaining the highest amount of variation in the data was identified. The number of core elements is of direct interest for the analyst, since the higher the number of core elements, the more factor combinations

II. Algorithms, models and applications

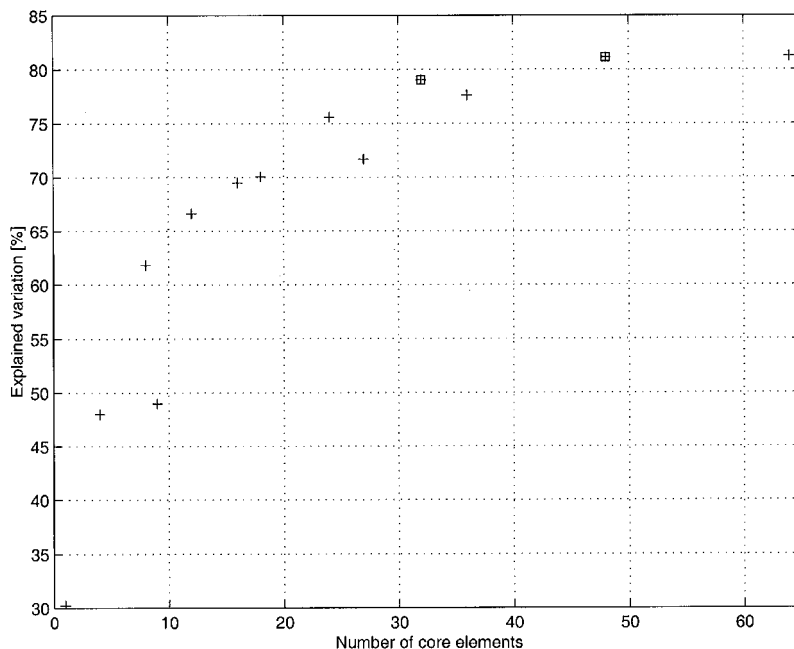


Fig. 3. A total of 37 three-way Tucker models of specified dimensions are calculated and each model is grouped according to the number of elements in the core. For each group the maximum degree of fit is plotted as a function of the number of core elements in the group. From the plot it is seen that the best model with 32 core elements explains 79.0% of the variation, see Section 5.2.

must be included in analysis and interpretation. One could undertake a view of model complexity in terms of the total number of parameters rather than just the number of parameters in the core. However, the complexity of the systematic behaviour of data is reflected by the dimensions of the core since the dimensions directly relate to the number of latent phenomenon in data. Thus, it is chosen to weigh the fit of the model against the complexity in terms of number of factors.

In Fig. 3 the highest explained variation in each of the 13 groups is plotted as a function of the number of core elements in the group. As indicated by the emphasized points, two groups are interesting; models having 32 and 48 core elements. Both these models provide a close fit to the data with a relatively low number of parameters in the core. When going from 32 core elements to 48, the explained variation increases merely from 79.0% to 81.1%. Thus, in order to make the interpretation manageable, the array with 32 elements is chosen for further analysis. The model with the highest explained variation in this group of models was found to have dimensions (4,4,2) indicating that four principal patterns prevail in the sample and fraction modes whereas two principal trends suffice to describe the variation of the filter combinations. The core array of the initial (i.e., un-rotated) model is

depicted by C^{raw} :

$$C^{\text{raw}} = \left(\begin{array}{cccc|cccc} 3256 & -2901 & 620 & 183 & 2702 & 2270 & -277 & -869 \\ 1986 & 1921 & 16 & 1601 & -1025 & 951 & 1632 & 152 \\ 742 & 735 & 949 & -940 & -329 & 67 & -1130 & 315 \\ -609 & 184 & 1168 & 548 & 232 & 249 & 30 & -580 \end{array} \right).$$

Bearing in mind that the squared value of any core element is proportional to the variation explained by the respective factor combination, inspection of C^{raw} reveals that there is no clear threshold allowing for a simple distinction between significant and insignificant core elements. This is a common problem when interpreting larger core arrays. Because the analyst cannot pin-point a few significant combinations of factors, interpretation may be rendered impossible. The variance-of-squares of C^{raw} is 2.22×10^{14} and the degree of variance-of-squares is 7.73%. Application of the algorithm described in Section 3 for optimizing variance-of-squares rotates C^{raw} into C^{vos} by orthonormal transformations.

$$C^{\text{vos}} = \left(\begin{array}{cccc|cccc} 4486 & 110 & -16 & -9 & 129 & 3509 & -198 & 373 \\ 301 & 2644 & 496 & -1215 & -1319 & -605 & 833 & -252 \\ 222 & -75 & -1249 & 662 & 37 & -537 & -3 & -609 \\ 39 & -414 & 569 & 1649 & 274 & -45 & -2009 & -324 \end{array} \right).$$

The variance-of-squares of C^{vos} is found to be 5.45×10^{14} which is 2.5 times higher than before rotation. With a sum of squared residuals at 1.443820401×10^7 the fit of the two models is verified to remain unaffected by the orthonormal transformation. In contrast to C^{raw} , the rotated core, C^{vos} , directs the analyst to a few significant combinations of factors. This is clearly illustrated in Fig. 4 where the squared value of each of the 32 elements is plotted against the respective ranking (solid lines). The squares of the elements level out slightly below 2×10^6 after the fifth element for the rotated core. Thus, the significant variation in data is accounted for by interpreting the factors represented by the five largest squared core elements. The sum of squares of these five squared elements is 4.62×10^7 , whereas the sum of squares of the five largest elements of the un-rotated core amounts to 3.54×10^7 as seen from the curves representing the cumulated values (dashed lines). The largest squared core element of the rotated core ($\approx 2 \times 10^7$) is approx. twice as high as the largest squared element of the unrotated core ($\approx 1 \times 10^7$), thus explaining twice the variation in the data. For comparison, a number of 9 core elements would have to be included in the interpretation of the un-rotated core to account for the same amount of variation.

As no body diagonal is defined for the (4,4,2) core array under investigation, the core cannot be optimized with respect to diagonality. For the sake of comparison and for proving the functionality of the algorithm, the core array has been optimized with respect to slice-wise diagonality over the last mode. The resulting core, C^{swdia} , is found to have a sum of squared slice diagonals of 3.80×10^7 corresponding to

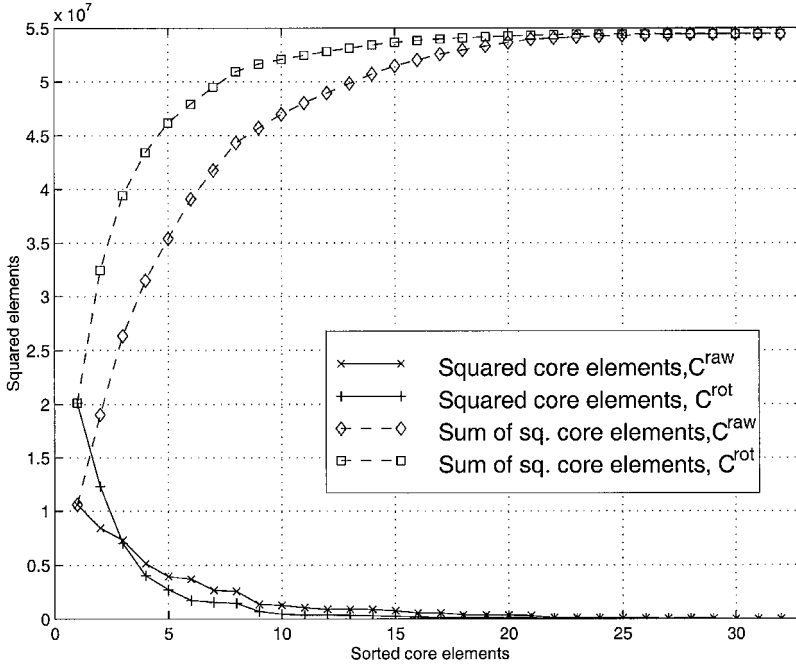


Fig. 4. Squared values of the 32 elements in the unrotated core and the rotated core are plotted against their ranking (solid lines). As expected, the rotated core has fewer and more significant core elements than does the unrotated core array. By following the course of the cumulated curves (dashed lines) it is concluded that for any given number of factor combinations the rotated core captures a significantly higher amount of variation of the data.

a degree of 69.8%:

$$C^{swdia} = \left(\begin{array}{cccc|cccc} 4252 & -762 & -8 & 554 & 1362 & 2213 & -356 & -1751 \\ 59 & 3179 & -191 & -224 & -1618 & 132 & 1217 & 773 \\ -42 & -628 & 1619 & -561 & 321 & -303 & -1533 & -489 \\ 283 & -54 & 363 & 1365 & 697 & 622 & 671 & -1049 \end{array} \right).$$

According to C^{swdia} the core can be diagonalized to some extent, albeit, not yielding few significant elements, although the diagonalization has provided the analyst with a core that is a little simpler than the initial core array, but not as simple as the core array that is optimal in a variance-of-squares sense.

6. Convergence properties of the algorithm

In this section, we study convergence properties of Algorithm 1 presented in Section 3.1. First, we are going to show that the sequence of iterates generated

II. Algorithms, models and applications

272 *C.A. Andersson, R. Henrion / Computational Statistics & Data Analysis 31 (1999) 255–278*

by this algorithm has monotonically nondecreasing values of the criterion to be maximized. As a preparatory step, we need the following lemma:

Lemma 1. *With a matrix A of order (n, n) associate the optimization problem*

$$\max\{\text{tr } PA \mid P \in \mathcal{O}(n)\}. \quad (16)$$

Then, the set of (global) solutions to (16) is given by

$$GS = \{P \in \mathcal{O}(n) \mid P = VU, (U, V) \in SV(A)\},$$

where

$$SV(A) = \{(U, V) \in \mathcal{O}(n) \times \mathcal{O}(n) \mid UAV = D, D \text{ is diagonal and nonnegative}\}$$

is the set of pairs of orthogonal matrices yielding an ‘unordered’ singular-value decomposition of A .

Proof. First note that $SV(A)$ consists of all pairs of orthogonal matrices providing a singular-value decomposition (in arbitrary order of singular values) of A . Now, writing down the first-order optimality conditions of (16), one verifies (similar to Section 3.1) the set of stationary solutions of this problem as being

$$SS = \{P \in \mathcal{O}(n) \mid PA \text{ is symmetric}\}.$$

Denote by $SEV(B)$ and $SSV(B)$ the sum of eigenvalues and singular-values, respectively, of a symmetric matrix B . Then,

$$\text{tr } PA = SEV(PA) \leq SSV(PA) = SSV(A) = \text{tr } QA \quad \forall (P, Q) \in SS \times GS \quad (17)$$

holds. Here, the first and second equality are obvious (recall the orthogonality of P), the inequality follows from the fact that the singular values of a symmetric matrix coincide with their absolute eigenvalues, and the last equality comes from the definition of GS :

$$\text{tr } QA = \text{tr } VUAVV^T = \text{tr } VDV^T = \text{tr } D = SSV(A),$$

due to the orthogonality of V and to D being a diagonal matrix of all singular values of A . Hence, the elements of GS realize a value of goal function which is not less than the value of the goal function of any element in SS , which in turn, being the set of stationary solutions to (16), contains the global solutions to (16). In conclusion, all elements of GS are global solutions. If, on the other hand, P is a global solution to (16), then $\text{tr } PA \geq \text{tr } QA$, where $Q \in GS$ is selected arbitrarily (a singular value decomposition of A always exists). As a global solution, P is a stationary solution as well, hence, $P \in SS$ and $SEV(PA) = SSV(PA)$ due to (17). Now, for the symmetric (due to $P \in SS$) matrix PA , there exists some $V \in \mathcal{O}(n)$ such that $V^T PAV = D$, where D is a nonnegative (by $SEV(PA) = SSV(PA)$) diagonal matrix. Consequently, D contains the singular values of PA and, hence, those of A . Defining $U := V^T P$, it follows that $P = VU$ and $(U, V) \in SV(A)$. This means $P \in GS$, hence the set of global solutions to (16) coincides with GS as was to be shown. \square

Corollary 1. *The choice of P_i^k in step 3 of Algorithm 1 corresponds to a selection*

$$P_i^k \in \text{argmax}\{\langle \nabla_{P_i} v(P_1^k, \dots, P_{i-1}^k, P_i^k, P_i^{k-1}, \dots, P_N^{k-1}), Q \rangle \mid Q \in \mathcal{O}(n_i)\}.$$

II. Algorithms, models and applications

Proof. By definition of step 3 of Algorithm 1 and according to Lemma 1, one has

$$P_i^k \in \operatorname{argmax} \left\{ \operatorname{tr} Q^T \left[\frac{\partial v}{\partial P_i} (P_1^k, \dots, P_{i-1}^k, P_i^{k-1}, \dots, P_N^{k-1}) \right] \mid Q \in \mathcal{O}(n_i) \right\}.$$

Now the assertion follows from (9). \square

Now, we are able to prove our first result on monotone convergence of functional values in Algorithm 1. To this aim, we refer to the criterion v as being partially convex, if it is convex in each variable P_i while the remaining ones are kept fixed. Of course, each convex v is partially convex, but the converse is not true. For instance, the function $f(x, y) = xy$ is partially convex (actually linear in both variables separately) but fails to be convex. We also recall that convexity of a differentiable function f implies the relation $f(y) - f(x) \geq \langle \nabla f(x), y - x \rangle$ for all x and y .

Lemma 2. *If the criterion v is partially convex, then the sequence $v(P_1^k, \dots, P_N^k)$ is nondecreasing with k .*

Proof. One has

$$\begin{aligned} & v(P_1^k, \dots, P_N^k) - v(P_1^{k-1}, \dots, P_N^{k-1}) \\ &= \sum_{i=1}^N v(P_1^k, \dots, P_{i-1}^k, P_i^k, P_{i+1}^{k-1}, \dots, P_N^{k-1}) \\ &\quad - v(P_1^k, \dots, P_{i-1}^k, P_i^{k-1}, P_{i+1}^{k-1}, \dots, P_N^{k-1}) \\ &\geq \sum_{i=1}^N \langle \nabla_{P_i} v(P_1^k, \dots, P_{i-1}^k, P_i^{k-1}, P_{i+1}^{k-1}, \dots, P_N^{k-1}), P_i^k - P_i^{k-1} \rangle \geq 0. \end{aligned}$$

Here, the first inequality relies on v being differentiable and partially convex, while the second inequality results from Corollary 1 due to $P_i^{k-1} \in \mathcal{O}(n_i)$. \square

For the three criteria v_1, v_2, v_3 of core simplicity, introduced in Section 2, one has $v_i = \tilde{v}_i \circ T$, where T and the \tilde{v}_i are defined by (11) and (12)–(14), respectively. Obviously, the \tilde{v}_i are convex functions (for \tilde{v}_1 , this follows from the invariance of the mean \tilde{C} in (6) under arbitrary orthogonal transformation T). On the other hand, the transformation T is multilinear, i.e. linear in each variable while the remaining ones are kept fixed. Consequently, the v_i are partially convex as compositions of a convex with a multilinear function. Furthermore, they are, of course, differentiable. Then, Lemma 2 allows to formulate the following result:

Corollary 2. *For the three criteria of core simplicity defined in Section 2, Algorithm 1 generates a sequence of iterates with monotonically nondecreasing values.*

II. Algorithms, models and applications

Now, we turn to the convergence of iterates themselves. For the purpose of abbreviation, we put bold face characters for N -tuples of matrices, i.e., $\mathbf{P} = (P_1, \dots, P_N)$. As a first immediate result, we have:

Lemma 3. *If the sequence \mathbf{P}^k of iterates generated by Algorithm 1 converges towards some \mathbf{P}^* , and if the criterion v is continuously differentiable, then \mathbf{P}^* is a stationary solution of Problem (P) introduced in Section 3.1.*

Proof. Let $i \leq N$ be arbitrarily given. By the remarks following the definition of Algorithm 1, one has that

$$P_i^{kT} \left[\frac{\partial v}{\partial P_i}(P_1^k, \dots, P_{i-1}^k, P_i^{k-1}, \dots, P_N^{k-1}) \right]$$

is a symmetric matrix. Passing to the limit $k \rightarrow \infty$, the above expression converges by the assumed continuous differentiability of v towards

$$P_i^{*T} \left[\frac{\partial v}{\partial P_i}(\mathbf{P}^*) \right],$$

which, as a limit of symmetric matrices, is symmetric itself and, according to (10) implies \mathbf{P}^* to be a stationary solution of Problem (P). \square

Hence, if the iterates converge, then their limit is a stationary point, as desired. However, there is no guarantee for the sequence \mathbf{P}^k to converge at all. On the other hand, since the \mathbf{P}^k belong to the compact set $S := \mathcal{O}(n_1) \times \dots \times \mathcal{O}(n_N)$, there must exist some convergent subsequence $\mathbf{P}^{k_l} \rightarrow_l \mathbf{P}^* \in S$. Unfortunately, Lemma 3 does not apply to this subsequence and one may not derive the usual convergence result, stating that all accumulation points of the sequence of iterates are stationary solutions. This will be possible after excluding some degeneracy: we shall call $\mathbf{P} \in S$ a nondegenerate point of v , if the singular values of $(\partial v / \partial P_i)(\mathbf{P})$ are pairwise distinct and strictly positive for all $i \leq N$. Then, we have:

Theorem 1. *Let v be continuously differentiable and partially convex (as it holds true for the three criteria of core simplicity defined in Section 2). Then each nondegenerate accumulation point of the sequence \mathbf{P}^k generated by Algorithm 1 is a stationary solution of problem (P) introduced in Section 3.1.*

Proof. Denote by $\mathbf{P}^* \in S$ any nondegenerate accumulation point of \mathbf{P}^k . The realization of step 3 in Algorithm 1 means that \mathbf{P}^{k+1} is defined by $P_i^{k+1} = (U_i^{k+1})^T (V_i^{k+1})^T$, where $U_i^{k+1}, V_i^{k+1} \in \mathcal{O}(n_i)$ provide a singular-value decomposition

$$U_i^{k+1} \left[\frac{\partial v}{\partial P_i}(P_1^{k+1}, \dots, P_{i-1}^{k+1}, P_i^k, \dots, P_N^k) \right] V_i^{k+1} = \text{diag} [d_{i,1}^{k+1}, \dots, d_{i,n_i}^{k+1}],$$

with $d_{i,1}^{k+1} \geq \dots \geq d_{i,n_i}^{k+1} \geq 0$ for $i = 1, \dots, N$. Since v was assumed to be continuously differentiable, the derivative $\partial v / \partial P_i$ is bounded on the compact set S for all i , hence

II. Algorithms, models and applications

so are its singular values. As a consequence, there exists a subsequence with

$$\begin{aligned} \mathbf{P}^{k_l} &\rightarrow_l \mathbf{P}^*; & (U_i^{k_l+1}, V_i^{k_l+1}, \text{diag}[d_{i,1}^{k_l+1}, \dots, d_{i,n_i}^{k_l+1}]) \\ & & \rightarrow_l (U_i^{**}, V_i^{**}, \text{diag}[d_{i,1}^{**}, \dots, d_{i,n_i}^{**}]). \end{aligned}$$

By definition of $P_i^{k_l+1}$ and by continuity of $\partial v / \partial P_i$, it follows that $\mathbf{P}^{k_l+1} \rightarrow_l \mathbf{P}^{**}$, where $\mathbf{P}_i^{**} = (U_i^{**})^T (V_i^{**})^T$ and

$$U_i^{**} \frac{\partial v}{\partial P_i} (P_1^{**}, \dots, P_{i-1}^{**}, P_i^*, \dots, P_N^*) V_i^{**} = \text{diag}[d_{i,1}^{**}, \dots, d_{i,n_i}^{**}] \tag{18}$$

with $d_{i,1}^{**} \geq \dots \geq d_{i,n_i}^{**} \geq 0$ for $i=1, \dots, N$. Furthermore, Lemma 2 along with the fact that $k_{l+1} \geq k_l + 1$ provide $v(\mathbf{P}^{k_{l+1}}) \geq v(\mathbf{P}^{k_l+1}) \geq v(\mathbf{P}^{k_l})$ and $v(\mathbf{P}^*) \geq v(\mathbf{P}^{**}) \geq v(\mathbf{P}^*)$, after passing to the limit $l \rightarrow \infty$. It results that $v(\mathbf{P}^*) = v(\mathbf{P}^{**})$.

Next we define the index set I to consist of those $i \leq N$ such that $P_i^* = U_i^T V_i^T$, where $U_i, V_i \in \mathcal{O}(n_i)$ provide any ‘unordered’ singular value decomposition

$$U_i \frac{\partial v}{\partial P_i} (P_1^{**}, \dots, P_{i-1}^{**}, P_i^*, \dots, P_N^*) V_i = \text{diag}[d_{i,1}, \dots, d_{i,n_i}],$$

with the $d_{i,j} \geq 0$ in arbitrary order. Suppose that $\{1, \dots, i'\} \subseteq I$ for some $i' \leq N$. Then, by definition of I , one gets $P_1^* = U_1^T V_1^T$, where $U_1, V_1 \in \mathcal{O}(n_1)$ provide an unordered singular value decomposition

$$U_1 \frac{\partial v}{\partial P_1} (P_1^*, \dots, P_N^*) V_1 = \text{diag}[d_{1,1}, \dots, d_{1,n_1}],$$

which after using some permutation matrix $\Pi \in \mathcal{O}(n_1)$ turns into a conventional singular value decomposition

$$\Pi U_1 \frac{\partial v}{\partial P_1} (P_1^*, \dots, P_N^*) V_1 \Pi^T = \text{diag}[d_{1,1}, \dots, d_{1,n_1}],$$

with $d_{1,1} \geq \dots \geq d_{1,n_1}$. From (18) it follows that $P_1^{**} = (U_1^{**})^T (V_1^{**})^T$, where

$$U_1^{**} \frac{\partial v}{\partial P_1} (P_1^*, \dots, P_N^*) V_1^{**} = \text{diag}[d_{1,1}^{**}, \dots, d_{1,n_1}^{**}]$$

provides another singular-value decomposition of the same derivative matrix. Now, the assumption of nondegeneracy of the accumulation point \mathbf{P}^* yields the uniqueness of the singular-value decomposition of $(\partial v / \partial P_1)(\mathbf{P}^*)$ (cf. Horn and Johnson, 1991, pp. 147–148). In particular, $U_1^{**} = \Pi U_1$ and $V_1^{**} = V_1 \Pi^T$ and, hence, $P_1^{**} = U_1^T \Pi^T \Pi V_1^T = U_1^T V_1^T = P_1^*$. In case that $i' \geq 2$, we proceed with the index 2 as before with the index 1 in order to see that $P_2^* = U_2^T V_2^T$ with some $U_2, V_2 \in \mathcal{O}(n_2)$ which provide a singular-value decomposition

$$\begin{aligned} \Pi U_2 \frac{\partial v}{\partial P_2} (P_1^*, P_2^*, \dots, P_N^*) V_2 \Pi^T &= \text{diag}[d_{2,1}, \dots, d_{2,n_2}] \\ &= \Pi U_2 \frac{\partial v}{\partial P_2} (P_1^*, \dots, P_N^*) V_2 \Pi^T, \end{aligned}$$

where again Π is some permutation matrix, and the last equation comes from the first one by using the identity $P_1^{**} = P_1^*$ proved before. Noting that, by (18),

$$U_2^{**} \frac{\partial v}{\partial P_2} (P_1^{**}, P_2^*, \dots, P_N^*) V_2^{**} = \text{diag}[d_{2,1}^{**}, \dots, d_{2,n_2}^{**}] = U_2^{**} \frac{\partial v}{\partial P_2} (P_1^*, \dots, P_N^*) V_2^{**}$$

II. Algorithms, models and applications

yields another singular value decomposition of the same derivative matrix on the right-hand side, the nondegeneracy of \mathbf{P}^* implies $P_2^{**} = P_2^*$ with the same argumentation as given before for the index 1. Proceeding like that for all indices $i \leq i'$, thereby consecutively exploiting the previously obtained relations $P_j^* = P_j^{**}$ for $j < i$, one ends up at the following statement:

$$\{1, \dots, i'\} \subseteq I \Rightarrow P_i^{**} = P_i^* \quad \forall i \leq i'. \tag{19}$$

Now suppose that $I \neq \{1, \dots, N\}$. Denote by $i^* \leq N$ the smallest index such that $i^* \notin I$. By definition of I , one has that $P_{i^*}^* \neq U^T V^T$ where U, V are arbitrary orthogonal matrices providing an ‘unordered’ singular-value decomposition of

$$\frac{\partial v}{\partial P_{i^*}}(P_1^{**}, \dots, P_{i^*-1}^{**}, P_{i^*}^*, \dots, P_N^*).$$

Then, Lemma 1 and (9) give (similar to the proof of Corollary 1)

$$P_{i^*}^* \notin \operatorname{argmax}\{\langle \nabla_{P_{i^*}} v(P_1^{**}, \dots, P_{i^*-1}^{**}, P_{i^*}^*, \dots, P_N^*), Q \rangle \mid Q \in \mathcal{O}(n_{i^*})\}. \tag{20}$$

On the other hand, a combination of (18), Lemma 1 and (9), implies for all $i \leq N$,

$$P_i^{**} \in \operatorname{argmax}\{\langle \nabla_{P_i} v(P_1^{**}, \dots, P_{i-1}^{**}, P_i^*, \dots, P_N^*), Q \rangle \mid Q \in \mathcal{O}(n_i)\}. \tag{21}$$

Now, (20) together with (21) applied to the index i^* leads to

$$\langle \nabla_{P_{i^*}} v(P_1^{**}, \dots, P_{i^*-1}^{**}, P_{i^*}^*, \dots, P_N^*), P_{i^*}^{**} - P_{i^*}^* \rangle > 0 \tag{22}$$

and

$$\begin{aligned} & v(\mathbf{P}^{**}) - v(\mathbf{P}^*) \\ &= \sum_{i=1}^N v(P_1^{**}, \dots, P_{i-1}^{**}, P_i^{**}, P_{i+1}^*, \dots, P_N^*) - v(P_1^{**}, \dots, P_{i-1}^{**}, P_i^*, P_{i+1}^*, \dots, P_N^*) \\ &\geq \sum_{i=1}^N \langle \nabla_{P_i} v(P_1^{**}, \dots, P_{i-1}^{**}, P_i^*, P_{i+1}^*, \dots, P_N^*), P_i^{**} - P_i^* \rangle > 0, \end{aligned}$$

where the first inequality relies on v being differentiable and partially convex as in the proof of Lemma 2. All terms in the last sum are nonnegative in view of (21), but at least the term with index i^* is strictly positive according to (22), whence the strict inequality. The last derivation, however, is in contradiction to the fact that $v(\mathbf{P}^{**}) = v(\mathbf{P}^*)$ which was proved above. Consequently, the assumption (following (19)) was false and it holds that $I = \{1, \dots, N\}$. As a result, for all $i \leq N$ the P_i^* may be written as products $U_i^T V_i^T$ where $U_i, V_i \in \mathcal{O}(n_i)$ and

$$U_i \frac{\partial v}{\partial P_i}(P_1^{**}, \dots, P_{i-1}^{**}, P_i^*, \dots, P_N^*) V_i = D = U_i \frac{\partial v}{\partial P_i}(\mathbf{P}^*) V_i$$

with some diagonal matrix D , where the second equality relies on (19). Then,

$$P_i^{*T} \frac{\partial v}{\partial P_i}(\mathbf{P}^*) = V_i D V_i^T$$

are symmetric matrices for all $i \leq N$ as required in the stationarity condition (10). Hence, we have shown, that \mathbf{P}^* is a stationary solution of problem (P). \square

We note that the proof of Theorem 1 follows the typical patterns of convergence proofs for algorithms in nonlinear optimization as developed, for instance, in Zangwill (1969). The nondegeneracy condition in Theorem 1 may be supposed to be satisfied in ‘almost all’ problems since it expresses the typical situation of all singular values of some matrix being distinct and strictly positive. Indeed, in all examples we considered so far, the algorithm asymptotically reached a stationary solution (characterized by (10)).

Acknowledgements

The authors wish to thank two anonymous referees for their constructive suggestions which led to an improved presentation of this paper. The first author is grateful to EU Affluence and FØTEK funds for financial support. The support provided by Prof. Lars Munck is greatly appreciated. Finally we thank Danisco Sugar for providing the week-samples of thick juice.

References

- Andersson, C.A., Munck, L., Henrion, R., Henrion, G., 1997. Analysis of N-dimensional data arrays from fluorescence spectroscopy of an intermediary sugar product. *Fresenius J. Anal. Chem.* 359, 138–142.
- Carroll, J.D., Chang, J., 1970. Analysis of individual differences in multidimensional scaling via an N-way generalization of the “Eckardt-Young” decomposition. *Psychometrika* 35, 283–319.
- Carroll, J.D., Wish, M., 1974. Models and methods for three-way multidimensional scaling. In: Krantz, D.H. (Ed.), *Contemporary Developments in Mathematical Psychology*, vol. 2, Freeman, San Francisco, pp. 57–105.
- De Leeuw, J., Pruzansky, S., 1978. A new computational method to fit the weighted Euclidean distance model. *Psychometrika* 43, 479–490.
- De Ligny, C., Spanjer, M., van Houwelingen, J., Weesie, H., 1984. *J. Chromatography* 301, 311–324.
- Harshman, R.A., 1970. Foundations of the PARAFAC procedure: model and conditions for an ‘explanatory’ multi mode factor analysis. *UCLA Working Papers in Phonetics*, vol. 16, pp. 1–84.
- Henrion, R., Andersson, C.A., 1999. A new criterion for simple-structure transformations of core arrays in N-way PCA. *Chemom. Intell. Lab. Syst.* 47, 189–204.
- Henrion, R., Henrion, G., Böhme, M., Behrendt, H., 1997. Three-way principal components analysis for fluorescence spectroscopic classification of algae species. *Fresenius J. Anal. Chem.* 352, 431–436.
- Horn, R.A., Johnson, C.R., 1991. *Topics in Matrix Analysis*. Cambridge University Press, Cambridge.
- Kapteyn, A., Neudecker, H., Wansbeek, T., 1986. An approach to n -mode components analysis. *Psychometrika* 51, 269–275.
- Kiers, H.A.L., 1992. TUCKALS3 core rotations and constrained TUCKALS modelling. *Statist. Appl.* 4, 659–667.
- Kiers, H.A.L., 1999. Three-way simplimax for oblique rotation of the three-mode factor analysis core to simple structure. *Comput. Statist. Appl. Data Anal.* 28, 307–324.
- Kroonenberg, P.M., 1983. *Three Mode Principal Component Analysis: Theory and Applications*. DSWO Press, Leiden.
- Larsson, H., 1989. *Svenskt Socker, Sockerbolaget, Vebjystelle, Sweden* (in Swedish).

II. Algorithms, models and applications

278 C.A. Andersson, R. Henrion / *Computational Statistics & Data Analysis* 31 (1999) 255–278

- Magnus, J.R., Neudecker, H., 1988. *Matrix Differential Calculus with Applications in Statistics and Econometrics*. Wiley, Chichester.
- Nørgaard, L., 1995. Classification and prediction of quality and process parameters of thick juice and beet sugar by fluorescence spectroscopy and chemometrics. *Zuckerindustrie* 120, 970–981.
- Smilde, A.K., 1992. Three-way analyses. Problems and prospects. *Chemom. Intell. Lab. Syst.* 15, 143–157.
- Tucker, L.R., 1966. Some mathematical notes on three-mode factor analysis. *Psychometrika* 31, 279–311.
- Zangwill, W.I., 1969. *Nonlinear Programming*. Prentice-Hall, Englewood Cliffs, NJ.
- Zeng, Y., Hopke, P.K., 1990. Methodological study applying three-mode factor analysis to three-way chemical data sets. *Chemom. Intell. Lab. Syst.* 7, 237–250.

II. Algorithms, models and applications

P4
**Improving the speed of multiway
algorithms. Part I: Tucker3**

Claus A. Andersson and Rasmus Bro



Improving the speed of multi-way algorithms: Part I. Tucker3

Claus A. Andersson^{*}, Rasmus Bro¹

Chemometrics Group, Food Technology, Department of Dairy and Food Science, Royal Veterinary and Agricultural University, Rolighedsvej 30, iii, DK-1958 Frederiksberg C, Denmark

Abstract

In an attempt to improve the speed of multi-way algorithms, this paper investigates several different implementations of the Tucker3 algorithm. The interest is specifically aimed at developing a fast algorithm in the MATLAB™ environment that is suitable for large data arrays. Nine different implementations are developed and tested on real and simulated data. In a subsequent paper, it will be demonstrated that a fast algorithm for the Tucker3 model provides a perfect basis for improving the speed of other multi-way algorithms. From the Internet address <http://newton.mli.kvl.dk/foodtech.html>, the developed algorithms can be downloaded. © 1998 Elsevier Science B.V.

Keywords: Tucker3; Three-mode factor analysis; 3-MFA; Three-way principal component analysis

1. Introduction

The Tucker3 model, or N -way PCA, is one of the most basic multi-way models used in chemometrics. It originates from psychometrics from the pioneering work of Tucker [1], and the algorithmic solution for estimating the model was later substantially improved by Kroonenberg and de Leeuw [2] and ten Berge et al. [3]. Several successful applications have been demonstrated in quite different areas such as chromatography [4], environmental analysis [5] and person perception analysis [6]. Having an efficient algorithm especially for large data sets is therefore of utmost importance. Several different algorithms have been described in the literature. Almost all are based on least squares regression, singular value decompo-

sition (SVD), Gram–Schmidt (GS) orthogonalization, or a modified Bauer–Rutishauer (BR) estimation. In this paper, all steps in the Tucker3 algorithm will be optimized with respect to speed. The focus will be on three-way models, but all results are equally applicable on models of higher orders [7]. In the sequel, nine different algorithms will be compared as they have been implemented in MATLAB, and it will also shortly be described how the algorithms can be modified to handle missing values and data with different uncertainties.

The sizes of the arrays considered are such that the computer has physical memory to hold the array and intermediate working arrays. If the array size exceeds what the physical computer memory can hold, other problems arise and other algorithms may be better (see Refs. [8–10]). These algorithms do not work with exact least-squares solutions, but rather try to approximate the solution by finding suitable bases

^{*} Corresponding author. E-mail: ca@kvl.dk.

¹ E-mail: rb@kvl.dk.

for the different modes. An efficient algorithm for the case of one large mode has also been proposed [11]. For arrays whose size does not exceed the potential computer power, it is not necessary to compress the array prior to modelling as most Tucker3 algorithms are quite fast. The purpose of this paper is to provide the fastest way of estimating the Tucker3 model, and implicitly providing suitable bases for the modes of large arrays.

2. Theory

In the following, scalars are indicated by italics, vectors by bold lower-case characters, bold capitals are used for two-way matrices, and underlined bold capitals for three-way arrays. The letters I , J , and K are reserved for indicating the dimension of the three different modes. The ijk th element of \mathbf{X} is called x_{ijk} and is the element in the i th row, j th column, and k th tube of \mathbf{X} . When three-way arrays are unfolded to matrices, the following notation will be used: If \mathbf{X} is an $I \times J \times K$ array and is unfolded to an $I \times JK$ matrix, the order of J and K indicates which indices are running fastest. In this case, the indices of J are running fastest, meaning that the first J columns of \mathbf{X} contain all variables for $k = 1$ and for $j = 1$ to $j = J$. In short, we will term the $I \times JK$ matrix $\mathbf{X}^{(1)}$, where the superscript indicates that it is the *first* mode that is preserved. Likewise $\mathbf{X}^{(2)}$ is a $J \times IK$ matrix and $\mathbf{X}^{(3)}$ a $K \times IJ$ matrix. If the arrangement of the array is clear from the context, the superscript will not be shown.

An $I \times J \times K$ array \mathbf{X} is given and a Tucker3 model of ranks R^A , R^B , and R^C respectively is sought. Written in matrix notation letting $\mathbf{X}^{(1)}$ be the $I \times JK$ unfolded array, and \otimes denoting the Kronecker product, the Tucker3 model reads

$$\mathbf{X}^{(1)} = \mathbf{A}\mathbf{G}^{(1)}(\mathbf{C}^T \otimes \mathbf{B}^T) + \mathbf{E}^{(1)}, \quad (1)$$

where $\mathbf{A}\mathbf{G}^{(1)}(\mathbf{C}^T \otimes \mathbf{B}^T)$ is the model of $\mathbf{X}^{(1)}$, $\mathbf{E}^{(1)}$ is the unmodelled part, i.e., the residuals of the model, and $\mathbf{G}^{(1)}$ is the core array \mathbf{G} arranged as an $R^A \times R^B R^C$ matrix. In Eq. (1), \mathbf{A} has size $I \times R^A$, \mathbf{B} has size $J \times R^B$, and \mathbf{C} has size $K \times R^C$ and the matrices hold the loadings in the first, second, and third mode, respectively. In the following, we will omit the residual part for simplicity. We restrict ourselves to

estimate the Tucker3 model with orthonormal \mathbf{A} , \mathbf{B} , and \mathbf{C} . We further restrict ourselves to algorithms based on iteratively estimating one of the four sets of parameters \mathbf{A} , \mathbf{B} , \mathbf{C} , and \mathbf{G} conditionally on the remaining parameters. In most cases, such an algorithm will be a so-called alternating least squares (ALS) algorithm.

The core array \mathbf{G} can be found conditional on \mathbf{A} , \mathbf{B} , and \mathbf{C} by a simple projection of \mathbf{X} onto \mathbf{A} , \mathbf{B} , and \mathbf{C} . In matrix notation this reads

$$\mathbf{G}^{(1)} = \mathbf{A}^T \mathbf{X}^{(1)} (\mathbf{C} \otimes \mathbf{B}) \quad (2)$$

If the model is perfect, then \mathbf{G} will express all variation of \mathbf{X} . For completeness, note that \mathbf{G} can also be computed from \mathbf{X} arranged as $\mathbf{J} \times \mathbf{IK}$ or a $\mathbf{K} \times \mathbf{IJ}$ matrices:

$$\mathbf{G}^{(2)} = \mathbf{B}^T \mathbf{X}^{(2)} (\mathbf{C} \otimes \mathbf{A}), \text{ and } \mathbf{G}^{(3)} = \mathbf{C}^T \mathbf{X}^{(3)} (\mathbf{B} \otimes \mathbf{A}), \quad (3)$$

From the definition of \mathbf{G} it follows that the Tucker3 model of \mathbf{X} can be stated

$$\begin{aligned} \mathbf{A}\mathbf{G}^{(1)}(\mathbf{C}^T \otimes \mathbf{B}^T) &= \mathbf{A}\mathbf{A}^T \mathbf{X}^{(1)} (\mathbf{C} \otimes \mathbf{B}) (\mathbf{C}^T \otimes \mathbf{B}^T) \\ &= \mathbf{A}\mathbf{A}^T \mathbf{X}^{(1)} (\mathbf{C}\mathbf{C}^T \otimes \mathbf{B}\mathbf{B}^T) \end{aligned} \quad (4)$$

For \mathbf{B} and \mathbf{C} fixed it follows that finding the optimal \mathbf{A} is equal to minimizing the norm of $(\mathbf{X} - \mathbf{A}\mathbf{A}^T \mathbf{M})$, where $\mathbf{M} = \mathbf{X}(\mathbf{C}\mathbf{C}^T \otimes \mathbf{B}\mathbf{B}^T)$. Using that

$$\begin{aligned} (\mathbf{C}\mathbf{C}^T \otimes \mathbf{B}\mathbf{B}^T) (\mathbf{C}\mathbf{C}^T \otimes \mathbf{B}\mathbf{B}^T)^T \\ = (\mathbf{C}\mathbf{C}^T \mathbf{C}\mathbf{C}^T \otimes \mathbf{B}\mathbf{B}^T \mathbf{B}\mathbf{B}^T) = (\mathbf{C}\mathbf{C}^T \otimes \mathbf{B}\mathbf{B}^T), \end{aligned} \quad (5)$$

and by tr denoting the trace of the square argument matrix, the sought norm is

$$\begin{aligned} \text{tr}((\mathbf{X} - \mathbf{A}\mathbf{A}^T \mathbf{M})(\mathbf{X} - \mathbf{A}\mathbf{A}^T \mathbf{M})^T) \\ = \text{tr}(\mathbf{X}\mathbf{X}^T) - 2\text{tr}(\mathbf{A}\mathbf{A}^T \mathbf{M}\mathbf{X}^T) \\ + \text{tr}(\mathbf{A}\mathbf{A}^T \mathbf{M}\mathbf{M}^T \mathbf{A}\mathbf{A}^T) \\ = \text{tr}(\mathbf{X}\mathbf{X}^T) - 2\text{tr}(\mathbf{A}\mathbf{A}^T \mathbf{M}\mathbf{X}^T) \\ + \text{tr}(\mathbf{A}\mathbf{A}^T \mathbf{M}\mathbf{X}^T \mathbf{A}\mathbf{A}^T). \end{aligned} \quad (6)$$

As $\text{tr}(\mathbf{X}\mathbf{X}^T)$ is fixed, minimizing this expression is equal to minimizing

$$\begin{aligned} -2\text{tr}(\mathbf{A}\mathbf{A}^T \mathbf{M}\mathbf{X}^T) + \text{tr}(\mathbf{A}\mathbf{A}^T \mathbf{M}\mathbf{X}^T \mathbf{A}\mathbf{A}^T) \\ - 2\text{tr}(\mathbf{A}^T \mathbf{M}\mathbf{X}^T \mathbf{A}) + \text{tr}(\mathbf{A}^T \mathbf{M}\mathbf{X}^T \mathbf{A}^T) \\ - \text{tr}(\mathbf{A}^T \mathbf{M}\mathbf{X}^T \mathbf{A}^T) \end{aligned} \quad (7)$$

and hence the optimal \mathbf{A} is found by maximizing

$$\text{tr}(\mathbf{A}^T \mathbf{M} \mathbf{X}^T \mathbf{A}^T) = \text{tr}(\mathbf{A}^T \mathbf{M} \mathbf{M}^T \mathbf{A}) \quad (8)$$

which shows that \mathbf{A} is the R^A largest eigenvectors of $\mathbf{M} \mathbf{M}^T$ or equivalently the first R^A left singular vectors of a singular value decomposition of \mathbf{M} .

For estimating \mathbf{B} and \mathbf{C} similar relations hold, and these relations form the basis for an algorithm for estimating the Tucker3 model. The essentials of such an algorithm are outlined in the generic algorithm below:

1. Initialize \mathbf{B} and \mathbf{C} .
2. Calculate $\mathbf{M}^{(1)}$ from \mathbf{B} , \mathbf{C} and $\mathbf{X}^{(1)}$. Calculate \mathbf{A} .
3. Calculate $\mathbf{M}^{(2)}$ from \mathbf{C} , \mathbf{A} and $\mathbf{X}^{(2)}$. Calculate \mathbf{B} .
4. Calculate $\mathbf{M}^{(3)}$ from \mathbf{A} , \mathbf{B} and $\mathbf{X}^{(3)}$. Calculate \mathbf{C} .
5. Goto step one until convergence
6. Calculate the core \mathbf{G}

Before going into the details of the algorithm, it is appropriate to elaborate on the computation of \mathbf{M} and $\mathbf{M} \mathbf{M}^T$. As \mathbf{A} is a basis for the column space of the best fitted rank R^A approximation of $\mathbf{M} = \mathbf{X}(\mathbf{C} \mathbf{C}^T \otimes \mathbf{B} \mathbf{B}^T)$, it follows that \mathbf{A} can also be determined from the much smaller matrix $\mathbf{X}(\mathbf{C} \otimes \mathbf{B})$. The cross-product of \mathbf{M} is derived from

$$\begin{aligned} & (\mathbf{X}(\mathbf{C} \mathbf{C}^T \otimes \mathbf{B} \mathbf{B}^T))(\mathbf{X}(\mathbf{C} \mathbf{C}^T \otimes \mathbf{B} \mathbf{B}^T))^T \\ &= \mathbf{X}(\mathbf{C} \mathbf{C}^T \otimes \mathbf{B} \mathbf{B}^T) \mathbf{X}^T \\ &= (\mathbf{X}(\mathbf{C} \otimes \mathbf{B}))(\mathbf{X}(\mathbf{C} \otimes \mathbf{B}))^T \end{aligned} \quad (9)$$

and can hence also be computed from the smaller matrix $\mathbf{X}(\mathbf{C} \otimes \mathbf{B})$.

There are several important steps in actually implementing the Tucker3 algorithm for large problems: (i) avoiding the use of Kronecker products and unnecessarily large working matrices, (ii) a good initialisation method, (iii) if possible, avoiding intermediate estimation of the core array, which is algorithmically unnecessary, and (iv) a fast method for estimating an F -component orthonormal basis for a matrix. In the following, we will use the update of \mathbf{A} as an example.

Ad (i) It is very common to express the Tucker3 model and algorithm using Kronecker products.

While intuitively appealing for providing simple matrix expressions for array models, this approach should not be adopted in the actual implementation, as it leads to very large intermediate arrays and excessively many elementary operations. Instead, one should rearrange the arrays continuously as exemplified below. This approach is justified by the fact that rearranging a matrix is very fast, as it only requires changes in indices, not real computations.

The projections $\mathbf{X}(\mathbf{C} \otimes \mathbf{B})$ can be written in matrix notation:

$$\begin{aligned} \mathbf{W}^{(2)} &= \mathbf{B}^T \mathbf{X}^{(2)} \\ \mathbf{V}^{(3)} &= \mathbf{C}^T \mathbf{W}^{(3)} \\ \mathbf{X}^{(1)}(\mathbf{C} \otimes \mathbf{B}) &= \mathbf{V}^{(1)} \end{aligned}$$

Though complicated to look at, this way of computing the projections is much faster than directly using the Kronecker products—in particular for large arrays. From version 5.0 of MATLAB, general arrays are supported, thus eliminating the need to specifically program these rearrangements.

Ad (ii) There is no need for initializing the first mode, i.e., \mathbf{A} , as this is given by $\mathbf{X}^{(1)}$, \mathbf{B} and \mathbf{C} in the first iteration according to the algorithm in question. The most straightforward method for initializing \mathbf{B} and \mathbf{C} is to use the R^B and R^C left singular vectors from an SVD of $\mathbf{X}^{(2)}$ and $\mathbf{X}^{(3)}$. A slight change is suggested here. As above, matrix \mathbf{B} is the first R^C left singular vectors from an SVD of the $J \times IK$ matrix $\mathbf{X}^{(2)}$. Subsequently, \mathbf{C} is obtained as the R^C first left singular vectors from an SVD of $(\mathbf{B}^T \mathbf{X}^{(2)})^{(3)}$. In this way, the initial \mathbf{B} and \mathbf{C} are likely to be closer to the solution than results from the SVDs on the separated modes would be. In addition, \mathbf{C} is derived from a matrix of size $K \times R^B I$. As such, this initialization scheme requires fewer computations than if the separate SVDs should be calculated. The order in which the component matrices \mathbf{B} and \mathbf{C} are calculated is of no importance, and one should choose the smallest of the two first.

Ad (iii) As the core array of the model is implicitly given by \mathbf{A} , \mathbf{B} and \mathbf{C} , one can simply calculate it once after convergence. But, instead of estimating the full model of \mathbf{X} to determine the error after each iteration, the sum of the squared core entries provides a robust and monotonically increasing parameter that may be used to detect convergence. During iterations, the sum of the squared residuals, \mathbf{E} , is mini-

mized. Denoting by $\|\cdot\|_2^2$, the square of the 2-norm of the argument, we formulate this as $\min\|\mathbf{E}\|_2^2 = \min\|\mathbf{X} - \mathbf{M}\|_2^2 = \min\|\mathbf{X}\|_2^2 - \|\mathbf{M}\|_2^2$. Since $\|\mathbf{M}\|_2^2 = \|\mathbf{G}\|_2^2$ for orthonormal factors, this corresponds to maximizing $\|\mathbf{G}\|_2^2$. Thus, in the implementations under discussion, we calculate the core to use the sum of the squared core elements to detect convergence.

Ad (iv) The very essential part of the Tucker3 algorithm is the derivation of orthonormal loading matrices. Using \mathbf{M} , the size of the matrix from which \mathbf{A} is calculated is $I \times JK$. Using $\mathbf{X}(\mathbf{C} \otimes \mathbf{B})$ the size is only $I \times R^A R^B$. In addition, the computation of $\mathbf{X}(\mathbf{C} \otimes \mathbf{B})$ is much faster than the computation of $\mathbf{X}(\mathbf{C}\mathbf{C}^T \otimes \mathbf{B}\mathbf{B}^T)$. The following procedures have been tested for determining \mathbf{A} given the matrix $\mathbf{X}(\mathbf{C} \otimes \mathbf{B})$:

- SVD on $\mathbf{X}(\mathbf{C} \otimes \mathbf{B})$
- Approximate Bauer–Rutishauser on $\mathbf{X}(\mathbf{C} \otimes \mathbf{B})(\mathbf{X}(\mathbf{C} \otimes \mathbf{B}))^T$
- Exact Bauer–Rutishauser on $\mathbf{X}(\mathbf{C} \otimes \mathbf{B})(\mathbf{X}(\mathbf{C} \otimes \mathbf{B}))^T$
- Gram–Schmidt orthogonalization of $\mathbf{X}(\mathbf{C} \otimes \mathbf{B})(\mathbf{X}(\mathbf{C} \otimes \mathbf{B}))^T$
- NIPALS on $\mathbf{X}(\mathbf{C} \otimes \mathbf{B})(\mathbf{X}(\mathbf{C} \otimes \mathbf{B}))^T$

Preliminary investigations did include QR factorization of $\mathbf{X}(\mathbf{C} \otimes \mathbf{B})(\mathbf{X}(\mathbf{C} \otimes \mathbf{B}))^T$, but since this approach invariably gives results similar to GS, we chose to leave this approach out of the discussion.

2.1. Algorithms

We will shortly describe the implemented variations of the Tucker3 algorithm by showing the update of the first mode loadings in pseudo-code. It is assumed that only the first R^A principal vectors are used in SVD and NIPALS. By *baurut* we mean an algorithm that estimates eigenvectors according to the principle of Bauer–Rutishauser and by *gsm* we mean an algorithm that orthonormalizes according to the Gram–Schmidt procedure. It should be noted that the calls to the *baurut* and *nipals* algorithms use the previous iterates of the factors as initial guesses in order to save computing time. Kroonenberg et al. [11] have compared the Gram–Schmidt orthogonalization with the method of Bauer–Rutishauser.

T1: SVD-based algorithm

$$\mathbf{M} = \mathbf{X}(\mathbf{C} \otimes \mathbf{B})$$

$$[\mathbf{A}, \mathbf{S}, \mathbf{V}] = \text{svd}(\mathbf{M})$$

T2: Bauer–Rutishauser I algorithm. One-step update in each mode

$$\mathbf{M} = (\mathbf{X}(\mathbf{C} \otimes \mathbf{B}))(\mathbf{X}(\mathbf{C} \otimes \mathbf{B}))^T$$

$$[\mathbf{U}, \mathbf{S}, \mathbf{V}] = \text{svd}(\mathbf{A}^T \mathbf{M}^2 \mathbf{A})$$

$$\mathbf{A} = \mathbf{M}\mathbf{A}\mathbf{U}\mathbf{S}^{-1/2}$$

T3: Bauer–Rutishauser II algorithm. Three-step update in each mode

$$\mathbf{M} = (\mathbf{X}(\mathbf{C} \otimes \mathbf{B}))(\mathbf{X}(\mathbf{C} \otimes \mathbf{B}))^T$$

for $i = 1$ to 3

$$[\mathbf{U}, \mathbf{S}, \mathbf{V}] = \text{svd}(\mathbf{A}^T \mathbf{M}^2 \mathbf{A})$$

$$\mathbf{A} = \mathbf{M}\mathbf{A}\mathbf{U}\mathbf{S}^{-1/2}$$

end

T4: Bauer–Rutishauser III algorithm. Repeated update in each mode until convergence of \mathbf{A}

$$\mathbf{M} = (\mathbf{X}(\mathbf{C} \otimes \mathbf{B}))(\mathbf{X}(\mathbf{C} \otimes \mathbf{B}))^T$$

while \mathbf{A} has not converged

$$[\mathbf{U}, \mathbf{S}, \mathbf{V}] = \text{svd}(\mathbf{A}^T \mathbf{M}^2 \mathbf{A})$$

$$\mathbf{A} = \mathbf{M}\mathbf{A}\mathbf{U}\mathbf{S}^{-1/2}$$

endwhile

T5: Bauer–Rutishauser IV algorithm. Advanced BR algorithm

$$\mathbf{M} = (\mathbf{X}(\mathbf{C} \otimes \mathbf{B}))(\mathbf{X}(\mathbf{C} \otimes \mathbf{B}))^T$$

$$\mathbf{A} = \text{baurut}(\mathbf{M}, \mathbf{A})$$

T6: Gram–Schmidt I algorithm. One-step update in each mode

$$\mathbf{M} = (\mathbf{X}(\mathbf{C} \otimes \mathbf{B}))(\mathbf{X}(\mathbf{C} \otimes \mathbf{B}))^T$$

$$\mathbf{A} = \text{gsm}(\mathbf{M}\mathbf{A})$$

T7: Gram–Schmidt II algorithm. Three-step update in each mode

$$\mathbf{M} = (\mathbf{X}(\mathbf{C} \otimes \mathbf{B}))(\mathbf{X}(\mathbf{C} \otimes \mathbf{B}))^T$$

for $i = 1$ to 3

$$\mathbf{A} = \text{gsm}(\mathbf{M}\mathbf{A})$$

end

T8: Gram–Schmidt III algorithm. Repeated update in each mode until convergence of \mathbf{A}

$$\mathbf{M} = (\mathbf{X}(\mathbf{C} \otimes \mathbf{B}))(\mathbf{X}(\mathbf{C} \otimes \mathbf{B}))^T$$

while \mathbf{A} has not converged

$$\mathbf{A} = \text{gsm}(\mathbf{M}\mathbf{A})$$

endwhile

T9: NIPALS-based algorithm.

$$\mathbf{M} = \mathbf{X}(\mathbf{C} \otimes \mathbf{B})$$

$$[\mathbf{A}, \mathbf{P}] = \text{nipals}(\mathbf{M}, \mathbf{A})$$

As the principles of SVD (Algorithm 1) and NIPALS (Algorithm 9) are well known and widely used in chemometrics, we will elaborate on the Bauer–Rutishauser algorithm and the Gram–Schmidt orthogonalization. For the Bauer–Rutishauser algorithm, we investigate four different methods: A simple one-step BR update (Algorithm 2) as suggested by Kroonenberg et al. [12], an approach repeating the simple update three times (Algorithm 3) and an approach, where the simple BR update is repeated until convergence of the eigenvector estimates is reached (Algorithm 4). In addition, we have implemented an advanced algorithm, which is referred to as the full Bauer–Rutishauser algorithm (Algorithm 5) (see Rutishauser [13]). To explore the continuity between the two extremes, i.e., the simple Algorithm 2 and the advanced Algorithm 5, we have added three-step and convergence-based implementations of Algorithm 2. The simple Algorithms 2 and 3 may be regarded as being equal to Algorithm 5, merely with a looser convergence criterion. Three implementations of the

Gram–Schmidt orthogonalization for estimating eigenvectors are investigated. Algorithm 6 is a simple one-step GS update as suggested by Kroonenberg [14], Algorithm 7 repeats the simple update three times and Algorithm 8 repeats the simple GS update until convergence is reached. By using repeated iterations better estimates of the true eigensolutions are obtained with a small computational effort, since the working matrices are present in directly accessible forms.

2.2. The Bauer–Rutishauser approach

In [15], Rutishauser proposes an algorithm that improves the convergence order of the bi-iteration method for estimating eigenvectors of matrices suggested by Bauer [16]. Using that \mathbf{Y} ($I \times I$), e.g., obtained as $\mathbf{X}\mathbf{X}^T$, is positive definite and symmetric, the aim of Rutishauser’s algorithm is to achieve the good numerical features offered by Bauer’s approach with a high convergence order. Rutishauser sets forth several suggestions to improve convergence as well as robustness of the algorithm. For the present purpose, we shall take a less general approach, since we do not require extreme accuracy of the obtained eigensolutions, and we desire to keep the computational requirements at a minimum. Thus, the implementation is kept simple and efficient in Algorithms 2, 3 and 4. Rutishauser’s strongest suggestions are implemented in the somewhat more advanced Algorithm 5 for comparative reasons. In Algorithms 2, 3 and 4, new orthogonal iterates of \mathbf{A} are provided through one, three or more Ritz-iterations such that the eigendirections, represented by matrix \mathbf{A}_n , are defined by the projected eigenvalue problem

$$\mathbf{A}_n^T \mathbf{Y}^{-2} \mathbf{A}_n = \mathbf{D}_n^{-2} \quad \mathbf{A}_n^T \mathbf{A}_n = \mathbf{I} \quad (10)$$

where \mathbf{D}_n ($R^A \times R^A$) is diagonal and holds the eigenvalues of \mathbf{Y} on the diagonal. \mathbf{A}_n is found as

$$\mathbf{A}_n = \mathbf{Y}\mathbf{A}_{n-1}\mathbf{Q}_n\mathbf{D}_n^{-1} \quad \mathbf{Q}_n^T\mathbf{Q}_n = \mathbf{I} \quad (11)$$

\mathbf{Q}_n ($R^A \times R^A$) and \mathbf{D}_n are found by, e.g. an SVD, according to

$$\mathbf{Q}_n\mathbf{D}_n^2\mathbf{Q}_n = \mathbf{A}_{n-1}^T\mathbf{Y}^T\mathbf{Y}\mathbf{A}_{n-1} = \mathbf{A}_{n-1}^T\mathbf{Y}^2\mathbf{A}_{n-1} \quad (12)$$

This approach gives results with improved numerical stability and higher convergence rate than the trivial rule $\mathbf{A}_n = \mathbf{Y}\mathbf{A}_{n-1}$ ($n = 1, 2, \dots$). The reader is referred to Refs. [13,16,17] for details and proofs. The

method may be seen as an extension of the method proposed by Bauer where

$$\mathbf{A}_n = \mathbf{Y}\mathbf{A}_{n-1}\mathbf{R}_n^{-1} \quad (13)$$

and \mathbf{R}_n ($R^A \times R^A$) is an upper triangular matrix with positive diagonal elements which may be derived directly from an extended Gram–Schmidt orthogonalization of $\mathbf{Y}\mathbf{A}_{n-1}$ (see [17] for advanced algorithmic approaches in this direction). One may argue that an algorithm based solely on Eqs. (10)–(12) is overly simplified. Hence, we also implemented a more complete Bauer–Rutishauser algorithm according to some of Rutishauser’s many suggestions [13]. In the implementation used here, a series of eigenprojections are calculated with the significant termination by a single Ritz iteration to estimate the orthogonal eigenvectors according to the projected eigenvalue problem.

2.3. The Gram–Schmidt approach

The Gram–Schmidt algorithm may be used for finding an orthonormal basis of any matrix. The orthogonalization is very cheap in terms of operations and it is non-iterative. For the present purpose we have applied a very simple GS algorithm with re-orthogonalization [13,17]. By the repeated eigenprojection of \mathbf{Y} onto \mathbf{A}_{n-1} the enforced response is returned in the new iterate \mathbf{A}_n according to

$$\mathbf{A}_n = \mathbf{Y}\mathbf{A}_{n-1} \quad (n = 2, 3 \dots) \quad (14)$$

However, after applying the eigenprojection several times, the columns of \mathbf{A}_n tend to become correlated, thereby compromising orthogonality. To ensure the condition of the estimated base and to avoid an uncontrolled increase in correlation between the columns of \mathbf{A} during iterations, we suggest to apply the GS orthogonalization continuously. Thus, the resulting sequence takes the form of

$$\mathbf{A}_n = \text{gsm}(\mathbf{Y}\mathbf{A}_{n-1}) \quad (n = 2, 3 \dots) \quad (15)$$

where *gsm* represents the orthogonalization of the matrix argument. To orthogonalize the columns of \mathbf{Z} ($I \times R^A$), assuming that \mathbf{Z} is non-singular, the GS algorithm will return an orthonormal basis in \mathbf{V} according to the following pseudo MATLAB code, in which $\mathbf{V}(:,i)$ designates the *i*th column of matrix \mathbf{V} , $\mathbf{V}(:,1) = \mathbf{Z}(:,1) / \|\mathbf{Z}(:,1)\|_2$

For $i = 2$ to R^A

$$\mathbf{V}(:,i) = \mathbf{Z}(:,i) - \mathbf{V}(:,1:(i-1))\mathbf{V}(:,1:(i-1))^T \times \mathbf{Z}(:,i)$$

$$\mathbf{V}(:,i) = \mathbf{V}(:,i) / \|\mathbf{V}(:,i)\|_2 \quad (16)$$

end

Some important special variations of the Tucker3 model are: How to incorporate different uncertainties for different elements and how to handle missing elements. We will shortly discuss different ways to approach these special cases.

2.4. Incorporating uncertainties

If the uncertainties of the individual data elements are known, it can be feasible to use these in the decomposition. If the uncertainties are almost equal for all elements, there is no need to change the algorithm, but otherwise at least two different possibilities exist. If the uncertainty of a given variable remains almost the same over all modes, it will suffice to scale the array accordingly, keeping in mind the ‘rules’ for scaling multi-way arrays (see Kroonenberg [14]). After scaling, an unconstrained model is estimated from the scaled array. If the uncertainties vary also over variables, or if an iteratively re-weighted solution is sought for robustness, then one cannot estimate the model using eigenvector-based methods, but has to use regression-based methods or the weighted least squares approach suggested by Kiers [18].

2.5. Missing elements

Missing elements can be effectively handled by the current algorithm by iteratively replacing missing elements with model estimates of the elements. The model is thus estimated from an array with no missing elements, and after each iteration the model of \mathbf{X} is estimated from the parameters. All elements that are missing are replaced with model estimates, and the algorithm is repeated until the convergence criterion is fulfilled and the estimates of the missing elements do not change significantly. That way, the missing elements do not directly influence the outcome of the model.

3. Experimental

The aim of this investigation is to find the fastest algorithm among the nine under discussion. The algorithms are compared on the time needed to obtain similar fits to (i) one measured and (ii) several synthesized data sets. For each data set, a model with many factors is estimated in order to ensure that all systematic information is modelled. To facilitate a discussion of the efficiency of the algorithms, we have shown the number of FLOPS (floating operations) required to obtain the solutions. The matrices **A**, **B** and **C** are initiated as previously suggested.

Due to the huge amounts of data handled during iterations, there is a lot of so-called *dead time*. The *dead time* of the algorithms has been estimated by removing the code specifically related to the updating schemes and only keeping the data management operations. By running 20 iterations of this void algorithm, an estimate on the average dead time per iteration, t_0 , caused by the size of the data array in question is obtained. After the various algorithms have been applied, the number of iterations, N , is known and the dead time may be subtracted from the total time, T , to give a clearer picture of the time used specifically by the updating schemes. The time used on handling the data is of course required to obtain any solution, but by removing the dead time, the common background is subtracted, thereby allowing us to discuss the sheer time differences caused by the specific updating schemes.

Given the array **X** the error f to minimize is given by

$$f(\mathbf{A}, \mathbf{B}, \mathbf{C}, \mathbf{G}; \mathbf{X}) = \|\mathbf{X}^{(1)} - \mathbf{A}\mathbf{G}^{(1)}(\mathbf{B}^T \otimes \mathbf{C}^T)\|_2^2 \quad (17)$$

where $\mathbf{X}^{(1)}$ is the frontal slice-wise unfolding **X** and component matrices **A**, **B** and **C** contain the orthogonal factors in their columns. All iterative procedures require a criterion to indicate if a sufficiently accurate model has been estimated. Given the dimensionality of the model, the desire of the analyst is to obtain the lowest possible value of f in the shortest possible time. As stated earlier, we do not calculate f explicitly, but we use the sum of the squared core entries instead, designated by g , as this is obtained with much fewer computations. We seek to maximize the value of g , since the variance (of **X**) described by the

model and g will be at maximum for the same set of **A**, **B** and **C** (rotation disregarded).

For checking convergence, we have taken one approach for the real data set and another for the 200 synthesized data sets. For the real data set, a minimum value of the sum of squared core entries, referred to as g^* , will be used as stopping criterion. The value of g^* has been set slightly below the asymptotic value of g , which was found by inspection. With regards to the numerous synthesized data sets, an unsupervised criterion to detect convergence is required, and for the present application, this is formulated as the maximum difference of g between two successive iterations. We will return to this later.

3.1. Data

The measured data set originates from spectrofluorometric measurements on 65 samples, and has dimensions $65 \times 40 \times 311$ representing approximately 6.5 MB of data. The values range from zero to approximately 1295. Investigations not reported here have revealed that the rank is in the range 6 to 8. Hence, a model of order $8 \times 8 \times 8$ is estimated. By inspection and evaluation of different solutions, the value of g^* for this data set was set to $3.720345874925 \cdot 10^{10}$. Using this value of g^* in all algorithms applied to this data set, the fit of the models will be comparable from the viewpoint of the analyst.

A number of 200 synthesized data sets of dimensions $120 \times 120 \times 120$ with PARAFAC rank not less than 8 are produced by synthesizing factors from Gaussian peaks in each of the three modes with randomly distributed peak centres and peak widths, and subsequently applying 5% homoscedastic (additive) and 5% heteroscedastic (multiplicative) normally distributed noise. With regards to spectral data, the resulting level of noise may be regarded as being high. To ensure the rank, the peak centres were forced to differ in locations within modes and the synthesized cores consisted of random values between 0 and 1, where the diagonal elements (1,1,1), (2,2,2), ..., (8,8,8) were forced to be 1. The convergence criterion was estimated for each synthesized data array in the following way: The SVD-based algorithm (Algorithm 1) was applied with the criterion that convergence was reached when two successive fits differed by less than 0.0005. If the algorithm

honoured this convergence criterion within 19 steps, the convergence criterion was divided by two, and the SVD-algorithm was restarted; this was repeated until the number of required steps exceeded 20. This feasible convergence criterion was then used for the remaining 8 algorithms. We estimate that at least 20 iterations are required to get accurate measurements on the computational time. Since very slow convergence of the most approximate algorithms (i.e., small changes between iterations in Algorithms 2 and 6) could erroneously cause the algorithms to exit too early, a subsequent evaluation of the errors of the final models was performed to reject models that did not fit data satisfactorily.

4. Results and discussion

The results from the models of the measured data set are listed in Table 1. Standard deviations are negligible and are not listed. It is readily seen that Algorithm 9 stands out with the lowest time consumption, T , and the highest efficiency in terms of FLOPS. This is likely due to the simplicity of the NIPALS algorithm, which is used to estimate eigenvectors in each of the three subproblems in this algorithm. Another important observation is the high number of required main iterations, N , for Algorithms 2 and 6. These two algorithms have a high degree of simplicity in common, but whereas this was intended to decrease the time consumption of the subproblems, the increase in the overall number of main iterations renders these approaches infeasible. Algorithms 2 and 6 provide too

inaccurate approximations to the eigensolutions; hence, they require more iterations to reach the exact eigensolutions. If the eigensolutions are inaccurately determined in one iteration, then the next iteration will suffer from this suboptimality in the posed problem. This is in contrast to the experiences reported by Kroonenberg [14] (p. 87), where he argues that it is not worthwhile to solve for highly accurate eigenvectors since the resulting algorithm will obtain an iteration-in-iteration structure requiring too much computational effort, since after all, during iterations, the eigenproblems posed are only formulated in terms of intermediate factors. Whereas this may be true for smaller sized problems, the compromise between spending computational time on estimating accurate eigensolutions and the overhead introduced by handling the large data arrays, appears to favour the updating schemes that are more accurate. From the viewpoint of the analyst Algorithms 2 and 6 are suboptimal in terms of FLOPS as well as time; thus, we will leave them out of the remaining discussion. With regards to time consumption, T , we see that Algorithms 1 and 4 use markedly more time on the same number of iterations. By inspection of T_c , we conclude that this is due to the time used in the updating schemes. Algorithm 1 includes an SVD which is stable and accurate, but very time consuming. So, in addition to the conclusions drawn from the very simple algorithms (i.e., that the eigenvectors must be accurate) it is indicated that there *is* an upper limit to the effort that should be used on improving the accuracy of the eigensolutions. When compared to Algo-

Table 1
Results from models of the measured data set

Algorithm number	Flops (10^9)	Number of iterations (N)	Time, T (s)	Corr. time ($T = T - N t_0$) (s)	Final value of $g g(N) 10^{10}$
1	1.46	21	63.54	28.03	3.72034587493
2	1.75	35	74.40	15.22	3.72034587493
3	1.33	22	52.56	15.36	3.72034587493
4	1.41	21	54.02	18.51	3.72034587493
5	1.15	21	49.18	13.67	3.72034587493
6	1.64	35	71.48	12.30	3.72034587493
7	1.10	22	46.96	9.76	3.72034587493
8	1.10	21	47.78	12.27	3.72034587493
9	0.81	21	42.54	7.03	3.72034587493

All values of required number of FLOPS, number of iterations (N), computation time (T), and corrected time (T_c) are averages of 20 model runs.

$t_0 = 1.69 \text{ s it}^{-1}$.

II. Algorithms, models and applications

rithm 3, Algorithm 4 appears to iterate too many times in the substeps judged from the value of T_c . This may be corrected by reducing the number of inner iterations, e.g., by adjusting the convergence criteria for the subiterations. Algorithms 5, 7 and 8 offers almost similar performance in terms of FLOPS and time consumption. In line with the findings of Kroonenberg et al. [12], the efficiency of the GS approaches, especially Algorithms 7 and 8, are certainly of interest. With regards to repeating the substeps, it holds for BR and GS that the three-step approaches significantly reduces the *overall* time needed to reach a solution. Since repeated application of the GS update improves the accuracy of the estimated eigensolutions, we attribute the decrease of iterations to the increased adequacy of the subsequently posed eigenproblems. Comparing columns four and three clearly shows that for all nine algorithms, most time is spent on handling data and *not* on solving the eigenproblems. Hence, improving the speed of data handling will contribute significantly in reducing the time consumption. The sum of squared core elements in the last iterations, $g(N)$, in Table 1 verifies that the final models are actually comparable in fit. Thus, the results from the measured data set suggest that Algorithms 5, 7, 8 or 9 are fastest, with Algorithm 9 being fastest for this data set.

The findings from the analysis of the 200 synthesized data sets are listed in Table 2. Since the synthesized data arrays are very different, we have listed the standard deviation next to the parameters. It is imme-

diately recognized that the observed standard deviations are high, thereby rendering interpretation difficult. This is mainly due to the very different properties of the data sets and not a matter of great concern. However, the pattern found in the mean values for T are verified by the fact that Algorithms 3, 7 and 9 are fastest in 41 (21%), 63 (32%) and 84 (42%) of the 200 models. Since the number of required inner iterations for all updates depends strongly on the size and the characteristics of the data under investigation, we investigated the correlation coefficients and the condition number of the synthesized factor matrices. Over all three modes, the synthesized factor matrices had absolute correlation coefficients ranging from 0.1319 to 0.8235 with a mean value of 0.5471 and a S.D. at 0.2852. Ranging from $2.01 \cdot 10^1$ to $3.19 \cdot 10^6$ the condition numbers (i.e., the ratio between the largest eigenvalue and the lowest) was found to have a mean value at $3.69 \cdot 10^4$ with a S.D. at $1.80 \cdot 10^5$. Based on these findings, we may conclude that the synthesized data sets were constructed from factors that were somewhat correlated, thereby introducing ill-posed subproblems. With regards to the time spent on the updating schemes, T_c , Algorithms 2 and 6 were fastest, but the eigensolutions provided within iterations were too simple and too inaccurate. This is in accordance with the findings from the measured data set. Thus, they (consistently) required the highest number of iterations. We consolidate the findings from the analysis of the measured data set; algorithms for analysis of large data arrays

Table 2

Mean values and standard deviations of required number of FLOPS, iterations (N), computation time (T), and corrected time (T_c) from 200 synthesized data sets

Algorithm number	FLOPS (10^9)		Iterations (N)		Time, T (sec)		Corr. time, T_c (s)	
	Mean	S.D.	Mean	S.D.	Mean	S.D.	Mean	S.D.
1	2.48	0.80	28.80	9.29	107.54	35.59	24.45	7.89
2	2.43	0.81	35.33	11.66	107.08	35.62	5.15	1.82
3	2.21	0.65	30.20	8.88	93.99	27.82	6.86	2.09
4	2.86	0.86	28.80	9.30	103.68	32.13	20.59	5.59
5	2.24	0.67	29.02	8.82	100.41	30.03	16.70	4.62
6	2.38	0.79	35.33	11.70	106.61	35.46	4.68	1.67
7	2.07	0.61	30.20	8.91	92.94	27.49	5.81	1.78
8	2.23	0.70	28.80	9.34	98.93	30.90	15.84	4.34
9	1.92	0.61	28.81	9.22	90.75	28.58	7.65	2.28

Compare with Fig. 1.

For the synthesized data sets t_0 is 2.89 s it^{-1} .

II. Algorithms, models and applications

must be based on fast, but accurate, algorithms for estimating eigensolutions of the involved subproblems. It should be noted that Algorithm 4 (convergence-based BR) and 8 (convergence-based GS) required the same number of outer iterations as Algorithm 1 (based on SVD) for all data sets, verifying that these three algorithms provide the same accurate eigensolutions. In accordance with Table 1, Algorithms 7 and 9 require less time and less FLOPS to reach a solution. To conclude, we find that Algorithm 9 offer the best combination of simplicity and accuracy of the eigensolutions of the synthesized data arrays.

Measurements of number of FLOPS, iterations N , total computing time T , and corrected time T_c , were arranged as matrices of dimensions 200 (data sets) \times 9 (algorithms), one matrix for each parameter. To illustrate the significant covariations of the parameters, we have extracted one principal component from each of the four matrices. The superposed factors for the nine algorithms in Fig. 1 are scaled such that the largest element in each factor has a value of one. The figure illustrates the essence of this investigation. The efficiency of the updating schemes in Algorithms 3, 7 and 9 are evident from the simultaneous low levels of FLOPS, iterations (N) and the total time required

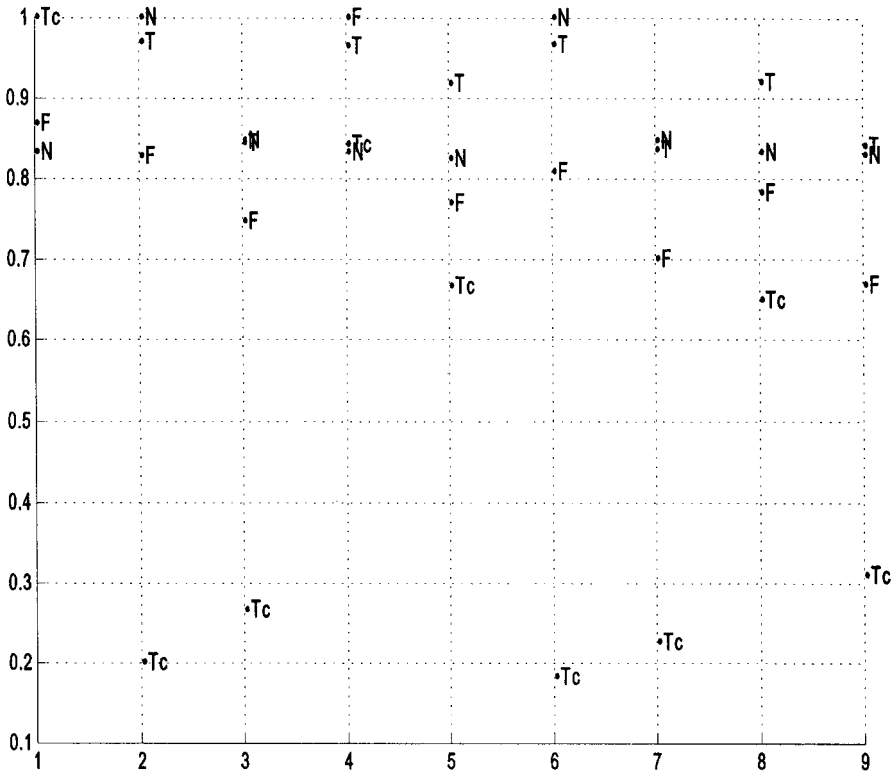


Fig. 1. Results from the models of 200 synthesized data sets with respect to the nine applied algorithms. The four superposed principal components represent the number of FLOPS (F), iterations (N), the total computing time (T), and corrected time (T_c). Compare with Table 2. The three factors explain 76.57%, 76.50%, 76.47%, and 80.38% of the variation in the matrices. The factors are scaled such that the largest element has a value of one.

(T) as seen from Fig. 1. We notice that the simple NIPALS algorithm (Algorithm 9), well known and widely used in chemometrics, substantiates itself as an excellent compromise between speed and accuracy. The huge gain in convergence when comparing single-step implementations (Algorithms 2 and 6) to the three-step implementations (Algorithms 3 and 7) is substantiated. The convergence-based iterations (Algorithms 4 and 8) are sensitive towards the threshold of the convergence criteria, and the optimal convergence criterion may depend on the data at hand.

5. Conclusion

We have compared nine algorithms for solving the Tucker3 model on very large data arrays. Through modelling of one measured and several synthesized data sets especially the NIPALS-based implementation appears to be feasible with regards to time consumption and FLOPS. The implementations based on three repeated simple Gram–Schmidt updates are suggested as alternative algorithms. Furthermore, we have found that accuracy, perhaps more than speed, is required in implementations of Tucker3 models of large data arrays to yield results in the shortest possible time.

Acknowledgements

Prof. Lars Munck is thanked for providing psychological support for what must be the most exploratory industry-related research group. The authors further wish to thank Professor Lars Munck for financial support through the Nordic Industry Foundation project P93149 and the FØTEK foundation. We also wish to thank Henk Kiers, Sijmen de Jong and Age Smilde and two anonymous referees for good comments on this paper.

References

- [1] L. Tucker, Some mathematical notes on three-mode factor analysis, *Psychometrika* 31 (1966) 279–311.
- [2] P.M. Kroonenberg, J. de Leeuw, Principal components analysis of three-mode data by means of alternating least squares algorithms, *Psychometrika* 45 (1980) 69–97.
- [3] J.M.F. ten Berge, J. de Leeuw, P.M. Kroonenberg, Some additional results on principal components analysis of three-mode data by means of alternating least squares, *Psychometrika* 52 (1987) 183–191.
- [4] C.L. de Ligny, M. Spanjer, J.C. van Houwelingen, H.M. Weesie, Three-mode factor analysis of data on retention in normal-phase high-performance liquid chromatography, *J. Chromatogr.* 301 (1984) 311–324.
- [5] P.J. Gemperline, K.H. Miller, T. West, E. Weinstein, J.C. Hamilton, J.T. Bray, Principal component analysis, trace elements and blue crab shell disease, *Anal. Chem.* 64 (1992) 523–532.
- [6] W.A. van der Kloot, P.M. Kroonenberg, External analysis with three-mode principal component analysis, *Psychometrika* 50 (1985) 479–494.
- [7] A. Kapteyn, H. Neudecker, T. Wansbeek, An approach to n -mode components analysis, *Psychometrika* 91 (1986) 269–275.
- [8] B.K. Alsberg, O.M. Kvalheim, Speed improvement of multivariate algorithms by the method of postponed basis matrix multiplications: Part I. Principal component analysis, *Chemometr. Intell. Lab. Syst.* 24 (1994) 31–42.
- [9] B.K. Alsberg, O.M. Kvalheim, Speed improvement of multivariate algorithms by the method of postponed basis matrix multiplications: Part II. Three-mode principal component analysis, *Chemometr. Intell. Lab. Syst.* 24 (1994) 43–54.
- [10] H. Kiers, R.A. Harshman, Relating two proposed methods for speedup of algorithms for fitting two- and three-way principal component and related multilinear methods, *Chemometr. Intell. Lab. Syst.* 39 (1997) 31–40.
- [11] H.A.L. Kiers, P.M. Kroonenberg, J.M.T. ten Berge, An efficient algorithm for TUCKALS on data with large number of observation units, *Psychometrika* 33 (1992) 415–422.
- [12] P.M. Kroonenberg, J.M.F. ten Berge, P. Brouwer, H. Kiers, Gram–Schmidt versus Bauer–Rutishauser in alternating least squares algorithms for three-mode principal component analysis, *Comp. Stat. Q.* 2 (1989) 81–87.
- [13] H. Rutishauser, F.L. Computational aspects of, Bauer’s simultaneous iteration method, *Numer. Math.* 13 (1969) 4–13.
- [14] P.M. Kroonenberg, Three-mode principal component analysis, DSWO Press, Leiden, 1983.
- [15] R. Bro, C.A. Andersson, Improving the speed of multi-way algorithms Part II: Compression, *Chemometr. Intell. Lab. Syst.* 42 (1998) 103–111.
- [16] F.L. Bauer, Das Verfahren der Treppeniterationen und verwandte Verfahren zur Lösung algebraischer Eigenwertprobleme, *ZAMP* 8 (1957) 214–235.
- [17] J.W. Longley, Least squares computations using orthogonalization methods, *Lecture Notes in Pure and Applied Mathematics*, Marcel Dekker, New York, 1984.
- [18] H.A.L. Kiers, Weighted least squares using ordinary least squares algorithms, *Psychometrika* 62 (1997) in press.

P5

**Improving the speed of multiway
algorithms. Part II:
Compression**

Rasmus Bro and Claus A. Andersson



Improving the speed of multiway algorithms Part II: Compression

Rasmus Bro^{*}, Claus A. Andersson¹

Chemometrics Group, Food Technology, Department of Dairy and Food Science, Royal Veterinary and Agricultural University, Rolighedsvej 30, iii, DK-1958 Frederiksberg C, Denmark

Abstract

In this paper an approach is developed for compressing a multiway array prior to estimating a multilinear model with the purpose of speeding up the estimation. A method is developed which seems very well-suited for a rich variety of models with optional constraints on the factors. It is based on three key aspects: (1) a fast implementation of a Tucker3 algorithm, which serves as the compression method, (2) the optimality theorem of the CANDELINC model, which ensures that the compressed array preserves the original variation maximally, and (3) a set of guidelines for how to incorporate optional constraints. The compression approach is tested on two large data sets and shown to speed up the estimation of the model up to 40 times. The developed algorithms can be downloaded from <http://\newton.mli.kvl.dk\foodtech.html>. © 1998 Elsevier Science B.V. All rights reserved.

Keywords: Tucker3; PARAFAC; CANDELINC; Constraints; Tucker1; Data compression

1. Introduction

An annoying aspect of estimating some multiway models using alternating least squares (ALS) is the time consumption of these algorithms. A way to increase the speed of ALS algorithms is to compress the data array initially and then subsequently estimate the model from the compressed data. This is natural since a multiway model is per se a compression of the original data into fewer parameters, implying that the systematic variation in the data is expressible in less than the original number of data points. Hence, the

model to be estimated should also be estimable from another (condensed) representation of the systematic variation in the data. Furthermore, since a multiway model can be considered a multilinear decomposition preserving the systematic variation in the data, it seems useful to use a multilinear decomposition for compression as well. After estimating the parameters of the model in the compressed space, these can then be transformed to the original space, and hopefully provide a good approximate solution to the solution that would be found if estimating the model directly from the raw data. In the sequel we will refer to the model used to compress the data as the *compression model* and the model operating on the compressed array as the *analytical model*.

Alsberg and Kvalheim have described in a series of papers a method for compressing high dimen-

^{*} Corresponding author. E-mail: rb@kvl.dk.

¹ E-mail: ca@kvl.dk.

sional arrays [1,2]. Kiers and Harshman [3] have shown that this approach is equivalent to the CANDELINC (CANonical DEcomposition with LINear Constraints) approach. In CANDELINC, only orthonormal bases are allowed but any non-orthonormal basis can be orthogonalized prior to compression without any loss of information [4]. The Alsberg and Kvalheim approach was developed specifically for estimating Tucker3 models, while the CANDELINC approach is valid for estimating any multiway model. Furthermore as stressed by Kiers and Harshman [3] there is no need for special algorithms in the CANDELINC approach. One simply regresses the data onto the bases, use any existing multiway algorithm on the compressed array, and decompress the result by premultiplying the solution with the projection bases. This, however, only holds for unconstrained models with a nonweighted least squares optimization criterion as will be shown. The only important constraint that does not require any special attention is orthogonality. If orthogonal loadings are found in, e.g., a PARAFAC model of the compressed array, then the backtransformed solution will also be orthogonal. In this paper Tucker3 is suggested for finding the compression bases as the Tucker3 algorithm is very fast and has the property of providing optimal bases in a least squares sense. Alsberg and Kvalheim suggest different bases in their work. If the size of the array is so large that estimation of the Tucker3 model is in practice impossible due to the computer capacity, then these suggested bases are sensible, but if the computer capacity is sufficient it is not sensible to use other bases than those defined by the Tucker3 model.

Note that the suggested compression approach is relevant for estimating most multiway models. Even in the case where one is merely interested in a Tucker3 model, compressing the array first, enables one to quickly estimate models of different dimensions and perhaps using different constraints in order to find the most appropriate model.

The compression method is developed and evaluated on several data sets. It is shown that the new method makes multiway modeling faster and more memory-efficient. It is discussed how to express important constraints and weighting schemes in the modeling of compressed arrays. Three-way arrays will be used as an example but the developed theory

is directly applicable for arrays of any order. The ALS procedure for estimating the PARAFAC model will be used throughout but the method is also applicable for other models and algorithms.

In the following, scalars are indicated by (lower-case) italics, vectors by bold lower-case characters, bold capitals are used for two-way matrices, and underlined bold capitals for three-way arrays. The ijk th element of \mathbf{X} is called x_{ijk} and is the element in the i th row, j th column, and k th tube of \mathbf{X} . When three-way arrays are unfolded to matrices, the following notation will be used: if \mathbf{X} is an $I \times J \times K$ array and is unfolded to an $I \times JK$ matrix, \mathbf{X} , the order of J and K indicates which indices of J are running fastest. In this case the indices of J are running fastest, meaning that the first J columns of \mathbf{X} contain all variables for $k = 1$ and for $j = 1$ to $j = J$. For short we will define the $I \times JK$ matrix $\mathbf{X}^{(1)}$ where the superscript indicates that it is the *first* mode that is preserved. Likewise $\mathbf{X}^{(2)}$ is a $J \times IK$ matrix and $\mathbf{X}^{(3)}$ a $K \times IJ$ matrix. If the arrangement of the array is clear from the context the superscript will not be shown.

2. Theory

An $I \times J \times K$ array \mathbf{X} is given. Suppose that the rank of the systematic variation in each of the three modes is R^A , R^B , and R^C , respectively. By the rank of the systematic variation is meant the minimum rank of an appropriate basis for the space spanned by the systematic variation in a particular mode, i.e., the rank if no noise was present [5]. For the first mode the rank of, and a basis for, the variable space can for example be determined from analyzing the $I \times JK$ unfolded matrix \mathbf{X} obtained by concatenating the K layers of size $I \times J$ of \mathbf{X} one after another.

Several methods exist for determining the proper rank, e.g., judging the residuals, using cross-validation [6,7] or methods similar to Malinowski's indicator function [8]. For compression, however, it is not essential to find the exact rank, but rather to define the rank so large that the correct rank is less than the defined rank. Let \mathbf{U} of size $I \times R^A$ be an orthonormal basis for the space spanned by systematic variation in the first mode. An orthonormal matrix \mathbf{V} of size $J \times R^B$ similarly defines the variable space of the

systematic variation in the second mode and an orthonormal matrix \mathbf{Z} of size $K \times R^C$ defines the variable space in the third mode. An F -component PARAFAC model is sought for the $I \times J \times K$ array \mathbf{X} . An F -component PARAFAC model is defined through \mathbf{A} ($I \times F$), \mathbf{B} ($J \times F$), and \mathbf{C} ($K \times F$) as

$$\min \left\| \left\| \sum_{k=1}^K \mathbf{X}_k - \mathbf{A} \mathbf{D}_k \mathbf{B}^T \right\|_F \right\|^2 \quad (1)$$

where \mathbf{X}_k is the k th layer of \mathbf{X} , i.e., the $I \times J$ matrix obtained by fixing the third mode at its k th value. The matrix \mathbf{D}_k is a diagonal matrix containing the k th row of \mathbf{C} in its diagonal. General information on the PARAFAC model can be found in many papers [9–13]. As the optimal \mathbf{A} is approximately describing the systematic variation in the first mode of \mathbf{X} it must hold that a matrix exists such that

$$\mathbf{A} = \mathbf{U} \mathbf{\Gamma}, \quad (2)$$

as \mathbf{U} is a basis for the systematic variation. Similar relations hold for the second and third mode:

$$\mathbf{B} = \mathbf{V} \mathbf{\Theta} \quad (3)$$

and

$$\mathbf{C} = \mathbf{Z} \mathbf{\Xi}. \quad (4)$$

This is the same as saying, that the PARAFAC model is linearly constrained to the subspaces \mathbf{U} , \mathbf{V} , and \mathbf{Z} . The CANDELINC model was developed for estimating multiway models under such linear constraints [4]. The theory of the CANDELINC model states that if a PARAFAC model of \mathbf{X} given by \mathbf{A} , \mathbf{B} , and \mathbf{C} is sought, subject to the above constraints, then it is only necessary to estimate the (much) smaller matrices $\mathbf{\Gamma}$, $\mathbf{\Theta}$, and $\mathbf{\Xi}$. More importantly these matrices can be found by estimating a PARAFAC model on an array \mathbf{Y} of size $R^A \times R^B \times R^C$ found by regressing \mathbf{X} onto the orthonormal bases \mathbf{U} , \mathbf{V} , and \mathbf{Z} . Written in matrix notation letting \mathbf{X} be the $I \times JK$ unfolded array, and \otimes denoting the Kronecker product these regressions read

$$\mathbf{Y}^{(1)} = \mathbf{U}^T \mathbf{X}^{(1)} (\mathbf{Z} \otimes \mathbf{V}). \quad (5)$$

Estimating an F -component PARAFAC model of \mathbf{Y} will give the loading matrices $\mathbf{\Gamma}$ ($R^A \times F$), $\mathbf{\Theta}$ ($R^B \times F$), and $\mathbf{\Xi}$ ($R^C \times F$), and through the relations of

Eqs. (2)–(4) the loading matrices in the original spaces can be calculated.

If the orthonormal bases are bases for the systematic variation, then the model estimated from \mathbf{Y} (Eq. (5)) will give the sought solution. In Ref. [4] this is shown for any model that can be regarded as a Tucker3 model or a restricted version of a Tucker3 model. The PARAFAC, PARATUCK2 [14], PARAFAC2 [15,16], and the Tucker2 [17] models can all be regarded as restricted versions of Tucker3 and can hence be estimated from the compressed array without loss of information under the constraints of Eqs. (2)–(4).

The crucial point in this method is to find good bases for the respective modes. If these are appropriate, one would expect the analytical model estimated from the compressed space to be equal to the model estimated from the raw data. One possibility for finding these bases would be to use the singular vectors from a singular value decomposition (Tucker1) of the array properly unfolded for each direction. That is, \mathbf{U} would equal the first R^A left singular vectors from an SVD of $\mathbf{X}^{(1)}$. The bases \mathbf{V} and \mathbf{Z} are found similarly. From these estimated bases and the relation in Eq. (5) the compressed array can be determined. In short for the Tucker1-based compression one obtains the projections matrices as

Tucker1-based compression

$$\begin{aligned} [\mathbf{U}, \mathbf{S}, \mathbf{T}] &= \text{svd}(\mathbf{X}^{(1)}, R^A) \\ [\mathbf{Z}, \mathbf{S}, \mathbf{T}] &= \text{svd}(\mathbf{X}^{(2)}, R^B) \\ [\mathbf{V}, \mathbf{S}, \mathbf{T}] &= \text{svd}(\mathbf{X}^{(3)}, R^C), \end{aligned} \quad (6)$$

where the function $[\mathbf{R}, \mathbf{S}, \mathbf{T}] = \text{svd}(\mathbf{X}, F)$ calculates the rank F truncated singular value decomposition of the matrix \mathbf{X} , the matrix \mathbf{R} holding the first F left singular vectors. Note that this approach has actually been suggested earlier for the PARAFAC model specifically in Ref. [18].

A better way, though, to define optimal bases is to say that \mathbf{U} , \mathbf{V} , and \mathbf{Z} should give a least squares estimate of the array \mathbf{Y} of Eq. (5). This will lead to a set of bases which preserves most of the original variation in the compressed array. The definition of the array \mathbf{Y} in Eq. (5) corresponds to the definition of the so-called core array in a Tucker3 model [19]. It therefore immediately follows that orthonormal load-

ing matrices of a $R^A \times R^B \times R^C$ Tucker3 model will provide optimal bases for calculating the compressed array. Further, the compressed array will be equal to the core array of the Tucker3 model. Realizing this, it then follows that a fast Tucker3 model is the key to a successful compression method. In part I [20], such an algorithm was developed for the MATLAB programming environment. After obtaining the array \underline{Y} any suitable model can be estimated as described in Refs. [3,4], and exemplified above for the PARAFAC model.

Tucker3-based compression

$$\operatorname{argmin}_{U, V, Z, Y} \|\underline{X} - \underline{UY}(Z^T \otimes V^T)\|_F^2 \quad (7)$$

It is important that most systematic variation be incorporated into the compressed array. This is especially true if the subsequent analytical model to be estimated is constrained in some sense. Henceforth, the goal of the Tucker3 model is not to find *the* model but rather to find a model that is not underestimated with respect to dimensions. It is of little concern whether the compressed array is of size $7 \times 7 \times 7$ or $11 \times 11 \times 11$ with respect to the speed of the algorithm, but it may have a significant influence on the quality of the model if not all systematic variation is retained in the $7 \times 7 \times 7$ array. In general, very few data types conform exactly to a mathematical model, which means that one must expect some systematic variation in the residuals. If, e.g., a three-component PARAFAC model is sought it will not necessarily be sufficient to compress the array using a $3 \times 3 \times 3$ Tucker3 model. The way to choose the appropriate number of components in the compression model depends highly on the data type. No general rules can be given, unless one is willing to settle for a quite large compressed array. One may for example compress the array using, say five extra components compared to the number of components in the analytical model, which would probably ensure a valid model. If this is not satisfactory, one has to resort to numerical rank-analysis or simply evaluate for increasing number of components in the compression model when the estimated final model no longer changes. The results presented in Ref. [21] as well as here indicate that using the same number of factors in the Tucker3 model as in the subsequent analytical

model will work satisfactory in many cases though not all.

2.1. Modifications of the compression approach

In the literature algorithms have been given for estimating the three-way PARAFAC and Tucker3 model in situations where only one mode is very high-dimensional [22,23]. These methods are exact and implicitly based on the fact, that the rank of the high-dimensional mode is limited by the dimensionalities of the remaining modes. If the product, d , of the two smallest dimensions of the array is smaller than the dimension in the mode of the largest size, then it can be shown that the rank of this mode is upper-bounded by d . In the present approach this means that in situations with one very high-dimensional mode, one can simply compress only in the high-dimensional mode using a basis of dimension d . This will provide a compressed array that exactly preserves the variation of the original array (A.K. Smilde, personal communication). It can be shown that such a compression model can be estimated by a Tucker1 model.

In general, if some modes are not to be compressed this is implemented in the compression method by estimating a Tucker2 or a Tucker1 model instead of the Tucker3 model. Avoiding compression in a certain mode can be useful, e.g., if the mode is to be estimated with constraints that do not easily translate into the compressed space.

If the uncertainties (e.g., standard deviations) of the individual elements are known, several possibilities exist for incorporating these uncertainties in the loss function of the analytical model. One may scale the data prior to compression [24–26] or compute the compression model using a weighted alternating least squares regression approach. The analytical model can henceforth be estimated with an unweighted loss function. Instead of using the uncertainties in the compression model, one may also simply estimate the compression model without considering these. The uncertainty of the elements of the *compressed* array may then be obtained by regressing the uncertainties (same size as \underline{X}) in the same way as \underline{X} is regressed (Eq. (5)). These uncertainties can hence be used when estimating the analytical model.

If the data array contains missing values, the compression must be performed taking this into account as described in Part I [20]. The resulting compressed array will have no missing entries and hence no special attention is needed in the algorithm for estimating the analytical model.

If the resulting loading matrices of the analytical model are required to be nonnegative this poses some problems, as the bounded least squares problem of the uncompressed problem turns into a more general and complicated inequality constrained least squares problem in the compressed space. Currently no method seems able to handle this special situation efficiently but the problem is being worked on, and will be the subject of a following paper.

3. Experimental

Two data sets arising from fluorescence spectroscopy were used for testing the compression on real data. The first called AMINO is a data set of five samples with different amounts of tryptophane, phenylalanine, and tyrosine. Each sample has been measured spectrofluorometrically at excitation 250–300 nm, emission 250–450 nm with 1 nm intervals. The data have also been described in Ref. [13]. The data array is of dimension 5 (sample) \times 51 (excitation) \times 201 (emission). Note that for these data the exact compression mentioned before is not possible. Even though the first mode is only of dimension 5, the product of the two smaller is 255 which is more

than the largest dimension. The proper PARAFAC-dimensionality of the data has been found to be three. The other data set stems from an investigation of a sugar plant process and is called SUGAR. It suffices here to say that 265 samples of sugar were dissolved in water and measured spectrofluorometrically from 275–560 nm at excitations 230, 240, 255, 290, 305, 325, 340 nm by a procedure according to Nørgaard [27]. Part of the data was significantly influenced by Rayleigh scatter. In order not to confound the results with the problems of missing values, this part of the data set was discarded in this analysis resulting in an array of size 265 \times 371 \times 7. The proper PARAFAC dimensionality is three.

For the AMINO data set, the following procedure was used. The unconstrained PARAFAC model was estimated for a two-, three-, and four-component model respectively. This way it is possible to judge separately what happens if the model is under- or over-specified with respect to the number of components. For the SUGAR data, only a three-component PARAFAC model was estimated. A relative change in fit (sum-of-squared errors) less than 10^{-6} was used as convergence criterion. Each model was estimated from the raw data and from an array compressed using two and up to seven components in the Tucker3 model to verify the influence of the degree of compression. Naturally one expects that the fewer components in the Tucker3 model, the faster the subsequent estimation will be as the array is smaller. However, one will also expect that the estimated analytical model resembles the model estimated from the

Table 1
Results from estimating a two-component PARAFAC model on the data set AMINO

Data set AMINO, two-component PARAFAC model				SVD-based component		
Tucker3 components	Time of comp/ model (s)	Time of model (s)	Time of raw (s)	Difference (% experimental)	Time of comp/ model (s)	Difference (% experimental)
2	97	43	324	$-0.6 \cdot 10^{-3}$	147	8.4
3	16	8	324	$6.3 \cdot 10^{-3}$	144	$6.8 \cdot 10^{-3}$
4	37	11	324	$2.4 \cdot 10^{-3}$	147	$2.4 \cdot 10^{-3}$
5	65	16	324	$1.9 \cdot 10^{-3}$	149	$2.0 \cdot 10^{-3}$
6	146	17	324	$1.6 \cdot 10^{-3}$	152	$1.9 \cdot 10^{-3}$
7	73	19	324	$0.4 \cdot 10^{-3}$	155	$0.4 \cdot 10^{-3}$

The first column gives the number of components used in the Tucker3 compression. The second column is the time spent in estimating both the compressed array and the model. The third column gives the time for only estimating the model from the compressed array, and the fourth column the time for estimating the model from the raw data. The fifth column gives the difference in the percentage of variation explained by the two models. The last two columns give the results from compressing with Tucker1 loadings.

II. Algorithms, models and applications

110

R. Bro, C.A. Andersson / Chemometrics and Intelligent Laboratory Systems 42 (1998) 105–113

Table 2

Results from estimating a three-component PARAFAC model on the data set AMINO

Data set AMINO, three-component PARAFAC model				SVD-based compression		
Tucker3 components	Time of comp/ model (s)	Time of model (s)	Time of raw (s)	Difference (% experimental)	Time of comp/ model (s)	Difference (% experimental)
3	32	24	849	$2.0 \cdot 10^{-5}$	151	$2.3 \cdot 10^{-4}$
4	56	29	849	$7.7 \cdot 10^{-5}$	157	$1.1 \cdot 10^{-4}$
5	82	35	849	$4.1 \cdot 10^{-5}$	162	$0.4 \cdot 10^{-4}$
6	165	41	849	$3.4 \cdot 10^{-5}$	168	$0.4 \cdot 10^{-4}$
7	101	48	849	$1.3 \cdot 10^{-5}$	175	$0.1 \cdot 10^{-4}$

For further explanation, see legend of Table 1.

raw data better, the more components are used for compression.

The time used for estimating the model is given in seconds and three times are tabulated: the time used for estimating the model from the raw data (using the same initialization as for the Tucker3 model), the time used for compression and estimating the model from the compressed array and finally the time used for estimating the analytical model from the compressed array. The last one is relevant as one will often estimate different models from the data in order to verify which is better. In such a case one would not re-compress the array each time, but rather use the same compressed array each time. We have chosen to use time rather than the number of FLOPS (floating operations) for indicating the computational complex-

ity, as the number of FLOPS seldom reflects the time consumption realistically. In order to be able to generalize the results obtained to other platforms than MATLAB, however, we will also mention the complexity of the methods with respect to FLOPS. The difference in fit between the model estimated from the raw data and from the compressed data is also given. The model estimated from the raw data is the 'truth' as it will per definition be the least-squares estimate; hence the fit of the model estimated from the compressed data, should give equally good fit.

For comparison, the results of using Tucker1-based compression instead of a Tucker3 is also shown. These Tucker1-defined bases are often suggested as appropriate bases for describing the respective variable spaces in the literature. Indeed, if differ-

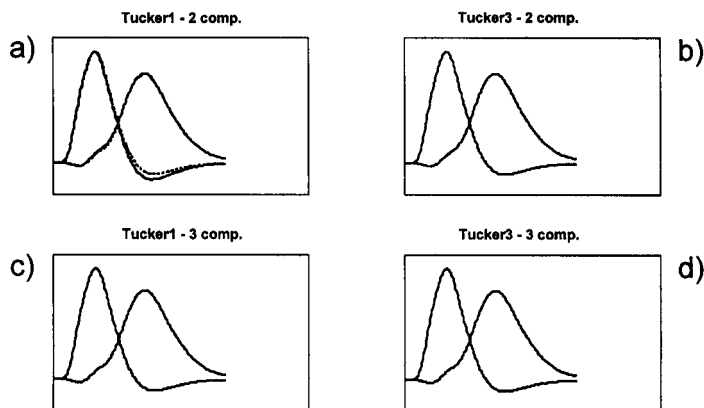


Fig. 1. Two-component PARAFAC model of AMINO. The broken lines indicate the loadings estimated directly from the raw data. (a) Using two-component Tucker1 for compression, (b) using two-component Tucker3 for compression, (c) using three-component Tucker1 for compression, (d) using three-component Tucker3 for compression.

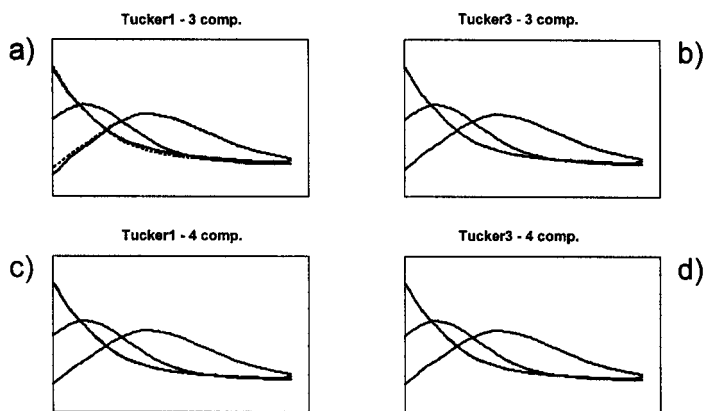


Fig. 2. Three-component PARAFAC model of SUGAR. The broken lines indicate the loadings estimated directly from the raw data. (a) Using three-component Tucker1 for compression, (b) using three-component Tucker3 for compression, (c) using four-component Tucker1 for compression, (d) using four-component Tucker3 for compression.

ences in time and fit between these two compression approaches are negligible there is little sense in using the more complicated iterative Tucker3 model for compression.

4. Results

The most important finding of the investigation is that the analytical model obtained from the compressed data is almost always identical to the one obtained from the raw data. Of all the models estimated only two compression based analytical models differ substantially from the models estimated directly from the raw data. These are the Tucker1-based models shown in Tables 1 and 2 with two- and three-com-

pression components, respectively. To illustrate qualitatively the difference between the Tucker1- and the Tucker3-based compression the estimated loadings in the emission mode are compared in Figs. 1 and 2 with the loadings estimated from the raw data.

The estimates are shown for the models mentioned above, and models including one more component in the compression bases. It is easily verified that only Tucker1-based models differ from the reference loadings (Fig. 1a Fig. 2a). Using more components will remedy this (Fig. 1c Fig. 2c) and the Tucker3-based compression is always better (Fig. 1b and d Fig. 2b and d). The overall conclusion as judged from the tables is, that Tucker3 compressed PARAFAC modeling is consistently faster than uncompressed modeling. Especially if the PARAFAC

Table 3
Results from estimating a four-component PARAFAC model on the data set AMINO

Data set AMINO, four-component PARAFAC model				SVD-based compression		
Tucker3 components	Time of comp/ model (s)	Time of model (s)	Time of raw (s)	Difference (% experimental)	Time of comp/ model (s)	Difference (% experimental)
4	874	580	1130	$14.0 \cdot 10^{-3}$	989	$14.0 \cdot 10^{-3}$
5	627	581	1130	$4 \cdot 10^{-3}$	669	$4 \cdot 10^{-3}$
6	671	547	1130	$2 \cdot 10^{-3}$	760	$4 \cdot 10^{-3}$
7	625	573	1130	$0 \cdot 10^{-3}$	710	$1 \cdot 10^{-3}$

For further explanation, see legend of Table 1.

Table 4

Results from estimating a three-component PARAFAC model on the data set SUGAR

Data set SUGAR, three-component PARAFAC model					SVD-based compression	
Tucker3 components	Time of comp/ model (s)	Time of model (s)	Time of raw (s)	Difference (% experimental)	Time of comp/ model (s)	Difference (% experimental)
3	307	111	1545	$5.4 \cdot 10^{-3}$	172	$64.8 \cdot 10^{-3}$
4	297	123	1545	$5.4 \cdot 10^{-3}$	172	$8.4 \cdot 10^{-3}$
5	447	150	1545	$0.5 \cdot 10^{-3}$	174	$0.5 \cdot 10^{-3}$
6	455	176	1545	$0.4 \cdot 10^{-3}$	177	$0.4 \cdot 10^{-3}$
7	450	202	1545	$0.2 \cdot 10^{-3}$	180	$0.2 \cdot 10^{-3}$

For further explanation, see legend of Table 1.

model is slightly overparameterized (too many components) the gain is large, as the estimation of the PARAFAC model from the raw data can then be very time-consuming (Table 3). Surprisingly, modeling based on Tucker3 compression is also faster than using the simpler Tucker1-based compression. This is because the Tucker1 estimation of bases is performed on quite large arrays. This could have been remedied by using instead an approach similar to the initialization of the Tucker3 algorithm as described in part 1. The Tucker3 compression though, consistently fits the reference model better than Tucker1-based compression. Especially if few compression components are used the difference can be large (Tables 1 and 4). There are thus no arguments for using Tucker1-based compression instead of Tucker3-based.

For all the models investigated the number FLOPS used for estimating the models were also registered. The main result is that estimating the PARAFAC model using the Tucker3-based compression is generally 5 to 80 times cheaper than estimating the model from the raw data in terms of FLOPS as compared to only a 3 to 40 times cheaper with respect to speed. Much of the computation (30–90%) is used for estimating the Tucker3 model, though with respect to time these figures are generally lower. Even though the compression approach is thus advantageous any improvement of the Tucker3 algorithm will be beneficial. A simple idea could be to only estimate the Tucker3 compression model using few iterations (< 10). The observation that the Tucker1 based approach is almost as efficient as the Tucker3 based approach seems to indicate, that even an approximate Tucker3 model can be beneficial. However, one must

keep in mind, that for all practical purposes, several analytical models will normally be estimated, but only one compression model is needed. Therefore the actual importance of the complexity of the compression algorithm is less important than indicated by the results presented here.

5. Conclusion

We have developed an efficient method for compressing large arrays using a fast Tucker3 algorithm for compression. The compression method has been shown to speed up estimation considerably. Incorporation of important constraints has also been discussed. It might be argued that there is little gain in using Tucker3 loadings instead of the more easily calculated Tucker1 models for compression. However, as the Tucker3 model is fast and because it *does* make a difference in some situations, the use of Tucker3 loadings seems an appropriate choice for compression. This, especially since the estimation of the compression model is mostly fast compared to the estimation of the possibly several analytical models. The conclusion of this work also applies to, e.g., the use of singular vectors for defining the variable space before doing generalized rank annihilation.

Acknowledgements

Professor Lars Munck is thanked for providing philosophical support for what must be the most exploratory industry-related research group. The authors further wish to thank Professor Lars Munck for

financial support through the Nordic Industry Foundation project P93149 and the FØTEK foundation. We are obliged to Age Smilde, Sijmen de Jong, Henk Kiers, and the anonymous referees for helpful comments.

References

- [1] B.K. Alsberg, O.M. Kvalheim, *Chemometrics Intell. Lab. Syst.* 24 (1994) 31.
- [2] B.K. Alsberg, O.M. Kvalheim, *Chemometrics Intell. Lab. Syst.* 24 (1994) 43.
- [3] H.A.L. Kiers, R.A. Harshman, *Chemometrics Intell. Lab. Syst.* 39 (1997) 31.
- [4] J.D. Carroll, S. Pruzansky, J.B. Kruskal, *Psychometrika* 45 (1980) 3.
- [5] V. Tomišić, V. Simeon, *J. Chemometrics* 7 (1993) 381.
- [6] S. Wold, *Technometrics* 20 (20) (1978) 397.
- [7] H. Martens, T. Næs, *Multivariate Calibration*, Wiley, Chichester, 1989.
- [8] E.R. Malinowski, *Factor Analysis in Chemistry*, Wiley, New York, 1991.
- [9] R.A. Harshman, *UCLA Work. Pap. Phonetics* 16 (1970) 1.
- [10] R.A. Harshman, *UCLA Work. Pap. Phonetics* 22 (1972) 111.
- [11] S. Leurgans, R.T. Ross, R.B. Abel, *SIAM J. Matrix Anal. Appl.* 14 (1993) 1064.
- [12] R.A. Harshman, M.E. Lundy, *Comp. Stat. Data Anal.* 18 (1994) 39.
- [13] R. Bro, *Chemometrics Intell. Lab. Syst.* 38 (1997) 149.
- [14] R.A. Harshman, M.E. Lundy, *Psychometrika* 61 (1996) 133.
- [15] R.A. Harshman, *UCLA Work. Pap. Phonetics* 22 (1972) 30.
- [16] H.A.L. Kiers, *Psychometrika* 54 (1989) 515.
- [17] P.M. Kroonenberg, *Three-Mode Principal Component Analysis*, DSWO Press, Leiden, 1989.
- [18] C.J. Appellof, E.R. Davidson, *Anal. Chem.* 53 (1981) 2053.
- [19] P.M. Kroonenberg, J. de Leeuw, *Psychometrika* 45 (1980) 69.
- [20] C.A. Andersson, R. Bro, *Chemometrics Intell. Lab. Syst.* 42 (1998) 91–101.
- [21] H.A.L. Kiers, *J. Chemometrics* (submitted).
- [22] H.A.L. Kiers, W.P. Krijnen, *Psychometrika* 56 (1991) 147.
- [23] H.A.L. Kiers, *Psychometrika* 57 (1992) 415.
- [24] J.M.F. ten Berge, in: R. Coppi, S. Bolasco (Eds.), *Multivariate Data Analysis*, Elsevier, North-Holland, 1989.
- [25] J.B. Kruskal, *Proc. Symp. Appl. Math.* 28 (1983) 75.
- [26] R.A. Harshman, M.E. Lundy, in: H.G. Law, C.W. Snyder, J.A. Hattie, R.P. McDonald (Eds.), *Research Methods for Multimode Data Analysis*, Praeger, New York, 1984.
- [27] L. Nørgaard, *Zuckerindustrie* 120 (1995) 970.

P6

**Further improvements of the
speed of the three-way Tucker3
algorithm**

Pentti Paatero and Claus A. Andersson



Further improvements of the speed of the Tucker3 three-way algorithm ¹

Pentti Paatero ^{a,*}, Claus A. Andersson ^{b,2}

^a Department of Physics, University of Helsinki, P.O. Box 9, FIN-00014 Helsinki, Finland

^b Food Technology, Chemometrics Group, The Royal Veterinary and Agricultural University, Denmark

Abstract

An improvement to the Andersson–Bro (A-B) alternating least squares (ALS) algorithm for the Tucker3 three-way model is presented. The published A-B algorithm deals cyclically with the three modes of the problem. In each ALS substep, the whole array is projected onto a different mode. The projections are the dominating workload. In the improved version, each whole-array projection is utilized for two ALS substeps. The same ALS steps are performed as before but the number of full-sized projections is cut to half. This almost doubles the speed of the algorithm without changing its convergence properties. The possibility to utilize each full-sized projection for more than two ALS substeps is discussed. © 1999 Elsevier Science B.V. All rights reserved.

Keywords: Three-mode factor analysis, 3-MFA; T3; Alternating least squares, ALS; Non-cyclical algorithm

Contents

1. Introduction	18
2. Notation	18
3. The basic A-B algorithm	18
4. Utilizing each first-level projection for two ALS substeps	18
5. Further possibilities	19
6. Experimental results: the real data set	19
7. Experimental results: synthetic data arrays	20
8. Conclusions	20
References	20

* Corresponding author. Tel.: +358-9-191-8337; Fax: +358-9-191-8680; E-mail: pentti.paatero@helsinki.fi

¹ Intended for publication in *Chemom. Intell. Lab. Syst.* Vol. 42, Nos. 1, 2, special issue in honour of Agnar Höskuldsson.

² E-mail: ca@kvl.dk.

1. Introduction

Recently, Andersson and Bro [1] published a thorough analysis of alternating least squares (ALS) algorithms for solving the three-way factor analytic Tucker3 model. The present note offers an improvement of the published Andersson–Bro (A-B) algorithm. The improved algorithm has been available through the Internet distribution of the A-B programs since May 1997. In its basic form, the modification enables a speed increase of almost a factor of two. This note is closely coupled to the A-B paper and it is assumed that the reader has the paper available. The notation of the A-B paper is mostly followed. Different notation will be explained.

2. Notation

Andersson and Bro work with arrays rearranged ('unfolded') into matrices. Thus projecting the array \mathbf{X} onto matrix \mathbf{B} is written as a matrix product, $\mathbf{W}^{(2)} = \mathbf{B}^T \mathbf{X}^{(2)}$. The superscript (2) indicates in which way the array is unfolded. In this work, the simpler notation suggested by Kruskal [2] is used, viz. $\mathbf{W} = \mathbf{X}^{\mathbf{B}}$ meaning $w_{isk} = \sum_j b_{js} x_{ijk}$. Similarly projections onto \mathbf{A} and onto \mathbf{C} are denoted by $\mathbf{Y} = \mathbf{A}\mathbf{X}$ and $\mathbf{Z} = \mathbf{X}\mathbf{C}$, meaning $y_{rjk} = \sum_i a_{ir} x_{ijk}$ and $z_{ijt} = \sum_k c_{kt} x_{ijk}$, respectively. A combined projection onto \mathbf{C} and \mathbf{B} is denoted in the A-B paper as $\mathbf{V}^{(1)} = \mathbf{X}^{(1)}(\mathbf{C} \otimes \mathbf{B})$. In Kruskal notation this is $\mathbf{V} = \mathbf{X}\mathbf{C}$, meaning $v_{ist} = \sum_j \sum_k b_{js} c_{kt} x_{ijk}$. Similar notations apply for double projections onto \mathbf{A} and \mathbf{B} , and onto \mathbf{A} and \mathbf{C} . A notation such as $\mathbf{W} = \mathbf{A}\mathbf{X}^{\mathbf{B}}$ may be understood equally well as projecting first on \mathbf{B} , then on \mathbf{A} or as projecting first on \mathbf{A} , then on \mathbf{B} .

In Ref. [1], one projection is discussed as representative of all three and the doubly projected array is called \mathbf{V} . In the present note, the notation \mathbf{V} is dropped as it is necessary to discuss all three cases separately. Instead, double projections of \mathbf{X} onto (\mathbf{B}, \mathbf{C}) , (\mathbf{C}, \mathbf{A}) , and (\mathbf{A}, \mathbf{B}) are called \mathbf{R} , \mathbf{S} , and \mathbf{T} , respectively.

3. The basic A-B algorithm

One full iteration step of the A-B ALS algorithm may be described as follows.

(1a) Project array \mathbf{X} onto factor matrix \mathbf{B} and further onto \mathbf{C} : $\mathbf{W} = \mathbf{X}^{\mathbf{B}}$, $\mathbf{R} = \mathbf{W}\mathbf{C}$.

(1b) Compute the new factor matrix \mathbf{A} as the first R^A singular vectors of the unfolded array \mathbf{R} .

(2a) Project array \mathbf{X} onto factor matrix \mathbf{C} and further to the new \mathbf{A} : $\mathbf{Z} = \mathbf{X}\mathbf{C}$, $\mathbf{S} = \mathbf{A}\mathbf{Z}$.

(2b) Compute the new factor matrix \mathbf{B} as the first R^B singular vectors of the unfolded array \mathbf{S} .

(3a) Project array \mathbf{X} onto the new matrix \mathbf{A} and further onto the new \mathbf{B} : $\mathbf{Y} = \mathbf{A}\mathbf{X}$, $\mathbf{T} = \mathbf{Y}^{\mathbf{B}}$.

(3b) Compute the new factor matrix \mathbf{C} as the first R^C singular vectors of the unfolded array \mathbf{T} .

The main contents of Ref. [1] is a thorough analysis of the algorithmic substeps 1b, 2b, and 3b. These substeps are refined so that the total number of iteration steps becomes as small as possible. In this note, these substeps are not discussed. As pointed out by Andersson and Bro, the main workload in the iteration is in the first level projections, i.e., in the computations $\mathbf{W} = \mathbf{X}^{\mathbf{B}}$, $\mathbf{Z} = \mathbf{X}\mathbf{C}$, and $\mathbf{Y} = \mathbf{A}\mathbf{X}$. In the second level projections, the arrays \mathbf{W} , \mathbf{Z} , and \mathbf{Y} are (much) smaller than the original array \mathbf{X} and the workload is correspondingly smaller.

4. Utilizing each first-level projection for two ALS substeps

The idea of the improved algorithm is that each first-level projection should be utilized as far as possible. The projections needed in two full ALS steps can be organized as follows, while keeping the A-B algorithm otherwise unchanged. This algorithm is designated as (2,2,2), indicating that two factor computations are performed after each first-level projection. The previous basic algorithm is correspondingly called (1,1,1).

(1) Project \mathbf{X} onto \mathbf{C} and further onto \mathbf{B} :

$$\mathbf{Z} = \mathbf{X}\mathbf{C}, \mathbf{R} = \mathbf{Z}^{\mathbf{B}}. \text{ Compute } \mathbf{A}.$$

(2) Project \mathbf{X} onto \mathbf{C} and further onto \mathbf{A} :

$$\mathbf{S} = \mathbf{A}\mathbf{Z}. \text{ Compute } \mathbf{B}.$$

(3) Project X onto B and further onto A :

$$W = X, T = AW. \text{ Compute } C.$$

(1') Project X onto B and further onto C :

$$R = WC. \text{ Compute } A.$$

(2') Project X onto A and further onto C :

$$Y = AX, S = YC. \text{ Compute } B.$$

(3') Project X onto A and further onto B :

$$T = Y. \text{ Compute } C.$$

Discussion of the algorithm. The matrix C does not change in step 1. Thus the first-level task of projecting X onto C is exactly the same in steps 1 and 2. The result of first-level projection from step 1, array Z , may thus be reused for the second-level projection in step 2. Similarly, W from step 3 may be used in step 1', and Y from step 2' may be used in step 3'. The net gain is that in two full steps, only three first-level projections are needed instead of six. The main part of workload is cut to half. The doubly projected arrays R , S , and T are the same as in the original algorithm, except for different rounding errors caused by a different order of computations. This algorithm has been distributed by Andersson and Bro through Internet.

5. Further possibilities

The idea presented in the previous section may be carried further. When X has been projected onto C , it is possible to recompute A and B several times while keeping C constant. There will be a problem-dependent optimum count of these subiterations where the improvement of fit produced by another

Table 2

Sequence of projections when first-level projections onto A are avoided

1st projection	2nd projection	Solve factor
C	A	B
–	B	A
–	A	B
B	A	C
–	C	A
–	A	C

subiteration step does not justify the additional workload caused by another subiteration step. Table 1 illustrates the projection sequence when each first-level projection is utilized for three second-level projections and factor solutions. After projecting onto C , A is solved, then B , and then again A . Similar patterns occur after first-level projections onto B and onto A . This arrangement is called (3,3,3).

It is straightforward to count the flops in different projections. If the three dimensions of the core array are not equal, then first-level projection to the mode having the largest core dimension causes the largest number of flops. As an example, consider a case where $I = J = K = 100$, $R^A = 10$, $R^B = R^C = 5$. Then the cost of first projecting onto A is twice the cost of the other alternatives. In this example one might wish to use a projection sequence where first-level projections are only performed onto B and onto C . Table 2 shows an example of such a sequence. This setup is called (0,3,3), where the zero code indicates that no first-level projection is made upon A .

6. Experimental results: the real data set

The experimental data set discussed in Ref. [1] was analyzed by using the modified algorithms. The results should be taken as representative examples, not as the final truth. The iteration counts needed for convergence will depend on the characteristics of individual data arrays. In addition, the relative timings will depend on technical details of the implementation, on caching characteristics of the hardware, and also on the dimensions of the three different modes.

The algorithmic variants are denoted by triples of numbers (na , nb , nc) where na denotes how many

Table 1

Sequence of projections when each first-level projection is followed by three second-level projections

1st projection	2nd projection	Solve factor
C	B	A
–	A	B
–	B	A
B	A	C
–	C	A
–	A	C
A	C	B
–	B	C
–	C	B

factor evaluations are performed after each first-level projection onto **A**, and so on. For the real data set of Ref. [1], the iteration counts for (1,1,1), (2,2,2), (4,4,4), and (10,10,10) were 21, 11, 7, and 4, respectively. The elapsed times were 58, 36, 30, and 26 s. These results demonstrate that the first-level projections are not the only significant workload when the subiteration counts increase above (2,2,2). Although the main iteration count decreases by 64% from (2,2,2) to (10,10,10), the elapsed time decreases only by 28%. Avoiding first-level projections in the third mode resulted in competitive timings, too: (8,7,0) and (20,19,0) converged in six and three iterations, requiring 32 and 27 s, respectively.

7. Experimental results: synthetic data arrays

Synthetic data arrays were generated in the manner described in Ref. [1]. With 39 such arrays, the results were ambiguous. The numbers of iterations seemed to vary randomly between different arrays and different iteration arrangements. A few extreme examples of iteration counts for (1,1,1)/(2,2,2)/(10,10,10) were 26/13/7, 34/36/16, and 23/16/23. Further experiments revealed the reason: With the used numbers of iterations (between 20 and 44 iterations for the (1,1,1) case) the convergence is pushed so far that numerical accuracy plays a decisive role. Projecting first onto **A** and then onto **B** leads to a different numerical result than projecting first onto **B** and then onto **A**. Which one is better, depends on the numerical data values.

Using the same projections but changing the (1,1,1) solution sequence from (A,B,C) to (A,C,B) also caused dramatic changes to iteration counts. Extreme examples: 54 iterations were changed to 13, 26 iterations to 47.

These numerical effects masked the convergence-rate differences almost completely. Thus it is not meaningful to report the results in more detail. In order to measure the convergence rates more reliably, a different test is needed. Then the required accuracy level should be set according to the requirements of a practical data analysis situation. Typically, one might be satisfied if the sum-of-squares value is obtained with five true significant digits. (In

the present test, six or seven correct digits were required.)

8. Conclusions

The suggested modifications may be trivially included in existing implementations of the A-B algorithm or in other similar algorithms. With two substeps, the gain in speed is almost a factor of two, which is worth the effort especially if large problems are solved. No complications are expected in convergence or numerical precision unless one tries to push the convergence so far that numerical effects (loss of significant figures in projections) play a decisive role.

With more than two substeps following each first-level projection, the gain probably depends on the data. In the single real-data test performed in this investigation, 10 subiterations were found to be marginally faster than four subiterations. It may be argued that just iterating two of the factor matrices while keeping the third one unchanged is almost worthless. On the other hand, this iteration is relatively cheap if the principal vectors are computed with an efficient algorithm. Only practical tests may decide how many subiterations give optimum performance.

An adaptive approach to organizing the subiterations seems possible. Instead of focusing on a fixed subiteration pattern (na, nb, nc), one could perform a variable number of second-level projections after each first-level projection. This would be based on a mild convergence criterion: each sequence of second-level projections would be continued until the improvement of fit from another second-level projection drops below a fixed percentage of the total improvement obtained so far under the current first-level projection.

References

- [1] C.A. Andersson, R. Bro, Improving the speed of multi-way algorithms: Part I. Tucker3, *Chemometrics and Intelligent Laboratory Systems* 42 (1998) 93–103.
- [2] J.B. Kruskal, Three-way arrays: rank and uniqueness of trilinear decompositions, with applications to arithmetic complexity and statistics, *Linear Algebra and its Applications* 18 (1977) 95–138.

II. Algorithms, models and applications

Chemometrics in food science - a demonstration of the feasibility of a highly exploratory, inductive evaluation strategy of fundamental scientific significance

Lars Munck, Lars Nørgaard, Søren B. Engelsen, Rasmus Bro and Claus A. Andersson



ELSEVIER

Chemometrics and Intelligent Laboratory Systems 44 (1998) 31–60

Chemometrics and
intelligent
laboratory systems

Chemometrics in food science—a demonstration of the feasibility of a highly exploratory, inductive evaluation strategy of fundamental scientific significance

L. Munck^{*}, L. Nørgaard, S.B. Engelsen, R. Bro, C.A. Andersson

Chemometrics Group, Food Technology, Department of Dairy and Food Science, The Royal Veterinary and Agricultural University, Rolighedsvej 30, DK-1958 Frederiksberg C, Denmark

Abstract

At the roots of science lies observation and data collection from the world as is and from which conclusions can be induced after classification. This is far from the present theory-driven, deductive, normative stage of science which depends heavily on modelling discrete functional factors in laboratory experiments and suppresses the aspect of interaction. In spite of its successes, science today has great difficulty in adapting to the changes which technology has created to cope with registering and evaluating real data from the world, such as in food production chains. This paper demonstrates that it is possible and profitable with the help of new technology to reintroduce an explorative, inductive strategy to investigate the chemistry of a complex food process as is with a minimum of a priori assumptions. The food process investigated is a sugar plant and the tools necessary in this strategy include a multivariate screening method (fluorescence spectroscopy), an arsenal of chemometric models (PCA, PLS, principal variables), including multiway models (PARAFAC, Tucker), and a computer. Not only can chemical criteria and process parameters throughout the process be validly predicted by the screening method, but process irregularities as well as chemical species can also be detected and validated by multiway chemometric techniques. Inspired by examples from the food area, the paper further discusses the nature of the exploration method in the selection of tools and data. The aim is to study complex processes as a whole in order to model interaction of the underlying latent functional factors which may later be defined more precisely by deductive methods. These methods in combination with an appropriate multivariate screening method allow for unique identification of objects—a significant prerequisite for a viable, exploratory, inductive data strategy which is needed as a fundamental complement to prevalent normative research in order to obtain a science on the interdisciplinary level. © 1998 Elsevier Science B.V. All rights reserved.

Keywords: Chemometrics; Food science; Multiway models

"... mathematics is bound to become an increasingly experimental science with less of a claim to absolute truth"

Gregory Chaitin [1]

1. The need for a new multivariate approach in interdisciplinary evaluation

The food and health area receives special attention from the public in the present accelerated change driven by technology. Chemistry and chemical data play decisive roles here. Classical basic research based on laboratory experimentation has made ap-

^{*} Corresponding author.

parent a wide range of natural and manmade chemical species which appear as functional and antifunctional factors in food science and nutrition. Food science is thus, today, in the very centre of the scientific cyclone, drawing on a wealth of disciplines from chemistry and physics [2,3], mathematics and statistics [4], to biology, genetics, medicine, microbiology [5], agriculture, technology and environmental science, and even further to the cognitive sciences like sensory [6] and consumer analysis and psychology as well as to other social disciplines like economy. Such an elaborate web of contacts increases the need for the establishment of basic principles for intercontextual multivariate data communication which are necessary tools to create a real science on the interdisciplinary level. Chemometrics might help here.

The present rapid change is supported but not primarily driven by science. Instead, inventors mainly outside the universities develop technology to advance to the forefront with a much more flexible operational strategy than science. The technologists are focusing on finding a surprising technological fix that is visible and attractive to the consumer and which thus can secure a market. Science often comes long afterwards and explains why technology works and what side effects it has by studying interferences to present hypotheses.

During the Second World War, the organisation of technological product development and the supporting science became much more effective, as vividly described in the classic OECD report by Erich Jantsch in 1967 [7]. The aim of the development outlined by Jantsch is essentially to 'invent the future' by technological forecasting, which Jantsch describes as a management discipline systematically exploiting goal-oriented science in order to realize technology or, in other words, to achieve technological transfer with a high degree of probability.

Exploratory technological forecasting starts by pragmatically evaluating the present knowledge base and is directed towards the future, while normative technological forecasting first defines a future goal or model by evaluating needs, wishes and possibilities and works backwards toward the present in order to realize it. In classical science, these two outlooks are related to inductive and deductive problem-solving, respectively [8]. When technology and science were young, they worked in an inductive, exploratory way,

for example to describe, classify and utilize the chemical compounds which were isolated by distillation, precipitation and crystallization and analyzed by their colour, smell, taste, solubility and reactivity. The patterns of relationships which could be induced from the information from these early studies inspired a theoretical model thinking in formulating general hypotheses from which new, specific and detailed principles and new, confirmative experiments could be deduced [9]. Thus, in food science and related industry, data evaluation today is primarily performed by classical statistical [10] and hard engineering methods [11] based on distributional assumptions and solution of complex differential equations, which were necessary before the advent of the computer. These methods are, however, only relevant for a part of real life where the sufficient causal understanding is already available and underlying assumptions fit, such as in representative sampling techniques, and on the molecular level when, e.g., modelling heat-transfer in food processes.

Before the advent of the computer, the necessary strategy to cope with issues in the multivariate complex world was through problem reduction. The different functional factors in the laboratory were isolated one by one at the expense of control of covariance and overview. Data are still evaluated by a mathematical language based on axioms which are more tuned to the logic of the mathematical machinery than to that of chemistry and the world outside the laboratory. Therefore, the present crisis in today's science is rooted in a lack of an accepted strategy in interdisciplinary science, despite the political quest for such a cooperation. We maintain that in the science of the future new strategies and data, analytical algorithms and procedures will play a fundamental role in creating a dialogue on equal terms between the normative, deductive and the exploratory, inductive principles. We will now focus on an example of how the computer, a specific screening method and a range of chemometric tools mostly funded on vector algebra adapted from mathematical methods of social science [12] may be used by the human brain to upgrade the exploratory, inductive research method which is greatly neglected today. Hempel [8] explains the current attitude: "Scientific knowledge is not obtained by the method of induction based on earlier collection of data but rather by 'The hypothe-

sis method': that is, to invent alternative hypotheses deduced from earlier known knowledge as preliminary answers of the problem under study and thereafter testing these hypotheses empirically''.

2. Exploring the beet sugar manufacturing process by spectrofluorometry and chemometrics—an example of a highly exploratory, inductive research strategy

We will begin by presenting the sequence of chemometric results of the exploratory investigation expressed as a graphic interface which is easily cognitively accessible for any person. In Appendices A–C, we will comment in more detail on how we use the chemometric machinery involved, with emphasis on the new multiway techniques.

Sugar or sucrose [13] is the most abundant disaccharide in nature and has been a world leading commodity for centuries mainly due to its sweet taste properties. Originally, it was extracted from sugar canes but today more than half of the world production comes from sugar beets. Sugar is probably the most chemically pure food component produced with a typical purity of 99.999%. Colour and purity play a great role when evaluating sugar quality.

In 1992, we heard from a sugar production expert that UV-lamps and filters were used in Denmark during the war for visual classification of sugar according to purity. There was a typical blue fluorescence for less pure sugars. With our background in fluorescence analysis in foods [14], but without any in-depth knowledge of sugar production, we contacted and established a dialogue with the Danish company Danisco Sugar. We started by analyzing samples which we knew nothing about in our Perkin Elmer LS50B spectrofluorometer. After presenting the results to the sugar technologists, we obtained successively more information about process conditions and about chemical analyses of the products for interpretation which we included in our chemometric models. The measurement conditions are described or referred to in the text of the figures and tables.

In Fig. 1A, we see the complex fluorescence spectra, each with 1023 data points from 34 different sugar samples from the year 1993. In order to get an

overview of this complex information, we performed a data reduction by principal component analysis (PCA) to reduce the data to a few (three) principal components (PCs).

The PCA score plot in Fig. 1B (PC#1 vs. PC#3) reveals 3 clusters which the sugar technologists identified as average weekly samples from the sugar campaign (production period) from week 1 to 14 for 3 sugar factories called A, B and C. The different raw material and processing conditions of the different factories in 1993 obviously had a unique fluorescence signature.

We then obtained 10 kinds of univariate chemical analyses for each of the 34 samples which are presented as spectra after scaling in Fig. 1C. We performed a separate PCA score analysis of the chemical data which also revealed 3 clusters (Fig. 1D) corresponding to 3 factories and similar to the spectrofluorometric investigation (Fig. 1B). When combining loadings and scores for the chemical analyses in a bi-plot (Fig. 1E), we could see that ash, colour and amino-N analyses are situated in the same area as samples from factory C which indicates that these have especially high values. Because the independent classification based on fluorescence data (Fig. 1B) indicates that factory C is especially high in fluorescence, we induced the hypothesis that fluorescence might be directly or indirectly related to some of the chemical analyses. In order to test this, we performed a partial least squares (PLS) regression analysis on the 34 samples correlating whole fluorescence spectra with ash. The result reveals a significant correlation coefficient of -0.92 , which indicates that fluorescence analysis could be a candidate as a screening method for quality in sugar production.

This indication is further verified in a PLS study [15] with 81 whole fluorescence spectra from 6 different factories showing especially high correlations with amino-N, ash and colour (Table 1). Five wavelengths were selected by the principal variables method (see Appendix C) which altogether gave reasonable prediction models with amino-N, colour and ash, indicating that an 'on-line' screening method could be devised based on a simple filter instrument.

When a PCA was performed on fluorescence information of mean weekly sugar samples during the campaign for one factory, a horseshoe-formed time

II. Algorithms, models and applications

34

L. Munck et al. / *Chemometrics and Intelligent Laboratory Systems* 44 (1998) 31–60

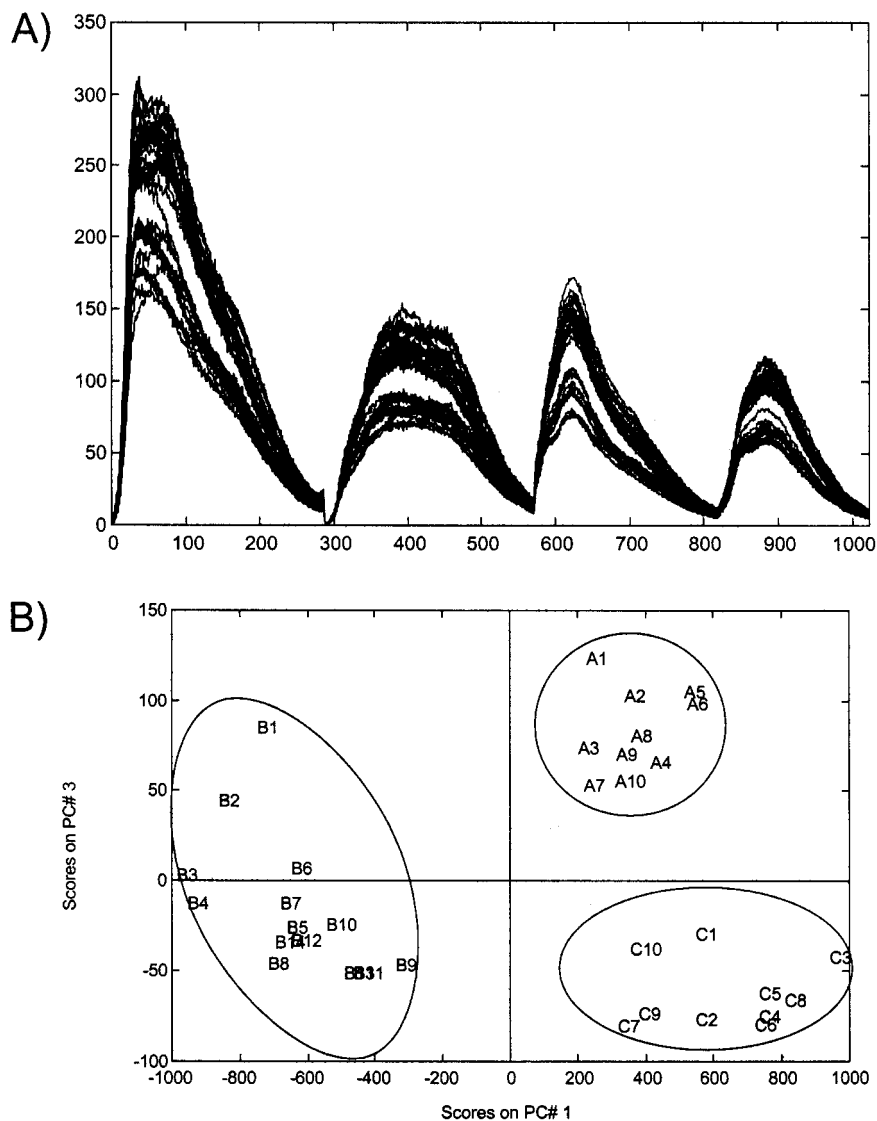
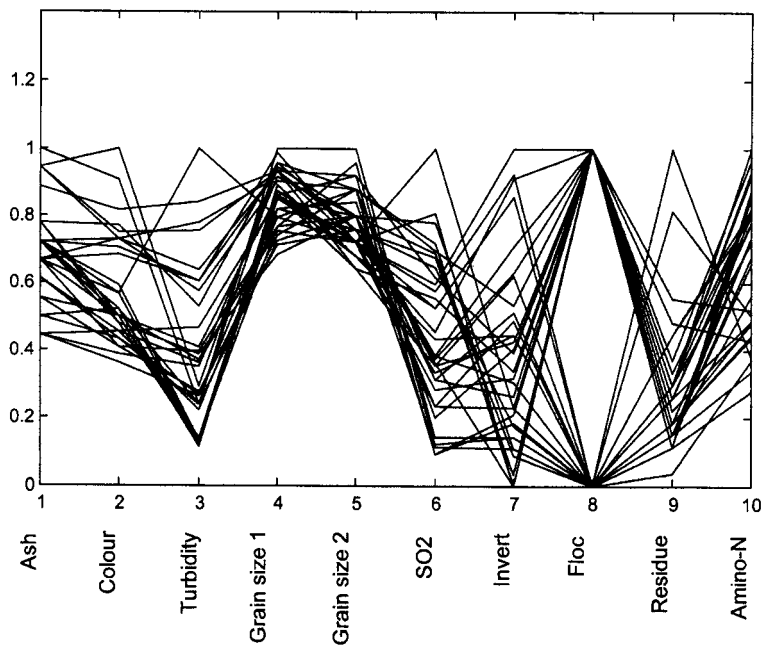


Fig. 1. (A) Uncorrected fluorescence emission spectra of 34 sugar samples. The spectra are recorded from a solution of sugar in water at excitation wavelengths 230 nm, 240 nm, 290 nm and 340 nm. The emission ranges sampled with 1 nm intervals are 275–560 nm, 275–560 nm, 311–560 nm, and 361–560 nm, respectively (in total 1023 data points). See Ref. [15] for further details. (B) A score plot from a PCA on the spectra; three clusters are seen corresponding to samples from three different factories (A, B, and C). (C) Chemical data on the same 34 samples (scaled to a maximum value of 1). (D) Score plot from a PCA on the chemical data; again three clusters are seen corresponding to samples from three different factories. (E) Bi-plot based on chemical data.

II. Algorithms, models and applications

C)



D)

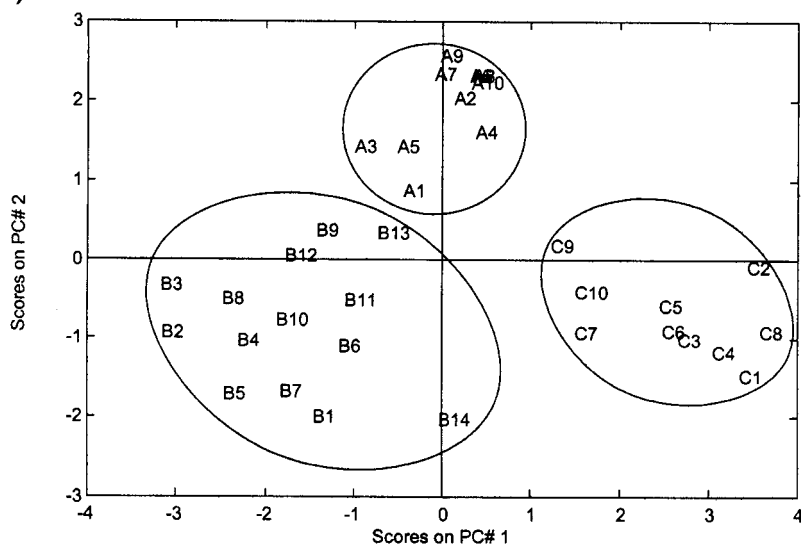


Fig. 1 (continued).

E)

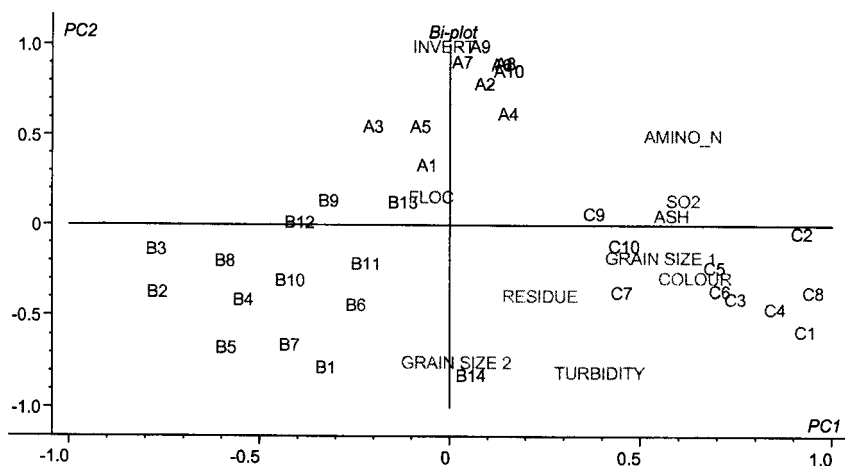


Fig. 1 (continued).

trend could be envisaged for some factories (Fig. 2A), but not for others (Fig. 2B) which were rather chaotic. These two extreme PCA score plots selected from six factories with data from 1993 were described by the sugar engineers as their best and worst functioning factories. The trend in the PCA analysis of spectra in Fig. 2A tentatively represents changes in beet raw material chemistry due to growing conditions, age, climate and storage and the resulting adjustments in process technology.

A similar PCA score plot of sugar fluorescence information from the campaign start of the best functioning sugar factory in 1994 is displayed in Fig. 2C. A total of 106 sugar samples were taken during the first three days of the sugar campaign. The PCA score plot representing these sugar spectra starts at the bottom with samples 3, 2, 5, 6, 4, 9, 8, 7, moving upwards to the right, then straight to the left and ending up in an area of balance from score -50 to score $+50$ of PC2. At the same time, the number of significant principal components diminishes from 4–5 to 1–2, indicating normal operating conditions. However, in the area of relative balance we can still envisage in a local PCA (Fig. 2D) a segregation in two sample clusters 40–74 and 75–106, indicating a fundamental change in the process conditions after sam-

ple 74. This change could be identified in the factory records as a process breakdown. Sample 88 is an unexplained outlier. We conclude that it would be worthwhile to investigate whether the fluorescence information could be used to assist the process engineer in indicating the balance of the process in the form of PCA graphics.

We now move upwards in the process chain from sugar to analyze thick juice—an important un-pure intermediate product in sugar production. In an earlier preliminary study on thick juice [15], we obtained results similar to those as with sugar with regard to fluorescence analysis, however less clear cut, in the classification of factories and correlation to chemical analyses. We then employed a more advanced analysis than two-way PCA, namely 4-way Tucker [16,17], which is explained in more detail in Appendix A. Undiluted thick juice does not display fluorescence due to concentration quenching. It is possible to 'develop' fluorescence information by dilution. By simultaneously using fluorescence landscapes for partially quenched (1:15 Fig. 3A) and unquenched dilutions (1:150 Fig. 3B) we obtain four external parameters with 47 samples, two levels of dilution, 20 excitation wavelengths and 311 emission wavelengths constituting a 4-way data array of order

Table 1

(A) Full spectrum prediction errors for sugar samples (dissolved in water)^a

	Mean	Range	# PC's	RMSEP ^b	r
Amino-N (ppm)	2.631	0.28–4.91	1	0.314	0.96
Colour	21.8	11–44	5	2.4	0.94
Ash %	0.0110	0.004–0.017	3	0.0012	0.91
SO ₂ (ppm)	4.16	0.8–8.2	3	1.08	0.85
Invert (ppm)	36.8	0–92	3	17.6	0.74
Turbidity	0.498	0.19–1.30	4	0.204	0.72

(B) Prediction results for colour, ash, and amino-N based on five excitation–emission wavelengths pairs selected by the principal variables algorithm^{cd}

	Mean	Range	# PC's	RMSEP ^b	r
Amino-N	2.631	0.28–4.91	1	0.280	0.96
Colour	20.9	11–34	5	2.6	0.90
Ash%	0.011	0.004–0.017	3	0.0013	0.91

^aAll models are PLS1 models [15].

^bRoot mean square error of prediction.

^cThe excitation (nm)/emission (nm) wavelengths used for prediction were 230/361, 230/310, 230/333, 230/454 and 340/419.

^dSee Appendix C.

II. Algorithms, models and applications

38

L. Munck et al. / Chemometrics and Intelligent Laboratory Systems 44 (1998) 31–60

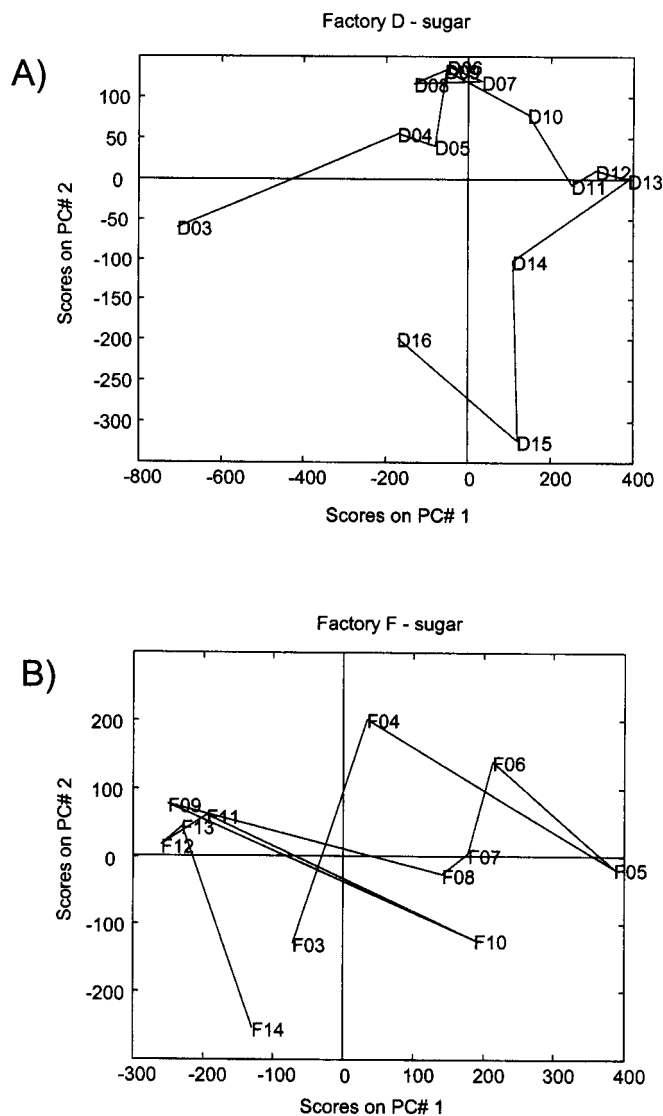


Fig. 2. (A) and (B) Score plots from a PCA of fluorescence spectra recorded on weekly collected samples from two factories. Factory D (A) was known to be the best functioning factory, while factory F (B) was known to be the worst functioning factory. (C) Score plot from a PCA of fluorescence spectra recorded on 106 sugar samples from the first three days of operation in a given sugar factory. (D) Score plot of a PCA on the last 87 samples. The numbering is chronological.

II. Algorithms, models and applications

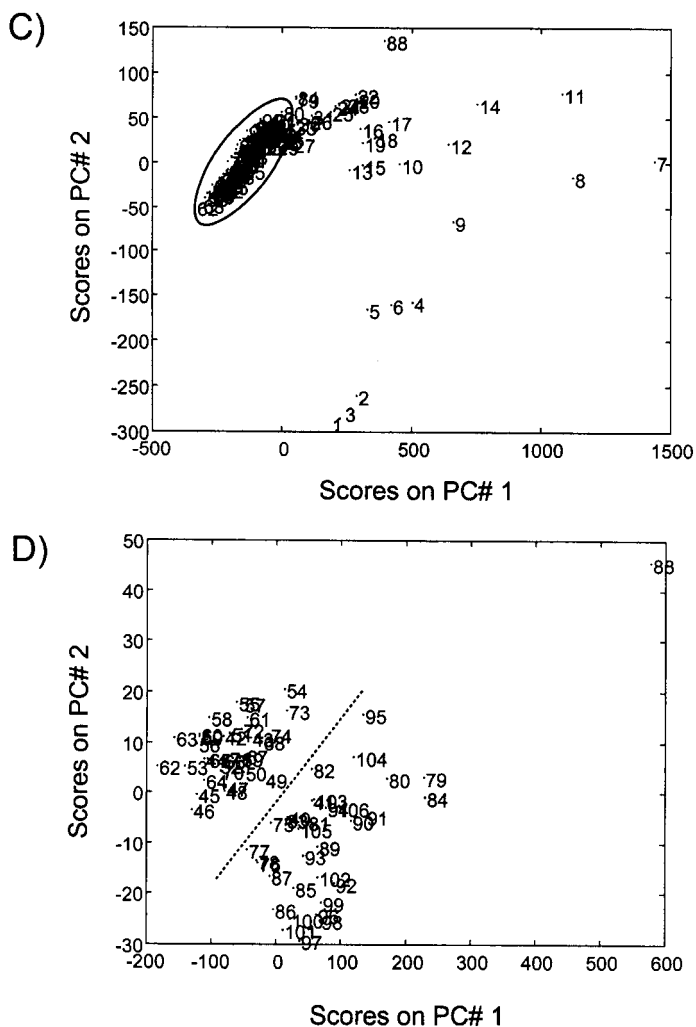


Fig. 2 (continued).

($47 \times 2 \times 20 \times 311$). The plot of the PC scores 2 and 3 is displayed in Fig. 3C showing a clear-cut classification into 5 factories (a, b, d, e and f) and with a clear tendency of timing within each cluster from below to above, ranging from the early to the late samples. This classification is much more clear-cut than

that obtained from the PCA score plots in the thick juice material from different factories investigated by Nørgaard [15] where factories were overlapping and where the time aspect of the samples could not be modelled in the same plot. This underlines the advantages of respecting and exploiting the structure of

II. Algorithms, models and applications

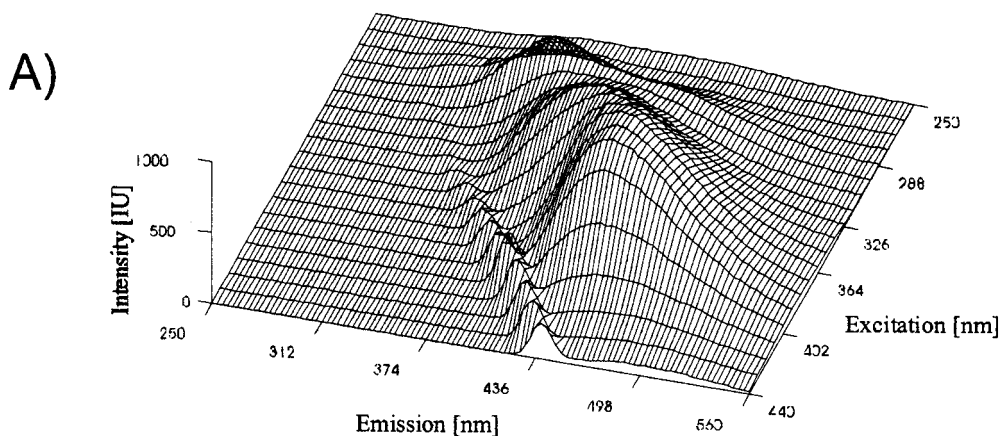
40

L. Munck et al. / *Chemometrics and Intelligent Laboratory Systems* 44 (1998) 31–60

the data and selecting chemometric algorithms accordingly, which are further discussed in Appendices A–C.

We will now proceed further upstream in the sugar process to beet production in agriculture. The price paid to the farmer for the beets is regulated by the

Thick Juice, 1:15, pH 9.00



Thick Juice, 1:150, pH 9.00

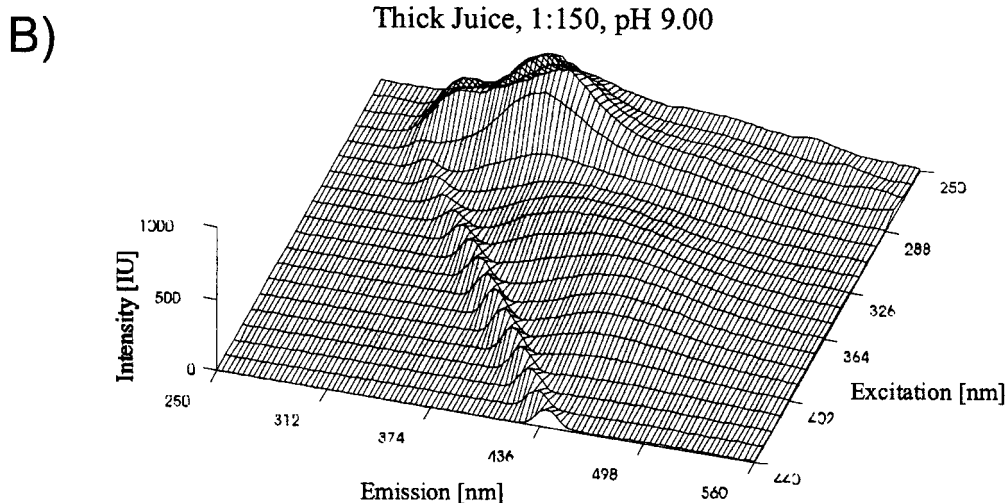


Fig. 3. (A) and (B) Fluorescence landscapes of one thick juice sample in two concentrations. Note how the fluorescence signal in the UV region is quenched in the 1:15 dilution (A) and becomes dominant in the lower concentration (B). (C) A Tucker score plot showing the pattern of principal components two and three of the sample mode from 4-way PCA. Two principles are illustrated by this plot: samples from the same factories (a, b, d, e, and f) are clustered nicely together and simultaneously the shift of the samples according to week number (e.g., d1 to d10) reveals that temporal information is present in the fluorescence landscapes.

II. Algorithms, models and applications

42

L. Munck et al. / Chemometrics and Intelligent Laboratory Systems 44 (1998) 31–60

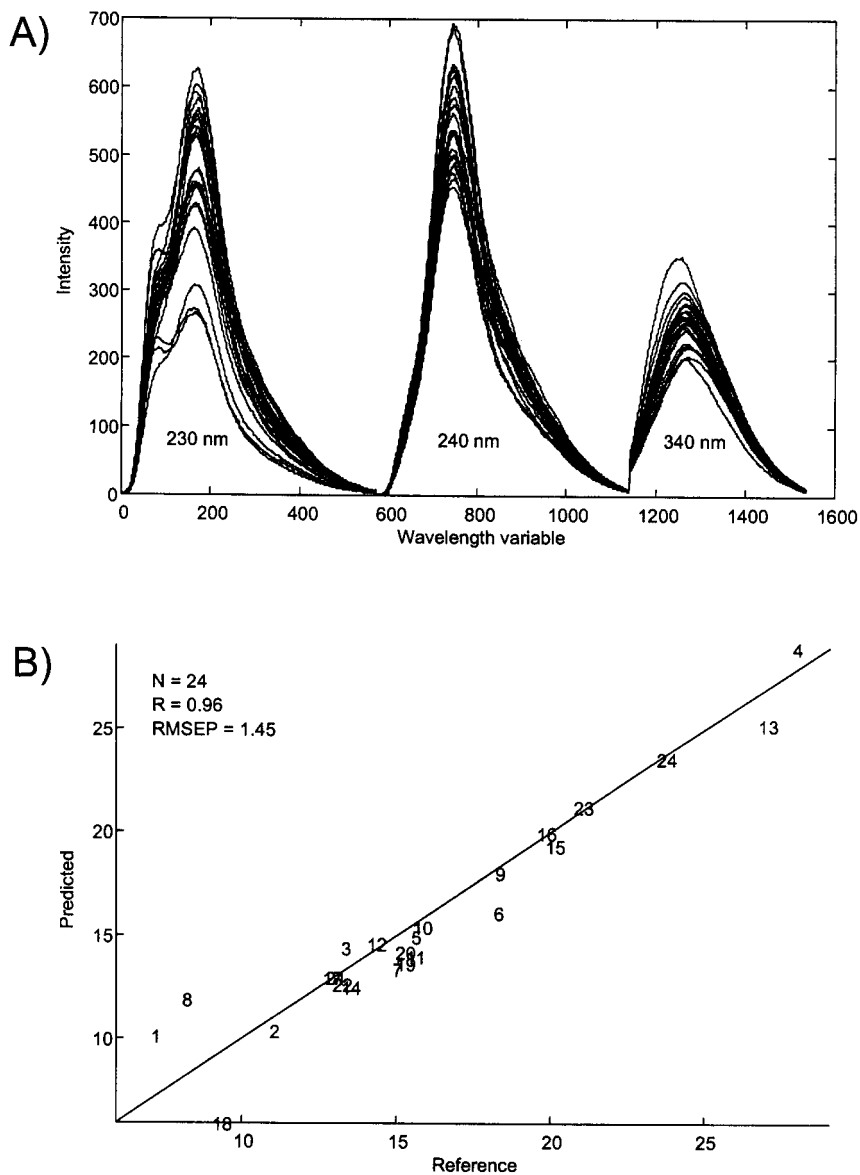
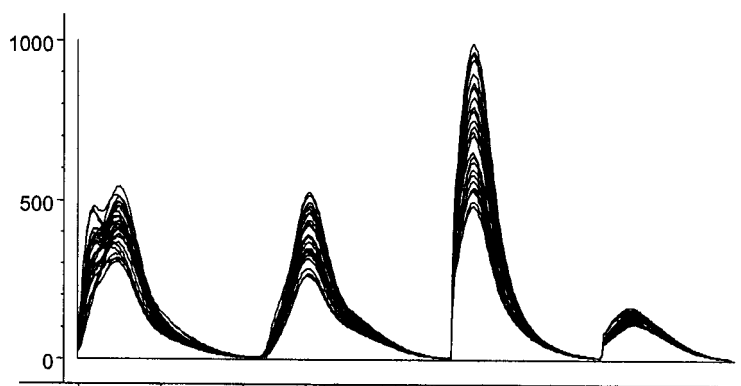


Fig. 4. (A) Fluorescence raw emission spectra of 24 sugar mash samples. Excitation 230 nm, 240 nm, and 340 nm (emission ranges 275–560 nm). (B) Predicted versus measured plot of amino-N values. Based on a three-factor PLS-model with fluorescence spectra as independent variables and amino-N as the dependent variable. (C) Raw fluorescence spectra recorded on sugar beet mash samples from nine different farms (three sample from each farm, i.e., in total 27 samples). The excitation/emission wavelengths are the same as those displayed in Fig. 1. (D) A score plot showing that the beets from the same farm no. 4, 7, 9, 10, 12, 15, and 19, in the fluorescent fingerprint seen in the mash samples.

II. Algorithms, models and applications

C)



D)

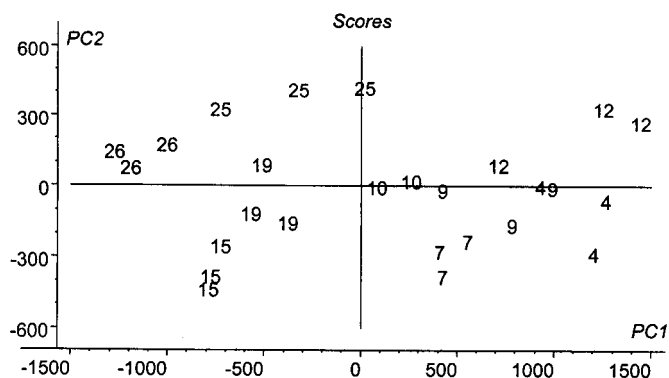


Fig. 4 (continued).

wavelengths) may allow direct recovery of some of the pure spectra from the underlying chemical substances.

In this study, four loadings called pseudospectra could be resolved, two of which were identified by comparing emission and excitation pseudospectra with the true spectra of tyrosine (Fig. 5B) and tryptophane (Fig. 5C, see also discussion in Appendix B). Fig. 5D shows the four emission pseudospectra and

their correlations to the process parameters colour and ash. In this preliminary study, it is observed that the four component candidates have different patterns of correlation, pointing at the possibility that they may be used as indicator substances, e.g., for colour or ash alone or in combination. Compound 4 is obviously the best indicator for colour.

In Fig. 5E, the scores for the four pseudospectra during the campaign are shown. The components

II. Algorithms, models and applications

44

L. Munck et al. / *Chemometrics and Intelligent Laboratory Systems* 44 (1998) 31–60

show a high degree of covariation, especially in the beginning of the campaign, revealing a tendency toward higher peaks during weekends. The variation

levels off during the season when outdoor temperature is decreasing. Around shift 200, on about the 15th of November, compound 4 scores steadily rise,

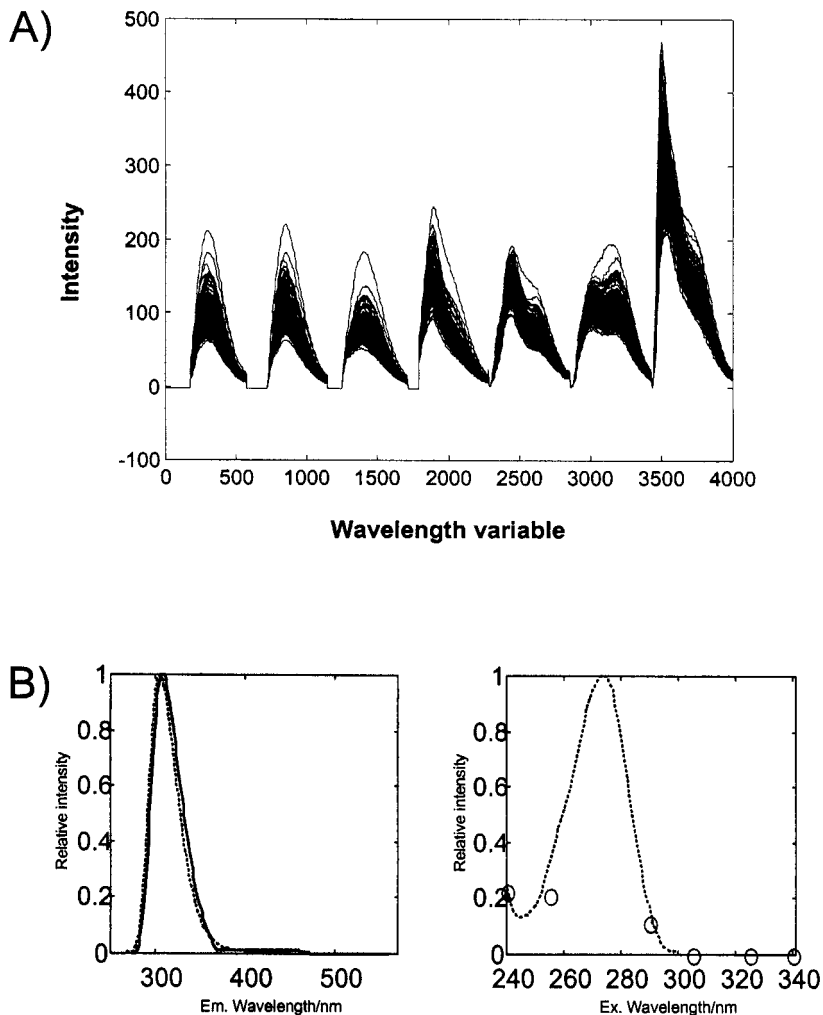


Fig. 5. (A) Raw fluorescence emission spectra of 268 sugar samples sampled as a mean spanning eight h equal to one shift during a three-month campaign (1995). The samples were measured at excitation wavelengths 230, 240, 255, 290, 305, 325, and 340 nm (emission ranges were all 275–560 nm). (B) Pseudo-emission and excitation spectra for compound 2 compared with pure tyrosine (dashed). To the left the emission parameters are shown and to the right the excitation parameters are shown. (C) Pseudo-emission and excitation spectra for compound 3 compared with pure tryptophane (dashed). To the left the emission parameters are shown and to the right the excitation parameters are shown. (D) PARAFAC emission loadings 1–4 and their correlations to ash and colour. (E) Concentrations (scores) of the four pseudocomponents.

II. Algorithms, models and applications

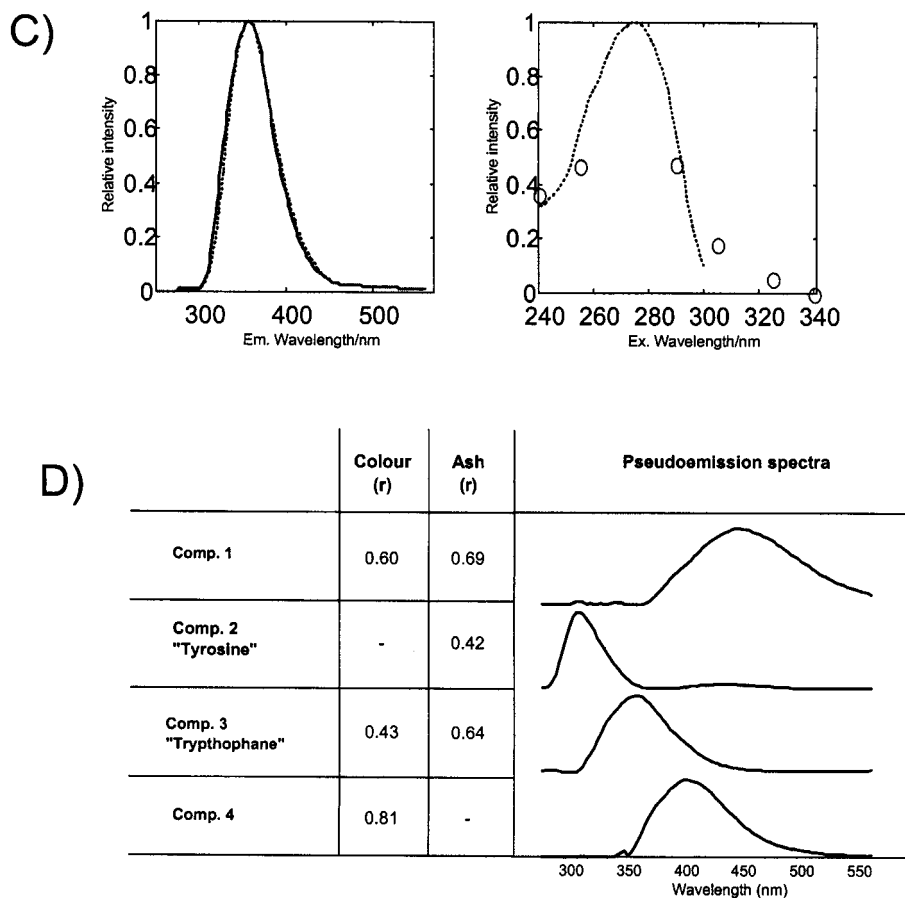


Fig. 5 (continued).

while scores for the other three components are more constant.

Factory records as well as interviews with the process engineers revealed that beets are stored longer during weekends which may produce heat due to microbiological activity which is reflected in higher fluorescence scores for all four components as well as an increase in colour. The change in the level of compound 4 and the increased colour development could be explained by frozen beets due to the coming winter and the resulting process adjustments. Compound 4 could thus be an indicator for colour as well as for frozen beets. These observations has to be

verified and generalized in more detailed studies with other factories and other production years.

The variation of the fluorescence pseudocomponents during the production campaign clearly indicates temperature effects covariant with colour of sugar. We may therefore induce a hypothesis from real life data that temperature in the receiving beet stores may have a major impact on the precursors of sugar colour which should be checked by monitoring temperature in the store.

We have demonstrated that with a minimum of prior knowledge of sugar technology and chemistry we are able to establish a constructive, exploratory

E)

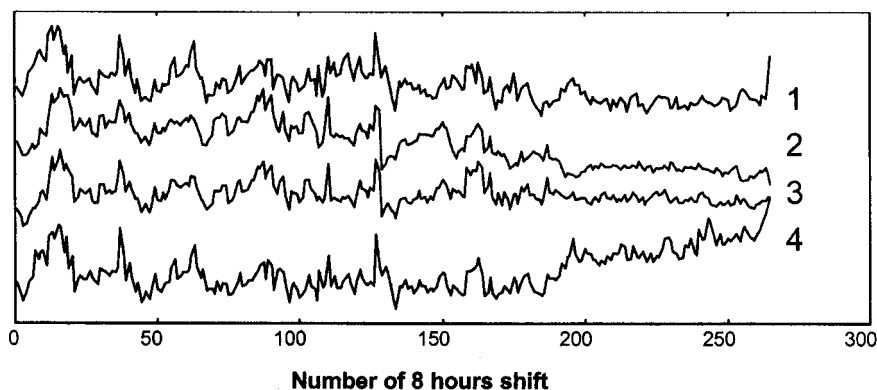


Fig. 5 (continued).

dialogue with the sugar technologists throughout the whole production chain using the tools of a fluorescence screening analysis, chemometric software and the computer. Together we have been able to identify a range of process events which the fluorescence analysis had picked up. At the same time we have shown that the fluorescence screening method has the potential for providing a holistic fingerprint of the state of chemistry in the process in the form of 4 fluorophores which correlates with a range of important quality parameters throughout the beet sugar manufacturing process and which may be used as indicator substances which is further demonstrated in Appendix B.

3. What chemometrics and food science can learn from each other

In his outline on the roots of mathematics in human culture, Barrow [4] emphasizes the inherent weakness of the human brain in multivariate analysis and the fundamental role of written symbols and basic assumptions axioms—the fundamental on which the mathematical machinery is built. It should be acknowledged that 'axioms' are also a fundamental part of human cognition—a method to keep a working platform of consistency in bookkeeping in a complex

universe. This is often practised without thinking too much, for example by the chemist in the laboratory as well as by the food consumer in daily life. However, when trying to exploit mathematics in real life, such as in food production, it becomes as crucial to define 'the axioms' of chemistry and food production as those of the mathematical models which are used to describe and predict events in data from food processes.

Food production is dependent on the demand of markets in thousands of complex production chains regulated by the monetary principle and governmental and international regulations. The functional unit is 'man as selector' [20] in different roles as consumer, distributor, manufacturer, as well as raw material and secondary material supplier.

This exploratory selection process with the individual consumer in the centre may be elucidated by a model for learning—'the selection cycle' (Fig. 6) [20] related to the concept of the perceptual cycle in psychology [21] (p. 37)—comprising different steps starting with a primary selection hypothesis inspired from the global area (0) proceeding with an inventory/screening analysis (I) and selection of material and methods (II), followed by testing/evaluating (III) which results in a secondary (IV) selection hypothesis are valid for the local area.

After an introductory round the individual selector proceeds in increasingly more focused and limited

II. Algorithms, models and applications

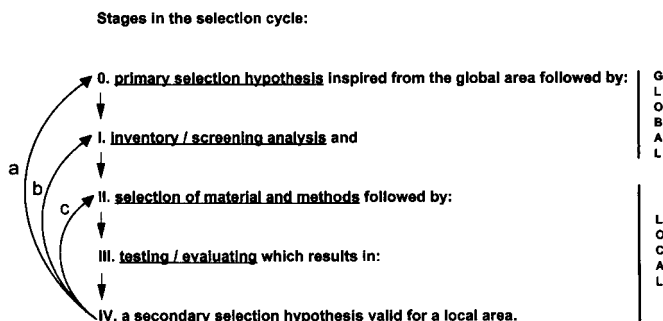


Fig. 6. The selection cycle [20].

rounds (Fig. 6a–c) (e.g., omitting point 0 (b) or even 0 and 1 (c)) in the selection cycle. Thus, in each cycle, the dynamically adapted secondary selection hypothesis (IV) is validated experimentally (III) in numerous revolutions. It is a common phenomenon that in the progress of time the secondary hypothesis (IV:n) and its derived propositions from the local area have often overshadowed the more global primary selection hypothesis derived from, e.g., society. It now lives its own life in the context of society in the mind of the selector in spite of its local limitations. In this way serious bias could be introduced unintentionally.

The food experience of the consumer tells that the selection cycle contains both global and local as well as visible and hidden domains. When buying food in the store, the selector starts with a primary selection hypothesis (0) implying acquisition of defined foods with expectations regarding culinary quality, health and economy in a long-range perspective. He/she then evaluates foods in the local area with regard to visible (screening) characteristics (I) like colour, packaging and price. After selection (II) the individual 'develops' hidden qualities such as smell, taste and tenderness by cooking the food at home (III). This may generate a reaction in the form of a new purchase policy (IV) which will then be checked in later cycles. The exploratory behaviour of the consumer creates information about foods in the local area which again may reinforce or weaken a specific behaviour of selection.

The global aspect of food selection [20] includes the part of the accumulated feedback on the physiolo-

gy of the consumer which is caused by his/hers own food selection and consumption. It also contains the hidden feedback effects [20] of nature which Darwin called 'natural selection', now also including the indirect influence of the selection force on the food production environment of the activity of a large population of human selectors exploiting resources and the resulting effects on their food quality and health.

Returning to our example on exploratory analysis by fluorescence screening, we find that indeliberately we worked exploratively according to the selection cycle model: we attempted an analysis in the 'global area'—the beet sugar production chain—by using chemometrics.

Without extensive knowledge of sugar manufacturing we used the fluorescence screening method to pose a question to the process as follows: "Is fluorescence analysis chemically and technologically relevant as a screening method for control and prediction of parameters of industrial interest?" This is the primary hypothesis (0) in the selection cycle. After analyzing (1:1) sets of sugar products with fluorescence spectroscopy, we could select (II:1) and evaluate (III:1) sugar samples belonging to defined factories and processes as well as identify time effects due to date of delivery throughout the season. We could also identify process balance in a start-up test (III:1) by analyzing the sugar product as well as indicating a minor breakdown in the balance point.

From these results, we could induce a preliminary secondary selection hypothesis (IV:1) that a sugar sample could be looked upon as 'a datalogger' which

integrates information from the production chain upstream that could be read by a fluorescence spectrophotometer and evaluated by PCA.

In our second selection cycle, we proceed on our data selection adventure in the local area—the laboratory—by comparing the classification of traditional sugar analyses (I:2) with fluorescence analyses in two separate PCAs. Due to the fact that samples with high fluorescence have high ash, colour and amino–nitrogen values, we selected (II:2) the PLS algorithm which gave good correlation in an evaluation (III:2) between fluorescence spectroscopy at 5 specific wavelengths and sugar quality, indicating direct or indirect relationships. This fact was used to formulate a new and more specific secondary selection hypothesis (IV:2) that fluorescence could be used as a preliminary screening method for direct analysis of purity in sugar. In a third selection cycle this hypothesis was expanded to the whole production chain. In a fourth selection cycle, we enlarged our third secondary hypothesis by suggesting that behind the fluorescence spectra lies information from discrete chemical compounds which may be used as ‘indicator substances’. These substances reflect chemical composition of sugar and intermediate products as well as process parameters. To solve this problem we selected multiway exploratory algorithms such as Tucker and PARAFAC. From a complete material of 8 h average sugar samples from an entire sugar campaign PARAFAC displayed 4 different pseudospectra (loadings) corresponding to 4 discrete compounds (fluorophores), two of which could be preliminarily identified. The four pseudospectra were shown to be able to model process observations, such as frozen beets and quality criteria like ash and colour, as well as other important process parameters as discussed in Appendix B.

Finally, in the fifth turn in the selection cycle we aim at more precisely identifying the underlying chemical compounds by high pressure liquid chromatography in the local area, the research laboratory, which is outside the scope of this paper. Thus, we do not forget to check the results from the exploratory screening with our chemical interpretation of the problem.

In the longer perspective, we aim to feed back the integrated experience of the multivariate fluorescence perspective from the five selection cycles into

the primary area (0), the beet sugar industry, in the form of an established ‘global’ control method covering the production chain from beet production to sugar.

In our sugar process example, with our sensitive spectrofluorometric method we are not measuring sugar, which is non-fluorescent, but rather a selection of impurities such as fluorescent amino acids, phenols and their reaction products with reducing sugars: the high molecular coloured melanoidines and melanines. The sugar processing engineer tries hard to avoid the formation of colour by adjusting pH with CaO and adding reducing agents in the form of SO₂.

In traditional chemical analysis, one starts by defining the hundreds of chemical substances involved in a process, as was done for the sugar industry by Madsen et al. [22] in order to understand color formation. If the target hypothesis is to find easily identifiable indicator substances by which to model quality and process characteristics, we suggest that our exploratory, inductive method by introducing a multivariate screening method in the global area of the sugar factory would be more economical than a normative, deductive strategy based only on a priori chemical knowledge, chromatography and classical statistics as studied in the local area—the research laboratory.

We can thus conclude that the strategy of exploratory chemometric analysis in the example is closer to the behaviour of ‘man as selector’ performing in the food production chain than to how statisticians operate today. While statistics is mainly directed toward probabilistic methods in modelling noise, identifying the object as a void in the space of noise, exploratory data analysis and chemometrics is more deterministic [23]. It instead tries to model the contours of data objects by data experimentation in the computer.

In our example, statistical validation is completed with two other alternatives: calibration/test set validation (data experimentation) and interviews with the processing engineers, including confirmation from process data banks. It must be pointed out that exploratory data analysis, which contains an important inductive, empirical element of validation through enumeration [8], does have a more humble profile [24] in a restricted context than classical mathematics and statistics. It places less demand on finding the abso-

lute (generalized) truth (see citation by Chaitin in the introduction), but instead aims at finding an adequate and more precise local truth of equal or higher importance which is time- and context-dependent. It is basically a provisional detective work [25], trying to explore the partly unknown territory of the world outside the laboratory where hard hypotheses are likely to neglect covariance and synergy and therefore are insufficient and inefficient. An endeavour of reversed logics might be fruitless in a classical situation relying on univariate analyses where each object has just a few characteristics, a multivariate analytical situation with many informative data points attached to each object increases the uniqueness of the description. In classification it allows safe detection of outliers, thus greatly increasing the validity of the results.

From our platform of data technology in chemometrics, we can clearly see how it was necessary before the computer to develop a very special form of deep, rigorous and general thinking [26] aimed at identifying the laws of nature. The goal is to obtain consensus in the form of a global rational opinion as a 'science map of reality' through organized, inter-subjective communication [26]. Such an inflexible outlook is rather strange for model creation in the normal human mind which is characterized by pragmatism and cognitive flexibility, although with a short memory.

In fact, as the physicist and historian Thomas Kuhn points out [27]: "The investigations of classical science have few quantitative points of contact with nature, because investigations of those contact points usually demand such laborious instrumentation and approximation and because nature itself needs to be forced to yield the appropriate result, the route from theory of law to measurement can almost never be travelled backward. Numbers gathered without some knowledge of the regularities to be expected almost never speak for themselves. Almost certainly they remain just numbers".

We have here applied our global (with regard to fluorescence) screening method and exploratory data analysis and gone from measurements of sugar samples to a theory of selected indicator substances for process control. Is it not this fairly straight forward travel from the measurement of phenomena from real life to construction of a theory which Kuhn calls

'backwards', which we have just humbly attempted and to a large extent succeeded in?

Obviously, new multivariate screening methods and data evaluation methods based on induction using the computer, which Kuhn [27] and Hempel [8] were unaware of (and still the vast majority of scientists are today), open up new possibilities for connecting data from the world as it is with science—if one can obtain a common platform for 'the axioms' and contexts of mathematics and those of the world under study. This issue is further exemplified in Appendices A–C.

We may thus conclude that there is a major conceptual distance between the aspiration of science of global understanding of natural phenomena in its generalized sense and global evaluation of measurements as is from the real world for prediction and control. This discrepancy has to be further understood and bridged by a new strategy combining screening methods, mathematics and information technology. We can thus look upon the flow of information in our sugar process example as a dialogue between two connected selection cycles—one global (sugar production) and one local (the laboratory).

Attempts by leading physicists to introduce a new paradigm change in science, such as in the now classic book by Prigogine and Stenger [9] (since 1979) 'Order out of chaos—Man's new dialogue with science' are only slowly being acknowledged. They see the world as an open self-organizing system which develops while consuming energy. The world is heterogeneous. It contains simple as well as complex, reversible as well as irreversible and probabilistic (e.g., due to thermal movement of molecules) and deterministic (e.g., due to DNA in organisms) including chaotic moments. This new outlook on the world, combined with exploratory data analysis, is much more relevant for describing the dynamic situation in food science than classical hard modelled science with its mathematics and statistics which, however, is still relevant in special cases. One should thus be cautious in introducing a priori biased statistical evaluation techniques in such a world without defining context in an inventory in the start of the selection cycle.

As food technologists we, of course, gratefully acknowledge the laws of nature as defined by science in our food technology research. But our pri-

many task is not to produce the eternal and general. We do not aim to make a factory which produces the same product from the same raw materials by the same technology forever. Instead, we are interested in controlling the timely, transient and specific traits of the production, so that the company may withstand competition for another year. The generally acknowledged mathematical language which should be used in the future to model such data should be more compatible with this context and to the new science of Prigogine and Stenger [9]. Today it is not.

We now see the great opportunity to directly study order out of chaos in Prigogine's and Stengers' sense by applying multivariate screening methods in real life (e.g., in a sugar factory) as evaluated by the computer and exploratory data analysis. It is therefore of great wonder to us that most scientists, including Prigogine, investigating self-organizing systems are still apparently working with hard modelling, deductive methods alone and have not yet found their way to supplement with the new multivariate methods. Science is indeed conservative. It has not yet discovered all the new kinds of freedom which the computer may introduce. It is possible within the limits of the screening analysis and the mathematical algorithm with the exploratory method to discover unknown phenomena directly. It is only possible for classic science to obtain new knowledge outside its traditional deductive system of hypotheses indirectly through unexpected interference, e.g., in discovering environmental problems.

The classical, positivistic science presumptions [9,26,27] of the world are still dominant in the present normative-deductive culture and severely restrict chemometrics. They focus on deduction from a priori hypotheses based on fully transparent factors which can be seen directly or revealed after experimentation. As long as the present consensus in statistical hard modelling and validation rules, the more flexible, soft exploratory data models which introduce latent factors and empirical validation, such as PLS regression, will not be accepted as a science. This is due to the incomplete transparency of these algorithms which for the mathematicians are undecidable by lack of mathematical proofs, in spite of their better robustness and ability to adjust to a changing context by experimental validation reflecting human behaviour in the selection cycle.

In fact, the operation of the PLSR algorithm makes a dialogue possible between screening data from the world as it is and laboratory data. This is expressed in finding common latent factors in a cyclic adaptation process which embodies a dialogue between the global and local principle, between the real world and sciences, just as in the selection cycle discussed previously.

It is obvious that chemometrics can contribute to food science with new more flexible data programs which display the exploratory results in cognitively accessible graphical data interfaces. Food science and chemistry on the other hand stimulates the chemometrician to take new contexts into consideration in the development of models suitable for real world data which is exemplified in the Appendices A–C.

In practical life, respect for the 'axioms' of the world in the form of contexts is more important than transparency. In science it seems to be the reverse. Transparency is preferred based on the axioms of the mathematical machinery, far from the contexts of the world which was supposed to be studied. Because of its lack of complete transparency we could thus for the moment look upon chemometrics more as a technology than as a scientific discipline—a very vital technology which already has proven its potential in chemistry and in other related technologies [23,28]—an invention the results of which science should explore and incorporate in its basic principles.

As early as 1941, Emil Post, one of the co-discoverers with Turing [4] (p. 292) of non-computable operations, wrote [29] the following comment regarding the divide between meaning and formalism in mathematics: "mathematical thinking is, and must be, essentially creative. It is to the writer's continuing amazement that ten years after Gödel's remarkable achievement current views on the nature of mathematics are thereby affected only to the point of seeing the need of many formal systems, instead of a universal one. Rather has it seemed to us inevitable that these developments will result in a reversal of the entire axiomatic trend of the late nineteenth and early twentieth centuries with a return to meaning and truth. Postulation thinking will then remain as but one phase of mathematical thinking".

It should thus be possible to assemble a mathematical algorithm to describe and predict complex conditions in the real world inspired by finding order

in observational measurements of nature by consulting the computer. Such an endeavour must respect the mechanisms how humans best senses complex information.

While we wait for the breakthrough of the new interdisciplinary science [9] where exploratory, inductive chemometrics is an integrated part as an established option, we could with the support of the relatively recently discovered computer contribute to the basic mathematical language of the new science by balancing the normative and exploratory principles in a dialogue, as described in our example. In this work food technology is an excellent Trojan horse in the conservative scientific city of Troy, harbouring research teams prepared to fight for the revolutionary new science and its new mathematics while awaiting the right moment and better times.

Acknowledgements

The inspiring cooperation with Ole Hansen, Lars Bo Jørgensen and John Jensen, Danisco Sugar Development Center Nakskov, Denmark in exploring beet sugar production is gratefully acknowledged. We also thank John Hørlyck and Peter Henriksen for professional assistance in maintaining equipment and in measuring the samples as well as Gilda Kischinovsky for valuable help in preparing the manuscript. The four years of research summarized in this paper was supported by Nordic Industrial Fund project No. P93149 (salary to Rasmus Bro), EU-AIR2 project No. CT94-1416 'AFFLUENCE' (equipment and salary to Claus Andersson), Føtek-2 project 'On-line/at-line screening methods - spectrometric structural analysis for process and quality control in food production' (salary to John Hørlyck and Gilda Kischinovsky), and by the Danish Veterinary and Agricultural Research Council (equipment and salary to Lars Nørgaard).

Appendix A. Selecting and adjusting chemometric models to represent different contexts of the world

Chemometrics has arisen as a hybrid with contributions from various sciences like econometrics, psychometrics, classical statistics and physics. The mixed background is reflected in the way the chemo-

metrician actually conducts the data analysis. Central aspects in data analysis are the selection of data as well as the selection of suitable models, combined with adaptation of the models to a given problem. Classification, for example through PCA, is a fundamental first step in an exploratory data investigation of a given data set (e.g., fluorescence spectra), employing data reduction into latent variables in this way revealing resemblances and outliers.

In the framework used throughout this paper we see the alternation between the selection of models and the selection of data which again influences the selection of material for analysis and the technological focus of the project. The data analyst might follow different chemical roads depending on the goal of the investigation. However, the exploratory approach starting with an inventory with a data classification from a multivariate screening method is to be preferred in the beginning of an investigation in order to minimize bias. After revealing the data structure, both surprising and expected elements can be identified from which more specific correlation models may be created using a range of new chemometric methods. These include the new multi-way methods employed in our example with sugar process fluorescence analyses.

There are various models for analysing multi-way data sets, see Kroonenberg [A1]. In Figs. 7 and 8 we shall focus on the N -way principal component analysis (N -way PCA) which is a generalization of the 3-way Tucker3 model [A2] to N -way data arrays as well as the PARAFAC model [A3]. The authors would like to draw the reader's attention to the fact that the generalization of bilinear PLSR to multilinear PLSR (N -PLS) was given by Bro [A4].

A.1. Tucker model

As with conventional two-way PCA, the model uses a projection technique whereby the systematic variation in data is reduced to a few representative factors. Due to some mathematical features (i.e., factors are non-unique and can be rotated) of the model and its solutions, the term N -way PCA is often used to describe the Tucker 3 model. Fig. 7 provides a basis for presenting the N -way PCA. The 3-way PCA model of a 3-way data array \mathbf{X} of order (r_1, r_2, r_3) is depicted in the figure. The array is decomposed into

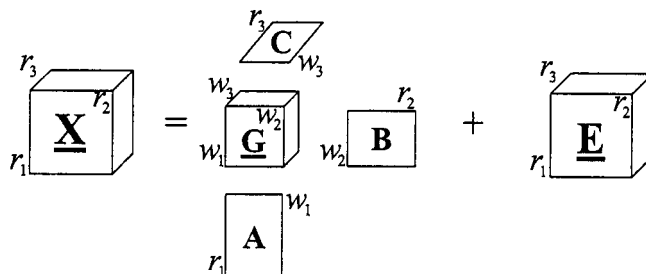


Fig. 7. Tucker.

a significant systematic part and a non-significant residual depicted by **E**. The systematic part is described by orthogonal factors which are stored columnwise in matrices **A** (r_1, w_1), **B** (r_2, w_2) and **C** (r_3, w_3). The mathematical representation is as follows

$$x_{ijk} = \sum_{f=1}^F \sum_{g=1}^G \sum_{h=1}^H a_{if} b_{jg} c_{kh} g_{fgh} + e_{ijk} \quad (1)$$

The number of factors in each of the three ways, i.e., w_1, w_2 and w_3 , must be determined by the analyst from a priori knowledge about **X** or by evaluating models with different combinations of w_1, w_2 and w_3 , choosing the order that gives the most accurate model of **X**. The correct number of factors is found as a compromise between having a good fit and as few factors as possible. The array **G** of order (w_1, w_2, w_3), referred to as the core array, allows the factors to interact in the model of **X**. Upon calculation of the model, the factors in the three component matrices **A**, **B**, and **C** and the core **G** must be interpreted. Since the factors are orthogonal, hence linearly independent, the squared core elements are proportional to the variation explained by the combination of factors in question. Thus, if $g_{i,j,k}$ is the largest squared element in **G**, the combination of factor i in the first mode, factor j in the second mode and factor k in the third mode explains most of the variation in **X** and the

analyst should give these factors special attention when interpreting the model.

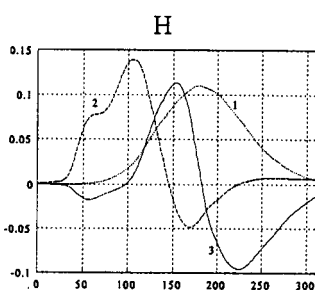
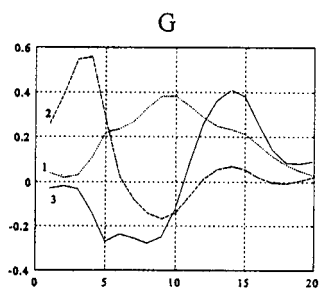
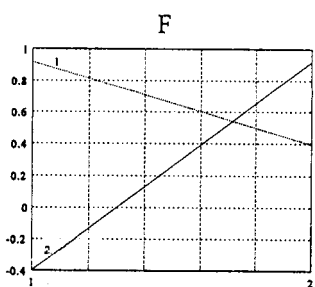
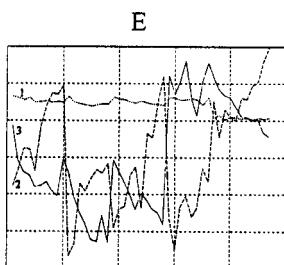
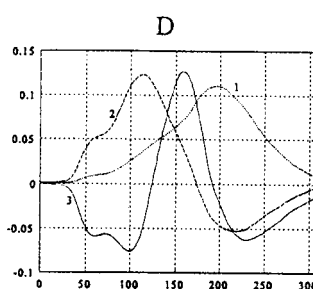
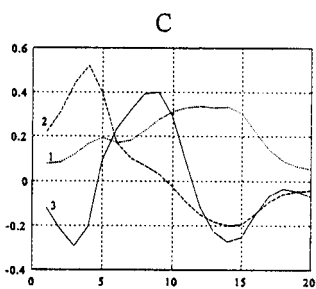
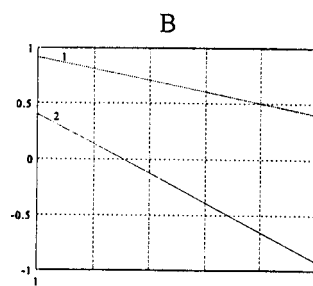
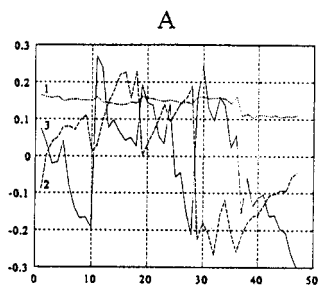
Factors from N -way PCA suffer from rotational ambiguity, i.e., the N -way PCA of **X** has an infinity of factors and cores, where one solution can be rotated into another having the exact same fit. Returning to the exploratory power of the squared elements of the core, one can perform *selective* transformations of a solution to give a core where only a few squared entries are significant [A5]. Having only a limited number of significant core entries allows the analyst to focus on a few combinations of more significant/general factors. Hence, we use an unsupervised algorithm to select a solution from this infinity of solutions to yield a model for interpretation which is simple as possible.

A.2. Data (an in-depth treatment of this data set was given in Andersson et al. [A6])

Fluorescence intensity landscapes, or excitation-emission matrices, were measured on 47 thick juice samples from the 1994 sugar campaign. Five factories contributed thick juice samples. Two typical landscapes from one sample are shown in Fig. 3A–B in the main text. Note that the peaks in the ultraviolet area do not decrease from A) to B) with dilution. This is caused by concentration quenching, or inner-ab-

Fig. 8. (A) Factors in the first way representing variation in the thick juice samples. (B) Factors in the second way describing concentration effects. (C) Factors explaining the excitation profiles. (D) Factors explaining the emission profiles. (E) Rotated sample factors. (F) Rotated concentration profiles. (G) Rotated excitation factors. (H) Rotated emission factors.

II. Algorithms, models and applications



sorption effect [A7]. Each sample has been diluted volumetrically 1:15 and 1:150 with pH 9.00 NH_4Cl in double ion exchanged and Si-free water. Both of these dilutions were measured using 20 excitation wavelengths (250–440 nm, 10-nm intervals) and 311 emission wavelengths (250–560 nm, 1-nm intervals). At the excitation and emission sites 10 nm slit widths were used. The instrument was the Perkin Elmer LS50B spectrofluorometer. As indicated by Fig. 3 (main text), the combination of a narrow emission slit width and generally low turbidity allows for neglecting the Rayleigh scattering. Since each intensity measurement in the collected data depends on four external parameters, the sample number (47 samples), the concentration (two levels of dilution, 1:15 and 1:150), the emission wavelength and the excitation wavelength, the measured intensities constitute a 4-way data table of order (47, 2, 311, 20). We will apply a 4-way PCA model for analysis of these data. The 4-way PCA used in this application can be conceived as an extension of the decomposition illustrated in Fig. 7 with a necessary introduction of an additional set of factors, \mathbf{D} , and by extending \mathbf{X} (r_1, r_2, r_3, r_4), \mathbf{G} (w_1, w_2, w_3, w_4) and \mathbf{E} (r_1, r_2, r_3, r_4) to be 4-way structures.

In order to find the optimal numbers of factors for the 4-way PCA model, several models of different orders were investigated. Table 2 shows the relative increase in explained sum-of-squares (SS) as the order of the models increase. The total number of parameters is shown in the far right column of Table 2. The findings shown in Table 2 suggest that a model of order (3, 2, 3, 3) should be chosen. For the factors to be representative a good fit to \mathbf{X} is paramount, hence 96.25% of SS explained seems appropriate in

comparison with the models of higher orders. The number of parameters should be kept as low as possible in accordance with the principle of parsimony. Parsimonious models reduce the risk for fitting non-systematic trends (i.e., noise). Note that the model does not improve in fit when using more than two factors in the second mode. This is in concordance with the number of observations in the second mode: one cannot derive three or more orthogonal solutions in a mode that is only spanned by two variables. When moving from analysis of two-way data to multi-way data, we expect increased stability towards outliers. This is due to the increase in selectivity. Measuring many independent characteristics of samples will offer more scales on which to evaluate the goodness or suitability of the sample for modelling by the model in question. This is the so-called second-order advantage. The N -way PCA and the two-way PCA have the non-uniqueness in common, since factors from these two classes of models may be rotated by orthogonal transformations without affecting the fit.

The sample-to-sample variation among the 47 samples is condensed in the factors in the first way. The three factors in the first way are depicted in Fig. 8. The factor denoted 1 describes a significant change of level in the samples. Factors marked 2 and 3 also reveal systematic behaviour. The factors describing the concentration levels are shown in Fig. 8. Fig. 8 reveals the behaviour of the intensities as a function of the excitation wavelength. However, it should be remembered that the factors are orthogonal. This makes interpretation with regard to chemical properties difficult. Fig. 8 shows the principal components describing the variation in the fourth way which relates to the emission wavelength. In the $54 (= 3 \cdot 2 \cdot 3 \cdot 3)$ element large core array the five most significant squared entries and their factor combinations are $2.04 \cdot 10^{10}$ (1,1,1,1), $2.27 \cdot 10^9$ (1,1,3,1), $1.20 \cdot 10^9$ (1,1,1,3), $9.92 \cdot 10^8$ (1,2,1,3) and $5.46 \cdot 10^8$ (1,1,2,2). From these values we see that no clear-cut factor combinations can be used for further data exploration. If the factors are properly rotated and the core correspondingly counter-rotated, a more simple structure of the core may be selected.

Thus, to improve the interpretability of the core array, the solution was rotated to yield maximum variance-of-squares of the core [A5]. After transfor-

Table 2

The explained sum-of-squares of the data as a function of the number of factors in the 4-way PCA model of sugar fluorescence measurements from the material in Fig. 3A–C

Model order	Expl. SS (%)	Par.
(1,1,1,1)	74.13	384
(2,1,2,2)	82.88	772
(2,2,2,2)	92.08	782
(3,2,3,3)	96.25	1201
(3,3,3,3)	96.24	1230
(4,2,4,4)	97.85	1656

mation, the variance-of-squares of the core array changed from $4.11 \cdot 10^{20}$ to $5.46 \cdot 10^{20}$, i.e. an increase of 32%. The variance-of-squares of the optimised core elements were $2.36 \cdot 10^{10}$ (1,1,1,1), $1.73 \cdot 10^9$ (1,1,2,2), $9.50 \cdot 10^8$ (1,2,1,3), $1.49 \cdot 10^8$ (1,2,2,3) and $1.03 \cdot 10^8$ (1,2,1,2). Note how the largest elements of the rotated core have absorbed variation described by the minor ones. Upon rotation the factors were as plotted in Fig. 8E–H. The variation expressed by the factors in Fig. 8 can be plotted in a more convenient way as in Fig. 3C (main text) where factor 2 and factor 3 are plotted against each other (corresponding to a PCA score plot). The conclusions drawn from this plot are presented in the main text.

Appendix B. parafac

B.1. Model

Consider a fluorescence data set with typical elements, x_{ijk} , where x_{ijk} is the intensity of the i th sample excited by light at the j th excitation wavelength and measured at the k 'th emission wavelength. Theoretically, such data can be approximated as

$$x_{ijk} = \sum_{f=1}^F a_{if} b_{jf} c_{kf} + e_{ijk} \quad (2)$$

where a_{if} is the concentration of the f th analyte in the i th sample, b_{jf} is the relative emission emitted at wavelength j of analyte f , and c_{kf} is the relative amount of light absorbed at the excitation wavelength k of analyte f . This relation holds for diluted solutions, and if b_{jf} is (approximately) independent of c_{kf} [A8].

The fluorescence model is equivalent to the PARAFAC (parallel factor analysis) model initially proposed by R.A. Harshman [A9] and Carroll and Chang [A10]. Leurgans and Ross [A11], Leurgans et al. [A12], Ross and Leurgans [A13], and Nørgaard [A14] describe in detail the rationale for using PARAFAC models for modelling fluorescence data. The PARAFAC model is very closely related to ordinary two-way PCA, as exemplified graphically in Fig. 9.

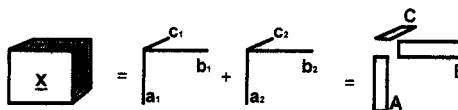


Fig. 9. A two-component PARAFAC model of the three-way array X (residuals omitted for brevity). The vector and matrix products to the right of the equal sign are equivalent to ordinary outer products, i.e. the first component represented by a_1 , b_1 , and c_1 gives a rank-one part of the model of the same size as X , each element being a triple product $a_{i1} b_{j1} c_{k1}$.

Where two-way PCA gives one score and one loading matrix, one gets one score matrix and two loading matrices in a PARAFAC model of a three-way data set; one for each variable mode in the data. Therefore, a PCA model is a bilinear model, while PARAFAC is a trilinear model. The PARAFAC model is unique [A3,A15]. This means that if the model is appropriate for the data one need not impose orthogonality or other mathematical constraints to identify the model. Furthermore, instead of abstract latent variables, the true underlying phenomena are found. In this case it means that it is possible to estimate the underlying emission and excitation spectra and concentration profiles simply by decomposing the fluorescence data by a PARAFAC model.

B.2. Data

Sugar was sampled every 8 h during a campaign (approximately three months) at a sugar plant in Scandinavia, providing a total of 268 samples three of which were discarded in this study. Each sugar sample was dissolved in un-buffered water (2.25 g/15 mL) and the solution was measured spectrofluorometrically (Perkin Elmer LS50B). For every sample the emission spectra from 275–560 nm was measured in 0.5 nm intervals (571 wavelengths) at seven excitation wavelengths (230, 240, 255, 290, 305, 325, 340 nm). Laboratory determinations of the quality of the produced sugar were also available. These quality measures are ash content and colour. In addition, several automatically sampled process variables were available, including temperature, flow, and pH determinations at different points in the process. Typically these variables are very noisy and sampled at quite different rates.

A four-component PARAFAC model of the fluorescence data is appropriate in this case. However, for an unconstrained model a large portion of the loadings have negative areas at lower wavelengths. The reason for this is that 60% of the data are missing in this area, due to Rayleigh scattering. Therefore, the model is based on only one to four excitations below 360 nm. This causes some of the estimated emission loadings to be uncertain.

As the parameters of the PARAFAC model reflect concentrations and emission and excitation spectra, non-negativity seems a valid constraint to use in order to remedy this problem. One may infer that non-negativity should not be necessary, since the model should be identifiable even without using non-negativity. The adequacy of the unconstrained model, however, only holds to the extent that the PARAFAC model is correct for the data. There is a portion of the data that is missing due to Rayleigh scatter. Also, very likely a portion of the data that has not been set to missing values may be influenced by Rayleigh scatter to a slight degree, and therefore the data do not necessarily behave according to a trilinear systematic variation plus random noise. Furthermore, heteroscedasticity, quenching and other deviations from the model can cause the estimated parameters to deviate from strict non-negativity.

Very similar results are obtained by an unconstrained and a non-negativity constrained model. In the sample and excitation modes the loadings of the two models are highly correlated ($r = 0.99$). Further,

the problems arising in the unconstrained model can be explained by the amount of missing values and model mis-specification. A four-component non-negativity constrained PARAFAC model results in the emission loading vectors displayed in Fig. 10a. The spectra seem mainly reasonable, but for one spectrum, the bump slightly above 300 nm seems to be more of a numerical artefact than real (Fig. 10b). This is plausible because many variables are missing in this area. One important aspect indicates that the spectrum should really be unimodal namely, that the most likely fluorophores in sugar (amino acids, simple phenols, and derivatives) have unimodal emission spectra due to the Kasha rule [A7,A8].

The above reasoning led to specifying a new model where all emission spectra were estimated under unimodality constraints and remaining parameters under non-negativity constraints. The estimated model was stable (Fig. 10c) and the estimated excitation spectra and relative concentrations did not vary considerably from that of the non-negativity constrained model. This strongly confirms the assumption that the cause of the artefact is mainly due to the amount of missing data in the specific region. It means that the unimodality is probably a valid constraint, and it also implies that unimodality is mainly necessary for improving the visual appearance of the emission loadings, hence enabling better identification of the underlying analytes.

Fig. 5B,C (main text) show selected estimated emission spectra, which fit well with the emission

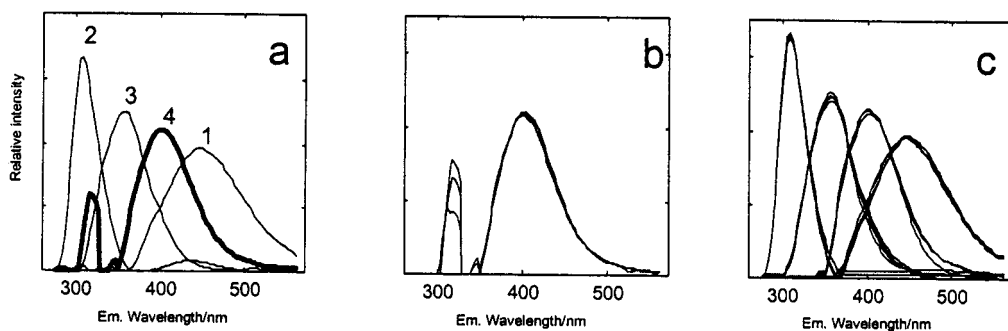


Fig. 10. Estimated emission spectra from fluorescence data. (a) Four spectra estimated using non-negativity. The 'suspicious' spectrum, 1, is marked with a thicker line. (b) Suspicious spectrum estimated from four different subsets using non-negativity. (c) Estimated spectra from different subsets using unimodality.

II. Algorithms, models and applications

spectra of pure tyrosine and tryptophane respectively, two substances of known technological importance. The excitation spectra of tyrosine and tryptophane crudely agreed with those of the pure chemicals due to the limited number of seven excitation wavelengths employed with a gap between 255 nm and 290 nm. The spectra of tyrosine and tryptophane were acquired under quite dissimilar circumstances (pH 9, whereas the solutions used here was unbuffered) in experiments unrelated to this study. Still, the striking similarity with regard to the emission spectra confirms that the PARAFAC model is capturing chemical information. In order to verify with more confidence the identity of the underlying analytes we have confirmed the fluorescence signatures of the pseudospectra in column chromatography fractions of thick juice.

B.3. Using PARAFAC scores for modelling quality

The scores (**A**) of the model of the fluorescence data are estimates of concentrations. Initially, the correlation between the PARAFAC scores and the pro-

cess variables was investigated. For some process variables there were almost no correlations, but for a large number excellent correlations were obtained. Examples of can be seen in Fig. 11.

A calibration model was made for predicting ash and colour from PARAFAC scores, The models for predicting ash content and colour of the sugar were excellent. The predicted values and the reference values are shown in Fig. 12. Note that, disregarding the fact that no cross- or test set validation has been performed, the prediction models are only based on four regression coefficients each, hence quite impressive. The above model substantiates, that it is possible to use fluorescence for on-line or at-line monitoring of sugar quality. This is important, as these parameters are currently only determined every 8 h and with a certain lag, as the laboratory analysis takes time.

The models described in this application based on fluorescence data are quite extraordinary. They give a direct connection between the raw material, process parameters and the final sugar quality (as defined by laboratory measurements defining the internal as well as the external consumer quality). As such,

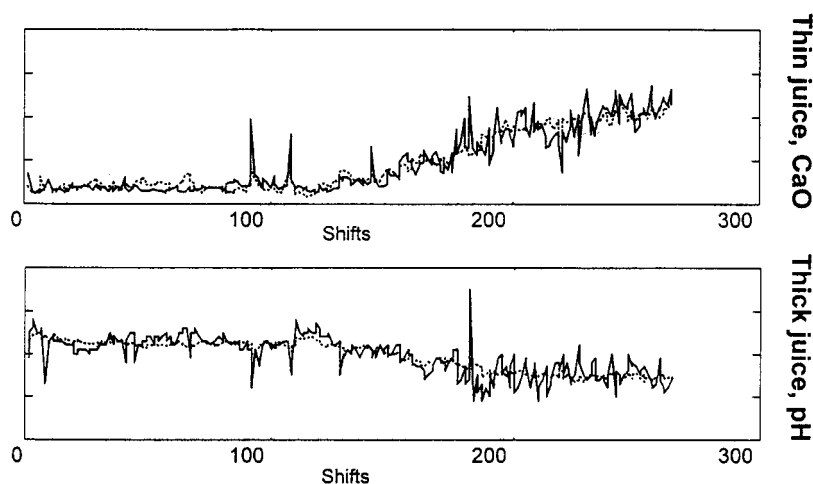


Fig. 11. Predictions of two important process variables. Unbroken lines are reference values. Notice the smoothing effect of the predictions based on fluorescence analysis of 8 h mean sugar samples representing one shift. The fitted values obtained using multiple linear regression (MLR) are shown. MLR was chosen, because the condition of the independent variables (265×4) is excellent, hence no problems arising from collinearity are expected.

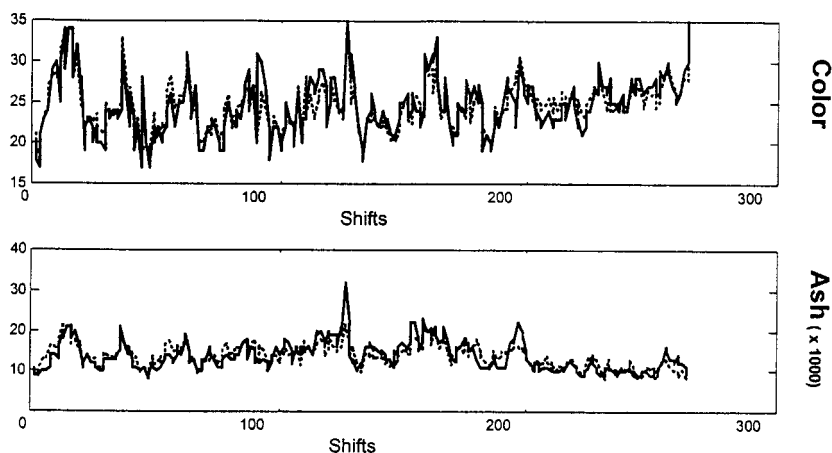


Fig. 12. Predictions of colour and ash from PARAFAC scores. Thick lines are reference values and thin lines the predicted values.

the conceptual idea behind the results reach far beyond the specific data treated here.

Appendix C. Principal variables (PV)

The PV model is based on exactly the same principles as is PCA and PLS. In PCA the first loading vector is the eigenvector corresponding to the largest eigenvalue of $(X'X)^2$, while in PLS we look for the weight vector which is the eigenvector corresponding to the largest eigenvalue of $(X'Y)^2$ [A16]. In PV we investigate exactly the same matrix products, but since we are interested in finding manifest variables and not latent factors we seek the largest diagonal elements of the matrices $(X'X)^2$ (in the 'PCA'-case) or $(X'Y)^2$ (in the regression case) corresponding to first principal variables. In PCA and PLS X is orthogonalised with the information described by the first latent factor. This also holds in the PV algorithm, where the X matrix is orthogonalised with the manifest variable: $X_{\text{new}} = X - v \cdot k$, where v is the column corresponding to the first principal variable and k is the loading.

Next the variables selected by the PV-algorithm are used in an ordinary multiple linear regression (MLR) with y as the dependent variable in order to develop a predictive model based only on the selected variables. We see here the synergistic combi-

nation of classical statistics (MLR) and new chemometric methods (principal variables). See the main text for applications (Table 1).

C.1. References to Appendices

- [A1] P.M. Kroonenberg, Three-mode component models, A survey of the literature, *Statistica Applicata*, 4 (1992) 619–633.
- [A2] L. Tucker, Some notes on three-mode factor analysis, *Psychometrika*, 31 (1966) 279–311.
- [A3] R. Bro, PARAFAC: Tutorial and applications, *Chemometrics and Intelligent Laboratory Systems*, 38 (1997) 149–171.
- [A4] R. Bro, Multi-way calibration. Multilinear PLS, *Journal of Chemometrics*, 10 (1996) 47–61.
- [A5] R. Henrion and C.A. Andersson, Diagonality versus variance of squares for simple-structure transformations of N-way core arrays, *Journal of Chemometrics*, submitted.
- [A6] C.A. Andersson, L. Munck, R. Henrion and G. Henrion, Analysis of N-dimensional data arrays from fluorescence spectroscopy of an intermediara sugar product, *Fresenius Journal of Analytical Chemistry*, 359 (1997) 138–142.
- [A7] S.G. Schulman, *Fluorescence and Phosphorescence Spectroscopy: Physicochemical Principles and Practice*, Pergamon Press, Oxford, 1977.

[A8] G.W. Ewing, *Instrumental Methods of Chemical Analysis*, McGraw-Hill Int. Ed., New York, 1985.

[A9] R.A. Harshman, *Foundations of the PARAFAC procedure: Model and conditions for an 'explanatory' multi-mode factor analysis*, *UCLA Working Papers in phonetics* 16 (1970).

[A10] J.D. Carroll and J. Chang, *Analysis of individual differences in multidimensional scaling via an N-way generalization of 'Eckart-Young' decomposition*, *Psychometrika*, 35 (1970) 283–319.

[A11] S. Leurgans, R.T. Ross, *Multilinear models in spectroscopy*, *Statistical Science*, 7 (1992) 289–319.

[A12] S. Leurgans, R.T. Ross and R.B. Abel, *A decomposition for three-way arrays*, *SIAM Journal of Matrix Analysis and Applications*, 14 (1993) 1064–1083.

[A13] R.T. Ross and S. Leurgans, *Component resolution using multilinear models*, *Methods in Enzymology*, 246 (1995) 679–700.

[A14] L. Nørgaard, *A multivariate chemometric approach to fluorescence spectroscopy*, *Talanta*, 42 (1995) 1305–1324.

[A15] R.A. Harshman and M.E. Lundy, *PARAFAC: Parallel factor analysis*, *Computational Statistics and Data Analysis*, 18 (1994) 39–72.

[A16] A. Höskuldsson, *Prediction Methods in Science and Technology*, Thor Publishing, Copenhagen, 1996.

References

- [1] G. Chaitin, in: J. Horgan (Ed.), *The End of Science — Facing the Limits of Knowledge in the Twilight of the Scientific Age*, Helix Books, Addison-Wesley, Reading, MA, 1996, p. 230.
- [2] P.C. Williams, K. Norris (Eds.), *Near Infrared Technology in Agricultural and Food Industries*, Am. Assoc. Cereal Chem., St. Paul, MN, 1987.
- [3] H. Martens, M. Martens, in: K.I. Hildrum, T. Isaksson, T. Næs, A. Tandberg (Eds.), *Near Infrared Spectroscopy—Bridging the Gap between Data Analysis and NIR Applications*, Ellis Horwood, 1992, 1–10.
- [4] J.D. Barrow, *Pi in the Sky—Counting, Thinking and Being*, Penguin Books, London, 1993.
- [5] J.C. Frisvad, M. Nørskær, *Use of correspondence analysis partial least squares on linear and unimodal data*, *J. Chemom.* 10 (1996) 677–685.
- [6] M. Martens, E. Risvik, H. Martens, *Matching sensory and instrumental analyses*, in: J.R. Piggott, A. Paterson (Eds.), *Understanding Natural Flavors*, Blackie Academic and Professional, Chapman & Hall, London, 1994, 61–76.
- [7] E. Jantsch, *Technological Forecasting in Perspective*, Organisation for Economic Cooperation (OECD), Paris, 1967.
- [8] C. Hempel, *Philosophy of Natural Science*, Prentice-Hall, Englewood Cliffs, NJ, 1968.
- [9] I. Prigogine, I. Stengers, *Order out of Chaos — Man's New Dialogue with Nature*, Flamingo Paperbacks, London, 1984.
- [10] Analytical Methods Committee, *Uncertainty of measurement: implications of its use in analytical science*, *R. Soc. Chem. London, Analyst* 120 (1995) 2303–2308.
- [11] R.P. Singh, J.R. Banga, *Recent advances in food process optimization*, *Chem. Industry*, London 13 (1994) 511–514.
- [12] C.W. Snyder, H.G. Law, J.A. Hattie, *Overview of multimode analytic methods*, in: H.G. Law, C.W. Snyder, J.A. Hattie, R.P. McDonald, *Research Methods for Multimode Data Analysis*, Praeger Scientific, New York, 1984, 2–35.
- [13] S.B. Engelsen, S. Pérez, *Internal motions and hydration of sucrose in a diluted water solution*, *J. Mol. Graph. Modelling* 15 (1997) 122–131.
- [14] L. Munck (Ed.), *Fluorescence Analysis in Foods*, Longman Scientific and Technical, Harlow, England, 1989.
- [15] L. Nørgaard, *Classification and prediction of quality and process parameters of beet sugar and thick juice by fluorescence spectroscopy and chemometrics*, *Zuckerindustrie* 120 (1995) 970–981.
- [16] L. Tucker, *Some notes on three-mode factor analysis*, *Psychometrika* 31 (1966) 279–311.
- [17] C.A. Andersson, L. Munck, R. Henrion, G. Henrion, *Analysis of N-dimensional data arrays from fluorescence spectroscopy of an intermediary sugar product*, *Fresenius J. Anal. Chem.* 359 (1997) 138–142.
- [18] R. Bro, *PARAFAC: Tutorial and applications*, *Chemom. Intell. Lab. Systems* 38 (1997) 149–171.
- [19] R.A. Harshman, M.E. Lundy, *PARAFAC: parallel factor analysis*, *Computational Stat. Data Anal.* 18 (1994) 39–72.
- [20] L. Munck, *Man as selector—a Darwinian boomerang striking through natural selection*, in: J. Aa. Hansen (Ed.), *Environmental Concerns*, Elsevier, London, 1991, 211–227.
- [21] M.W. Eysenck, *Principles of Cognitive Psychology*, Lawrence Erlbaum Associates, UK, 1993.
- [22] R.F. Madsen, W. Kofod Nielsen, B. Winström-Olsen, T.E. Nielsen, *Formation of colour compounds in production of sugar from sugar beet*, *Sugar Technology Reviews*, Elsevier, Amsterdam, 6 (1978/79) 49–115.
- [23] S. Wold, *Chemometrics, what do we mean with it, and what do we want from it?* *InCINC'94* (1994), http://www.emsl.pnl.gov:2080/docs/incinc/chem_phd/SWdoc.html.
- [24] P. Gould, *Destructive retrieval in the realm of three-mode thinking*, in: H.G. Law, C.W. Snyder, J.A. Hattie, R.P. McDonald, *Research Methods for Multimode Data Analysis*, Praeger Scientific, New York, 1984, 536–591.
- [25] J.W. Tukey, *Exploratory Data Analysis*, Addison-Wesley Publishing, 1977.
- [26] J. Ziman, *Reliable Knowledge - An Exploration of the*

II. Algorithms, models and applications

60

L. Munck et al. / Chemometrics and Intelligent Laboratory Systems 44 (1998) 31–60

- Grounds for Belief in Science, Cambridge Univ. Press, Cambridge, 1978.
- [27] T.S. Kuhn, *The Essential Tension - Selected Studies in Scientific Tradition and Change*, The Univ. of Chicago Press, Chicago and London, 1977.
- [28] H. Martens, *Multivariate Calibration: Combining harmonies from an orchestra of instruments into reliable predictions of chemical composition*, Proceedings, International Statistical Institute, Tokyo, 1987, 1–18.
- [29] E.L. Post, Absolutely unsolvable problems and relatively undecidable propositions: Account of an anticipation (1941), printed in the book *The Undecidable: Basic Papers on Undecidable Propositions, Unsolvable Problems and Computable Functions*, Raven Press, New York, 1965.

II. Algorithms, models and applications

P8

**Multi-way chemometrics for
mathematical separation of
fluorescent colorants and colour
precursors from
spectrofluorimetry of beet sugar
and beet sugar thick juice as
validated by HPLC analysis**

Dorrit Baunsgaard, Claus A. Andersson, Allan Arndal and Lars
Munck



Multi-way chemometrics for mathematical separation of fluorescent colorants and colour precursors from spectrofluorimetry of beet sugar and beet sugar thick juice as validated by HPLC analysis

Dorrit Baunsgaard*, Claus A. Andersson, Allan Arndal, Lars Munck

Chemometrics Group, Food Technology, Department of Dairy and Food Science, The Royal Veterinary and Agricultural University, Rolighedsvej 30, 1958 Frederiksberg C, Denmark

Received 10 September 1999; received in revised form 3 December 1999; accepted 6 December 1999

Abstract

In previous analyses of colour impurities in processed sugar, a multi-way chemometric model, CANDECOMP-PARAFAC (CP), has been used to model fluorescence excitation-emission landscapes of sugar samples. Four fluorescent components were found, two of them tyrosine and tryptophan, correlating to important quality and process parameters. In this paper HPLC analyses are used to chemically verify and extend the CP models of sugar. Thick juice, an intermediate in the sugar production, was analysed by size exclusion HPLC. Tyrosine and tryptophan were confirmed as constituents in thick juice. Colorants were found to be high molecular weight compounds. Fluorescence landscapes on collected column fractions were modelled by the CP model and seven fluorophores were resolved. Apart from tyrosine and tryptophan, four of the fluorophores were identified as high molecular weight compounds, three of them possible Maillard reaction polymers, whereas the seventh component resembled a polyphenolic compound. It is concluded that the relevance of CP for mathematical separation of fluorescence landscapes has been justified on two levels by HPLC; firstly as a screening method of fluorophores in complex samples and secondly as a confirmation of peak purity in chromatographic separation. © 2000 Elsevier Science Ltd. All rights reserved.

1. Introduction

White sugar produced industrially from sugar beet contains minute traces of unwanted colorants. Extensive research into the origin and development of the sugar colorants has been carried out for many years (Godshall, 1996). The earliest works date more than 130 years back (Scheibler, 1869). The fact that significant components have not yet been identified reflects the extreme complexity of the sugar streams as they occur in the sugar factory. Approaches that use isolated laboratory experiments tend to diverge from the natural seasonal variations of the streams, whereby the findings become too specialised to have any practical value in the real process streams at the factories. We have chosen a new approach to reach conclusions that adapt to the

natural (co)variations of the constituents in the sugar streams. With the use of exploratory data analysis, functional components in the process streams are found by soft adaptive modelling instead of using hard chemical analysis to identify actual chemical substances (Munck, Nørgaard, Engelsen, Bro & Andersson, 1998). Advanced multi-way models, such as the CANDECOMP-PARAFAC (CP) model, can be used to decompose complex excitation-emission fluorescence landscapes into excitation and emission spectral profiles of characteristic components (Leurgans & Ross, 1992). Bro (1999) used the CP model on fluorescence landscapes from 268 sugar samples collected from a factory during a sugar campaign. A model with four fluorescent components was found to capture the variation in that time period. Two of them had pseudo-spectra, which showed a close similarity to pure fluorescence spectra of tyrosine and tryptophan. In addition, the concentrations of the four components estimated from the sugar samples could be correlated to several quality and process parameters. Thus, the four fluorescent components found in the final

* Corresponding author. Tel.: +45-3528-3500; fax: +45-3528-3505.

E-mail address: dba@kvl.dk (D. Baunsgaard).

sugar product are considered as indicator substances of the chemistry in the sugar process.

In the sugar process streams, there are several potential fluorophores. These include colour precursors such as amino acids and polyphenolic compounds (Wolfbeis, 1985). Colour precursors can interact in colour forming reactions such as amino acids with reducing sugars in Maillard reactions or enzymatic oxidation of phenolic compounds to form melanins (Godshall, Clarke, Dooley & Blanco, 1991). Coloured Maillard reaction products have been reported to exhibit fluorescence (Adhikari & Tappel, 1973). One of the preferred methods for analysing colorants and colour precursors has been gel permeation chromatography (GPC) since many of the colorants are considered as high molecular weight compounds (Madsen, Kofod Nielsen, Winstrøm-Olsen & Nielsen, 1978a; Reinefeld, Schneider, Westphal, Tesch & Knackstedt, 1973; Shore, Broughton, Dutton & Sissons, 1984).

In this paper, we combine CP modelling of fluorescence excitation-emission landscapes with HPLC size exclusion analysis. After separating the sample on the column, collected fractions are measured as fluorescence landscapes and modelled with the CP model. Thick juice, an intermediate product from the sugar manufacturing process, is analysed instead of sugar since the latter is too pure and not suitable for chromatographic analysis. The purpose of the chromatography is two-fold. It can be used to verify the identity of the mathematically modelled fluorophores in sugar with peak identification. Also, the number of identifiable components may be improved by the pre-separation of the components on the column before the fluorescence measurements. The pre-separation is used to reduce quenching and other interactions in the complex sample, which influences the fluorescence, and may violate the assumptions made prior to application of the CP model.

2. Materials and methods

2.1. Chemicals

L-tyrosine, L-tryptophan and L-phenylalanine were purchased from Sigma (USA). The reagents for the HPLC buffer were obtained from Merck KGaA (Germany). Water was distilled and deionized (Milli-Q, Waters, USA). HPLC eluents were filtered and degassed before use.

2.2. Samples

Beet sugar samples and beet sugar thick juice samples were all provided by Danisco Sugar A/S, Denmark. Ten thick juice samples from five different sugar factories,

two from each, were dissolved in water 1:500 (v/v) and used to measure fluorescence landscapes. Five sugar samples collected from one of the sugar factories were prepared by dissolving 7 g sample in 15 ml water for the fluorescence measurements. For the HPLC analyses thick juice samples from one of the five factories was prepared by diluting 100 μ l thick juice with 100 μ l 0.2 M ammonium buffer, pH = 8.9 and 300 μ l water. Due to the high viscosity of the thick juice sample, a pipette designed for viscous samples (Microman 250, Gilson, USA) was used to take samples of the thick juice.

2.3. HPLC analyses

The HPLC size exclusion analyses were performed on a Gilson system with a Gilson 170 UV-VIS diode array detector (range: 210–550 nm) and a Jasco FP-920 fluorescence detector (excitation/emission wavelengths: 280/325 nm). A Waters 250 Ultrahydrogel column (range 1–80 kDa) was used equipped with a guard column of the same material and thermostatted at 30°C. The mobile phase consisted of 0.2 M ammonium buffer ($\text{NH}_4\text{Cl}/\text{NH}_3$), pH = 8.9 and water (20:80 v/v) at a flow rate of 0.5 ml/min. All sample solutions were filtered through a 0.22 μ m hydrophilic PVDF membrane filter (Millipore, USA) before injecting an aliquot of 100 μ l onto the column. In this publication, two representative HPLC runs of thick juice were selected for fluorescence landscape measurements of 41 collected fractions of 750 μ l (1.5 min) from 10 to 71.5 min in each run.

2.4. Amino acid standards

Tyrosine and tryptophan were identified by peak identification of spiked thick juice samples with amino acid standards. The spiked thick juice samples were prepared by mixing 50 μ l thick juice and 100 μ l 0.2 M ammonium buffer, pH = 8.9 with 350 μ l tyrosine solution (192 mg/l) or 350 μ l tryptophan solution (43 mg/l). The two amino acid solutions and a phenylalanine solution (1.4 mg/l) were used to establish the size exclusion range of the column in a 1:2 (v/v) dilution with the ammonium buffer.

The fluorescence spectra of the tyrosine and tryptophan standards were measured with the same parameters as with the other samples using a tyrosine concentration of 1.6 mg/l and a tryptophan concentration of 0.3 mg/l.

2.5. Fluorescence landscape measurements

A Perkin-Elmer LS50 B fluorescence spectrometer was used to measure fluorescence landscapes using excitation wavelengths between 230–300 nm with 5 nm intervals and 310–460 nm with 10 nm intervals. The emission wavelength range was 288–700 nm. Excitation

and emission monochromator slit widths were set to 10 nm, respectively. Scan speed was 1500 nm/min. A micro quartz cuvette with the dimensions 5×5 mm was used to avoid dilution and to reduce any concentration quenching effects of the sample solution.

2.6. The CANDECOMP-PARAFAC model

The CANDECOMP-PARAFAC (CP) model was proposed in 1970 (Carroll & Chang, 1970; Harshman, 1970) and fits the premises of fluorescence spectroscopy for resolving pure excitation and emission spectra from measured net signals of mixtures. To allow for a discussion of the CP model, we consider a fluorescence data set with elements denoted by x_{ijk} , where x_{ijk} is the intensity of the i th sample excited by light at the j th excitation wavelength and measured at the k th emission wavelength. The resulting data set thus spans a three-dimensional table structure, where each entry represents an observation that depends on discrete levels of the three parameters, (sample number×excitation wavelength×emission wavelength). The three-way data array can be approximated by

$$x_{ijk} = \sum_{f=1}^F a_{if} b_{jf} c_{kf} + e_{ijk} \quad (1)$$

In (1) it is assumed that the measured net signal is a sum of F individual contributors, or fluorophores. For fluorophore number f , a_{if} is the concentration in the i th sample, b_{jf} is the relative amount of light absorbed at excitation wavelength j , and c_{kf} is the relative intensity emitted at wavelength k . This tri-linear structure of the light intensity model is similar to the tri-linear CP model for which solution algorithms have been devised (see Carroll & Chang, 1970; Harshman, 1970). Under the assumption of tri-linearity in the signal/concentration ratio and additivity of the intensities, the CP model parameters will be estimates of the underlying excitation spectra, i.e. the b_{jf} parameters, and the emission spectra, i.e. the c_{kf} parameters of each of the f contributing fluorophores. However, based on the observations or a priori knowledge, the task of defining the correct number of fluorophores, f , remains. The mathematical uniqueness of the CP-model will provide parameters in A, B and C of the individual fluorophores contributing to the net signal. Not only will the parameter estimates be unique to the individual fluorophores, but since the fundamental mechanistic model of the net signal of a single fluorophore is in exact accordance with the CP-model for $F=1$, the resolved parameters will be relative estimates of concentration level, excitation ability (absorbance spectrum) and emission ability (emitted spectrum).

Furthermore, the CP model allows for simultaneous presence of many such single contributors to the overall observed emitted intensity, x_{ijk} . Thus, by estimating the CP parameters, the collection of net signal can be separated mathematically into a number of characteristic profiles for each of the fluorophores/contributors. See Leurgans and Ross (1992) for an in-depth discussion of multi-linear models in spectroscopic contexts. For a more thorough presentation of the model, the reader is referred to a tutorial on the CP model (Bro, 1997).

The CP results have been obtained with the use of the N -way Toolbox for MATLAB (Andersson & Bro, 1998) running MATLAB 5.3 under Microsoft Windows NT 4 SP5 on a dual 450 MHz Intel PII Xeon PC. For the tri-linear CP model to be valid, infeasible measurements (i.e. Rayleigh scatter and emission wavelengths less than excitation wavelengths) have to be treated as missing values. To circumvent the scaling ambiguities of the CP model and to enhance the interpretability of the model, the profiles were constrained to non-negativity while minimising the sum of squared errors, i.e. the constrained model parameters were estimated from a total least squares optimisation of Eq. (1).

3. Results and discussion

3.1. Fluorophores in sugar and thick juice

Since thick juice is used instead of sugar in the HPLC separations, it is important to know the differences and similarities between fluorophores found in sugar and in thick juice. In addition, the changes in the properties of an intermediate sugar product to the properties of the final product can be useful, e.g. in process control.

The CP analysis on fluorescence landscapes of sugar samples previously made by Bro (1999) was repeated by making a CP model using five sugar samples from another sugar factory. In addition, fluorescence landscapes were measured on ten thick juice samples from five different sugar factories, two samples from each factory, and modelled with the CP model. A four-component model was generated from the sugar data and a five-component model from the thick juice data. The CP modelling estimates excitation and emission spectra of measured fluorophores as well as a sample profile relating the concentration of each fluorophore in the samples measured. Fig. 1 (rows 1–4) and Fig. 2 present the excitation and emission spectra of the modelled components in the sugar and thick juice samples, respectively. The components are displayed in the same order as they are modelled depending on their contribution in the sample profile. The resolved spectra show reasonable spectral shapes, but they are dependent on the appearance of the measured fluorescence data and the premises of the model. Therefore some of the spectra may display artefacts such

4

D. Baunsgaard et al. / Food Chemistry 0 (2000) 1–9

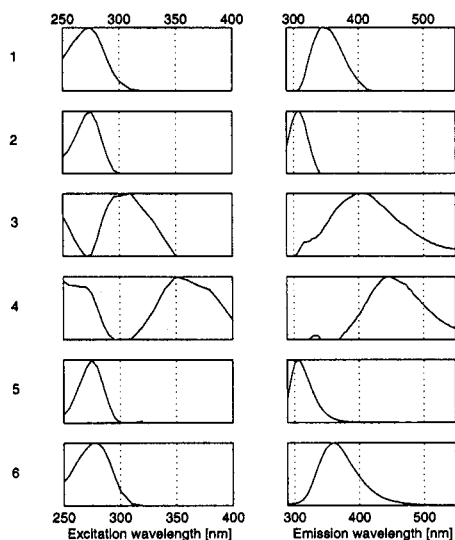


Fig. 1. The results of a four-component CP model of fluorescence landscapes of five beet sugar samples. Rows 1–4 contain the excitation and emission spectra of the four resolved components. The left column shows the excitation profiles and the right column shows the emission profiles. Rows 5 and 6 show the fluorescence excitation and emission spectra of pure tyrosine and pure tryptophan, respectively, for a comparison. All profiles have been normalised to unit length.

as extra bands in the emission spectra, e.g. the emission spectrum of component 4 in Fig. 2. The excitation (1st excited state) and emission wavelength maxima of the spectra in Figs. 1 and 2 are presented in Table 1. The shape and maxima of the emission spectra of the sugar model in Fig. 1 are comparable to the previously modelled spectra of the four-component sugar model by Bro (1999). In Fig. 1 the excitation and emission spectra of pure tyrosine and tryptophan standards are displayed in rows 5 and 6, respectively. Comparing the spectra of the two amino acids with the spectra of the modelled components in Fig. 1, there is a close similarity between tyrosine and component 2 and between tryptophan and component 1. The spectral profiles of thick juice fluorophores in Fig. 2 are consistent with the spectra of the sugar components in Fig. 1, although there are some differences in the profiles. This is also evident by comparing the excitation and emission maxima in Table 1. The tyrosine-like fluorophore is component 1 in Fig. 2. Component 2 in Fig. 2 resembles the tryptophan-like component in Fig. 1, but the emission profile is shifted towards lower wavelengths and a fifth component (component 3) is introduced in the thick juice model. The spectral properties of the new component are close to tryptophan. Thick juice contains much more impurities

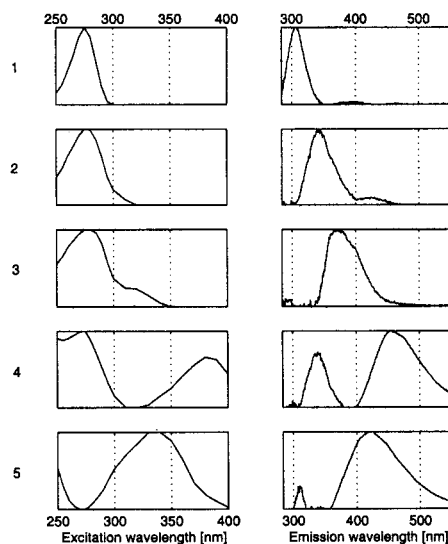


Fig. 2. A five-component CP model of fluorescence landscapes of 10 thick juice samples. The left column shows the resolved excitation profiles and the right column shows the resolved emission profiles of the five components. All profiles have been normalised to unit length.

than sugar and the fluorescence data is more difficult to model. If component 2 is tryptophan, component 3 might be another fluorophore or a tryptophan-derived component with somewhat changed fluorescent properties, either of which affecting the estimated tryptophan profile. Using a larger sample set, it will be possible better to solve such ambiguities.

In the modelling of sugar and thick juice fluorescence data, samples from several factories have been used. It is found that sugar models from different factories contain the same four fluorophores, e.g. the similarity of the modelled spectra of the five sugar samples in Fig. 1 with the previously modelled spectra from another factory (Bro, 1999). Furthermore, the thick juice model in Fig. 2 was based on samples from five different sugar factories and HPLC analyses made on the thick juice samples from the five factories all showed the same qualitative chromatographic pattern. Therefore, the modelled fluorophores from the sugar and thick juice fluorescence data are considered to be common constituents of sugar and thick juice and not factory related.

3.2. Peak identification using HPLC analyses

It is important to validate the results of the CP modelling of fluorescence landscapes of sugar and thick juice. When comparing the resolved pseudo-spectra

Table 1

The excitation and emission maxima of the modeled spectra of sugar, thick juice and HPLC fractions of thick juice

Component ^a	Sugar _{max} (nm)		Thick juice _{max} (nm)		HPLC fractions of thick juice _{max} (nm)	
	Excitation	Emission	Excitation	Emission	Excitation	Emission
1	275	350	275	305	275	305
2	275	305	275	340	275	360
3	310	400	280	370	375	460
4	350	450	380	455	340	440
5	–	–	335	420	385	460
6	–	–	–	–	290	400
7	–	–	–	–	290	330

^a The component numbers correspond to the row numbers given in Figs. 1, 2 and 6 for each of the three CP models.

with pure spectra of tyrosine and tryptophan, a level of uncertainty is involved due to the limited number of samples as well as quenching and non-linearities in the measured fluorescence data. Using chromatographic peak identification, it is possible to verify that the two amino acids really are constituents of thick juice. Drewnowska, Walerianczyk, Butwilowicz, Jarzebinski, Fitak and Gajewska (1979) have previously estimated the contents of tyrosine and tryptophan in thick juice with the use of liquid chromatography. Fig. 3 shows a HPLC size exclusion separation of one of the thick juice samples before and after spiking the sample with the two amino acids and monitored by fluorescence detector set at 280/325 nm. The three chromatograms show good overlap and the spiked peaks confirm that the two dominating components eluting at 25 and 42 min are the free amino acids, tyrosine and tryptophan, respectively. In addition, the identities of the peaks were confirmed by comparison with chromatograms of amino

acid standards. The tyrosine and tryptophan peaks at 25 and 42 min were also found in the chromatograms of the thick juice samples from the four other factories used in the thick juice model. The corresponding diode array scans of the two spiked peaks in Fig. 3 are also displayed in the figure. The spectra are practically identical with pure spectra of tyrosine and tryptophan, which is an additional certainty of the identification of the peaks.

It is difficult to analyse the very pure sugar on a HPLC system. However, the similarity of the spectral profiles in the sugar model with the thick juice model and the spectra of the amino acid standards confirm indirectly the identification of the corresponding fluorophores.

3.3. HPLC size exclusion analyses of thick juice

When using a size exclusion column (range 1–80 kDa), it is possible to separate the thick juice samples according to molecular weight. This can be used to separate the colorants as high molecular weight compounds from low molecular weight colour precursors. The column dead time was determined to 12.4 min using Blue Dextran 2000. The amino acid standards tyrosine and phenylalanine were used to establish the end of the size exclusion area of the column to 25 min. The fact that tryptophan elutes at 42 min is probably caused by *adsorptive* retention on the column. In Fig. 4 three simultaneously recorded chromatograms of a thick juice sample are shown. The two upper chromatograms are captured from the diode array detector at 280 and 420 nm, whereas the lower chromatogram is from the fluorescence detector at 280/325 nm. 420 nm is the normal wavelength chosen by the sugar industry to represent colour. Many of the known components absorb at 280 nm (amino acids, polyphenols, Maillard reaction products, etc.), which is consistent with the multiple peaks in the chromatogram. The 420 nm chromatogram, on the other hand, shows a limited number of small peaks in the beginning of the run between 15 and 25 min. The estimated size exclusion range was approx. 12–25 min, which means that the colorants are smaller than 80 kDa

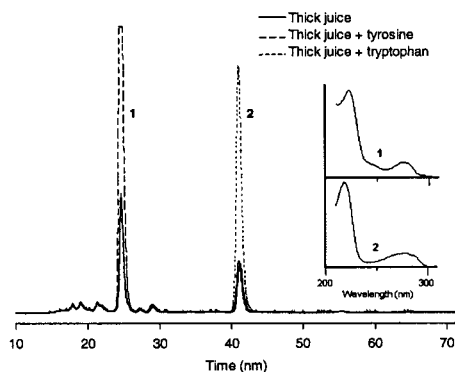


Fig. 3. HPLC size exclusion chromatograms with qualitative standard additions of tyrosine (1) and tryptophan (2) to thick juice monitored by fluorescence detection at 285/325 nm. The chromatograms verify the expected presence of tyrosine and tryptophan. The corresponding UV/VIS absorbance spectra from the diode array scans of the two peaks are also displayed.

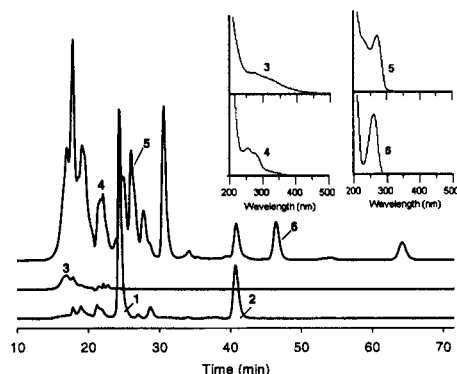


Fig. 4. HPLC size exclusion chromatograms of a thick juice sample. Upper curve: UV detection at 280 nm; middle curve: UV detection at 420 nm; bottom curve: fluorescence detection at 280/325 nm. Diode-array spectra of selected peaks (4–6) are also displayed. The spectra of peaks 1 and 2 are identical with the spectra of the corresponding tyrosine and tryptophan peaks in Fig. 3.

but extend the range down to 1 kDa. Colorants have been estimated to 5 kDa in white beet sugars, though for some sugars up to 40 kDa, and in molasses colorants up to 50 kDa have been found (Godshall et al., 1991). Their findings agree well with the range of the colorants in thick juice separated on the HPLC column. Apart from the two very dominating peaks at 25 and 42 min identified as tyrosine and tryptophan, the fluorescence chromatogram in Fig. 4 also shows a number of smaller peaks in the colorants area in the first 25 min.

A few selected diode array scans with very different spectral appearance are also displayed in Fig. 4. Apart from confirming the findings in the chromatograms, the diode array absorbance spectra can provide more detailed information for the identification of the components in thick juice. The absorbance spectra of peaks 1 and 2 are identical to the displayed spectra of corresponding peaks in Fig. 3. The spectra of peak 3 reveals that the highest molecular weight colorants absorb light up to 500 nm, which is consistent with the golden-orange appearance of the thick juice sample. Peaks 4–6 display different spectra mainly absorbing at 280–300 nm whereas peaks 4 and 5 appear to be composed of multiple components. The displayed spectra demonstrate the complexity of the thick juice sample and the fact that the separation of thick juice on the HPLC size exclusion column is insufficient to separate the colorants in thick juice.

3.4. A CP model of fluorescence landscapes of HPLC fractions of thick juice

To improve the CP model of thick juice as well as the HPLC separation, 41 fractions of 1.5 min (10–71.5 min)

were collected during the HPLC separation shown in Fig. 4. A fluorescence landscape was recorded of each fraction by off-line measurements in a scanning spectrofluorometer. In Fig. 5 the fluorescence landscape of fraction 9 serves as an example of such a landscape. There are clearly multiple overlapping fluorescent peaks in the landscape and a resolution method is required. The 41 landscapes form a three-dimensional data array consisting of the 41 fractions in the first dimension, 31 excitation wavelengths (230–460 nm) in the second dimension, and 431 emission wavelengths (288–700 nm) in the third dimension. The array was modelled by the three-way CP model and seven components were found. The modelling results are shown in Fig. 6. Each component is represented by the estimated excitation and emission spectra as well as a chromatographic profile, which shows the concentration of each component in the 41 collected fractions. The excitation and emission maxima of the seven components are presented in Table 1. The spectral shapes in Fig. 6 are all reasonable. Again extra bands appear in some of the emission spectra. The fluorescence landscape of fraction 9 in Fig. 5 demonstrate that a large part of the landscape has to be treated as missing values due to first and second order Rayleigh scattering (Bro, 1999). In the estimations of these areas, extra bands may appear depending on the condition of the fluorescence data. Components 1 and 2 in Fig. 6 are recognised as the two modelled components tyrosine and tryptophan, which are also found in the sugar and thick juice models (Figs. 1 and 2). In the corresponding chromatographic profiles in Fig. 6 the two components show two dominant peaks in fraction 10 (23.5–25 min) and fraction 21 (40–41.5 min), respectively, which are consistent with the position of the spiked peaks in the fluorescence chromatogram in Fig. 3. The chromatographic profile of tryptophan in row 2 in Fig. 6 also shows contributions in fractions 3–12 similar to the small peaks displayed in the fluorescence chromatogram in Fig. 4. Tyrosine, on the other hand, is only found in fractions 9–11. Tryptophan has very distinct fluorescent properties, which are kept intact even as a functional group in a larger molecule, whereas tyrosine loses the fluorescent properties very easily. For example, in proteins the fluorescence is dominated by the tryptophan residue (Lakowicz, 1983). The fact that the tryptophan fluorophore is modelled in the higher molecular weight fractions in the chromatographic profile could be due to tryptophan residues behaving as individual fluorophores in polymers. This demonstrates that the chromatographic profile from a CP model can be used as a mathematical purification of the overlapping peaks in a chromatogram, provided that the assumptions of linearity and additivity of the model hold. The area of the chromatogram from 15–25 min with many overlapping peaks in Fig. 4 is simplified by the CP model and more information can be obtained.

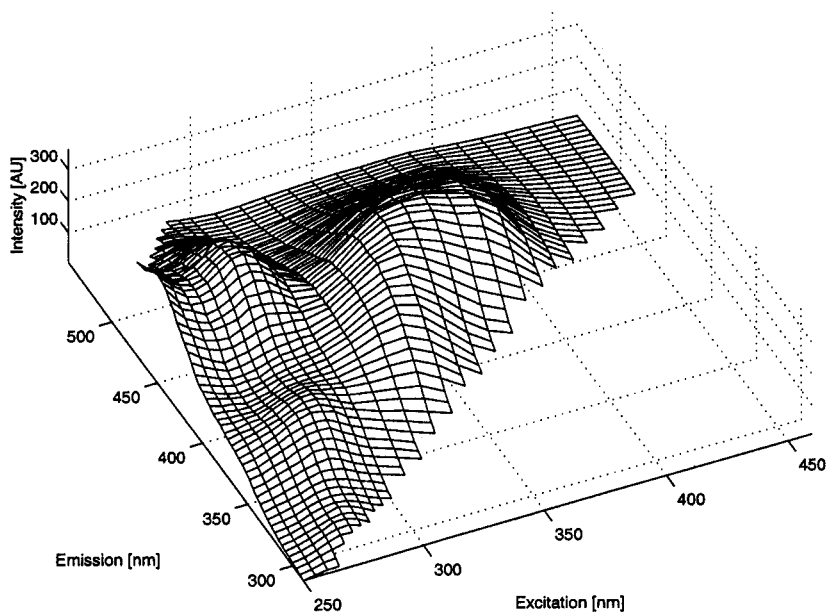


Fig. 5. An example of a fluorescence landscape from HPLC fraction no. 9 (22–23.5 min) of thick juice measured with 31 excitation wavelengths (230–460 nm) and 431 emission wavelengths (288–700 nm). The blank regions hold Rayleigh scatter signals and are thus treated as missing values.

Components 3–5 in Fig. 6 are very similar in their spectral shapes and position of the emission spectra. They are modelled as three individual components because of the differences in the excitation and chromatographic profiles. It can be argued that they are part of the same group of fluorophores, but are resolved individually due to small differences in molecular sizes and/or small differences in the fluorophore environments. The size exclusion on the HPLC column is not good enough in the high molecular weight area and a more refined fraction collection is necessary to obtain a clearer separation. This is supported by the chromatogram at 280 nm in Fig. 4, where there is only one peak at 20–23 min. The three components (3–5) in Fig. 6 have excitation profiles that reach into the visible area above 400 nm, which implies that they contribute to the colorants in thick juice. They are all found in the first fractions of the chromatographic profiles and are thus high molecular weight compounds. The spectral characteristics of these colorants resemble conjugated Schiff bases derived from malonaldehyde and amino acids as reported by Chio and Tappel (1969). The authors ascribed the absorption and fluorescence properties of the Schiff bases to the chromophoric system $-N=C-C=C-N-$. Pongor, Ulrich, Bencsath, and Cerami (1984) isolated a fluorophore from a product of a browning reaction of polypeptides with glucose, which show similar fluorescence

spectra. The structure of the isolated fluorophore contained a conjugated system of nitrogen and carbon in an imidazole derivative. Similar compounds isolated from real samples in the sugar processing have not been reported, but quantitative elementary analysis on high molecular weight fractions from GPC separations of thick juice showed an element ratio of carbon and nitrogen as 7:1, which indicated that amino acids were built into the high molecular weight fractions (Madsen, Kofod Nielsen & Winstrøm-Olsen, 1978). All this suggests that some or all of components 3–5 are colorant polymers formed during the sugar processing in Maillard reactions involving amino acids and reducing sugars.

Component 6 in Fig. 6 is also a high molecular weight compound with contributions in the first fractions in the chromatographic profile. The emission spectrum is in the visible area, but the excitation spectrum is well below 400 nm and the component is therefore not a colorant. The component is similar to component 3 in the sugar model in Fig. 1 and partly comparable to component 5 in the thick juice model in Fig. 2. At present the component is not associated with any known fluorophore.

Component 7 in Fig. 6 is the only component not comparable to any component in the sugar model in Fig. 1. This component may be the reason that the

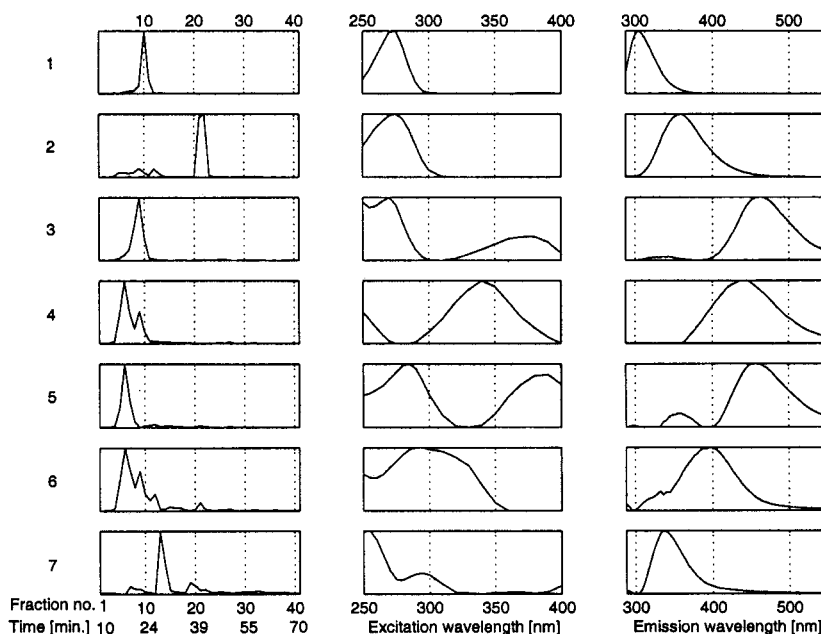


Fig. 6. The results of a seven-component CP model of the measured fluorescence landscapes of 41 collected HPLC fractions (10–71.5 min). The left-most column holds the chromatographic profiles, which show the concentration of each of the seven fluorescent components in the fractions. The centre column holds the excitation profiles and the right-most column holds the emission profiles of the fluorophores. All profiles have been normalised to unit length.

tryptophan component is not estimated as clearly in the thick juice model (Fig. 2) as in the sugar model (Fig. 1), since it has spectral properties close to tyrosine. Its concentration is low in thick juice and therefore the CP model of the 10 thick juice samples in Fig. 2 could not resolve it. Pre-separation on the column made it possible to measure the fluorescence of component 7 without interference like concentration quenching from other fluorophores in thick juice. The component contributes only slightly in the first fractions when looking at the chromatographic profile in Fig. 6, but is spread over several of the later fractions with a dominant peak in fraction 13 (28–29.5 min), which indicates either a low molecular weight compound or a compound with high column affinity. The excitation and emission profiles of this component are suggesting a fluorophore with a polyphenolic group (Duggan, Bowman, Brodie & Udenfriend, 1957).

4. Conclusion

It is possible to capture the same fluorescent information from the CP models of fluorescence landscapes

of sugar samples and thick juice samples. Four principal components are resolved from the sugar model, where two of them have spectra similar to tyrosine and tryptophan. The tyrosine component is also found in the five-component thick juice model, whereas the estimation of the tryptophan component is less certain due to the more complex sample. However, the presence of the two amino acids in the thick juice model is verified by HPLC peak identification, which also confirms the spectral identification of the model components. The HPLC size exclusion separation of thick juice further confirms that the fluorescent colorants, which are found in the CP analysis of the sugar and thick juice samples, are high molecular weight compounds. Landscape measurements on HPLC collected fractions of thick juice are successfully modelled and seven components are found. The resolved chromatographic profile of the model can be used as a mathematical purification of the not perfectly separated chromatogram. Two of the seven modelled components are identified as the free amino acids, tyrosine and tryptophan, but the latter also appears in higher molecular weight fractions in the chromatographic profile implying intact tryptophan residues in polymers. Four out of the seven modelled components

are identified as high molecular weight components; three of them are suggested to be Maillard reaction polymers of amino acid origin with different molecular weights. The seventh component is of low concentration and has a spectral appearance of a polyphenolic-like compound. It is important to improve further the fluorescence information of the sugar streams by modelling a larger data material to improve the CP model estimations, and it is currently in progress. Future research will also include CP models of fluorescence data from samples taken throughout the sugar process to increase the information of the origin and development of the fluorophores in the sugar streams.

Thus, this paper demonstrates the usefulness of mathematical deconvolution by the CP model of fluorescence data from complex sample matrices as well as for peak purity evaluation in chromatography.

Acknowledgements

The authors thank Ole Hansen, Lars Bo Jørgensen and John Jensen, Danisco Sugar Development Center, Nakskov, Denmark for inspiring cooperation and in providing the sugar and thick juice samples. We also thank Dr. Rasmus Bro for valuable discussions.

References

- Adhikari, H. R., & Tappel, A. L. (1973). Fluorescent products in a glucose–glycine browning reaction. *Journal of Food Science*, *38*, 486–488.
- Andersson, C. A. & Bro, R. (1998) The *N*-way toolbox for MATLAB. Can be downloaded from <http://models.kvl.dk/source/nwaytoolbox/>
- Bro, R. (1997). PARAFAC: tutorial and applications. *Chemometrics and Intelligent Laboratory Systems*, *38*, 149–171.
- Bro, R. (1999). Exploratory study of sugar production using fluorescence spectroscopy and multi-way analysis. *Chemometrics and Intelligent Laboratory Systems*, *46*, 133–147.
- Carroll, J. D., & Chang, J. (1970). Analysis of individual differences in multidimensional scaling via an *N*-way generalization of "Eckart–Young" decomposition. *Psychometrika*, *35*, 283–319.
- Chio, K. S., & Tappel, A. L. (1969). Synthesis and characterization of the fluorescent products derived from malonaldehyde and amino acids. *Biochemistry*, *8*, 2821–2827.
- Drewnowska, W., Walerianczyk, E., Butwilowicz, A., Jarzebinski, J., Fitak, B., & Gajewska, M. (1979). Contents of free amino acids and amides in sugar and sugar industry semiproducts. *Acta Alimentaria Polonica*, *5*, 315–321.
- Duggan, D. E., Bowman, R. L., Brodie, B. B., & Udenfriend, S. (1957). A spectrophotofluorometric study of compounds of biological interest. *Archives of Biochemistry and Biophysics*, *68*, 1–14.
- Godshall, M. A. (1996) Recent progress in sugar colorants. In *Proceedings of the 1996 Conference on Sugar Processing Research* (pp. 262–305), New Orleans, USA.
- Godshall, M. A., Clarke, M. A., Dooley, C. D., & Blanco, R. S. (1991). Progress in beet sugar colorant research. *Journal of Sugar Beet Research*, *28*, 155–165.
- Harshman, R. A. (1970). Foundations of the PARAFAC procedure: models and conditions for an "explanatory" multi-modal factor analysis. *UCLA Working Papers in Phonetics*, *16*, 1–84.
- Lakowicz, J. R. (1983). *Principles of fluorescence spectroscopy*. New York: Plenum Press p. 347.
- Leurgans, S., & Ross, R. T. (1992). Multilinear models: applications in spectroscopy. *Statistical Science*, *7*, 289–319.
- Madsen, R. F., Kofod Nielsen, W., Winstrøm-Olsen, B., & Nielsen, T. E. (1978a). Formation of colour compounds in production of sugar from sugar beet. *Sugar Technology Reviews*, *6*, 49–115.
- Madsen, R. F., Kofod Nielsen, W., & Winstrøm-Olsen, B. (1978b). Juice purification system, sugar house scheme, and sugar quality. *Sugar Journal*, *41*, 15–19.
- Munck, L., Nørgaard, L., Engelsen, S. B., Bro, R., & Andersson, C. A. (1998). Chemometrics in food science — a demonstration of the feasibility of a highly exploratory, inductive evaluation strategy of fundamental scientific significance. *Chemometrics and Intelligent Laboratory Systems*, *44*, 31–60.
- Pongor, S., Ulrich, P., Bencsath, F. A., & Cerami, A. (1984). Aging of proteins: isolation and identification of a fluorescent chromophore from the reaction of polypeptides with glucose. *Proceedings of the National Academy of Sciences of the USA*, *81*, 2684–2688.
- Reinefeld, E., Schneider, F., Westphal, K., Tesch, K., & Knackstedt, H. G. (1973). Model studies on the browning reaction in technical sugar juices. *Zucker*, *26*, 581–588.
- Scheibler, C. (1869). Über das Betaïn, eine im Saft der Zuckerrüben (*Beta vulgaris*) vorkommende Pflanzenbase. *Zeitschrift des Vereines für die Rübenzucker-Industrie im Zollverein*, *19*, 549–558.
- Shore, M., Broughton, N. W., Dutton, J. V., & Sissons, A. (1984). Factors affecting white sugar colour. *Sugar Technology Reviews*, *12*, 1–99.
- Wolfbeis, O. S. (1985). The fluorescence of organic natural products. In S. G. Schulman, *Molecular luminescence spectroscopy: methods and applications—part I* (pp. 167–370). New York: John Wiley and Sons.

P9

**Analysis of N -dimensional data
arrays from fluorescence
spectroscopy of an intermediate
sugar product**

Claus A. Andersson, Lars Munck, Rene Henrion and Gunther
Henrion

ORIGINAL PAPER

C. A. Andersson · L. Munck · R. Henrion · G. Henrion

Analysis of N -dimensional data arrays from fluorescence spectroscopy of an intermediary sugar product

Received: 13 January 1997 / Revised: 18 March 1997 / Accepted: 25 March 1997

Abstract Unwanted formation of colour takes place during the production of crystalline sugar. The degree of colouration depends partly on the necessary processing conditions, e.g. heating and pH, and partly on the initial composition and condition of the sugar beets used as raw material. Reducing sugars are formed during the process. These are reactive compounds forming a variety of coloured complexes and strong precursors to further formation of colour and many of these compounds contain fluorophores. In the present work it is discussed if spectrofluorometric screening of intermediary sugar products prior to the final heating stages combined with a multi-way chemometric approach can provide information that significantly reflects the condition of the process and the beets. The model used is the N -way PCA (Principal Component Analysis) which is an exploratory model, not necessitating explicit modelling of single parameters nor any assumptions towards parameter interaction. By use of a 4-way PCA of order (3,2,3,3) satisfactory classification of 47 thick juice samples belonging to 5 factories has been obtained from a spectrofluorometric screening method. Also, a temporal trend has been found to evolve during the time of production. The investigation substantiates the use of modern models from data analysis for extracting significant information from large and complex data sets.

Dedicated to Professor Dr. Gerhard Werner on the occasion of his 65th birthday

C. A. Andersson · L. Munck
Chemometrics Group, Food Technology,
Royal Veterinary and Agricultural University, Rolighedsvej 30,
DK-1958 Frederiksberg, Denmark

R. Henrion
Weierstrass-Institute of Applied Analysis and Stochastics,
Mohrenstrasse 39, D-10117 Berlin, Germany

G. Henrion
Institute of Chemistry, Humboldt University of Berlin,
Hessische Strasse 1–2, D-10115 Berlin, Germany

1 Sugar production

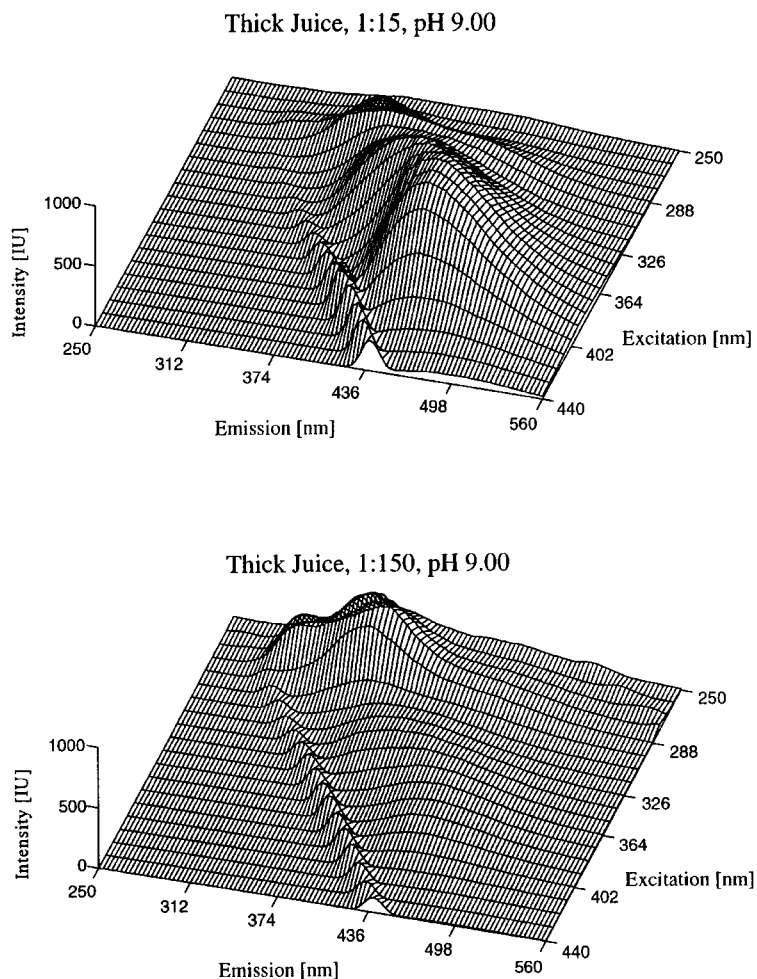
In northern Europe the most important source of sucrose for the production of crystalline sugar is the sugar beet, *Beta Vulgaris*. Harvesting of sugar beets and, immediately following, production of sugar is concentrated to a yearly period of approx. 4 months. This period is called the campaign and runs typically from October to January. During the campaign the factories continuously receive beets from many different beet farmers. Due to premises of growing, e.g. fall of rain, frost, soil characteristics, fertilizer type and harvesting machinery, there is a high variation between the truckloads delivered by the farmers. A consequence of this variation is that the parameters for the chemical unit processes are difficult to control with regard to securing a white and uniform final product (see [1] for an overview of the process). The quality class of the sugar is determined according to European standards in which colouration is a main parameter. The classification influences the price at which the product can be sold, hence there is a strong economical motivation for minimizing the formation of colour during the process. Chemometrics has successfully been applied to the prediction of selected quality parameters in sugar [2].

A spectrofluorometrically based screening method has been applied to samples taken weekly of a preliminary sugar product, *thick juice*. Data from this screening have been explored with multi-way, multivariate chemometric methods.

2 Experimental

Fluorescence intensity landscapes, or excitation-emission matrices, have been measured on 47 thick juice samples from the 1994 campaign. Five factories have contributed thick juice samples. Each sample has volumetrically been diluted 1:15 and 1:150 with NH_4Cl pH 9.00 buffer in doubly ion-exchanged and Si-free water. The buffer was made only once. Both of the dilutions were measured using 20 excitation wavelengths (250 nm–440 nm, 10 nm intervals) and 311 emission wavelengths (250 nm–560 nm, 1 nm intervals). Two typical landscapes for one sample are shown in Fig. 1.

Fig. 1 Two fluorescence landscapes – one for each dilution – are measured per thick juice sample



Note that the peaks in the ultraviolet do not decrease with dilution, this is caused by concentration quenching, or inner-absorption effect, see [3]. At the excitation and emission sides 10 nm slits were used. The instrument was the Perkin Elmer LS50B spectrofluorometer. As indicated by Fig. 1, the combination of a narrow emission slit width and generally low turbidity allows neglecting the Rayleigh scattering. The 47 samples were measured in arbitrary order.

3 Analysis of N -way data arrays

Each intensity measurement in the collected data depends on four external parameters; the sample number (47 samples), the concentration (two levels of dilution), the detection wavelength (311 emission wavelengths) and the exci-

tation wavelength (20 excitation wavelengths). Hence, the intensities measured constitute a 4-way data array of order (47,2,311,20).

Various models exist for analyzing three-way data sets, see [4]. In the present work we focus on the N -way principal component analysis (N -way PCA) which is a generalization of the 3-way Tucker3 [5] model to N -way data arrays. Taking a starting point in the 3-way case, Fig. 2 provides a basis for presenting the N -way PCA. The 3-way PCA model of a 3-way data array \mathbf{X} of order r_1, r_2, r_3 is depicted in the figure. The array is decomposed into a significant systematic part and a non-significant residual depicted by \mathbf{E} . The systematic part is described by orthogonal factors which are stored columnwise in matrices

II. Algorithms, models and applications

140

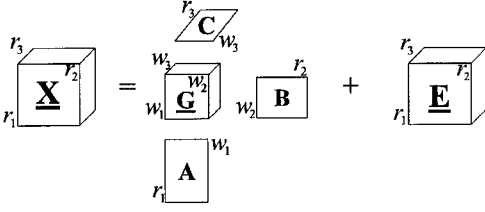


Fig. 2 The three-way principal component analysis (PCA) model

\mathbf{A} (r_1, w_1), \mathbf{B} (r_2, w_2) and \mathbf{C} (r_3, w_3). The number of factors in each of the three ways, i.e. w_1, w_2 and w_3 , must be determined by the analyst from *a priori* knowledge about \mathbf{X} or by evaluating models with different combinations of w_1, w_2 and w_3 , choosing the order that gives the most accurate model of \mathbf{X} . The array \mathbf{G} of order (w_1, w_2, w_3), referred to as the core array, allows the factors to interact in the model of \mathbf{X} . Interaction of factors is not encountered in conventional, i.e. bilinear, PCA but is only feasible for $N \geq 3$. After having estimated the orthogonal factors and the core array the squared entries in the core express how significant the factor combinations are for the model. The 4-way PCA can be conceived as an extension of the decomposition illustrated in Fig. 2 with a necessary introduction of an additional set of factors, \mathbf{D} , and by extending \mathbf{X} (r_1, r_2, r_3, r_4), \mathbf{G} (w_1, w_2, w_3, w_4) and \mathbf{E} (r_1, r_2, r_3, r_4) to be 4-way structures. The general N -way PCA may be formulated according to (1).

$$\text{vec } \mathbf{X} \approx (\mathbf{A}_1 \otimes \dots \otimes \mathbf{A}_N) \text{vec } \mathbf{C} \quad (1)$$

In (1) \mathbf{X} represents the N -way data array of order (n_1, \dots, n_N) and \mathbf{A}_i (n_i, w_i) is the orthogonal component matrix belonging to the i th way. The array \mathbf{C} of order (w_1, \dots, w_N) designates the core array. \otimes represents the Kronecker product. For details of the general N -way model the reader is referred to [6]. A tutorial on N -way PCA is given in [7]. A common algorithm calculating component matrices and core array from the data array in (1), is described in [8].

Factors from N -way PCA suffer from rotational ambiguity, i.e. the N -way PCA of \mathbf{X} has an infinity of factors and cores, where one solution can be rotated into another giving the exact same fit to \mathbf{X} . Returning to the exploratory power of the squared elements of the core, one can perform controlled transformations of a solution to give a core where only a few squared entries are significant, see [9]. Having only a limited number of significant core entries allows the analyst to focus on a few combinations of more significant and general factors. In contrast, having no significant combinations of factors, interpretation is rendered impossible due to the high number of non-significant factors that must be evaluated.

4 Principal component analysis of the 4-way data array

In order to find the optimal order of the 4-way PCA model, several combinations of different orders were in-

Table 1 Sum-of-squares explained by PCA models of different orders

Model order	Expl. SS [%]	Num. Par.
(1,1,1,1)	74.13	384
(2,1,2,2)	82.88	772
(2,2,2,2)	92.08	782
(3,2,3,3)	96.25	1201
(3,3,3,3)	96.24	1230
(4,2,4,4)	97.85	1656

vestigated. Table 1 shows the relative increase in explained sum-of-squares (SS) as the orders of the models increase. The total number of parameters is shown in the rightmost column of Table 1. The findings from this table suggest that a model of order (3,2,3,3) should be chosen since 96.25% of SS explained seems appropriate in comparison with the models of higher orders. Also, the number of parameters should be kept as low as possible in accordance with the principle of parsimony. Parsimonious models involve as few parameters as possible, hence the risk for fitting non-systematic trends (noise) in \mathbf{X} is minimized. Note, that the model does not improve in fit when using more than two factors in the second dimension, this is in concordance with the number of observations: One cannot derive three or more orthogonal solutions in a dimension that is only spanned by two variables.

In order to improve the interpretability of the (54 elements large) core array, the solution was transformed to yield maximum variance-of squares of the core as proposed in [9]. By transformation the variance-of-squares of the core array, which is an indicator of how few significant entries are present in the core, changed from 4.11×10^{20} to 5.46×10^{20} , i.e. an increase of 32%. The resulting profiles are plotted in Fig. 3A–D. Inspection of the variance-of-squares maximized core elements yields (with the involved factors of the four modes in parentheses) 2.36×10^{10} (1,1,1,1), 1.73×10^9 (1,1,2,2) 9.50×10^8 (1,2,1,3), 1.49×10^8 (1,2,2,3) and 1.03×10^8 (1,2,1,2). For convenience of the reader the squared elements of the core have been sorted, and the values of the 5 largest entries are depicted in Fig. 4. From this figure it is clear that the combination indicated by (1,1,1,1), being the first sample profile, first dilution factor and the first excitation and emission profiles, is most important in the model of \mathbf{X} . Therefore we shall initially concentrate on explaining these factors since they are most general. In Fig. 3A, profile 1 shows that the main variation between samples is caused by two levels of the fluorescence intensities. In Fig. 3A the samples are arranged factory-wise in ascending week number such that samples 1–10 are from factory a, 11–18 from b, 19–28 from d, 29–36 from e and 37–47 from f. Hence, we may conclude that the samples from the last factory (number 37–47) generally have lower levels of intensity. Similarly, the major trend in the data is that the fluorescence intensities descend when the samples are diluted. This is deduced from Fig.3B since the factor de-

Fig. 3A–D The rotated factors from PCA on the 4-way data set. The sample profiles are shown in **A**. Emission and excitation profiles are shown in **C** and **D**, respectively. The factors explaining the variation caused by dilution are illustrated in **B**. 1–3 see text

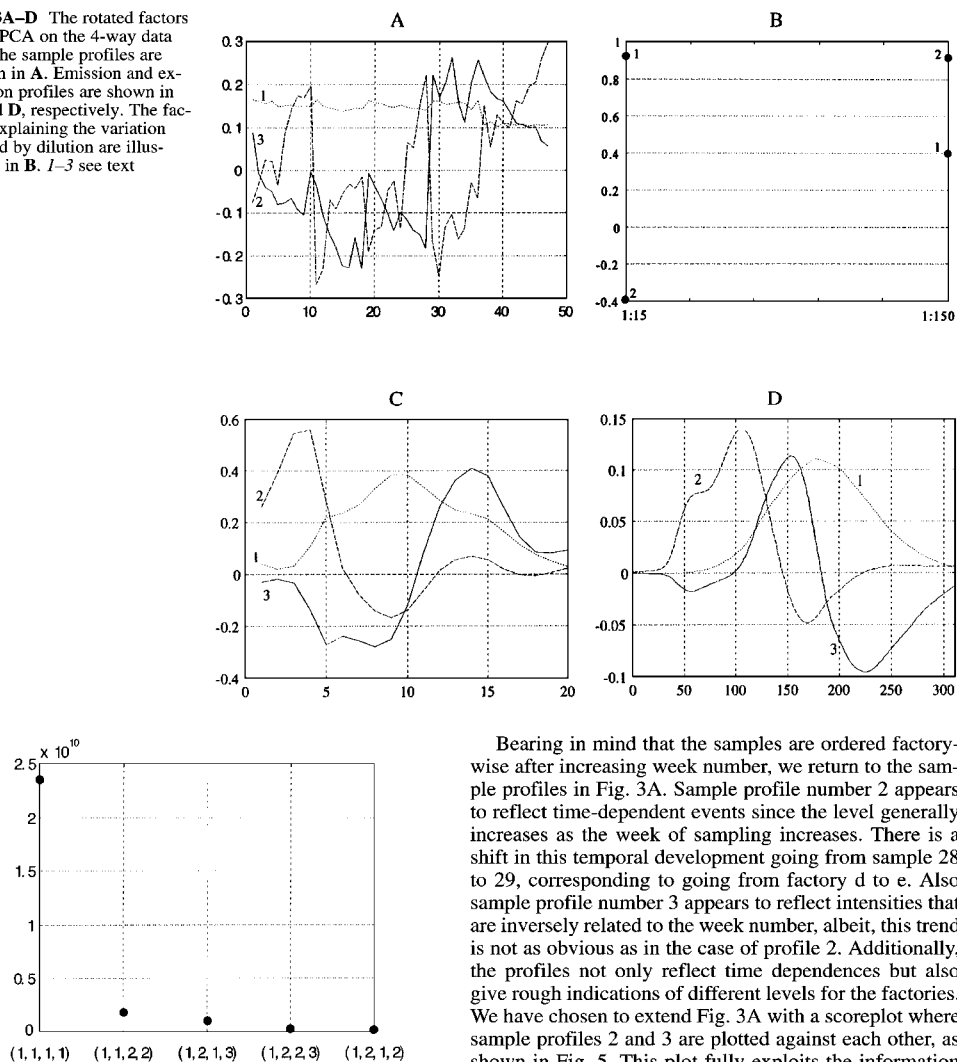
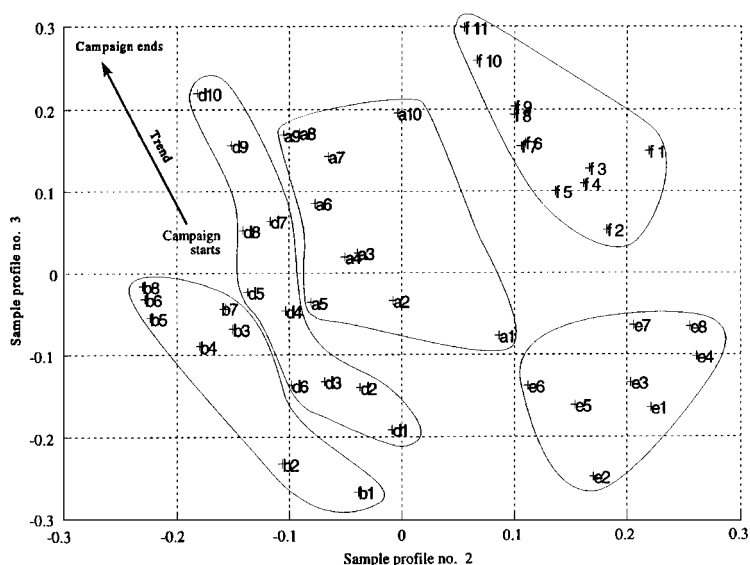


Fig. 4 The 5 largest squared elements of the core array. The remaining 49 elements are in the same range, or lower, than the lowest two elements shown here. Hence, the three most significant factor combinations are (1,1,1,1), (1,1,2,2) and (1,2,1,3)

increases from 0.93 to 0.40 upon dilution. The reason that this is not true for all samples, as indicated by factor two, may be due to concentration quenching, i.e. that the intensity does not decrease with dilution from 1:15 to 1:150. The spectral excitation and emission profiles marked 1 in Fig. 3C–D give indications to the profiles of the fluorophores being common to the samples.

Bearing in mind that the samples are ordered factory-wise after increasing week number, we return to the sample profiles in Fig. 3A. Sample profile number 2 appears to reflect time-dependent events since the level generally increases as the week of sampling increases. There is a shift in this temporal development going from sample 28 to 29, corresponding to going from factory d to e. Also sample profile number 3 appears to reflect intensities that are inversely related to the week number, albeit, this trend is not as obvious as in the case of profile 2. Additionally, the profiles not only reflect time dependences but also give rough indications of different levels for the factories. We have chosen to extend Fig. 3A with a scoreplot where sample profiles 2 and 3 are plotted against each other, as shown in Fig. 5. This plot fully exploits the information in the two profiles as discussed above by combining the trends from two independent factors in one plot. The relationship among the samples becomes clear since samples from the same factories are grouped almost without overlaps. Furthermore, these two factors reveal a development in time, that is, there is a trend in the plot that the samples are dispersed within the clusters according to the time of sampling (as indicated by the inserted arrow). Hence, sample profiles 2 and 3 contain fluorometric information that describes the temporal behaviour of the thick juices as the campaign runs. Also, plots of sample profiles 1 vs. 2 and 3 have been investigated, but as indi-

Fig. 5 A scoreplot combining the information in sample profiles no. 2 and 3. The letters a, b, d, e and f each relate to a factory and the numbers designate the week of sampling. This plot reveals two important trends in the fluorescence data: Grouping according to factory and a development in time



cated by sample profile 1 in Fig. 3A, this factor contains only very general information that cannot reveal detailed differences between neither time nor factory among the samples.

5 Results

Explorative soft modelling, *in casu* 4-way PCA, has substantiated the use of spectrofluorometry as a screening method. By showing that the collected 4-way data array cannot only classify samples according to factories, but also give an indication of temporal conditions, fluorometry gives promise as a very relevant source of information that is related to variations in the raw beets and the state of the factory as well. Without explicit modelling of the many uncontrollable parameters (some being difficult to assess or quantify, e.g. growing conditions and weather conditions) causing the differences between samples, the results from the 4-way PCA has proven that spectrofluorometric measurements give promise as an important screening method for process control. By temporal characterizing of the thick juice, the process control will be able to adjust conditions accordingly. On the basis of the presented results a project has been initiated aiming at developing a spectrofluorometer for in-line screening. This

will improve our understanding of the relation between measured fluorescence signals and the extent of colouration. The data analytical part of the project will include extensive use of chemometric multi-way models, as the one presented.

Acknowledgments We wish to thank Danisco Sugar for providing the thick juice samples. C.A. and L.M. are grateful to the Affluence AIR2-CT94-1416 project fund and the Føtek-2 grant "On-line". The present work is a result of cooperation between the universities HUB, Berlin and KVL, Copenhagen.

References

1. Andersson CA (1995) Flow injection analysis, fluorometry and chemometrics. Master thesis. Royal Veterinary and Agricultural University, Food Technology, Copenhagen
2. Nørgaard L (1995) *Zuckerindustrie* 120:970-981
3. Schulman SG (1977) *Fluorescence and Phosphorescence Spectroscopy: Physicochemical Principles and Practice*. Pergamon Press, Oxford
4. Kroonenberg PM (1992) *Stat App* 4:619-633
5. Tucker L (1966) *Psychometrika* 31:279-311
6. Magnus JR, Neudecker N (1988) *Matrix differential calculus with applications in statistics and econometrics*. Wiley, Chichester
7. Henrion R (1994) *Chemom Intell Lab Syst* 25:1-23
8. Kroonenberg PM, De Leeuw J (1980) *Psychometrika* 45: 69-97
9. Henrion R, Andersson CA (1997) *J Chemometrics* (submitted)

P10
**PARAFAC2 - Part II. Modeling
chromatographic data with
retention time shifts**

Rasmus Bro, Claus A. Andersson and Henk A. L. Kiers

II. Algorithms, models and applications

JOURNAL OF CHEMOMETRICS
J. Chemometrics 13, 295–309 (1999)

PARAFAC2—PART II. MODELING CHROMATOGRAPHIC DATA WITH RETENTION TIME SHIFTS

RASMUS BRO,^{1*} CLAUS A. ANDERSSON¹ AND HENK A. L. KIERS²

¹*Chemometrics Group, Food Technology, Department of Dairy and Food Science, The Royal Veterinary and Agricultural University, Denmark*

²*Heymans Institute (PA), University of Groningen, Groningen, The Netherlands*

SUMMARY

This paper offers an approach for handling retention time shifts in resolving chromatographic data using the PARAFAC2 model. In Part I of this series an algorithm for PARAFAC2 was developed and extended to N -way arrays. It was discussed that the PARAFAC2 model has a number of attractive features. It is unique under mild conditions though it puts fewer restrictions on the data than the well-known PARAFAC1 model. This has important implications for the modeling of chromatographic data in which retention time shifts can be regarded as a violation of the assumption of parallel proportional profiles underlying the PARAFAC1 model. The PARAFAC2 model does not assume parallel proportional elution profiles, but only that the matrix of elution profiles preserve its 'inner-product structure' from sample to sample. This means that the cross-products of the matrix holding the elution profiles in its columns remain constant. Here an application using chromatographic separation based on the molecular size of thick juice samples from the beet sugar industry illustrates the benefit of using the PARAFAC2 model. Copyright © 1999 John Wiley & Sons, Ltd.

KEY WORDS: multiway; curve resolution; fluorescence spectroscopy; shifted profiles

INTRODUCTION

In order to understand the chemistry of the color formation during sugar processing from beets, an experiment was conducted to explore the presence and amount of chemical analytes in thick juice, which is an intermediate product in the sugar production. The molecular entities of thick juice samples were separated by size and affinity on a chromatographic system and detected by fluorescence in the hope that the individual fluorophores could be separated and detected. However, it turned out to be impossible to separate the analytes completely; that is, the elution peaks/profiles were partly overlapping. The analysis was further complicated by the fact that there were huge shifts in retention time of specific analytes from sample to sample.

Overlapping chromatographic peaks can sometimes be separated mathematically. If a univariate detection system is used in a chromatographic system, an experiment results in a time profile which is conveniently held in a vector. If several such experiments are performed on different samples, a matrix X results, of which each row holds the profile of each individual sample. If there are no

* Correspondence to: R. Bro, Chemometrics Group, Food Technology, Department of Dairy and Food Science, The Royal Veterinary and Agricultural University, Denmark. E-mail: rb@kul.dk
Contract/grant sponsor: Nordic Industry Foundation; Contract/grant number: P93149
Contract/grant sponsor: FØTEK

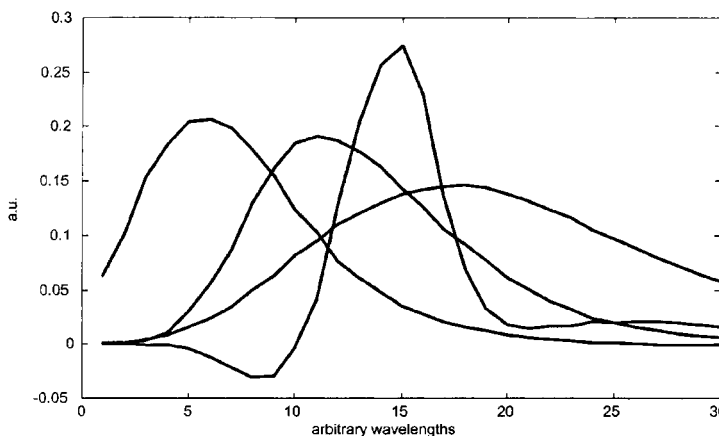


Figure 1. Spectra used in simulated data

retention time shifts in the data, every analyte will give rise to the same elution profile in every sample, except for a change in magnitude (area) depending on the concentration of the analyte. Assuming there are R analytes, the data held in the $I \times J$ matrix \mathbf{X} can be modeled by R bilinear components as

$$\mathbf{X} = \sum_{r=1}^R \mathbf{b}_r \mathbf{a}_r^T + \mathbf{E} \quad (1)$$

where \mathbf{b}_r is an I -vector holding the concentration of the r th analyte in the I samples, \mathbf{a}_r is the time profile of the r th analyte, and the matrix \mathbf{E} holds the residual variation. For each sample the time profile is described as a sum of the individual profiles weighted by the corresponding concentrations of the analyte, $b_i \mathbf{a}_r$. This model implies that the time profiles do not change from sample to sample. If the analytes are completely separated, the individual profiles can immediately be extracted, in which case no additional mathematical modeling is required. If the time profiles overlap, this corresponds mathematically to the vectors \mathbf{a}_r , $r = 1, \dots, R$, being non-orthogonal. Resolving or rather estimating the profiles of the pure analytes in such a case has received a lot of attention in chemometrics, starting with the work of Lawton and Sylvestre.¹ Owing to the fundamental rotational indeterminacy in bilinear modeling, it is not possible to estimate the pure profiles from the data without employing some sort of external knowledge in the decomposition in order to obtain a unique model. The word 'external' is to be taken lightly here, since the necessary knowledge may sometimes be obtained directly from the data. The main way of obtaining uniqueness is to identify selective variables (or samples), i.e. elution times where only one analyte is present (or absent). As described theoretically in Reference 2, this may lead to a unique or partially unique decomposition. The presence of selective variables forms the basis for most traditional resolution techniques in chemistry. Another approach is based on the use of constraints. One may estimate the parameters in the bilinear model under constraints such as non-negativity of concentration estimates or unimodality of elution profiles.³ While constraints are useful for improving the estimates of model parameters, they do not lead to uniqueness in general. Rather, they help reduce the feasible set of solutions.

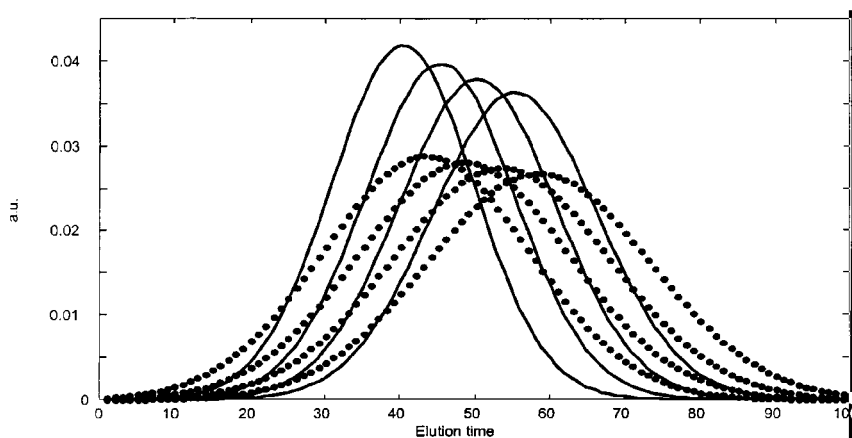


Figure 2. Elution profiles F_k from first experiment (full lines) and last experiment (dotted lines). The first and last experiments have the most dissimilar elution profiles, and the profiles change gradually throughout the experiments. Note that as the profiles shift, their width expands as well

When spectral detection rather than univariate detection is used, a three-way array is obtained, the third mode consisting of measurements at different wavelengths. It is well known that for *three-way* chromatographic data with no retention time shifts it is possible to resolve uniquely the underlying components without any additional constraints by the use of the PARAFAC1 model.⁴ Thus the addition of a third spectral mode is highly convenient, since otherwise resolving the individual components may not be possible.

The primary concern in this paper is the problem of modeling three- and higher-way chromatographic data *with retention time shifts*. In the following we will first describe the chromatographic data and a set of simulated data used for introducing the PARAFAC2 model with respect to modeling retention time shifts. A short description of the possible models for resolving chromatographic multiway data is given. Finally the results of modeling the simulated as well as the real data are provided.

DATA

Simulated data

A three-way data set was generated for simulating spectrally detected chromatographic data with retention time shifts. Four analytes with overlapping chromatographic peaks were used. The data were generated according to the model

$$\mathbf{X}_k = \mathbf{F}_k \mathbf{D}_k \mathbf{A}^T + \mathbf{E}_k \quad (2)$$

where \mathbf{X}_k is the measured data from sample (i.e. experiment) k , \mathbf{F}_k is a 100×4 matrix holding the elution profiles of the four (fictitious) analytes present in sample k , \mathbf{D}_k is a 4×4 diagonal matrix holding the concentrations of the four analytes in sample k in its diagonal, and the matrix \mathbf{A} is a 30×4 matrix holding the spectra of the four analytes, chosen as in Figure 1. The matrix \mathbf{E}_k holds the added noise. Thus only the spectra in \mathbf{A} are constant over the samples. The data set consists of data from ten

samples. In different samples the concentrations of the analytes were chosen randomly (evenly distributed between zero and one) and the elution profiles were shifted differently as described below. Thus the data array is of size 100 (time) \times 30 (spectrum) \times 10 (sample).

Normally distributed heteroscedastic noise was added proportional to the size of the signal such that the variance of the noise was 5% of the variance of the systematic variation. Note that this is a relatively large amount of noise.

The following choice of structure in \mathbf{F}_k (containing the elution profiles) was used. In any specific experiment all elution profiles had identical shifts. The amount of shift was gradually increased from zero in experiment 1 (Figure 2, full lines) to four time units in experiment 10 (Figure 2, dotted lines). With increasing shifts the width of the peak area was also increased accordingly, being proportional to the square root of the elution time.

If the data fit the premises of the PARAFAC2 model, the PARAFAC2 model gives unique parameters (up to trivial scaling and permutations). Since the 'true' parameters (pure spectra, concentrations and elution profiles) will provide a model that also gives the best fit, the PARAFAC2 parameters will thus be estimates of the true parameters. This is quite dissimilar from bilinear modeling where the rotational invariance of the solution makes it impossible to estimate the parameters unless auxiliary information is available. However, in this case it is known *a priori* that the data do not fit the PARAFAC2 model perfectly. For this to hold, the cross-product of the matrix holding the elution profiles, \mathbf{F}_k , should be constant over k as elaborated on in Part I.⁵ Thus $\mathbf{F}_k^T \mathbf{F}_k = \mathbf{G}$ for any k . That this is not the case in the above example is easily shown from

$$\mathbf{F}_1^T \mathbf{F}_1 = \begin{bmatrix} 1.00 & 0.82 & 0.93 & 0.96 \\ 0.82 & 1.10 & 0.60 & 1.01 \\ 0.93 & 0.60 & 0.96 & 0.80 \\ 0.96 & 1.01 & 0.80 & 1.05 \end{bmatrix}$$

and

$$\mathbf{F}_{10}^T \mathbf{F}_{10} = \begin{bmatrix} 1.00 & 0.90 & 0.96 & 0.98 \\ 0.90 & 1.05 & 0.77 & 1.00 \\ 0.96 & 0.77 & 0.98 & 0.89 \\ 0.98 & 1.00 & 0.89 & 1.02 \end{bmatrix}$$

The cross-products shown above have been normalized by scaling the first element to the value one for easier comparison. It is readily seen that these matrices are not identical and hence the requirements for the PARAFAC2 model to hold are not valid here. Thus the PARAFAC2 model will not fit the data perfectly, though still give unique estimates of parameters. The crucial aspect is to investigate if PARAFAC2 is still a reasonable model to use and if it can provide sensible estimates of the underlying parameters (spectra, profiles and concentrations). It is less constrained than a corresponding PARAFAC1 model, hence it is the main hypothesis in this paper that it can be expected to perform better than PARAFAC1. We aim to show that for reasonable deviations from perfect data, PARAFAC2 will still provide good estimates of the underlying parameters.

Chromatographic data

Fifteen samples of thick juice from different sugar factories were introduced into a Sephadex G25 low-pressure chromatographic system using a 0.02 M $\text{NH}_4\text{Cl}/\text{NH}_3$ buffer (pH 9.00) as carrier. In this

way the high-molecular reaction products between reducing sugars and amino acids/phenols are separated from the low-molecular free amino acids and phenols. The high-molecular substances elute first, followed by the low-molecular species. Aromatic components are retained the longest time owing to a high affinity to the Sephadex material. The sample size was 300 μl and a flow of 0.4 ml min^{-1} was used. Twenty-eight discrete fractions of 1.2 ml were sampled and measured spectrofluorometrically on a Perkin Elmer LS50B spectrofluorometer.

The column was a 20 cm long glass cylinder with an inner radius of 10 mm packed with Sephadex G25 fine gel. The water used was doubly ion exchanged and millipore filtrated upon degassing. The excitation–emission matrices were collected using a standard 10 mm \times 10 mm quartz cuvette, scanning at 1500 nm min^{-1} with 10 nm slit widths in both excitation and emission monochromators (250–440 nm excitation, 10 nm intervals; 250–560 nm emission, 4 nm intervals). For each sample, 28 excitation–emission matrices are measured, one for each fraction collected. Thus the size of the four-way data set is 28 (fraction) \times 20 (excitation) \times 78 (emission) \times 15 (sample).

METHODS

A structural model of chromatographic data will first be developed for the ideal situation in which there are no retention time shifts. Subsequently it will be shown how to accommodate this model for handling retention time shifts. First only three-way data will be considered and afterwards it will be shown how to extend the results to four-way data as well as the mathematical consequences of such an extension. Then the results of applying the PARAFAC2 and competing models to the simulated three-way and real four-way chromatographic data are shown.

Consider data such as the above-mentioned where fluorescence spectroscopy is used for detection. When the emission wavelength is fixed, then at each elution time an excitation spectrum is measured. This corresponds conceptually to the normal situation in UV-vis detection chromatography. Let x_{ijk} be the emission intensity of the i th fraction (elution time) of the k th sample measured at the j th excitation wavelength. For a dilute solution in which no quenching occurs it holds that this intensity is the sum of intensity contributions from the individual fluorophoric entities in the sample plus some additional noise. Assume there are R independent fluorophores. For each fluorophore r the emission intensity is linearly dependent on the concentration c_{kr} in the k th sample. It is also linearly dependent on the ‘quantum yield’ at excitation wavelength j , a_{jr} . Finally it is linearly dependent on the relative amount of sample present in the i th fraction, f_{ir} . Thus the model of the data can be stated as

$$x_{ijk} = \sum_{r=1}^R f_{ir} a_{jr} c_{kr} + e_{ijk} \quad (3)$$

This model may also be stated in terms of matrices. Let \mathbf{X} be the $I \times JK$ matrix holding the $I \times J \times K$ three-way array with typical elements x_{ijk} . The first J columns of \mathbf{X} correspond to the $I \times J$ slab obtained from the three-way array by setting k equal to one. The $I \times R$ loading matrix \mathbf{F} holds the parameters f_{ir} , and \mathbf{A} ($J \times R$) and \mathbf{C} ($K \times R$) are defined likewise. The columns of \mathbf{F} will be the estimated elution profiles, the columns of \mathbf{A} the estimated spectra, and the elements in \mathbf{C} the estimated concentrations. Then it holds that the PARAFAC1 model can be stated as

$$\mathbf{X}_k = \mathbf{F} \mathbf{D}_k \mathbf{A}^T + \mathbf{E}_k \quad (4)$$

where \mathbf{X}_k is the k th frontal slab of the three-way array and \mathbf{D}_k is a diagonal matrix holding the k th row of \mathbf{C} in its diagonal.

From the theory of the PARAFAC1 model^{4,6} it immediately follows that given the appropriateness

of the model it is possible to resolve the data into meaningful components pertaining to individual analytes. This is so because the PARAFAC1 model is uniquely identified up to scaling and permutation of the components under mild conditions.⁷⁻¹⁰ The model of the chromatographic data derived above assumes that the elution profiles of individual components, i.e. the columns \mathbf{f}_r of \mathbf{F} , are identical in each sample. However, this is not the case in the presence of retention time shifts. In such situations, using the PARAFAC1 model will be problematic. We then have to replace the first mode loadings \mathbf{F} with a set of loadings \mathbf{F}_k specific to sample k . The elution profiles \mathbf{F}_k for a specific experiment k are then unrelated to the profiles from another experiment, so as to allow for retention time shifts in the model. A model of shifted data may therefore generically be stated as

$$\mathbf{X}_k = \mathbf{F}_k \mathbf{D}_k \mathbf{A}^T + \mathbf{E}_k \quad (5)$$

The parameters and residuals in this model are different in general from the ones given in equation (4), but the matrices are given the same names in order to stress that ideally these should be identical. This model is problematic for several reasons. First of all it possesses no uniqueness properties in the sought sense since it can be shown to be equivalent to a bilinear model of the data unfolded to a two-way matrix. Also important, though, is that it assumes no relation at all between equivalent elution profiles in different samples. If the elution profiles *are* somehow related, not using this will lead to an unnecessarily high uncertainty in the estimated components.

Between the two extremes of having all \mathbf{F}_k equal to \mathbf{F} and having \mathbf{F}_k unconstrained there are several possibilities for imposing structure in \mathbf{F}_k . It is the choice of the structure of \mathbf{F}_k that determines the structure of the model. The PARAFAC2 model offers one such intermediate model. In the PARAFAC2 model each loading matrix \mathbf{F}_k is modeled as

$$\mathbf{F}_k = \mathbf{P}_k \mathbf{F}, \quad k = 1, \dots, K \quad (6)$$

where \mathbf{P}_k is an $I \times R$ column-wise orthonormal matrix and \mathbf{F} is of size $R \times R$. The matrix \mathbf{F} represents the common part of the elution profile matrices from different experiments in an R -dimensional subspace, while the matrix \mathbf{P}_k determines the specific manifestation of these profiles in the I -dimensional space of the k th experiment.[†] One may of course also envision other ways of imposing structure in \mathbf{F}_k , but it seems that this type of structure is adequate for approximating many occurring deviations from the strict linearity required in the standard PARAFAC1 model. A very important feature of the PARAFAC2 model is that it retains the advantage of intrinsic structural uniqueness as discussed at length in References 5, 11 and 12.

The structure imposed in \mathbf{F}_k can also be formulated differently by observing that equation (6) is equivalent⁵ to requiring

$$\mathbf{F}_k^T \mathbf{F}_k = \mathbf{F}^T \mathbf{F}, \quad k = 1, \dots, K \quad (7)$$

This means that for every sample k a set of elution profiles \mathbf{F}_k is estimated under the constraint that the cross-products of the profile matrix are identical. It is simple to show that if for example the profiles of all analytes are shifted the same amount, if there is no peak broadening and the elution baseline is represented both before and after all analytes appear, then this assumption will be valid. If these assumptions are not met, the PARAFAC2 model is still less restrictive than the PARAFAC1 model while being unique. Thus even data that do not conform exactly to the restrictions may be better

[†]Note that the matrix \mathbf{F} appearing in the PARAFAC2 model is not of the same size as the one appearing in the PARAFAC1 model.

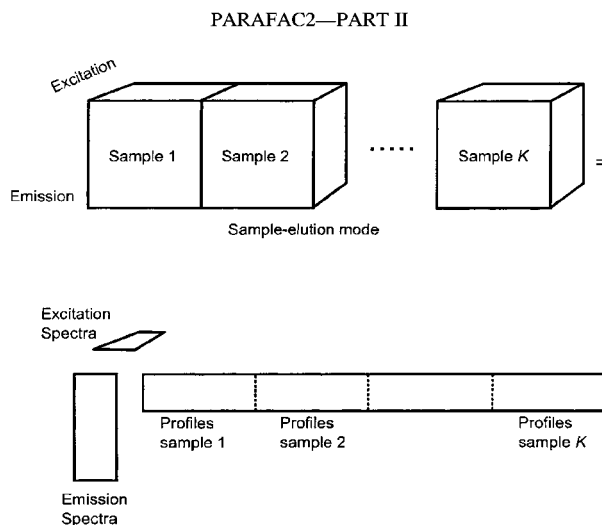


Figure 3. Four-way chromatographic data represented as a three-way array where sample and elution profile modes are combined into one. Below the corresponding three-way PARAFAC1 model is depicted, showing that for this unfolding the PARAFAC1 model estimates the elution profiles from each sample independently

modeled by PARAFAC2 than by PARAFAC1, since the model misspecification will be less pronounced for PARAFAC2.

Having discussed the three-way version of the PARAFAC2 model, it is appropriate to discuss aspects of modeling four-way data. As discussed in References 3 and 5, the PARAFAC2 model is easily extended to higher orders. An interesting aspect of the four-way model is that even if no constraints are imposed on F_k , the model will still be unique, since the four-way model with unconstrained F_k is equivalent to a three-way PARAFAC1 model of the four-way data unfolded to a three-way array.[‡] Since the chromatographic data are four-way, it is therefore possible to validate the four-way PARAFAC1 and PARAFAC2 models against the results of the three-way PARAFAC1 model fitted to the unfolded four-way data. Regardless of the presence of retention time shifts the three-way PARAFAC1 model will give reasonable estimates of the model parameters if the elution and sample modes are combined in the unfolding (Figure 3).

Determining the model complexity

For PARAFAC1 as well as PARAFAC2 it is essential to use the correct number of components. In two-way analysis this is also important, but for multiway models the importance is even more pronounced. In most two-way analyses one is mainly interested in determining a suitable subspace, while in PARAFAC models the specific orientation within the subspace is also important. Moreover, PARAFAC models are not nested, so choosing e.g. a four-component model instead of a three-component model has implications not only for the additional component but also for the orientation of *all* four components.

[‡]Still, if the added structural constraint of the PARAFAC2 model is valid, it is preferable to use it, since added constraints (on F_k) will in general provide more robust and precise parameter estimates.³

In order to determine the proper number of components for PARAFAC1 as well as PARAFAC2 models, several possibilities exist. As for ordinary two-way principal component analysis, methods based on judging residuals and on resampling are possible. For multiway models, however, some additional tools are available that are very helpful in determining the proper number of components. The split-half analysis³ is founded on exploiting the uniqueness properties of the PARAFAC1 and PARAFAC2 models. If the right number of components is chosen, the 'true' underlying latent variables will be found. This will hold regardless of which samples are used for estimating these. If the proper number of components is not used, the estimated parameters will be linear combinations of the true parameters and therefore depend on which samples are used.

Another powerful tool for assessing the model complexity of PARAFAC1 models is the core consistency diagnostic suggested in Reference 3 and elaborated on in detail in Reference 13. It is based on the fact that the PARAFAC1 model can be posed as a restricted Tucker3 model where the core array is fixed to be a superidentity array.¹⁴ The core consistency diagnostic amounts to first calculating the optimal unconstrained core array for a Tucker3 model where the loading matrices are the ones obtained by the PARAFAC1 model at hand. Then the core consistency diagnostic given as a percentage is defined as

$$\text{core consistency} = 100 \left(1 - \frac{\sum_{d=1}^F \sum_{e=1}^F \sum_{f=1}^F (g_{def} - t_{def})^2}{\sum_{d=1}^F \sum_{e=1}^F \sum_{f=1}^F t_{def}^2} \right) \quad (8)$$

where g_{def} and t_{def} denote the elements of the calculated core and of the intrinsic superdiagonal core respectively. If \mathbf{G} is equal to \mathbf{T} , the core consistency is perfect and has a value of unity (100%), which indicates that the PARAFAC1 model at hand is indeed appropriate. At the other extreme the consistency may be below zero if the PARAFAC1 model is inappropriate or the variation is purely random, hence mostly off-superdiagonal.

As demonstrated in Reference 13, if the number of components in the hypothesized model exceeds the proper number of components, the Tucker3 core array will deviate considerably from superdiagonality. This will not be the case if the proper number of components is used. Thus the highest number of components that maintains a sufficiently superdiagonal Tucker3 core array will be the adequate number of components to use.

RESULTS

Simulated data

The results of fitting PARAFAC1 and PARAFAC2 models to the simulated data using the correct number of components (i.e. four) are shown in Figure 4. The PARAFAC2 estimates are closer to the true values than the PARAFAC1 estimates. Furthermore, it can be seen that the PARAFAC2 estimated elution profiles are less smooth than the corresponding PARAFAC1 estimates. This is an indirect illustration of the important property of PARAFAC2 that it puts fewer restrictions on the elution profiles. This is needed because such restrictions are infeasible when there are shifts. In this case, where a substantial amount of noise was added to the data, the estimated elution profiles become rather unsmooth, but they do follow the original profiles closely.

In order to verify that the PARAFAC2 model is superior to the PARAFAC1 model for the given data, 100 simulations were performed according to the above data but with different random concentration matrices. For every simulated data set the two models were fitted and the correlations

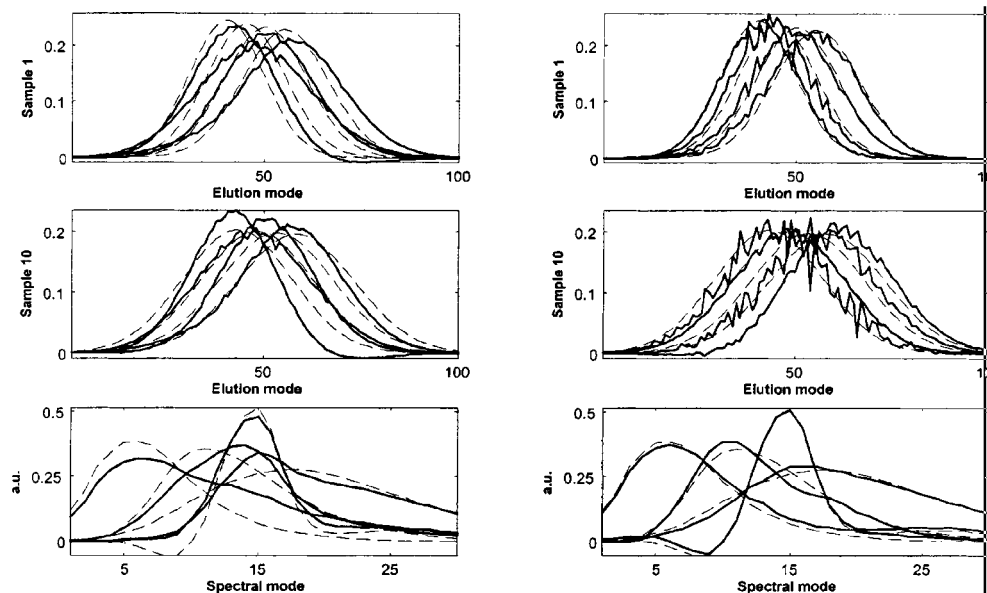


Figure 4. Estimated profiles and spectra from simulated data. The top plots show the true profiles (broken lines) together with estimates (full lines). PARAFAC1 estimates are to the left and PARAFAC2 estimates to the right. The middle plots show the same for experiment 10 and the bottom plots shows the reference spectra (broken lines) compared with the estimates

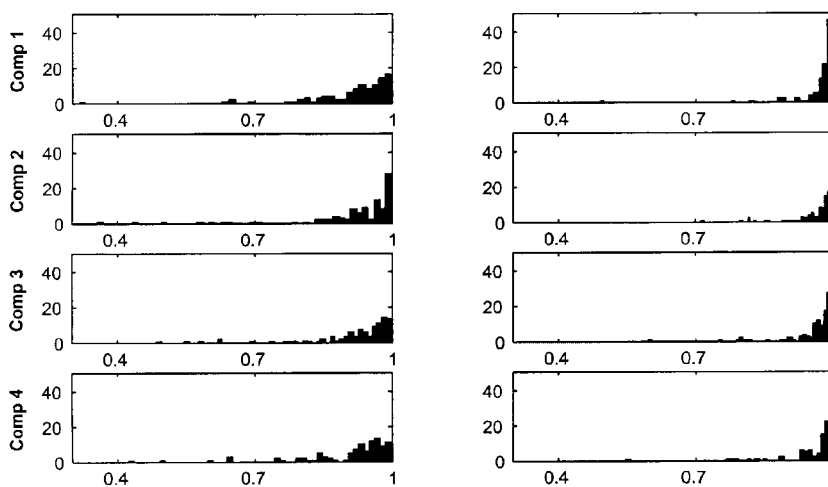


Figure 5. Histograms showing correlation between estimated and true concentrations for each component for PARAFAC1 (left) and PARAFAC2 (right). The histograms are based on 100 different models with different random concentration matrices

Table 1. Explained variation and core consistency for different three-way PARAFAC1 models, of chromatographic data

Number of components	Explained variation (%)	Core consistency (%)
3	96.4	91.9
4	98.9	96.3
5	99.3	20.6
6	99.4	15.1

between estimated and true concentrations calculated. In Figure 5 these correlations are shown. Each plot is a histogram containing the absolute correlation between the estimated and true concentrations of one specific analyte for one specific model over all 100 data sets. It is evident that the PARAFAC2 model is generally superior to the PARAFAC1 model. The correlations between true and estimated concentrations for the PARAFAC2 model are much more skewed towards one than for the PARAFAC1 model.

Chromatography

The first step in modeling the chromatographic data is to determine how many components to use in the model. In order to establish the correct number of components, a three-way PARAFAC1 model was investigated in which the sample and elution modes were concatenated into one mode (see Figure 3). In this way, retention time shifts will not affect the model, since the profiles of each sample will be modeled independently. For three-, four-, five- and six-component models the core consistency (equation (8)) as well as the percentage of variation explained was calculated. The percentage of explained variation was defined as

$$\text{variation explained} = 100 \left(1 - \frac{\sum_{i=1}^I \sum_{j=1}^J \sum_{k=1}^K \sum_{l=1}^L (x_{ijkl} - m_{ijkl})^2}{\sum_{i=1}^I \sum_{j=1}^J \sum_{k=1}^K \sum_{l=1}^L x_{ijkl}^2} \right) \quad (9)$$

where x_{ijkl} is an element of the four-way array and m_{ijkl} is the corresponding element of the model of the array.

For the posed models the results are given in Table 1. Note that based on the percentage of variation explained, it is difficult to assess which of the four candidate models is the most preferable since they all explain approximately the same amount of variation. Using the core consistency, however, the picture is much clearer. Three- and four-component models are seen to be suitable since they both have very high consistencies. A five- or six-component model is definitely not appropriate, since the loading matrices that should reflect the subspace of the systematic variation are mainly descriptive of variation on the off-superdiagonal part of the array (indicated by the low core consistency). Since four is the highest number of components for which the model assumptions hold, it may be concluded that four components provide an adequate model complexity of the given data under the premises of the PARAFAC1 model.

Having established the number of components to use, the two competing four-way models of the data were fitted: a four-way four-component PARAFAC1 model and a four-way four-component PARAFAC2 model. For both models, non-negativity was imposed on all parameters except the

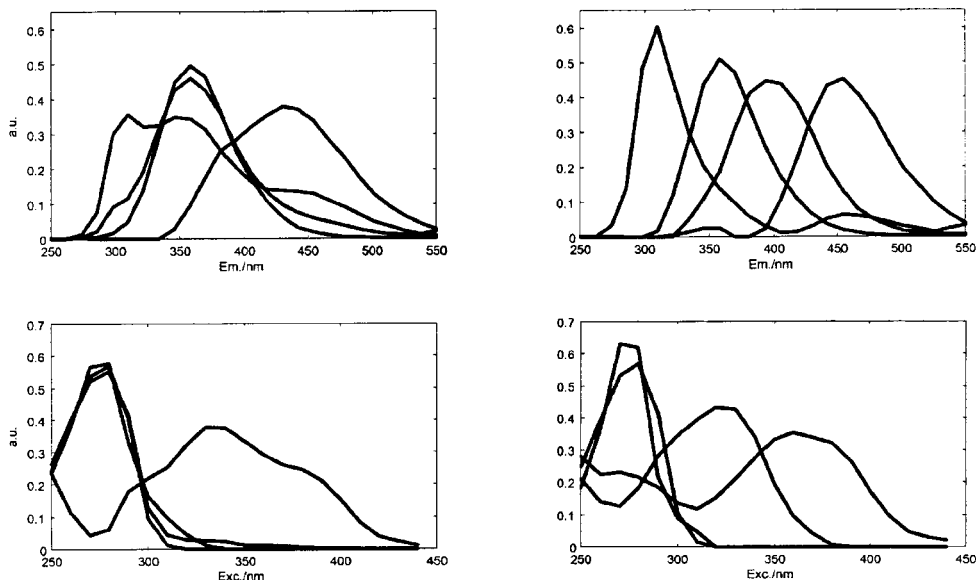


Figure 6. Estimated emission (top) and excitation (bottom) spectra from four-way PARAFAC1 (left) and four-way PARAFAC2 (right)

elution profiles in PARAFAC2, since imposing non-negativity on these is difficult.⁵ In Figure 6 (left) the excitation and emission mode loadings of a four-component PARAFAC1 model are shown. The parameters are not very appealing. The likeness of several components suggests that the model may not be valid. However, the solution is stable in the sense that it was obtained several times from different starting values. In Figure 6 (right) the excitation and emission mode loadings of a non-negativity-constrained PARAFAC2 model are also shown. These parameters look reasonable and are very different from the PARAFAC1 loadings, especially in the emission mode. The PARAFAC2 model seems to be better. Based on these results alone, it is difficult, though, to conclusively claim that the PARAFAC2 model is valid and better than the PARAFAC1 model.

A very simple way of validating which model is better admits itself as mentioned before. The sample and elution modes may be combined into one mode and the subsequent three-way array uniquely modeled by a three-way PARAFAC1 model. Since each elution mode will then be modeled separately for each sample, possible retention time shifts will not affect the appropriateness of the model.

For the model of the three-way data the excitation and emission mode loadings are shown in Figure 7. Note the close similarity between the three-way PARAFAC1 and four-way PARAFAC2 solution. All three models (three-way PARAFAC1, four-way PARAFAC1 and four-way PARAFAC2) should theoretically be identical if no retention time shifts are present. Since the four-way PARAFAC1 model gives substantially different parameter estimates, it may safely be concluded that this model does not fit the characteristics of the data. The most likely reason for this is retention time shifts.

From the three-way model of the data a set of loadings is also obtained in the combined elution/sample mode. Reshaping the loading for one specific component to a matrix, a set of elution profiles for this 'analyte' is obtained, one for each sample. In Figure 8 this is shown for component 1. These

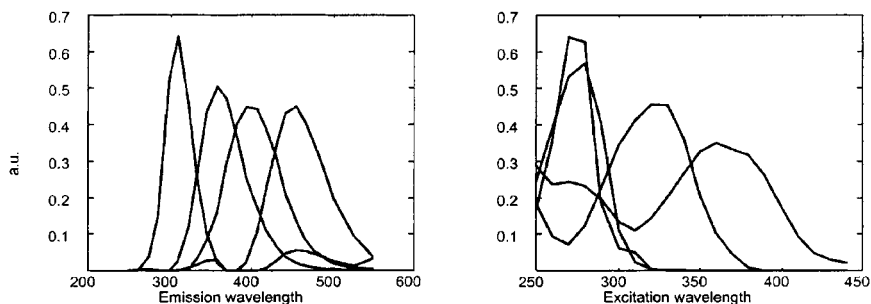


Figure 7. Emission (left) and excitation (right) mode loadings estimated from three-way non-negativity-constrained PARAFAC1 model

estimated profiles are not subjected to model error due to retention time shifts, since they stem from the three-way model.

It is readily seen that even though the elution profiles should be identical in each run, this is certainly not the case. There are huge shifts in the retention times from sample to sample, probably caused by the very different contents of the samples. This explains why four-way PARAFAC1 cannot fit these data well. The gel in the column is known to be sensitive toward the concentration of phenolic compounds and certain amino acids. The inter-sample variation in the elution profiles is probably due to different contents of such compounds with high affinity for the chosen gel causing the shifts in retention times.

It is interesting to compare the elution profiles estimated by three-way PARAFAC1 with the

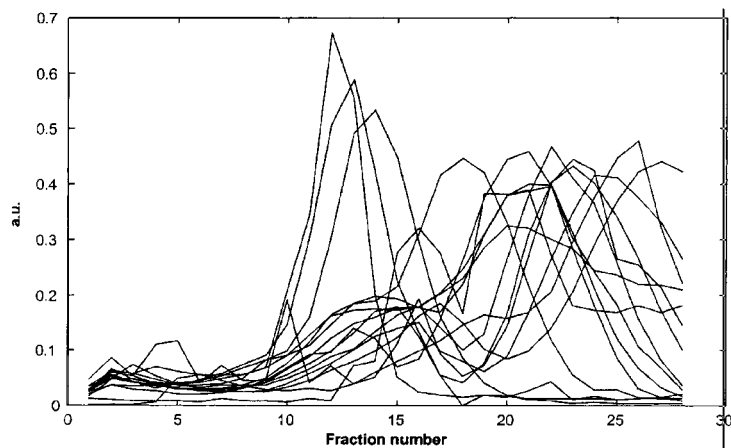


Figure 8. Estimated elution profiles of component 1 (not scaled) estimated from a three-way PARAFAC1 model. Each line is the estimated profile of the component in one specific sample. If no retention time shifts were present, all profiles should be identical!

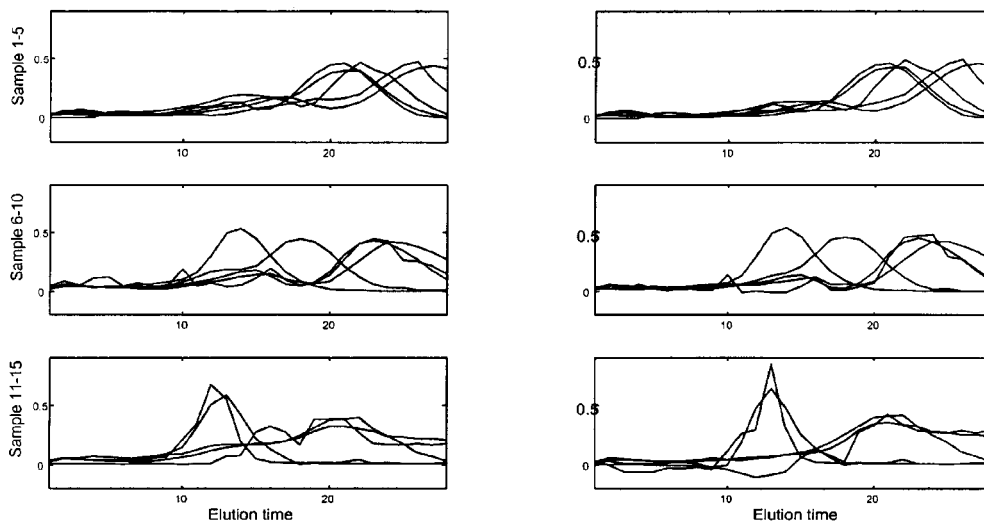


Figure 9. Estimates of elution profiles of component 1 in 15 different samples. Estimates from three-way PARAFAC1 are shown to the left and from four-way PARAFAC2 to the right. The top plots show the estimates of the first five samples, etc.

estimates obtained from PARAFAC2. As for the three-way model and unlike the four-way PARAFAC1 model, PARAFAC2 provides individual profiles for each sample (F_k). In Figure 9 the estimated profiles of component 1 in all samples are compared for three-way PARAFAC1 and four-way PARAFAC2. Note that the PARAFAC1 elution profiles are identical to the ones shown in Figure 8. As for the spectral parameters the similarity is very high even though the deviations between the 15 elution profiles are not of a type expected to be perfectly modeled by PARAFAC2.

Performing a split-half analysis for both the four-way PARAFAC1 and the PARAFAC2 model substantiated that the four-way PARAFAC1 model is not suitable, since the parameters did not replicate over different subsets. The data were divided into two groups by assigning eight samples to one group and seven to another. For both subsets a PARAFAC1 and a PARAFAC2 model were fitted. In Figure 10 the resulting emission and excitation mode loadings are shown. There are large discrepancies in the PARAFAC1 parameters depending on which subset is used, while for the PARAFAC2 model these discrepancies are smaller and probably caused by the very low sample size (seven and eight respectively).

CONCLUSION

In this application a suggestion has been given for the solution of a very important and frequently arising problem, namely shifted data. It has been shown that even though the data are severely shifted, PARAFAC2 apparently is capable of modeling the data. In this case, validation could be very elegantly performed by unfolding the four-way data to a three-way structure for which the PARAFAC1 model, and its ensuing uniqueness, holds. However, usually, shifted chromatographic data are at most three-way and therefore such a rearrangement in order to attain uniqueness is impossible. Furthermore, using the four-way PARAFAC2 model, more structure is imposed in the model than with the three-way PARAFAC1 model for the unfolded data, which is preferable from an

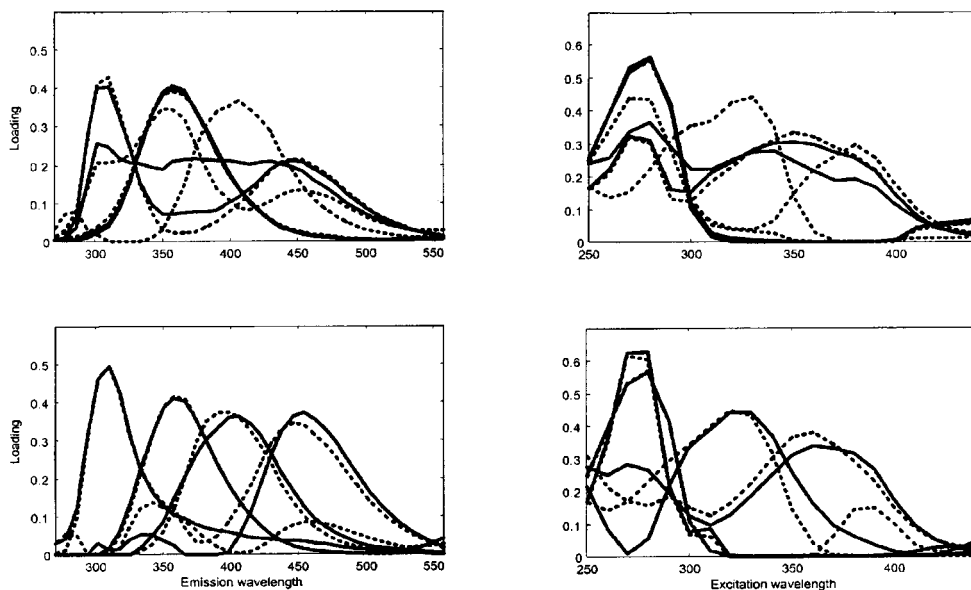


Figure 10. Split-half analysis. The top plots give the results from four-way PARAFAC1 and the bottom plots the results from PARAFAC2. The left plots show the emission mode parameters and the right plots the excitation mode parameters. Loading vectors estimated from a subset of eight samples are shown with full lines, and loading vectors estimated from a subset of seven samples are shown with dotted lines

interpretation as well as a noise reduction point of view.

The three-way PARAFAC2 model appears to provide a good approach for solving variable shifts for three-way data, and further applications to chromatographic data will help substantiate this conclusion.

ACKNOWLEDGEMENTS

For the first two authors, financial support was obtained from Professor Lars Munck, Food Technology, Department of Dairy and Food Science, Royal Veterinary and Agricultural University, Denmark through Nordic Industry Foundation project P93149 and FØTEK for part of the work reported here.

REFERENCES

1. W. H. Lawton and E. A. Sylvestre, *Technometrics*, **13**, 617 (1971).
2. R. Manne, *Chemometrics Intell. Lab. Syst.* **27**, 89 (1995).
3. R. Bro, *Multi-way Analysis in the Food Industry. Models, Algorithms, and Applications*, University of Amsterdam, Amsterdam and Royal Veterinary and Agricultural University, Amsterdam (1998).
4. R. A. Harshman, *UCLA Working Papers Phonet.* **16**, 1 (1970).
5. H. A. L. Kiers, J. M. F. ten Berge and R. Bro, *J. Chemometrics*, **13**, 275 (1999).
6. R. Bro, *Chemometrics Intell. Lab. Syst.* **38**, 149 (1997).
7. R. A. Harshman, *UCLA Working Papers Phonet.* **22**, 111 (1972).
8. J. B. Kruskal, *Psychometrika*, **41**, 281 (1976).

II. Algorithms, models and applications

9. J. B. Kruskal, in *Multiway Data Analysis*, ed. by R. Coppi and S. Bolasco, p. 8, Elsevier, Amsterdam (1989).
10. J. B. Kruskal, *Linear Algebra Appl.* **18**, 95 (1977).
11. J. M. F. ten Berge and H. A. L. Kiers, *Psychometrika*, **61**, 123 (1996).
12. R. Harshman and M. E. Lundy, *Psychometrika*, **61**, 133 (1996).
13. R. Bro and H. A. L. Kiers, 'A new efficient method for determining the number of components in PARAFAC models', submitted (1999).
14. L. R. Tucker, *Psychometrika*, **31**, 279 (1966).